UNIVERSITY OF BIRMINGHAM

The immunobiology of human hepatic gamma delta T cells

Stuart Hunter

A thesis submitted to the University of Birmingham
for the degree of
DOCTOR OF PHILOSOPHY

Institute of Immunology and Immunotherapy
College of Medical and Dental Sciences
University of Birmingham
September 2017

Abstract

The liver is home to a number of tissue associated lymphocyte populations, of which many have been implicated in the pathogenesis of chronic liver diseases. γδ T cells, particularly the $V\delta2^{neg}$ subset, are known to comprise a substantial proportion of tissue associated lymphocytes, although their immunobiology remains poorly understood. Here, the localisation, TCR diversity, immunophenotype and function of human intrahepatic γδ T cells was explored with an emphasis on highlighting any potential role in chronic liver disease and also to further understanding of tissue associated γδ T cells, using the liver as a model tissue. Intrahepatic γδ T cells were predominantly localised in the sinusoids and did not increase in frequency with chronic inflammation. $V\delta2^{neg}$ cells exhibited private TCR clonal focussing, with complex CDR3 regions suggestive of antigen-driven expansions, concordant with a loss of naïve-like $CD27^{hi}$ cells present in the periphery. Expanded clonotypes were phenotypically T_{EM}- or T_{EMRA}-like, with T_{EMRA}-like clonotypes shared between liver and blood and resembling vasculature-associated virus specific $CD8^+$ T cells while T_{EM} clonotypes were identified only in the liver and resembled tissue-resident $CD8^+$ T cells. These findings suggest that disease has minimal impact on intrahepatic γδ T cells, while supporting an adaptive paradigm for these cells in the formation of tissue-associated subsets.

For William and Emilia

While we try to teach our children all about life,

our children teach us what life is all about

Acknowledgements

I would like to thank my supervisor and mentor Prof. Ben Willcox, who took me on as a Masters project student after I'd spent twelve years in the scientific wilderness – without him I would likely not have gained a PhD studentship and my newly rekindled career in science would have fizzled out before it even got started. His relentless good humour, enthusiasm and positivity have been a driving force in the completion of this thesis, not to mention his discerning scientific eye and willingness to engage in research that attempts to ask the bigger questions.

My co-supervisor, Dr Ye Oo, has similarly formed a bastion of good natured calm throughout the project, putting up with my grumpiness on an almost daily basis and always a welcome source of encouragement and ideas – thank you. In the lab, there have been many people who have helped along the way, foremost amongst them Dr Carrie Willcox, who's help with the single cell PCR was invaluable, and Dr Martin Davey, who provided a great deal of help with flow cytometry and data analysis. Dr Hannah Jeffery helped me find my feet in the liver labs and was always on hand to assist with day to day queries and issues. Many thanks to these three and all in the Willcox group and liver labs who have contributed over the last 4 years.

Without the belief, encouragement and support of my wife Jo I would not have even started out on this endeavour, let alone completed it. My mum, Christine, has likewise always been there for me while my life has taken unexpected twists and turns – my love and thanks to both of you, and to the rest of my family, who I suspect have been following my progress with that immortal question: "When are you going to get a real job?"

Contents

Figures

Tables

Abbreviations

AIH	Autoimmune hepatitis
ALD	Alcoholic liver disease
APC	Antigen presenting cell
BCR	B cell receptor
CAR	Chimeric antigen receptor
CCL	Chemokine ligand
CCR	Chemokine receptor
CD	Cluster of differentiation
CDR	Complementarity determining region
CMV	Cytomegalovirus
CTL	Cytotoxic T lymphocyte
CTLA	Cytotoxic T lymphocyte-associated molecule
DAB	3,3'-Diaminobenzidine
DAMP	Damage associated molecular pattern
DC	Dendritic cell
DETC	Dendritic epithelial T cell
DNA	Deoxyribonucleic acid
EBV	Epstein Barr virus
ECM	Extracellular matrix
EDTA	Ethylenediaminetetraacetic acid
FACS	Fluorescence activated cell sorting
FBS	Foetal bovine serum
FFPE	Formalin fixed paraffin embedded
HBV	Hepatitis B virus
HCC	Hepatocellular carcinoma
HCV	Hepatitis C virus
HLA	Human leucocyte antigen
HMB-PP	(E)-4-Hydroxy-3-methyl-but-2-enyl pyrophosphate
HRP	Horseradish peroxidase
HSC	Hepatic stellate cell
HSEC	Hepatic sinusoidal endothelial cell
IBD	Inflammatory bowel disease
IEL	Intra-epithelial lymphocyte
IFN	Interferon
Ig	Immunoglobulin
IHC	Immunohistochemistry
IL	Interleukin
ILC	Innate lymphoid cell
IPP	Isopentenyl pyrophosphate
ISH	In-situ hybridisation
IU	International units
KC	Kupffer cell
KIR	Killer activation receptor
LDL	Liver derived lymphocytes
LPS	Lipopolysaccharide
LSEC	Liver sinusoidal endothelial cell
mAb	Monoclonal antibody
MHC	Major histocompatibility complex
MMP	Matrix metalloprotease
MSC	Mesenchymal stem cell
NAFLD	Non-alcoholic fatty liver disease
NASH	Non-alcoholic steatotic hepatitis
NGS	Next generation sequencing
NK	Natural killer cell
NKT	Natural killer T cell
PAMP	Pathogen associated molecular pattern
PBC	Primary biliary cholangitis
PBMC	Peripheral blood mononuclear cells
PBS	Phosphate buffered saline
PCR	Polymerase chain reaction
PMA	Phorbol myristate acetate
PRR	Pattern recognition receptor
PSC	Primary sclerosing cholangitis
RACE	Rapid amplification of cDNA ends
RAG	Recombination activating gene
RNA	Ribonucleic acid
sc-PCR	Single cell polymerase chain reaction
SMA	Smooth muscle actin
TCR	T cell receptor
TGF	Transforming growth factor
TH1	T helper 1
TIMP	Tissue inhibitors of metalloprotease
TLR	Toll like receptor
Treg	Regulatory T cell

1

Introduction

1.1 The mammalian immune response

The immune response has evolved to protect host organisms from attack by exogenous intracellular and extracellular pathogens, including bacteria, viruses and parasites, and also has a significant role in the homeostasis of host tissues through modification of the microenvironment, removal of dead or dying cells, and wound repair. Two arms of the immune system have developed, one, the innate immune response, forming the first line of defence against invading pathogen and playing a major role in tissue homeostasis, the other, the adaptive immune response, responsible for removal of pathogens that escape the innate response and for the formation of immunological memory, enabling rapid and effective responses to any repeated insult.

1.1.1 The innate immune response

Many common pathogens share molecular elements that are not found in the host organism. These are termed pathogen-associated molecular patterns (PAMPs), and include lipopolysaccharide (LPS) found in bacterial cell walls, and viral RNA, amongst many others (Medzhitov and Janeway, 2002). Damage to cells from physical or chemical sources can also trigger the release of damage-associated molecular patterns (DAMPs) (Bianchi, 2007). Through the evolution of immune cell surface receptors that recognise these elements (pattern recognition receptors, or PRRs), innate immune cells are capable of quickly identifying pathogens and instigating an immune response. This response occurs either through direct means such as endocytosis or cytolysis, indirectly through the release of inflammatory cytokines and recruitment of other immune cells to the site of infection, or very often a mix of both (Brightbill *et al*., 1999, Svanborg *et al*., 1999).

Cells of the innate immune response also have a critical role as antigen presenting cells (APC), priming the adaptive immune response, as will be discussed below.

Cells of myeloid origin are particularly important in innate immunity, with monocyte-derived macrophages and dendritic cells (DC) playing key roles, but lymphoid cells also play a role, particularly natural killer (NK) cells (Yokoyama and Plougastel, 2003), NKT cells (Kronenberg and Gapin, 2002) and innate-like lymphocytes (ILC) (Hwang and McKenzie, 2013).

1.1.2 The adaptive immune response

While PRR such as the Toll-like receptors (TLR) expressed by cells of the innate response are capable of detecting many pathogens based on generic molecular features (Takeda *et al*., 2003), cells of the adaptive immune response, namely T lymphocytes and B lymphocytes, have highly targeted antigen recognition capabilities. This takes the form of the T cell receptor (TCR) or B cell receptor (BCR) respectively. These receptors are generated by somatic rearrangement of the genes at the TCR/ BCR locus, orchestrated in part by enzymes encoded by the RAG1 and RAG2 genes (Shinkai *et al*., 1992). This results in T cells and B cells being able to recognise a hugely diverse repertoire of potential antigens – potentially up to 10^{15} individual specificities (Davis and Bjorkman, 1988).

As with PRR, activation of the T cell receptor by binding with its cognate antigen triggers the lymphocyte to either develop cytotoxic properties or to secrete cytokines specific to the cytokine milieu encountered by the cell during antigen recognition (Croft *et al*., 1994, Nakamura *et al*., 1997). In B cells, recognition of cognate antigen through the BCR

triggers differentiation of the cell into a plasma cell, capable of secreting immunoglobulin (Ig) antibodies (Slifka *et al*., 1998).

In addition, long-lasting immune protection can only be conferred by the creation of immune cells capable of rapidly expanding in response to challenge. The formation of these memory cells is carried out by the adaptive immune response, through clonal expansion of lymphocytes that have been exposed to antigen via their TCR/ BCR (Kaech *et al*., 2002).

1.1.3 Conventional T cells

Conventional T cells express a TCR composed of a heterodimer of a disulphide linked α chain and β chain. These chains consist of an extracellular immunoglobulin-like domain, a short cytoplasmic domain and a transmembrane domain that allows association with the CD3 tetramer complex, together forming the TCR complex (Clevers *et al*., 1988). Antigen specificity is conferred by the highly variable membrane distal domains of the TCR chains, which share structural homology with Ig variable (IgV) domains. Like IgV, these domains contain three complementarity determining regions (CDR), loops of the protein chain with highly varied amino acid sequence. The three CDR of the α chain combine with those of the β chain to form the antigen binding site, and due to the unique combination of amino acids present, each binding site will have a unique conformation, polarity and hygroscopicity, being therefore highly selective for a particular antigen (Garboczi *et al*., 1996).

The TCR complex is unable to bind free antigen. Instead, antigen in the form of short peptide sequences must be presented by another molecule on the surface of the target

cell, namely the major histocompatibility complex (MHC) (Germain, 1994). In humans, there are nine genes encoding for the MHC, termed the human leucocyte antigen (HLA) complex. Three of these genes, HLA-A, HLA-B and HLA-C, encode for MHC class I molecules, while the HLA-D family of six genes encode MHC class II. Antigens derived from intracellular pathogens and processes are typically presented on MHC class I molecules, while those derived from extracellular pathogens are presented on MHC class II. While MHC class I molecules are normally expressed on all nucleated cells, MHC class II molecules are normally expressed only by professional APC, such as macrophages and DC (Steimle *et al*., 1994). Diversity of the HLA locus genes is very high due to an extensive number of polymorphisms, and as such the protein products of these genes constitute a marker of "self" in terms of cellular recognition.

In addition to recognition and binding of the target cell MHC-peptide complex by the TCR, T lymphocytes require additional stimulation to gain effector function (Rudolph *et al*., 2006). CD8 is a co-stimulatory molecule expressed by a subset of T cells that recognises the invariant domain of MHC class I molecules and amplifies the intracellular signalling cascade triggered by MHC-peptide binding through the TCR (Gao *et al*., 1997). T cells expressing CD8 that are activated in this way become cytotoxic T lymphocytes (CTL), capable of secreting perforin and granzyme and thereby killing the target cell, or inducing programmed cell death (Green *et al*., 2003). In this way the source of intracellular antigen will be destroyed. CD4 is another co-stimulatory molecule that recognises the invariable domain of MHC class II (Wang and Reinherz, 2002). $CD4^+$ T cells are generally termed T helper cells (T_H) due to their influence on other immune cell subsets. Due to the varied nature of extracellular pathogens, $CD4^+$ T cells require an additional signal to

differentiate, in the form of cytokine stimulation (Mucida and Cheroutre, 2010). Binding of MHC class II and CD4 co-stimulation in the presence of IL-12 will commit the T cell to the T_H1 phenotype, expressing the pro-inflammatory IFN-γ and TNF-α, which helps activate CTL, NK and bactericidal macrophages (Berberich *et al*., 2003). IL-4 in the microenvironment will result in adoption of a T_H2 phenotype by the $CD4^+$ T cell, capable of stimulating B cell differentiation to generate a humoral response against parasites (Kaplan *et al*., 1998). Antigen binding in the presence of IL-6 and IL-1β leads to a T_H17 phenotype, with expression of IL-17 and IL-22 leading to recruitment of polymorphonuclear cells capable of dealing with invading bacteria and fungi. Finally, recognition of antigen in the presence of TGF-β leads to generation of a regulatory T cell phenotype (Treg), capable of expressing IL-10, TGF-β and T cell inhibitory molecules such as cytotoxic T lymphocyte antigen 4 (CTLA-4), thereby dampening an immune response and limiting immunopathology (Sakaguchi, 2005).

1.1.4 Kinetics of the adaptive immune response

Proteins inside the cell are continuously degraded by the proteasome complex in the cytosol and the resulting short peptides are transported into the endoplasmic reticulum (ER) via the transport-associated with antigen processing complex (TAP). In the ER these peptides associate with the MHC class I subunits and the entire complex is assembled and transported to the cell surface. In cells capable of expressing MHC class II, i.e. professional APCs, antigenic pathogens are phagocytosed, or extracellular proteins are endocytosed, degraded, and these vesicles are fused with ER derived vesicles containing nascent MHC class II molecules before being transported to the cell surface (Guermonprez *et al*., 2002). Uptake of pathogen and antigen presentation is associated

with migration of APC, specifically DC, to the lymph nodes or spleen, where they can interact with naïve T lymphocytes, or the release of chemoattractants that recruit T cells to the site of infection (Allan *et al*., 2006). In either case, passing naïve T cells with specificity for the presented MHC-peptide complex will bind with the target cell or APC, a process also requiring the interaction of signal 2 molecules such as CD28, expressed by T cells (Acuto and Michel, 2003), with CD80 or CD86, expressed by many APC (Greenwald *et al*., 2005). This priming interaction will trigger T cell effector function development, as well as proliferation and migration to the site of infection (Kapsenberg, 2003). A proportion of these cells will not follow these differentiation steps but will instead acquire a memory phenotype. This generates a central pool of long-lived, antigen-specific cells capable of rapid response to further challenge by previously encountered antigen. While the innate immune response mediated by macrophages, neutrophils and NK cells is very rapid, the adaptive immune response requires a longer timeframe due to the need for migration, APC and T cell interaction and consequent expansion of effector cell populations. However, it is becoming apparent that another branch of adaptive immunity may be capable of bridging the gap between the innate and adaptive response, a branch composed for the most part of unconventional T cells. Unconventional T cells all express a TCR but are generally incapable of recognising MHC-peptide complex, instead binding with MHC-like molecules, including CD1 and MR1 (Treiner and Lantz, 2006). While several subsets of unconventional T cells exist, including natural killer T cells (NKT) and mucosal associated invariant T cells (MAIT), this thesis will focus on γδ T cells, and in particular their role in the liver.

1.2 Gamma delta T cells

1.2.1 Defining the immunological niche of γδ T cells

γδ T cells express a TCR composed of a γ chain and a δ chain, encoded by γ and δ genes that rearrange in the same way as Ig and $\alpha\beta^+$ TCRs (Elliott *et al*., 1988). Although these chains have far fewer corresponding variable (V) region gene segments than αβ T cells, with only 70 possible combinations of Vγ and Vδ segments compared with 2,500 for αβ TCRs, the variability of the γδ TCR is increased hugely by use of multiple reading frames for transcription and recombination of the Vδ segment with diversity (D) regions in the δ chain, resulting in up to 10^{18} individual specificities (Davis and Bjorkman, 1988). In both mice and humans however, use of the Vδ segment is often restricted, and in mice in particular specific combinations of Vγ and Vδ regions are often observed, especially in tissue associated γδ T cell populations. For example, in mice, the dermal epithelium is populated exclusively with γδ T cells expressing the Vγ5Vδ1 combination, while in humans the blood subset of γδ T cells expresses the Vγ9Vδ2 combination at a frequency of 90 – 99%. In human epithelial tissue, γδ T cells primarily express Vδ1 or Vδ3, in combination with a variety of Vγ segments, and they may constitute up to 50% of the total $CD3^+$ lymphocyte population (Guy-Grand *et al*., 2013). This observed enrichment of γδ T cells in epithelial tissue suggests a role for these cells in innate-like protection against invading pathogen, especially since it is apparent that these cells do not migrate to the lymphoid tissue for priming in the same way that naïve αβ T cells do, and therefore will not be exposed to the large number of diverse antigens presented there by DC.

Although monoclonal proliferation of antigen specific γδ T cells has been documented in response to infectious agents such as listeria, salmonella and toxoplasmosis, as indeed has the formation of an effector memory population of virus specific $V\delta2^{neg}$ T cells following cytomegalovirus (CMV) infection in some patients (Pitard *et al*., 2008), in general previous studies of γδ T cells have suggested that they do not seem to form genuine memory cells as occurs in true adaptive immunity.

As well as the TCR, γδ T cells express a variety of cell surface receptors common to cells of the innate lineage, including both activatory and inhibitory NK receptors, such natural killer group 2 member D (NKG2D), TLRs and the Fc receptor CD16. This supports the notion of γδ T cells as predominantly innate-like, but several studies have in fact highlighted the importance of TCR engagement in the acquisition of functionality by these cells. If this is the case, understanding the nature of the ligand recognised by the γδ TCR may be crucial in attempts to understand their function.

1.2.2 γδ TCR ligands

Ligand recognition by the γδ TCR is one of the chief mysteries pursued by researchers in the γδ T cell field. A lack of diversity amongst V chain composition, especially in the tissue resident population of γδ T cells, suggests that foreign antigen may not be the primary target of these cells, and, together with evidence of NK receptor expression, suggests a role for γδ T cell in lymphoid stress surveillance, perhaps with self-stress molecules representing the primary group of γδ TCR ligand (Vantourout and Hayday, 2013). Nevertheless, the highly variable nature of the CDR3 region of the δ chain may suggest this is not the case, and efforts to determine the γδ TCR ligands have discovered several targets, both endogenous and exogenous in nature.

Several MHC-like molecules have been found to act as antigen for the γδ TCR. These include, in mice, the non-peptide-binding MHC molecules H2-T10 and H2-T22 (Crowley *et al*., 2000), and in humans CD1c and CD1d (Adams, 2014). Additionally, the MHC class I-like (MIC) proteins MICA and MICB have been proposed to act as ligands for the γδ TCR (Coulthard *et al*., 2003). This evidence is derived from functional studies rather than direct binding, and as such remains unproven, especially since these molecules are recognised ligands for NKG2D, also expressed by γδ T cells. Indeed, direct binding and structural evidence has only been determined for T22 and CD1d, and that from small numbers of γδ TCR clones, so the physiological relevance remains unproven.

An important aspect of these studies into MHC-like molecule binding by the γδ TCR is that peptide or lipid presentation by these molecules is generally not required as part of the binding process. Since many antigen-presenting molecules are upregulated during cellular stress, it is possible that this recognition by γδ T cells is part of the lymphoid stress surveillance mechanism (Hayday, 2009).

Phosphoantigens (P-Ag) are small non-peptidic phosphorylated moieties produced during isoprenoid biosynthesis by pathogenic prokaryotes and in higher eukaryotes. They are therefore, potentially both endogenous and exogenous in nature. They include hydroxymethyl-but-2-enylpyrophosphate (HMB-PP), which is not produced by vertebrates but is a strong agonist of the human Vγ9Vδ2^{+} TCR, suggesting a role as a PAMP in this setting (Eberl and Jomaa, 2003). Isopentenyl pyrophosphate (IPP) is produced by both bacteria and in eukaryotes, where its production through altered metabolism in transformed cells has been linked with a role for the Vγ9Vδ2^{+} T cell subset in tumour immunosurveillance (Morita *et al*., 1999). The sensitivity of these γδ T cells for

IPP is several logs lower than for HMB-PP, consistent with the possible role for IPP as an auto-antigen in examples of cell stress. Evidence for direct binding of P-Ag to the γδ TCR is weak and it is likely that processing by an intermediate cell type such as monocytes or a presentation molecule is involved in the binding process. The crystal structure of the Vγ9Vδ2^{+} TCR suggested all CDR loops are involved in antigen binding (Wang *et al*., 2010), suggestive of a much larger epitope than a simple P-Ag. Recently, a candidate presentation molecule has been proposed, butyrophilin 3A1 (BTN3A), although the exact mode of recognition remains controversial (Harly *et al*., 2012). BTN3A has been demonstrated to be upregulated on potential target cells such as epithelia following cytokine or hypoxia-mediated stress, as well as tumour tissue (Compte *et al*., 2004). Through knockdown and mutation studies, the intra-cellular B30.2 domain of BTN3A was demonstrated to be indispensable to P-Ag sensitivity (Harly *et al*, 2012); (Sandstrom *et al*., 2014), however, exactly how the P-Ag, which is often secreted by pathogen, is taken up by the lymphocyte to bind the intra-cellular B30.2 domain remains unresolved.

Furthermore, the B7-family butyrophilin-like (BTNL) family of molecules has been associated with regulation of murine and human γδ T cells. Homologous with the *Skint1* gene, which is critical to the thymic development of Vγ3^{+}Vδ1^{+} in mice (Chodaczek *et al*., 2012) and expressing intra-cellular B30.2 domains, the conserved BTNL family have been demonstrated to critically and selectively promote survival of Vγ5^{+} γδ T cells in murine small intestine (*Btnl1*) (Di Marco Barros *et al*, 2016). This paradigm may extend to human epithelial tissue, where BTNL3 and -8 have been demonstrated to specifically activate Vγ4+ γδ T cells (Di Marco-Barros *et al*, 2016). It is possible that BTNL molecules are co-stimulatory in this scenario, rather than direct-TCR ligands (Nielsen *et al*., 2017).

The likelihood of the γδ TCR being employed in recognition of foreign antigen is supported by the work of Chien and colleagues who determined that that algal protein phycoerythrin was a ligand for murine and human γδ TCR, and that the CDR3 region was critical in determining binding specificity (Zeng *et al*., 2012). Again, the physiological relevance of this particular antigen remains in question, but nevertheless as a proof of principle this work offers persuasive evidence. As with MHC-like binding, antigen presentation in γδ TCR binding of phycoerythrin does not seem necessary, distinguishing this interaction from that of αβ T cells and their target antigen whilst simultaneously expanding the range of potential targets for lymphocytes in general. In addition, early studies of human γδ T cells suggested that clonal expansion and formation of memory cells does not seem to occur, suggesting that even on the recognition of genuinely foreign peptide, γδ T cells behave with more innate-like kinetics than a conventional adaptive T cell response.

1.2.3 Function of gamma delta T cells

1.2.3.1 γδ T cell effector functions

Activated γδ T cells in both mice and humans express a range of cytokines associated with conventional CTL responses, including IFN-γ and TNF-α, as well as cytotoxicity proteins granzyme, perforin, Fas ligand and TNF-related apoptosis-inducing ligand (TRAIL). In this way γδ T cells are clearly capable of functioning as cells of the late adaptive immune response (Salerno and Dieli, 1998). However, γδ T cells can simultaneously also express a range of factors, particularly cytokines, chemokines and growth factors normally

associated with helper T cell subsets and the early phase of an adaptive immune response, including Th2 and Th17 cytokines. Chemokines secreted by γδ T cells are involved with recruitment of macrophages, NK cells, B cells and T cells. Studies have highlighted interaction between γδ T cells and both B cells and DC, and work by Moser's group has demonstrated the capacity of human Vγ9Vδ2^{+} T cells to act as antigen presenting cells; phagocytosing opsonised target cells, subsequent expression of CCR7 and migration to lymph nodes with concomitant expression of CD80 and CD86 (Brandes *et al*., 2005). This suggests a vast array of potential functions for activated γδ T cells.

1.2.3.2 Anti-pathogenic protection

The direct, critical involvement of γδ T cells in combating infections has only been demonstrated in a limited number of mouse TCRδ knockout studies, for example, during lung-tropic *Nocardia asteroides* infection (Tam *et al*., 2012). However, many studies have demonstrated increased inflammation, morbidity and mortality with γδ T cell deplete mice, although the mode by which γδ T cells contribute to immunoprotection varies. While mortality is increased in TCRδ knockout mice infected with vaccinia virus, memory cell formation and successful immunity on secondary infection is not affected in these mice, suggesting they are functioning as innate-like cells and not contributing towards a successful adaptive response (Selin *et al*., 2001). IL-17 production and consequent inflammation seems to be important in protecting mice against several bacterial pathogens including *Klebsiella pneumonia* (Matsuzaki and Umemura, 2007), while induction of CD8^{+} memory cells by γδ T cells has been highlighted in establishing immunological memory against West Nile virus (Wang *et al*., 2006). As previously mentioned, Vδ2^{neg} γδ T cells expand in an apparently antigen-specific manner following

CMV infection, particularly in immunosuppressed patients following transplantation or chemotherapy (Couzi *et al*., 2009). This potential role of γδ T cells to behave like αβ T cells in response to certain pathogens in the absence of an αβ T cell response may reflect the fact that they are the first cells of the immune system to develop in neonates and have a clear role in neonatal protection (Gibbons *et al*., 2009).

1.2.3.3 Lymphoid stress surveillance

As has been mentioned, various potential antigens of the γδ TCR, as well as ligands for NKG2D expressed by γδ T cells, are upregulated in response to cellular stress, including infection and transformation. This enables γδ T cells to quickly identify such infected or stressed cells, and instigate either a direct cytotoxic response or to stimulate an adaptive response. Since the myeloid lineage DC are classically associated with this sort of immune surveillance, Hayday and colleagues coined the phrase "lymphoid stress surveillance" to distinguish the role of lymphocytic γδ T cells (Hayday, 2009). The localisation of discrete γδ T cell populations to epithelial tissues supports this hypothesis, at least in murine studies. Since these tissues are the first to be exposed to invading pathogen, having a local subset of immune cells capable of mounting a rapid, and perhaps antigen-specific, response would seem to make evolutionary sense. In addition, these tissues exhibit a high rate of cellular turnover and consequentially are prone to DNA replication errors and transformation. Several studies have demonstrated γδ T cell mediated killing of various cancer cell lines, and the importance of γδ T cells in preventing the formation of tumours in murine models of cutaneous and colon carcinogenesis (Girardi *et al*., 2001). As such, there have been several clinical trials over the past few years that have attempted to utilise stimulated autologous $V\gamma9V\delta2^{+}$ T cells in adoptive

transfer as a means of treating various cancers in humans (reviewed by Fournie *et al*., 2013).

1.2.3.4 Immunoregulation and homeostasis

A growing body of work has highlighted the contribution of γδ T cells to immune regulation, particularly in epithelial tissues. In experiments in mice, γδ T cell depletion has been demonstrated to increase inflammation and IFN-γ levels in both lung (Liu *et al*., 2013) and gut (Waters *et al*., 1999) epithelia following introduction of pathogen. However, this may be due to the lack of an effective early γδ T cell response in controlling the pathogen and subsequent prolonged activation of an αβ T cell-mediated response. Despite this, γδ T cells are known to interact with a number of immune and stromal cells in a potentially regulatory fashion, both in sterile and pathogenic inflammatory scenarios (Hayday and Tigelaar, 2003).

Although the exact nature of the interactions between αβ T cells and γδ T cells is yet to be fully elucidated, there is some evidence that the two subtypes compete for pro-proliferative factors such as DC-derived IL-15, and thereby γδ T cells could loosely be said to have a regulatory effect on αβ T cell function (Do and Min, 2009). Generally, γδ T cells are capable of producing the immunosuppressive cytokines IL-10, TGF-β as well as expressing LAG3, FasL and TRAIL, all of which have been implicated in regulation of T cell activity through induction of anergy or apoptosis (Hayday and Tigelaar, 2003). γδ T cells have also been linked with regulation of pro-inflammatory macrophages, contributing towards resolution of inflammatory processes. During *L. monocytogenes* infection, γδ T cells have been demonstrated to induce cytolysis of pro-inflammatory macrophages (Tramonti *et al*., 2008). Several studies have also highlighted the importance of

monocyte/ macrophage derived factors in the recruitment and stimulation of γδ T cells, so, as with most of the γδ T cell – immune cell interactions, there is a degree of reciprocity. Mesenchymal stem cells (MSC) are important precursors to a variety of stromal cells, including osteoblasts, chondrocytes and myocytes. Through expression of prostaglandin E2, MSC have been demonstrated to suppress the proliferation of γδ T cells *in vitro* (Martinet *et al*., 2009). Although constrained to the Vγ5Vδ1 expressing murine dendritic epidermal T cells (DETC), some studies have also suggested a role for γδ T cells in regulation of neighbouring stroma, for example through the secretion of insulin-like growth factor 1 (IGF) and keratinocyte growth factor (KGF) (Toulon *et al*., 2009). In addition, chemokine secretion by γδ T cells following trauma such as burn injury has been linked with recruitment of macrophages and promoting wound repair (Rani *et al*., 2014).

1.3 Liver biology

1.3.1 Liver physiology

Certain subsets of γδ T cells have been found to localise to specific tissues in both mice and humans. In humans, while the Vδ9 Vδ2^{+} subset are mainly found in the periphery, γδ T cells with the Vδ1 chain have been demonstrated to localise to epithelial tissues, with an enlarged δ1/δ2 ratio in gut, lung and dermis compared with that in blood (Groh *et al*., 1989). During the last 20 years, studies demonstrated a similar δ1/δ2 ratio and increased percentage of γδ T cells of the total T cell population in liver compared with the periphery (Kenna *et al*., 2004), suggesting the possibility of a similar role for these cells in the liver as in gut and other epithelial tissues. However, the nature of that role remains unclear. To begin to understand the function of γδ T cells in the liver, it is important to have an

understanding of the unique physiology and functions of the liver organ, and its vital role in human immunity.

1.3.1.1 Liver function

The liver is the largest internal organ in humans and receives up to 30% of the total blood volume of the body every minute. As well as receiving up to 20% of its blood from the main arterial supply, the liver is the first destination of venous blood from the gut. This blood contains carbohydrates, proteins and lipids absorbed into the blood stream following digestion. The liver is responsible for metabolising these nutrients, as well as clearing any toxins or pathogens that reach it from the gut. Nutrient-rich blood drains from the gastrointestinal tract through the hepatic portal vein, where, in combination with arterial blood supplied by the hepatic arteries, it passes into the liver sinusoids, and then into contact with hepatocytes by passing through fenestrations of the liver sinusoidal endothelial cells (LSEC). Hepatocytes are the majority cell type in the liver, accounting for ~80% of the cytosolic organ mass, and form the liver parenchyma. These cells carry out a vast number of functions related to metabolism and catabolism of various nutrients, including synthesis of many proteins, including lipo- and glycoproteins, metabolism of carbohydrates - the liver being the primary site of gluconeogenesis in the body, and storage of fats, triglycerides, carbohydrates and iron. Hepatocytes produce and secrete bile salts which emulsify lipids during digestion in the duodenum. Hepatocytes also have a major role in detoxification and removal of many exogenous ingested and endogenous compounds such as drugs, ammonia and steroids.

In addition to nutrients, any pathogens or pathogen derived antigen such as LPS that evade the predominantly innate immune response in the gut also move to the liver, so

the immune system there has to be able to deal with these to prevent infection. Despite this, the liver also has an important role in establishing immunotolerance to many antigens that may otherwise cause inflammation and damage to the sensitive liver parenchyma (Horst *et al*., 2016). This necessary balance between removal of pathogens and induction of immune tolerance is exploited successfully by several hepatotrophic pathogens including Hepatitis B and C viruses (Knolle *et al*., 2015) and *Plasmodium* spp. sporozoites (Wunderlich *et al*., 2014). Cells of the immune system resident in the liver are critical in both defense against pathogens and establishment of immunotolerance toward foreign antigen.

1.3.1.2 Liver microanatomy

Within the liver a vast meshwork of hexagonal lobules are formed, with the portal venules, arteries and interlobular bile ducts clustered at each corner of the hexagon, forming the "portal triad", and a central vein that receives the draining blood supply (Figure 1.1). The liver sinusoids have a very small diameter but form a huge endothelial bed, resulting in a five-fold drop in blood pressure between the portal arteries and these sinusoids, running between the portal tract and the central vein. This yields a blood flow of around half the speed of other capillary beds. This allows prolonged contact between the hepatic blood and the specialised cells of the liver, cells including LSEC, hepatic stellate cells (HSC), liver-resident macrophages called Kupffer cells and intra-hepatic lymphocytes. This long interaction is particularly important for the immune system cells, allowing time for pathogen or pathogen-derived antigen to be taken up by antigen-

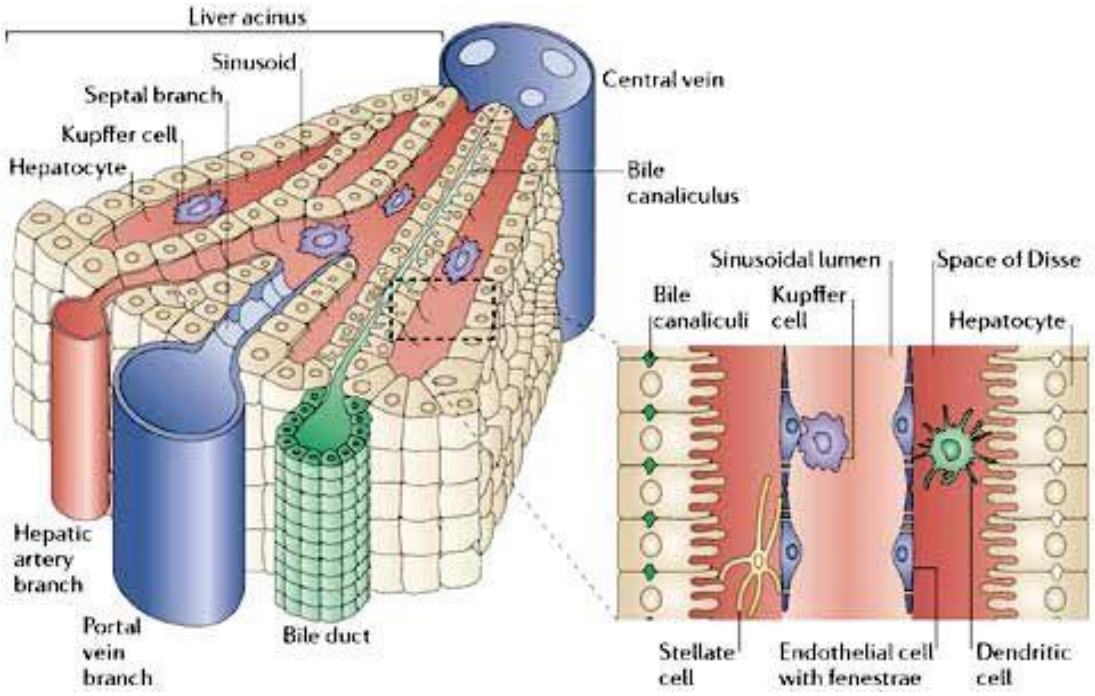

Figure 1.1: Microanatomy of the liver

From: Adams *et al. Nature Reviews Immunology* **6**, 244–251 (March 2006) | doi:10.1038/nri1784

presenting cells, as well as time for passing lymphocytes to be recruited from the blood supply into contact with the parenchymal cells.

The first point of contact for blood leaving the portal tract and entering the liver sinusoids is the hepatic sinusoidal endothelial cells. These cells effectively form a barrier between the blood and the hepatocytes, although this barrier is relatively permeable due to their sieve-like, fenestrated formation, and is indeed breached by the hepatocytes themselves on occasion via extensions of the hepatocyte membrane (Wisse *et al*., 1996). Despite this porous structure, the fenestrations are in fact tightly regulated and only allow passage of specific macromolecules from the endothelial lumen into the underlying tissue.

As such, the LSEC form an important gateway for anything attempting to reach the hepatocytes, and accordingly have a vital role in regulation of liver function (Knolle and Wohlleber, 2016).

Lacking a contiguous basement membrane structure, the LSEC have a gap between them and the underlying parenchyma, the Space of Dissé. This gap is occupied by a loose network of phenotypically astral cells that extend long dendritic processes around the sinusoids. These are the hepatic stellate cells (HSC), normally involved in lipid and Vitamin A storage. Under inflammatory conditions HSC go from a quiescent state to adopt a fibrinogenic phenotype, and are the major contributors towards fibrosis in chronically inflamed livers (Weiskirchen and Tacke, 2014).

Also present in the sinusoids are liver-resident immune cells, including macrophages, termed Kupffer cells (KC), dendritic cells and lymphocytes. Recent studies have suggested that KC may develop from liver-based haematopoitic cells, rather than from

monocytes derived from bone marrow stem cells (Perdiguero *et al*., 2015). While their ontogeny remains unclear, KC have been demonstrated to adhere to LSEC and as such represent a unique population of macrophages that remain static, rather than crawling to search for pathogen (Jenne and Kubes, 2013). Indeed, KC are the only subset of macrophages yet known that are capable of capturing bacteria under flow conditions, rather than static, using a unique combination of shear-stress activated receptors for the complement protein C3b (Gorgani *et al*., 2008). Loss of KC has been demonstrated to contribute to bacteremia and host death in *Listeria monocytogenes* infection, highlighting their critical role in immune protection (Ebe *et al*., 1999). KC also function as important APCs in the liver, as will be discussed later.

Dendritic cells are present in the liver, clustering around the portal tract and central vein, and have been demonstrated to mature as they progress via the sinusoids from one to the other (Sato *et al*., 1998). Activated DC can translocate across the LSEC membrane, enter the Space of Dissé and thereby drain via the lymphatic system to lymph nodes to orchestrate an immune response. Lymphocytes, including natural killer cells, NKT, $CD8^+$ T cells and γδ T cells, are found in the portal tracts and dotted throughout the liver parenchyma. Relative numbers of all of these cell types are increased over those found in the periphery, with the liver exhibiting the highest density of NK and NKT cells anywhere in the body. The role of these cells will be examined in the following section.

1.3.2 Liver immunology

Blood from the gut typically bypasses the usual lymphatic circulation, particularly if the gut epithelium is damaged or dysfunctional, avoiding contact with tissues normally responsible for immune surveillance – lymph nodes and the spleen. Accordingly, the liver

likely represents the first line of defense against blood-borne pathogens, regardless of whether these enter via the gut or elsewhere. Depletion of liver-resident immune cells leads to increased pathogen burden and animal death, whereas in contrast, removal of the spleen does not, indicating the crucial role this organ has in immunosurveillance. How the liver performs this function has been extensively studied, but there are many questions remaining.

1.3.2.1 The innate immune response in the liver

Three immune cells subtypes that play key roles in the innate immune response are present in high densities in the liver; KC, NK and NKT. KC can directly phagocytose invading pathogen that has been targeted by complement or antibody, and express PRRs such as mannose receptors and TLRs which enable these cells to identify exogenous and endogenous antigen and instigate cell activation and phagocytosis (Bilzer *et al*., 2006). Upon activation, KC secrete CXCL3, IL-12 and IL-18, inducing activation and expansion of nearby NK and NKT cells, which in turn can produce high levels of the anti-viral IFNγ. Also, CXCL2, TNF-α, IL-6 and IL-1β secreted by KC have been demonstrated to recruit and activate neutrophils to the liver sinusoids, where they secrete pro-inflammatory cytokines inducing influx and activation of T cells, as well as directly phagocytose KC-bound bacteria (Gregory *et al*., 1996).

NK cells compose around one third of all the intra-hepatic lymphocytes, more than three times the ratio found in blood, likely reflecting the importance of an efficient innate response in the liver. As well as the normal NK functions described earlier, liver NK cells can modulate MHC expression by hepatocytes and HSC, thereby forming an additional layer of tuning to the immune response (Doherty and O'Farrelly, 2000). IFNγ secreted by

activated NK cells causes hepatocytes and LSEC to produce CXCL9, recruiting T cells to the site of inflammation. The importance of the liver derived NK population was highlighted in a study that demonstrated that resolution of acute HCV infection is mediated at least in part by particular KIR haplotypes (Khakoo *et al*, 2004). In addition, recent work with mouse models and human tissue has determined there to be a liver-resident memory NK population, although the ontogeny and mechanism of this memory phenotype remains to be fully elucidated (Melsen *et al*., 2016).

CD1d is expressed by KC, hepatocytes and DC in the liver, and accordingly CD1d-restricted NKT cells have an important role in mediating the innate response to non-peptidic antigen in the liver (Yanagisawa *et al*., 2013). As well as having cytotoxic function via perforin and granzyme and being key modulators of the immune response via fast release of either Th1 or Th2 cytokines, NKT cells are the only liver resident immune cell that has been demonstrated as actively crawling to find pathogen, independent of the direction of blood flow in the sinusoids (Geissmann *et al*., 2005).

Together, the actions of these cells result in a typically fast response to the presence of sinusoidal pathogen, resulting in rapid elimination of the pathogen.

1.3.2.2 Antigen presentation and the induction of immune tolerance in the liver

Induction of an effective adaptive immune response requires activation of primed T cells via binding of their TCR to cognate MHC-bound antigen, as well as the presence of certain pro-inflammatory soluble factors in the immune microenvironment. T cells are usually primed by interacting with dendritic cells loaded with antigenic peptide that have drained to the lymph node, where they interact with naïve T cells. However, as well as DC, the

liver contains a number of additional cell subsets that express all the surface molecules required to present antigen to naive T cells and instigate an adaptive immune response, including MHC Class I and II, as well as costimulatory molecules CD80 and CD86, without the initial priming in the lymph node (Jenne and Kubes, 2013).

LSEC express a wide variety of PRR, including TLRs and mannose receptors, which enable them to endocytose not only pathogenically-derived antigen but also cellular debris containing intracellular antigen released by a dying cell. They can then process and present these antigens on their MHC Class I and, unusually, Class II molecules in a process called cross-presentation. LSEC are particularly effective cross-presenting cells, and have been demonstrated to directly instigate T cell responses (Limmer *et al*., 2000). However, as part of the MHC:TCR interaction, the costimulatory molecule PD-L1 is upregulated in the LSEC, which induces the expansion of non-responsive T cells following TCR engagement via interaction with the PD-L1 receptor, PD-1 (Carambia *et al*., 2013). This results in a large population of antigen-nonresponsive T cells and contributes toward immune tolerance in the liver.

KC also express antigen presentation molecules but in normal resting state have poor APC function. Continual exposure to low levels of exogenous antigen such as LPS reduces the ability of KC to stimulate a T cell response, as also occurs in LSEC; an important mechanism in preventing continuous damaging inflammation in response to commonly encountered gut derived antigen (Knolle *et al*., 1999). Both KC and LSEC produce anti-inflammatory IL-10 and TGFβ in these circumstances, which further dampens any T cell mediated response through loss of effector functions following priming with IL-10 and change of chemokine receptor expression in DC that reduces their migration to lymph

nodes (Knolle *et al*., 1995). In pro-inflammatory conditions however, KC have been demonstrated to act as strong APC and trigger normal T cell activation and maturation.

Hepatocytes express MHC Class I and limited Class II, as well as CD80 and CD86, and therefore although they cannot cross-present they may be able to induce direct T cell activation. They have been demonstrated to express PRR such as TLRs, and therefore may be capable of taking up pathogenic antigen from their surroundings (Chen *et al*., 2005). Similarly, HSC also express the cellular machinery required to activate T cells, although no mechanism for antigen uptake has been described in HSC, suggesting their role as APC in the liver may be limited (Winau *et al*., 2007).

Therefore, despite the abundance of potential APC in the liver, it seems likely that antigen presentation in these cells has evolved in such a way as to in fact induce tolerance towards regularly encountered antigen that may otherwise cause a damaging inflammatory response, particularly under normal basal conditions. However, robust adaptive immune responses can and do occur in the liver; they simply require the correct inflammatory signals.

1.3.3 Immune mediated liver pathology

Chronic liver inflammation, resulting in fibrosis and potentially leading to cirrhosis and hepatocellular carcinoma, occurs in a number of clinically relevant situations. Some hepatotrophic pathogens, primarily the hepatitis B and C viruses, have evolved mechanisms that prevent their rapid elimination by the liver immune system and instead perpetuate in the hepatocytes, inviting a low level continuous immune response that can lead to fibrosis and ensuing pathogenesis (Horner and Gale, 2013). Damage to

hepatocytes caused by long term exposure to certain toxins, primarily alcohol, can induce a similar prolonged immune response, again leading to fibrosis, as can metabolic disorders such those attributed to non-alcoholic fatty liver disease (Wang *et al*., 2012). Finally, several auto-immune disorders in liver tissues have been described, and although each has a different aetiology, the outcome, chronic liver inflammation, fibrosis and liver dysfunction, is always associated with an unchecked or unwarranted immune response.

1.3.3.1 The immunology of liver fibrosis

Induction of type-I collagen-derived fibrosis is part of the normal wound repair response to tissue damage in the liver and contributes to the protection of hepatocytes from toxins. However, excessive fibrosis and the resulting scar tissue caused by prolonged tissue injury leads to liver dysfunction, portal hypertension and ultimately liver failure (Parsons *et al*., 2007).

While there are several known causes of fibrosis, including tumours and foreign objects in tissue, it is important to note that all of them are associated with the instigation of an immune response. Without this immune response, fibrosis does not occur. In the context of the liver, the two main causative factors are tissue damage through exposure to toxins and pathogenically/ autoimmune mediated inflammation.

As part of the normal immune response to hepatocyte injury, whether it be toxin-induced, metabolically induced or pathogenically induced, a number of pro-inflammatory cytokines and growth factors are secreted by both the damaged cells and cells of the immune system that are recruited to the site of injury. These include TGFβ, platelet derived growth factor (PDGF), IL-13 and connective tissue growth factor (CTGF), and are

thought to contribute towards the differentiation of liver mesenchymal cells, namely HSC and portal fibroblasts, into myofibroblasts (Li *et al*., 2008). TGFβ induces the upregulation of type-1 collagen and α-smooth muscle actin (α-SMA) in these cells, while PDGF induces their expansion (Xu *et al*., 2016). These activated cells then secrete the extra-cellular matrix (ECM) proteins that form the basis of the scar tissue and also pro-inflammatory cytokines that further promote HSC differentiation in an autocrine feedback loop and chemokines that recruit immune cells to maintain HSC differentiation (Marra and Tacke, 2014).

Macrophages are key mediators of fibrosis. Following typical acute tissue injury, macrophages will break down ECM deposited by activated myofibroblasts, once the source of the injury has been removed. They do this through the action of a variety of matrix metalloproteinases (MMPs) (Duarte *et al*., 2015), which are inhibited by myofibroblast-derived tissue inhibitors of metalloproteinases (TIMPs) (Iredale *et al*., 1992). However, during inflammation macrophages have been observed to be pro-fibrotic, secreting TGFβ and PDGF to maintain the myofibroblast population. Additionally, recent studies have suggested that these pro-fibrotic macrophages are likely circulating monocyte-derived rather than KC, and that KC numbers actually decline during induction of fibrosis (Liaskou *et al*., 2013).

Other immune cells have also been demonstrated to have both pro- and anti-fibrotic activity. Th1 cells have exhibited anti-fibrotic activity, likely through the action of IFNγ, which modulates the balance between MMP and TIMP enzymes. Th2 and Th17 have been described as having pro-fibrotic properties. NK cells and γδ T cells have been shown to have potential anti-fibrotic effects via the induction of apoptosis in myofibroblasts

(Hammerich *et al*., 2013, Radaeva *et al*., 2006). Despite an increasing body of work in the field, in remains unclear precisely what role these subsets are having in the fibrosis scenario, and it is likely that the response will vary depending on disease aetiology and perhaps even on a case by case basis.

Fibrosis is generally a reversible process, with breakdown of excessive ECM carried out by macrophages and other cells expressing MMPs (Pellicoro *et al*., 2014). However, during chronic inflammation, the scar tissue often undergoes pathological changes that render it less susceptible to breakdown. Extensively cross-linked mature scar tissue is more resistant to protease action, and large deposits are inaccessible to MMPs and the macrophages that produce them.

As well as induction of ECM deposition by activated HSC, liver damage caused by chronic inflammation also causes hepatocytes to undergo proliferation in an attempt to regenerate lost tissue. In severely damaged livers, stem-like liver progenitor cells, located in the biliary tree, proliferate, generating the hepatic nodules indicative of liver cirrhosis (Shang *et al*., 2016). Although the exact molecular mechanisms remain to be elucidated, it is apparent that the rapid proliferation of these cells against a background of high inflammation would potentially generate the DNA damage and ensuing genetic mutations that could lead to the development of neoplastic cells and the onset of HCC (Affo *et al*., 2017).

1.3.3.2 The immunology of hepatitis viruses

Hepatitis B, a hepadnavirus, and Hepatitis C, a flavivirus, are hepatotrophic, non-cytopathic blood-borne viruses with multiple genotypes that lead to acute and chronic

infections. While hepatitis B virus (HBV) is a self-limiting infection that resolves in 90% of cases, the downstream effects of chronic hepatitis B infection, namely liver cirrhosis and HCC, still account for one million deaths per year, with over 350 million people infected with the virus (Nannini and Sokal, 2017). Hepatitis C virus (HCV) chronically infects around 200 million worldwide and acute infection leads to chronic infection in up to 90% of cases, and the same outcomes as HBV are likely for those untreated (Ahmed *et al*., 2017). Although a vaccine and a non-curative therapy are available for HBV, and curative therapy is now available for HCV, the costs and logistics involved with these mean many millions of people will remain infected with these viruses for decades to come.

Both HBV and HCV infect hepatocytes, and the immune system has been implicated both in the clearance of virus in acute infections and disease progression in chronic infection. Viral clearance in acute infections is associated with a strong CD4 and CD8 T cell response, and neutralising antibodies are an important part of HBV immunity. However, if the CD4/ CD8 anti-viral response is not strong or widespread enough to control the infection, the natural induction of tolerance to prolonged antigen observed in the liver occurs, and virus-specific T cells become phenotypically and functionally exhausted and are then eliminated (Rosen, 2013). Mutation of the viral epitopes recognised by these T cells is the final stage in immune escape, so that in chronic HBV and HCV infection, virus-specific T cells play little to no role in either controlling the infection or development of fibrosis. So, rather than antigen-specific T cells playing a role in disease progression, it is likely that non-specific immune cells, including T cells, NK cells and macrophages, which are recruited to the site of infection by pro-inflammatory signals, mediate the onset of fibrosis (Golden-Mason and Rosen, 2013). On the other hand, cytolytically active but non

anti-viral NK cells have also been attributed with the regulation of fibrosis via cytolysis of activated HSC (Radaeva *et al*., 2006).

1.3.3.3 Autoimmune liver diseases

There are three common liver diseases that have a basis in autoimmune disorders, each potentially inducing fibrosis, cirrhosis and cancer. Primary sclerosing cholangitis (PSC) is a disease of unknown aetiology affecting over 1 in 100,000 people in northern Europe and currently with no known cure, other than liver transplant, which is not always effective and often not possible since late stage PSC often develops into tumourigenesis. It is mediated by gut-derived lymphocytes erroneously targeting cells of the hepatobiliary tree, specifically cholangiocytes, epithelial cells lining the bile ducts. Chronic inflammation, bile duct destruction leading to cholestasis and fibrosis of the portal regions lead to cirrhosis (Karlsen *et al*., 2017).

60-80% of patients with PSC also present with inflammatory bowel diseases (IBD), usually a form of ulcerative colitis, an immunological disorder that has genetic underpinnings and involves targeting of the commensal gut microbiota by the host immune system. The exact mechanism of the link between IBD and PSC is not fully understood, although there are genetic factors common to both (Eksteen, 2016). Theories include the translocation of gut microbiota across an inflamed gut epithelium and subsequent activation of an immune response in the liver. In addition, inflammation in the liver has been demonstrated to increase expression of usually gut-specific adhesion molecules such as mucosal addressin cellular adhesion molecule 1 (MAdCAM1) and vascular adhesion protein 1 (VAP-1), resulting in the recruitment of gut-primed T cells that contribute to pathogenesis in the liver (Grant *et al*., 2001, Trivedi *et al*., 2017). Once inflammation of

the bile duct area has begun, destruction of the bile resistant epithelia may lead to further damage to hepatocytes by toxic bile, generating further inflammation.

Autoimmune hepatitis (AIH) affects up to 3 in 100,000 people and usually presents in young people, particularly women. It is associated with the production of liver autoantibodies, specifically anti-nuclear antibodies and anti-α-SMA antibodies, which defines Type I AIH, and anti-liver kidney microsomal type 1 antibody, which defines Type II AIH (Liberal *et al*., 2016). Like PSC, AIH has an unknown aetiology, but is also linked with genetic factors, with a high frequency of cases associated with possession of certain alleles of the HLA genes, which encode the human MHC molecules and are therefore involved with TCR recognition. A number of postulated triggers exist, including infection with hepatitis C, which has regions that share a high amino acid homology with the target of the auto-antibodies associated with AIH (Himoto and Masaki, 2012). Generation of antibodies to such an infection may then generate an antibody response to self-antigens, in a case of molecular mimicry.

There is also a possible role for impaired Treg function in AIH, as well as impaired self-regulation by autoreactive T cells through the loss of expression of usual inhibitory co-receptors such as PD-L1 and CTLA-4 (Herkel, 2015). The mechanisms involved in the development of these pathways and their contribution to AIH pathogenesis remain unclear.

The third auto-immunity linked liver disorder is primary biliary cholangitis (PBC), which is classically linked with patient development of autoantibodies against mitochondrial enzymes, particularly the E2 domain of the pyruvate dehydrogenase complex (PDC-E2) (Gershwin *et al*., 2000). Bile duct epithelia exhibit intact PDC-E2, and mouse models have

demonstrated a loss of tolerance to this autoantigen in the development of PBC. Autoreactive $CD4^+$ and particularly $CD8^+$ T cells then mediate destruction of the small bile ducts and on occasion instigate portal fibrosis and chronic liver damage (Liaskou *et al*., 2014). The vast majority of PBC cases are female, and up to 40 people per 100,000 are affected depending on geographical location. A reduction in the frequency of circulating Tregs has been observed in PBC patients (Lan *et al*., 2006).

1.3.3.4 Fatty liver diseases

There are two forms of fatty liver disease, alcoholic liver disease (ALD) and non-alcoholic fatty liver disease (NAFLD) which can develop into the more severe non-alcoholic steatohepatitis (NASH). The pathogenesis of both diseases can involve the immune system, and both can lead to liver cirrhosis and HCC.

ALD is one of the leading causes of morbidity and mortality worldwide, and stems from excessive consumption of alcohol. Alcohol is directly toxic to hepatocytes, and also potentiates other liver diseases such as NAFLD and chronic HCV infection. Steatosis, that is, abnormal retention of fat within hepatocytes, occurs in the liver of 90% of heavy drinkers, and although reversible through abstinence, this leads to fibrosis in 20 – 40% of patients that continue to drink, with ensuing cirrhosis and risk of HCC development. As well as being a direct toxin to hepatocytes, and inducing a large pro-inflammatory neutrophilic infiltration in response to injured and dying cells, alcohol and its derivatives activate HSC to produce collagen, inhibits anti-fibrotic NK function and increases gut permeability to exogenous toxins such as LPS, thereby inducing release of pro-

inflammatory cytokines and the development of chronic steatohepatitis (Wang *et al*., 2012).

NAFLD affects around one third of the Western world, making it the most common liver disease in the world. The more severe NASH, associated with chronic inflammation, affects 10 – 20% of patients with NAFLD. NAFLD is associated with obesity, which can lead to disruption of normal lipid metabolism and insulin resistance, increased free fatty acids and gut permeability, both of which trigger inflammation via production of various PAMPs and DAMPs (Benedict and Zhang, 2017).

1.4 Gamma delta T cells in the liver

1.4.1 Recruitment of γδ T cells to the liver

An important question in γδ T cell biology is how these cells are recruited to specific parts of the body, particularly in tissues where the TCR repertoire is altered from that of the circulating blood, such as in skin, gut and liver. Other than preferential survival or proliferation, it is only through recruitment or retention via chemokine and integrin axes that these altered repertoires can be established. Data on γδ T cell recruitment to the liver is very limited, but several studies have been conducted focussing on other tissues and in pathological scenarios such as autoimmunity and cancer, which may help build a foundation for further research in the context of the liver.

CCR9, CCL25 and α4β7 are gut-tropic molecules and recruit murine γδ T cells to the gut. These cells leave the gut but rapidly recirculate, creating a stable yet dynamic population (Guy-Grand *et al*., 2013). This supports the suggestion that the intra-hepatic lymphocyte

population is shaped by the dynamics of the entry and exit processes, rather than proliferation *in situ*, as proposed by Klugewitz (Klugewitz *et al*., 2004). In human IBD patients, including UC and Crohn's disease, circulating γδ T cells expressed higher levels of gut-homing CCR9 than healthy controls (Mann, McCarthy *et al*. 2012). In a murine model of allergic reaction, CCL25 induced specific migration of IL-17$^+$ γδ T cells to the site of inflammation, mediated by α4β7 integrin and the CCR6 chemokine receptor. In mice, these are expressed by IL-17$^+$ as opposed to IFNγ producing cells (Costa *et al*., 2012).

In a mouse melanoma model, CCR2/ CCL2 mediated accumulation of γδ T cells at the site of the tumour. These cells also were mainly Vδ1$^+$, which in humans express CCR2 (Lanca *et al*., 2013). CCL2 expression is dysregulated in many human tumours, including HCC. In addition, Vδ1$^+$ cells have been shown to accumulate in squamous cell carcinoma in vitro and oesophageal tumour tissue *ex vivo* based on expression of CD11a, CD49d and other integrins (Thomas *et al*., 2001).

Th17 CD4$^+$ T cells are recruited to the liver via CXCR3 and CCR6 (Oo *et al*., 2010), suggesting that expression of these molecules may be important in recruitment of lymphocytes to the liver. In an acute liver injury mouse model, γδ T cells accumulated in the liver via CXCR3/ CXCL9 axis and initiated acute liver toxicity via CD8 T cell recruitment and activation, perhaps by APC function (Ajuebor *et al*., 2008). In a mouse model of chronic liver injury, CCL20 recruited IL-17- and IL-22-producing CCR6$^+$ γδ T cells, which induced apoptosis of HSC independently of the action of IL-17, suggesting a possible protective role for γδ T cells against fibrosis (Hammerich *et al*., 2013). In the same study, sections of human chronic liver disease patients were analysed by immunohistochemistry and displayed CCL20 and CCR6 expression. In humans, the CXCR6/ CXCL16 axis is

responsible for recruiting NKT to the livers of chronic liver disease patients, leading to enhanced fibrosis and liver injury (Wehr *et al*., 2013). Whether this has a role in γδ T cell recruitment is not known.

In mice, evidence suggests that γδ T cells receive functional and locational instruction in the thymus, depending of the degree of engagement of the TCR received there, and potentially the ligand they are exposed to (Haas *et al*., 2012). Accordingly, γδ T cell subsets will be recruited to different locations in the murine body based on a chemokine receptor repertoire that is linked to function and possibly TCR specificity.

While data are limited, humans do not seem to share an equivalent method of thymic selection and differentiation of γδ T cells (Ribot *et al*., 2014), so data obtained from mouse models, especially when concerning chemokine receptor expression and postcoding to specific tissues, has to be treated with care when being applied to humans. This is also relevant for functional differentiation, discussed in the next section.

1.4.2 The function of γδ T cells in the liver

In chronic HCV patients, increased γδ T cell infiltration was observed in infected livers compared with blood (Nuti *et al*., 1998). $V\delta1^+$ γδ T cells increased in the liver of HCV patients compared with blood, up to 8.7% of the $CD3^+$ lymphocyte population (Agrati *et al*., 2001). Mitogenic stimulation of these cells *ex vivo* induced a Th1 cytokine expression profile. Care must be taken when interpreting the results of such studies however, since normal healthy liver is not easily accessible as a control, and very few studies have examined the γδ T cell burden in a truly healthy liver. In tissue taken from healthy donor

livers, 15% (6.8 – 34%) of liver-infiltrating $CD3^+$ lymphocytes express the γδ TCR, compared with 0.9 – 2.7% in PBMCs (Norris *et al*., 1998).

The ratio of γδ T cells to $CD3^+$ lymphocytes may not be the best marker of γδ T cell burden in the liver, since many chronic liver diseases are associated with a large lymphocytic infiltration to the portal areas, and unless γδ T cells are recruited at the same frequency or greater than αβ T cells, it is likely that the proportion of γδ T cells: $CD3^+$ lymphocytes will drop during chronic inflammation, even if the absolute number of infiltrating cells increases. In an IHC-based study, Kasper *et al* observed that the number of infiltrating γδ T cells in patients with HCV infection of varying aetiologies did not change, and was led to conclude that it was increasing numbers of αβ T cells that were responsible for increased inflammation (Kasper *et al*., 2009). There is no doubt however, that liver does contain a greater proportion of γδ T cells than the periphery, in both healthy and diseased livers, and even if they are not directly involved with necro-inflammatory processes in chronic disease, they may have a supporting or perhaps even anti-inflammatory role.

A growing body of evidence suggests that γδ T cells are likely to contribute to disease progression in acute liver injury, although this work is mainly restricted to mouse models where Th17-like γδ T cells are a more clearly identified subset than in humans. A Poly I:C RNA virus mimetic induced IL-17 production by hepatic γδ T cells in a mouse model of acute liver injury, and in combination with macrophage IL-23 production this led to increased liver damage (He *et al*., 2013). In an adenovirus-mediated acute liver injury model, γδ T cell-derived IL-17 production increased liver injury and recruitment of $CD8^+$ Th1 cells (Hou *et al*., 2013). As well as IL-17 as a γδ T cell derived mediator of liver

damage, Lu noted an increase in the number of γδ T cells and subsequent TNF-α production led to hepatocyte destruction in hepatitis virus strain 3-induced hepatitis in mice (Lu *et al*., 2012).

In a study by Ren's group, γδ T cell frequencies in peripheral blood were lower in patients with chronic HBV infection, although these cells exhibited a high cytotoxicity and TNF-α and IL-17 production. This was mainly attributed to the acute-on-chronic HBV patients, and suggests there may be a role for γδ T cells with a pro-inflammatory phenotype in acute liver disease (Chen *et al*., 2012). The same group had previously noted a decrease in the proportion of Vδ2 γδ T cells in the blood of chronic HBV patients, and reduced cytotoxicity and IFNγ production by these cells (Chen *et al*., 2008).

In chronic HCV infection, peripheral Vδ9Vδ2 cells decrease in frequency compared with the blood of healthy donors (Par *et al*., 2002), and also appear to lose their cytotoxic responsivity to phosphoantigen stimulation, although it is rescued by Type 1 interferon treatment (Cimini *et al*., 2012). γδ T cells expanded from HCV- and HBV-infected liver biopsies had high cytotoxicity and IFNγ production but failed to recognise any HCV antigen (Tseng *et al*., 2001). However, Vδ9Vδ2^{+} T cells can inhibit subgenomic HCV replication *in vitro*, via IFNγ production (Agrati *et al*., 2006). Expression of NK activating receptors, including CD226, enables Vδ9Vδ2^{+} cells to kill HCC cell lines *in vitro* (Toutirais *et al*., 2009). The potential protective role of the Vδ2 subset in the liver was explored by Wu *et al*, who found that Vδ2 T cell frequencies in both peripheral blood and liver tissue decreased in immune-activated HBV-infected patients. The authors suggest that these cells regulated Th17 CD4^{+} cells, through cell: cell contact and that with fewer Vδ2^{+} cells liver damage was increased (Wu *et al*., 2013).

Gamma delta T cells are enriched in the normal liver compared with matched blood from the same donors (6.6% of total $CD3^+$ compared with 2%) and these cells can be induced to kill tumour cell lines and release IFNγ. Of these cells, 21.2% were found to contain the Vδ3 chain (Kenna *et al*., 2004). In HCC, γδ T cells lose their anti-tumour effect in the immunosuppressive microenvironment of the tumour itself. They exhibit decreased infiltration of the tumour compared with the peri-tumoural tissue, with decreased cytotoxicity and IFNγ production. Tumour-infiltrating Tregs secreting TGFβ and IL-10 were attributed to this downregulation of effector function of γδ T cells (Yi *et al*., 2013). However, this process is likely reversible, since in a study by Mao *et al*, γδ T cells isolated from the peripheral blood of gastric cancer patients that were then cultured in vitro with syngeneic tumour cells were capable of killing tumour cell lines in vitro, inducing a $CD4^+$/$CD8^+$ T cell expansion, perhaps via APC function, and abrogating Treg-mediated immunosuppression (Mao *et al*., 2014). Additionally, γδ T cells with the Vδ1 chain exhibited anti-metastatic properties in a mouse xenograft model of colon carcinoma (Devaud *et al*., 2013). A recent study by Huang's group has observed that IL-17 producing γδ T cells contribute to myeloid-derived suppressor cell accumulation in human colorectal cancer tissue samples, leading to immunosuppression and aiding tumour progression (Wu *et al*., 2014).

Gamma delta T cells have been implicated in macrophage regulation. Murine $V\delta1^+$ γδ T cells kill macrophages as part of the resolution of immune response to various pathogens (Egan *et al*., 2005). In an *in vitro* study of γδ T cells interaction with liver-tropic *L. monocytogenes*-activated macrophages, $V\delta2^+$ and $V\delta4^+$ γδ T cells increased cytokine production by these macrophages and were in turn induced to express IL-10 by the

activated macrophages, thereby controlling the infection and the immune response to it and preventing liver damage (Tramonti *et al*., 2006). In mice, IL-17A production by γδ T cells plays a role in the innate immune response against *L. monocytogenes* in the liver (Hamada *et al*., 2008).

Regulation of γδ T cells in a liver-specific context has also been linked to Vα14 invariant NKT cells, which were activated by TLR-3 ligand expression in the livers of mice injected with the hepatotropic poly I:C virus. Suppression of γδ T cell accumulation and activation was mediated by induction of apoptosis in the γδ T cells by the iNKT cells (Gardner *et al*., 2009).

Although only one murine study to date has directly linked γδ T cells and liver fibrosis (Hammerich *et al*., 2013), where they appear to be protective, γδ T cells also appear to have a protective role in a murine model of lung fibrosis, via the Th17 cytokine IL-22, although the mechanism remains unclear (Simonian *et al*., 2010). In a second, bleomycin instigated model of pulmonary fibrosis, γδ T cells exhibited an anti-fibrotic effect via CXCL10 production (Pociask *et al*., 2011). The potential for an anti-fibrotic effect of human intrahepatic γδ T cells is clearly worth investigating for a potential therapeutic benefit.

1.4.3 The potential role of the γδ TCR and antigen specificity in the liver

Although the existing evidence suggests liver-derived γδ T cells are likely to have a predominantly innate-like phenotype and function, the potential role of the γδ TCR in liver homeostasis and pathology should not be discounted. As described in section 1.3.2, there are few known ligands for the γδ TCR. In the liver, where an elevated ratio of $V\delta2^-$

γδ TCRs is typically found, it may be possible to draw comparisons with findings from the gut. The MHC-like CD1 lipid-presentation family of molecules has been associated with recognition by γδ T cells, including the Group 1 CD1c (Spada *et al*., 2000) and the normally NKT associated CD1d. Although CD1d is only expressed at low levels in healthy human liver (Canchis *et al*., 1993), studies have demonstrated an increased expression of CD1d in chronic HCV infection and PBC (Durante-Mangoni *et al*., 2004). Gamma delta T cells are able to bind CD1d loaded with endogenous lipids such as cardiolipin (Dieude *et al*., 2011) and sulfatide (Luoma *et al*., 2013) in both mice and humans, in particular those possessing the Vδ1 and Vδ3 (Mangan *et al*., 2013) chains, which are the dominant subsets in liver tissue. This occurs via the TCR, demonstrating an MHC-like restriction, antigen specific binding by γδ TCRs (Bai *et al*., 2012). The crystal structure of a Vδ1 TCR in complex with CD1d has recently been published, verifying previous functional data (Uldrich *et al*., 2013). Since these studies have been performed on expanded populations of gamma delta T cells, it is unclear whether these interactions are physiologically relevant, however HCV has been demonstrated to induce an expansion of CD1d reactive NKT cells, perhaps as part of the innate defense against acute infection in both mice (Liu and Huber, 2011) and humans (Yanagisawa *et al*., 2013). In addition, HBV produces modified self-lipids that are presented on CD1d molecules and activate NKT cells (Zeissig *et al*., 2012). It is possible that the liver may use endogenous or exogenous lipids as an indicator of cellular stress, particularly since the liver is the major site of lipid processing and metabolism in the body, and that gamma delta T cells may be involved in recognition of this. If this is the case, determining the relevance of gamma delta T cell mediated recognition of CD1d lipid presentation when compared with NKT cells will be important. It is possible that the two cell types may have overlapping functions, with NKT cells

primarily associated with innate immune response, or it may be that a γδ T cell mediated interaction has additional properties, perhaps associated with immune regulation and tissue homeostasis. In a study conducted on tissue biopsied from gut epithelium, isolated CD1d reactive gamma delta T cell clones expressed both Th1 and immunoregulatory TGFβ and IL-10, when compared with αβ T cells isolated from the same tissue (Russano *et al*., 2007). The possible identity of liver-specific and even disease-γδspecific lipid antigens for gamma delta T cells would also be worth investigating in any attempt to utilise this potential pathway for immunotherapy.

Other known γδ TCR ligands that may have a role in the liver include phosphoantigens presented by butyrophilin, a molecule upregulated in HCC (Matos *et al*., 2009), and which may have a role in other forms of liver disease as a marker of cell stress or infection. Also, EPCR has been demonstrated to be expressed by HSC when activated to become myofibroblasts (Gillibert-Duplantier *et al*., 2010), suggesting a possible anti-fibrotic role for gamma delta T cells capable of recognising EPCR (Willcox *et al*., 2012).

1.5 Thesis aims

The liver is a key immunological organ that plays a vital role in tolerisation of the immune response toward gut derived non-harmful antigen whilst simultaneously acting as a firewall against pathogen-associated antigen. Dysregulation of the immune homeostasis via potentially numerous chronic insults can result in chronic inflammation, fibrosis and ultimately cirrhosis and development of cancer.

Gamma delta T cells are important effector cells capable of recognition and elimination of typically dysregulated-self targets, thereby playing a significant role in lymphoid stress

surveillance. While our knowledge of the phosphoantigen-reactive Vδ2^{+} subset is reasonably well developed, Vδ2^{neg} gamma delta T cells are less well studied. Despite previous studies highlighting a tissue tropism for Vδ2^{neg} gamma delta T cells, the nature of these cells and their role in immunosurveillance in human tissues is relatively poorly understood.

In this study, the primary aim was to characterise the human gamma delta T cell population in human liver, through localisation, immuno-phenotyping and TCR sequencing studies. Particular emphasis would be placed on comparing healthy liver with diseased tissue. Additionally, this study afforded the opportunity to address fundamental questions regarding gamma delta T cell biology, such as their role in adaptive or innate-like processes, and the role of the TCR in their function.

2

Materials and Methods

2.1 Tissue handling and cell isolation

2.1.1 Lymphocyte isolation from blood

Peripheral blood was collected in EDTA with informed consent from otherwise healthy haemochromatosis patients (ethical approval: Use of venesected blood from patients with haemochromatosis to isolate and culture immune cells, REC reference 04/Q2708/41) as well as patients with autoimmune hepatitis and alcoholic liver disease (ethical approval via the University of Birmingham Human Biomaterials Resource Centre (NRES Committee North West – Haydock; Ref 15/NW/0079)). In the case of matched blood and liver samples, venous blood was obtained from patients undergoing liver transplantation before the induction of anaesthesia. Subsequently explanted diseased liver was obtained from the same patients to allow the isolation of matched blood and liver-derived cells (ethical approval: Cellular trafficking and immune response in the human liver, REC reference 06/Q2708/11). Venous blood was also obtained from consenting healthy donors (protocol approved by the NRES Committee West Midlands ethical board; REC reference 14/WM/1254) in heparin. Umbilical cord blood units were obtained from the Anthony Nolan Cell Therapy Centre Nottingham (ANCTC) under generic tissue bank ethics held by ANCTC and extended to the researchers under a material transfer agreement (MTA).

Peripheral blood mononuclear cells were then isolated from whole blood by layering on top of Lympholyte-H Cell Separation Media (Cedarlane, Burlington, Canada) before centrifugation at 800g for 25 minutes at room temperature allowing separation based on gradient density. PBMCs were aspirated from the cloudy partition layer and washed twice with sterile phosphate buffered saline (PBS) before counting using an improved

Neubauer haemocytometer with dead cells excluded using Trypan-blue (Sigma-Aldrich, Gillingham , UK) and further experimental procedure.

2.1.2 Lymphocyte isolation from human liver

Diseased liver tissue was taken with informed consent from patients undergoing liver transplant at Queen Elizabeth Hospital, Birmingham UK. Chronically inflamed livers from the following patient groups were studied: alcoholic liver cirrhosis (ALD), non-alcoholic steatohepatitis (NASH), primary sclerosing cholangitis (PSC), primary biliary cholangitis (PBC), auto-immune hepatitis (AIH), chronic hepatitis C virus infection (HCV) and chronic hepatitis B virus infection (HBV). Additionally, livers explanted for non-inflammatory chronic conditions including polycystic liver disease and α-1 antitrypsin deficiency were also studied in some cases, where a comparison between inflamed and non-inflamed liver tissue was required. Non-diseased liver tissue was obtained from surplus tissue from cadaveric registered organ donors or from uninvolved liver tissue removed at the time of resection for colorectal hepatic metastases. All samples were collected with informed patient consent and local research ethics committee approval (local research ethics committee approval 04/Q2708/41 and REC 2003/242).

Explanted livers were cut into slices by a qualified pathologist at Queen Elizabeth Hospital and then transported to the Centre for Liver Research for further processing. Under sterile conditions, liver slices weighing approximately 50 – 150 g were diced into 3 - 5 mm cubes using scalpels and then washed at least 5 times in PBS to remove any blood associated lymphocytes and erythrocytes. Once washed, tissue was then transferred to Stomacher 400 Circulator bags (Seward, Worthing, UK) in approximately 150 ml chilled RPMI-1640 lymphocyte medium (Sigma-Aldrich) and then stomached for 5 – 7 minutes,

depending on severity of fibrosis, at 230 rpm in a Stomacher 400 machine (Seward, Worthing). Mechanical homogenisation in this manner prevented loss of surface markers by enzymatic cleavage as well as being quicker and cheaper than enzymatic digestion. In cases where very small amounts of tissue were obtained (typically less than 20 g), mechanical digestion was performed using GentleMACS dissociation C tubes (Miltenyi Biotech, Bergisch Gladbach, Germany) in a GentleMACS dissociator, running the mouse spleen standard protocol.

Following homogenisation, liver tissue was filtered through a fine (63 micron) nytal mesh (John Stanniar and Co, Manchester, UK) and washed with twice the initial volume of chilled PBS. Large cellular debris was then removed by centrifugation at 55 g for 5 minutes. Supernatants were then re-centrifuged at 2,000 rpm at $4^{O}C$, the supernatant discarded and the cell pellet washed at $4^{O}C$ with PBS a further 3 – 5 times depending on the extent of steatosis present in the liver tissue. Finally, washed cell pellets were re-suspended in PBS, layered on Lympholyte-H cell separation medium and centrifuged at 800 g for 25 minutes at room temperature. Liver derived lymphocytes (LDL) were aspirated from the partition band and washed twice with cold PBS before counting using an improved Neubauer haemocytometer with dead cells excluded using Trypan-blue (Sigma-Aldrich).

2.1.3 HSEC isolation and culture

Primary human hepatic sinusoidal endothelium cells (HSEC) were isolated from explanted liver disease tissue or from normal donor liver surplus to transplant requirements. Slices of liver tissue (20 – 50 g) were diced into 5 mm cubes using scalpels, washed with cold PBS as before and then incubated with collagenase type 1A (Sigma, St. Louis, USA) at $37^{O}C$

for 20 minutes in a shaker incubator. Following digestion the tissue was layered on top of a 33%/ 77% Percoll: 1M NaCl solution gradient and centrifuged at 500 g for 30 minutes. The interface layer was aspirated and cells washed in cold PBS three times before cholangiocytes were labelled using a cholangiocyte specific mAb for HEA125 (Progen, Heidelberg, Germany) at 4^{o}C for 20 minutes. Following incubation, cholangiocytes were removed from the cell suspension by incubation with anti-mouse IgG1-coated Dynabeads (Invitrogen, Carlsbad, USA) and subsequent magnetic separation. 25 µL pre-washed and re-suspended Dynabeads were added to 1 mL of labelled cells in a polypropylene FACS tube and incubated for 20 minutes at 4^{o}C before inserting the tube into a magnet for 2 minutes to allow labelled cells to adhere to the tube walls. With the tube still in the magnet, the supernatant containing non-labelled cells was then removed.

HSEC were then isolated from the resultant cell suspension by labelling using Dynabead-conjugated anti-CD31 antibody (10 µg/mL; Invitrogen) and subsequent magnetic separation. The protocol was identical to that for cholangiocyte removal except after magnetic incubation the supernatant was discarded and the adherent cells washed three times with PBS with an additional incubation in the magnet at each step, discarding non-adherent cells each time to ensure cell purity.

Isolated CD31^{+} HSEC were cultured in complete endothelial media (Gibco, Invitrogen, United Kingdom) supplemented with penicillin, streptomycin (100 µg/ml) and glutamine (2 mM, Gibco, CA, USA), heat-inactivated human AB serum (10% v/v, HD Supplies, Buckingham, UK), hepatocyte growth factor (10 ng/ml Peprotech, Rocky Hill, NJ, USA) and vascular endothelial growth factor (10 ng/ml Peprotech), referred to hereafter as HSEC media. Endothelial cells were grown in 25 cm^{2} tissue culture flasks coated with rat

tail collagen with regular medium exchanges until they became a confluent monolayer, then expanded in 75 cm^2 tissue culture flasks coated with rat tail collagen.

2.2 Cell based assays

2.2.1 Flow cytometry – surface marker staining of blood- and liver-derived T cells

Phenotyping of freshly isolated intrahepatic and peripheral blood derived T cell populations, including but not limited to pan-gamma delta T cells, $V\delta1^+$, $V\delta2^+$ and $CD8^+$ cells was performed using flow cytometry. In all protocols used in this study, dead cells were labelled using e506 viability dye (eBioscience, Hatfield, UK) prior to staining with antibodies. This was performed at a dilution of 1:500 in 2% foetal bovine serum (FBS) (Sigma) diluted in PBS and incubated at 4^oC for 20 minutes before washing twice with cold PBS to remove unbound dye. Using this method, autofluorescent cells could also be excluded from the analysis by gating out all cells positive for e506. For cell surface antigen expression analysis, cells were then incubated for 30 minutes at 4^oC with antibodies against CD3, CD8, pan-γδ TCR, Vδ2 TCR, and depending on the experiment Vδ1 TCR and/ or αβ TCR, as well as the antigen(s) of interest in 2% foetal bovine serum (FBS) diluted in PBS. In some experiments, after washing with 2% FBS, cells were analysed immediately by flow cytometry or else they were fixed for 10 minutes with 3% formaldehyde solution at room temperature (Sigma Aldrich), washed again and analysed later.

The following mouse anti-human antibodies were used for multi-colour flow cytometry: TCR αβ PE (IP26; 1:50), TCR γδ PEcy7 (B1; 1:100), CD3 BV421 (UCHT-1, 1:100), CD8 BV650

(SK1; 1:200), CD69 BV605 (FN50; 1:100), CD25 BV421 (2A3; 1:100), CD27 PE/ Dazzle 594 (M-T271; 1:200), CD45RA PeCy7 (HI100; 1:200), CCR7 (G043H7; 1:100), CD62L (DREG-56; 1:100), CD28 (28.2; 1:80), CD16 (3G8; 1:100), CD54 (HA58; 1:100), CXCR3 PE (G025H7), CD103 PE (BerACT8) and TCR Vδ2 PE (B6; 1:100); all BioLegend, San Diego, USA. Mouse anti-human CXCR3 PE (FAB160P, FAB160F; 1:20), CXCR6 PE (56811/FAB699P; 1:20), CD18 PE (2127011; 1:20) and CCR7 FITC (150503; 1:20) all from R&D Systems. Mouse anti-human CX_3CR1-PE (2A9-1; 1:20), CD11a FITC (HI111; 1:10), CD49d PE (9F10; 1:50), CD29 FITC (TS2/16; 1:20), β7 integrin FITC (FIB504; 1:20) from Immunotools, Friesoythe, Germany. Mouse anti-human TCR γδ PeCy7 (IMMU510; 1:200), TCR Vγ9 PeCy5 (IMMU360; 1:400) and CD127 (IM1980U; 1:20); Beckman Coulter, Brea, CA, USA. TCR Vδ1 FITC (REA173; 1:100) and TCR Vδ2 APC (123R3; 1:200); Miltenyi Biotec.

Single-fluorophore labelled anti-mouse IgGκ /negative control (FBS) compensation particles (BD Biosciences) were used for compensation. All data was collected using either a nine colour, 3-laser CyAn ADP flow cytometer (Beckman Coulter) an LSR II 4-laser flow cytometer (Beckton Dickinson Biosciences, Franklin Lakes, NJ, USA) or an LSR Fortessa X20 4-laser flow cytometer (Becton Dickinson) and data analysed with FlowJo v. 10.1 (TreeStar, Ashland, OR, USA), Summit 4.3 software (Dako Cytomation) or BD FACSDiva (Becton Dickinson).

2.2.2 Intracellular staining of blood- and liver-derived T cells

Freshly isolated liver infiltrating lymphocytes and/ or peripheral blood from different explanted diseased livers were used. For intracellular staining, cells were stimulated with 100ng/ml of PMA and 1 μg/ml of ionomycin for 4 hours and incubated with 4μg/ml of Brefeldin A for the last 3 hours of stimulation. For intracellular staining of IL17, IL-22 IFN-γ

and RORc liver infiltrating lymphocytes were fixed and permeabilized with staining buffer (eBioscience) according to the manufacturer's protocol. $1x10^6$ cells stained with an anti-mouse-IL17 mAb, IL-22mAb directly conjugated to PE and APC and IFN-γ mAb conjugated to FITC, or RORγt conjugated to PE (eBioscience).

To analyse expression of intracellular transcription factors and cytotoxicity factors, cells were stained for surface markers TCR γδ, TCR Vδ2 and TCR Vδ1 then fixed overnight in IC Fixation buffer (eBioscience), permeabilised and stained using the Foxp3/Transcription factor staining set (eBioscience) with antibodies directed against CD3, CD8 and the transcription factors Tbet PE, Hobit APC, and EOMES APC and Granzyme A FITC (CBO9; 1:100), Granzyme B APC (GB11; 1:100) and Perforin BV421 (B-D48; 1:80); all BioLegend. For intracellular cytokine staining, antibodies used were IFN-γ BV421 (340449; 1:200), TNF-α PE (554512; 1:200); BD Pharmingen, IFN-γ eFluor450 (4S.B3; 1:100), TNF-α FITC (Mab11; 1:50), eBioscience.

2.2.3 Magnetic cell sorting of blood- and liver-derived T cells

In certain experiments, purified populations of T cells were obtained from blood and/ or liver derived lymphocytes using magnetic sorting. This was achieved primarily using a positive sorting method using CD3 specific antibodies, as the negative sorting kits available all used CD56 and CD16 specific antibodies to deplete NK cells and monocytes, however, gamma delta T cells express both of these surface markers at variable levels and would therefore be removed from the final population. Liver or peripheral blood derived lymphocytes were incubated with biotinylated mouse anti-human CD3 antibody (eBioscience) in 5 mL FACS tubes at room temperature for 10 minutes, before washing in

2% FCS in cold PBS + 10 mM EDTA and incubation with streptavidin coated MagniSort™ Positive Selection Beads (eBioscience) for a further 10 minutes at room temperature.

Labelled cells were then inserted into EasySep separation magnets (Stemcell Technology, Vancouver, Canada) and incubated at room temperature for 5 minutes, after which the supernatant was discarded, the tube removed from the magnet and magnetised cells washed in 2% FCS. This process was repeated twice to ensure good purity of $CD3^+$ cells in the final population – typically greater than 98% of cells were $CD3^+$.

2.2.4 Static lymphocyte adhesion assay

36 hours prior to the assay being performed, T25 cell culture flasks (Corning, New York City, USA) were coated with rat-tail collagen (Sigma-Aldrich) and allowed to dry in sterile conditions. ~$1x10^6$ trypsinized primary human HSEC cells per flask were then added in HSEC medium and allowed to form a confluent monolayer at 37^0C, 5% CO_2 overnight, with cell free medium used as a control in one flask per experiment. Six hours prior to the assay the HSEC were either stimulated with addition of TNF-α (10 ng/ml) and IFN-γ (10 ng/ml) (Peprotech) to the medium or left untreated. Typically $1x10^6$ PBMC-derived lymphocytes were then either magnetically sorted to isolate $CD3^+$ T cells or added in bulk and, following thorough aspiration of the HSEC medium and two washes with sterile PBS to remove trace cytokines and non-adherent cells, were re-suspended in RPMI-1640 supplemented with 10% (vol/vol) heat-inactivated FCS (all Invitrogen), benzylpenicillin/streptomycin (100 IU/ml), and glutamine (2 mM) (all from Sigma Aldrich) and added on top of the HSEC monolayer in a total typical volume of 5 mL. The culture flasks were then incubated for 15 minutes at 37^0C, 5% CO_2 to allow adhesion of lymphocytes to the HSEC monolayer, before the non-adherent cells were harvested, the

cells washed with PBS and dead cells stained using the e506 viability dye (eBiosciences) at 4°C for 30 minutes. Surface staining of γδ TCR antigens was then performed on the non-adherent cells as described earlier and gamma delta T cell populations quantified by flow cytometry. Data are expressed as the change in γδ TCR^+ cells as a proportion of $CD3^+$ T cells in the adherent cell population, calculated as the inverse of the non-adherent population measured by flow cytometry.

2.2.5 Lymphocyte-endothelium transmigration assay

36 hours prior to the assay being performed, 5 μm pore polycarbonate membrane Transwell inserts (Corning, New York City, USA) were coated with rat-tail collagen (Sigma-Aldrich) and allowed to dry in sterile conditions. ~100,000 trypsinized HSEC cells per well were then added on top of the Transwell insert in HSEC medium and allowed to form a confluent monolayer at 37 ^{0}C, 5 % CO_2 overnight. Six hours prior to the assay the HSEC were either stimulated with addition of TNF-α (10 ng/ml) and IFN-γ (10 ng/ml) (Peprotech) to the medium or left untreated. Typically 250,000 PBMC-derived lymphocytes were then either magnetically sorted to isolate $CD3^+$ T cells or added in bulk and, following thorough aspiration of the HSEC medium and two washes with sterile PBS to remove trace cytokines and non-adherent cells, were re-suspended in RPMI-1640 supplemented with 10% (vol/vol) heat-inactivated FCS (all Invitrogen), benzylpenicillin/streptomycin (100 IU/ml), and glutamine (2 mM) (all from Sigma Aldrich) and added on top of the HSEC monolayer with cell-free medium added to the lower chamber to prevent drying out. Transwell chambers were then incubated for 48 hours at 37^{0}C, 5% CO_2 to allow transmigration of lymphocytes across the HSEC monolayer, before the entire contents of both upper and lower chambers was harvested, the cells were

washed with PBS and dead cells stained using the e506 viability dye (eBiosciences) at 4°C for 30 minutes. Surface staining of γδ TCR antigens was then performed as described earlier and gamma delta T cell populations quantified by flow cytometry. Data are expressed as the fold change in γδ TCR^+ cells as a proportion of $CD3^+$ T cells in both upper and lower chambers following incubation.

2.2.6 Fluorescence activated cell sorting (FACS)

For cell sorting, $V\delta1^+$ and $V\delta2^+$ populations were labelled with anti-CD3 (UCHT1; 1:100), TCR αβ (IP26; 1:50), TCR Vδ1 (TS8.2 or REA173; 1:100) or TCR Vδ2 (123R3; 1:100) and where indicated CD27 (M-T271; 1:200) and CD45RA (HI100; 1:200). Alternatively, $V\delta2^{neg}$ T cell populations were sorted by labelling with anti-CD3 (UCHT1; 1:100), TCR αβ (IP26; 1:50), TCR γδ (IMMU510; 1:200), TCR Vδ2 (123R3; 1:100). Cells were filtered using a 25 micron mesh to remove aggregates and resuspended in 2% FCS in cold PBS + 10 mM EDTA before sorting using a MoFlo Astrios Flow Cytometer Cell Sorter (Beckman Coulter) or a FACSAria II (Becton Dickinson).

2.2.7 T cell activation assay

Magnetically-sorted $CD3^+$ T cells (section 2.2.3) were seeded in 24-well plates (Corning) in RPMI-1640 supplemented with 10% (vol/vol) heat-inactivated FCS, benzylpenicillin/streptomycin (100 IU/ml), and glutamine (2 mM) and incubated for 72 hours either untouched, with washed Human T-Activator CD3/CD28 Dynabeads™ (Gibco) at a ratio of 1:1, or with recombinant cytokines IL-7 (25 ng/ mL), IL-12 (5 ng / mL), IL-18 (5 ng/ mL) (all Peprotech) and IL-15 (25 ng/ mL, Miltenyi). Gamma delta T cell subsets, CD8

T cells and activation markers CD69, CD54 and/ or CD25 were then determined by flow cytometry (2.2.1).

2.2.8 *In vitro* activation of intrahepatic T cells by *E. coli*

Liver-derived mononuclear cells were seeded in 12-well plates in RPMI-1640 supplemented with 10% (vol/vol) heat-inactivated FCS, benzylpenicillin/streptomycin (100 IU/ml), and glutamine (2 mM) and incubated for 72 hours either untouched, with paraformaldehyde-fixed *Escherichia coli* (*E. coli*) (DH5α, Invitrogen) at 1000 bacteria per cell respectively or with *E. coli* and blocking antibodies against IL-12p40/70 (5 μg/ml, C8.6, eBioscience) and IL-18 (5 μg/ml, 125-2H, MBL International, USA). Cell subsets were subsequently identified and activation assessed by flow cytometry labelling with IFNγ, as described previously.

2.3 Cell localisation studies

2.3.1 Immunohistochemistry

Localization of gamma delta T cells in human inflammatory liver sections was performed using immunohistochemistry staining on formalin fixed paraffin embedded (FFPE) cubes of liver tissue. Liver slices were cut and immediately fixed in 10% neutral buffered formalin for 24 – 48 hours prior to rinsing, dehydration and embedding in paraffin and subsequently sectioned into 5 μm thick sections and mounted on poly-L-lysine coated glass slides. Sections were then de-paraffinised in multiple washes of xylene and then re-hydrated in a series of decreasing strength ethanol baths.

Endogenous peroxidase activity was quenched by incubation in 0.3% hydrogen peroxide (Sigma Aldrich) in methanol for 20 minutes. Antigen retrieval was then conducted by boiling the sections while immersed in 1% EDTA solution for 15 minutes in a microwave. After washing using 0.1% Tween in PBS, non-specific antibody binding was blocked using casein (1 in 10 in PBS) (Vector Laboratories, Burlingame, CA) for 20 minutes. This was followed, after washing, by incubation for 1 hour in primary antibody (goat polyclonal – anti-human pan-VγVδ (50 µg/ mL, A-20, Santa Cruz Biotechnology, Santa Cruz, USA) or rabbit polyclonal – anti-human CD3 (2 µg/ mL, ab5690, Abcam, Cambridge, UK) or relevant IgG1 isotype control) diluted in PBS. After washing, sections were covered with Impress HRP-linked anti-goat or anti-rabbit secondary antibody (Vector Labs Laboratories) and incubated for 30 minutes at room temperature. Following washing, sections were developed using ImmPACT^{TM} DAB reagent (Vector Laboratories) diluted as per the manufacturer's instructions. After desired level of staining was achieved, typically 2 - 5 minutes, excess DAB was removed by rinsing with distilled water. Finally, sections were counterstained with filtered Mayer's haematoxylin solution (Leica Biosystems) for 2 minutes or until desired level of staining was achieved. This was developed by incubation in cold water for 2.5 minutes followed by hot water for 2.5 minutes. Once dry, slides were mounted using DPX (Cellpath, Newtown Powys, UK) and imaged on a Zeiss Axioskop 40 Microscope with a x20 or x40 objective lens. Regions of parenchymal and portal tract tissue were identified and numbers of $CD3^+$ or γδ-TCR^+ cells were counted per region identified, with 5 high power fields scored for each section.

2.3.2 In situ hybridisation (ISH)

Localisation of chain-specific gamma delta TCR^+ cells was performed in this study using two protocols, either the ViewRNA™ ISH Tissue 2-Plex Assay developed by Affymetrix and performed manually, or the RNAscope® 2.5 LS Duplex Assay (ACD) . Although 2-Plex staining was not always performed, the protocol followed the manufacturer's instructions up to the point of the second colour being developed in the case of 1-Plex staining. For both protocols, liver slices were cut and immediately fixed in formalin for 24 – 48 hours prior to embedding in paraffin and subsequently sectioned into 5 µm thick sections and mounted on poly-L-lysine coated glass slides, and immediately prior to the assay these slides were baked at 60 ^{o}C for 1 hour to immobilise the sections.

2.3.2.1 Visualisation of γδ T cell subsets using manual ViewRNA^{TM} ISH

Baked slides were then deparrafinised using three 5 minute xylene incubations, replacing the xylene with fresh each time, and dehydrated using two 5-minute incubations in 100% ethanol, before being allowed to air dry until completely dry in a fume hood. Slides were then heated in a beaker containing Pretreatment Solution (Affymetrix) placed in a water bath at 90 – 95 ^{o}C for 15 minutes, and then washed three times in ddH_2O. Slides were then incubated for 30 minutes in a humidified hybridisation chamber pre-warmed to 40 ^{o}C with protease solution diluted 1:100 in PBS (Affymetrix), and then washed three times in PBS before being fixed in 10% neutral buffered formalin for 10 minutes at room temperature. Following 2 washes in PBS, slides were then incubated in the hybridisation chamber for 2 hours at 40 ^{o}C with the thawed target probeset diluted in Probe Set Diluent QT (Affymetrix). Target probes were used as follows:

- a 20 ZZ probe targeting CD3E
- a 20 ZZ probe targeting TRDC
- a 7 ZZ probe targeting 2-564 of gi|99345462:619422-619991 (TRDV1)
- a 7 ZZ probe targeting 4-481 of gi|99345462:946632-947128 (TRDV2)
- a 8 ZZ probe targeting 2-470 of gi|28436398:56456-56931 (TRGV9)

Slides were then washed 3 times in Wash Buffer (Affymetrix) before a 25 minute incubation in the hybridisation chamber at 40^{o}C with pre-warmed PreAmplifier Mix QT (Affymetrix), a further three washes in Wash Buffer and then a 15 minute incubation in the hybridisation chamber with Amplifier Mix QT (Affymetrix). Following 3 washes in Wash Buffer and depending on the probe set being used (Type 1 or Type 6), slide were then incubated with Label Probe 6-AP or Label Probe 1-AP at 1:1000 in prewarmed Label Probe Diluent QF (Affymetrix) in the hybridisation chamber for 15 minutes. For 2-Plex assays, Label-6 probe sets were visualised using Fast Blue – following 3 washes with Wash Buffer, slides were incubated with Fast Blue substrate (Affymetrix) in the dark for 30 minutes in the hybridisation chamber. After washing, the fast blue reaction was quenched using AP Stop QT (Affymetrix) in a further 30 minute incubation in the dark in the hybridisation chamber. For the second probeset, typically Type-1, and for 1-Plex assays, positive hybridisation was visualised using FastRed Substrate (Affymetrix). After 3 washes with Wash Buffer, sections were incubated for 5 minutes at room temperature with AP Enhancer Solution (Affymetrix) with Fast Red Substrate (one fast red tablet dissolved in 5 mL naphthol buffer) added immediately afterwards and incubated for a further 30 minutes at 40 ^{o}C in the hybridisation chamber. Slides were then washed in PBS

and counter-stained using Mayer's haematoxylin solution as described before and mounted using ProLong Gold (Invitrogen). Imaging was performed on a Zeiss Axioskop 40 Microscope with a x20 or x40 objective lens.

2.3.2.2 Visualisation of γδ T cell subsets using automated RNAscope™ ISH

Although manufactured by a different company, the technology and protocol used in the RNAscope assay is very similar in most respects to that of the ViewRNA assay, with pretreatment, wash, probe incubation and signal amplification steps occurring in the same format. However, this protocol had been optimised by the manufacturers to be used in conjunction with the BOND RX Research Advanced Staining System (Leica Biosystems), using proprietary BOND dewaxing, wash, and antigen retrieval buffers (Leica) and amplification buffers manufactured by ACD. Minor modification of the staining protocol supplied by ACD was required but otherwise sample preparation, counterstaining and mounting was performed as for the ViewRNA assay.

2.4 Sequencing studies

2.4.1 γδ TCR sequencing

For next-generation sequencing studies, peripheral blood or liver derived lymphocytes were labelled with antibodies and FACS sorted according to the protocol detailed in section 2.2.6. Sorted $V\delta2^{+}$, $V\delta1^{+}$ or $V\delta2^{neg}$ cells were collected in numbers from 8,000 to 50,000 directly in RNAlater (Sigma Aldrich), vortexed and frozen at -80^{o}C for subsequent RNA extraction. This was performed using the RNeasy Mini extraction kit made by Qiagen (Hilden, Germany). Following centrifugation, the cell pellet was lysed and homogenised using Buffer RLT + 1% β-mercaptoethanol followed by thorough vortexing.

1:1 volume of 70% ethanol was then added before transferring the mixed lysate to an RNeasy spin column and centrifuged at 12,000 rpm for 15 seconds. To remove genomic DNA, 350 µl Buffer RW1 was added to the column and centrifuged at 12,000 rpm for 15 seconds before 80 µl of DNase I incubation mix was added to the column and incubated at room temperature for 15 minutes. To remove ethanol, the column was then washed again with RW1 before 500 µl Buffer RPE was added to the column and centrifuged at 12,000 rpm for 15 seconds and then again for 2 minutes with fresh Buffer RPE. To elute RNA, the column was transferred to a new collection tube and 30 µl RNase-free water added directly to the spin column membrane before centrifugation at 12,000 rpm for 1 minute. This was then repeated to ensure high RNA yield. RNA concentration was then determined using a NanoDrop^{TM} 3300 spectrophotometer (ThermoFisher, Waltham, MA, USA) and stored at -80 ^{o}C.

For high throughput deep sequencing of TCRs, amplicon rescued multiplex (ARM)-PCR and NGS methods were employed to analyse all sorted gamma delta T cell populations (iRepertoire Inc. Huntsville, USA). Following initial first-round RT-PCR using high concentrations of gene-specific primers, universal primers were used for the exponential phase of amplification (Patent: WO2009137255A2), allowing deep, quantitative and non-biased amplification of TCR γ and TCR δ sequences. All cDNA synthesis, amplification, NGS library preparation and sequencing were performed by iRepertoire. V, D and J gene usage and CDR3 sequences were identified and assigned and tree maps generated using iRweb tools (iRepertoire). For more detailed analysis and error correction, data sets were then processed using the MiXCR software package. Diversity metrics, clonotype overlap and gene usage were plotted in R, by VDJTools.

2.4.2 Single cell PCR γδ TCR sequencing

For exploration of the intrahepatic gamma delta TCR repertoire, single cell PCR was used. Individual Vδ1^{+} or Vδ3^{+} cells were sorted using a FACSAria II cell sorter (Becton Dickinson) (2.x.x) into a RNAse-free 96-well PCR plate (Axygen) containing 2 µL SuperScript^{TM} VILO reaction mixture containing 0.21 µL 1% Triton-X, 0.4 µL 5x VILO reaction mix, 0.2 µL SuperScript RT enzyme and 1.2 µL molecular grade water (Sigma) to lyse the cells and catalyse subsequent cDNA synthesis. Two wells per plate were left empty and two wells per plate filled with 50 cells as negative and positive controls respectively. Following brief centrifugation to ensure the cell was at the bottom of each well, the plate was incubated in a 2720 thermal cycler (Applied Biosystems) at 25°C for 10 minutes and then at 42°C for 120 minutes. The reaction was terminated at 85°C for 5 minutes before cooling to 4^{o}C and subsequent storage at -20^{o}C.

TCRγ and TCRδ cDNAs were then amplified in a nested 2-round PCR procedure. Firstly, 0.5 µL of "external" primers for TRDV1/3, TRDC, TRGV9 and TRGV1-8 (see Table 2.1) at 0.5 µM were included with 12.5 µL GoTaq mastermix (Promega, Madison, USA), 2 µL template cDNA and 9.5 µL molecular grade water (Sigma) and annealed at 50 ^{o}C over 35 cycles. Then, 2 µL of the PCR product from this first round was used as a template for a second PCR round using GoTaq mastermix and 0.5 µM of the "internal" primers of corresponding genes included in the first round, using the same PCR protocol. All primers were generously donated by Adam Uldrich, University of Melbourne.

To ensure effective amplification, 10 µL of second round PCR product was then run on a 1.2% agarose gel. Samples were diluted in 1X loading dye (40% sucrose, 0.5% bromophenol blue) and loaded into an agarose gel (1% agarose (Sigma)) in TBE Buffer

(89mM Tris base, 89mM Boric acid and 2mM EDTA) with the addition of ethidium bromide for visualization by ultraviolet light. Samples were separated by size by the application of 80V across the gel until the desired separation was achieved. The 1kb plus ladder (Life Technologies) was used for fragment size determination. Samples with correctly visualised bands on the gel were then purified using ExoSAP-IT (ThermoFisher) to remove excess primers and nucleic acids. 5 µL of PCR product was added to a fresh 96-well plate together with 1 µL ExoSAP-IT and the mixture incubated at 37^{o}C for 15 minutes and then 85^{o}C for a further 15 minutes to inactivate the ExoSAP-IT enzyme.

Finally, the PCR products were prepared for Sanger sequencing by cycle sequencing with BigDye Terminator 3.1 (Applied Biosystems) using 1 µL of the 0.5 µM "internal" reverse primers , 1 µL Big Dye (Applied Biosystems), 1 µL DMSO, 5 µL Dilution Buffer (Applied Biosystems), 6 µL molecular grade water and 6 µL PCR product template. The mixture was then incubated in a thermal cycler at 95^{o}C for 5 minutes, followed by 35 cycles of 96^{o}C for 10 sec for denaturation, 50^{o}C for 5 sec for annealing, and 60^{o}C for 4 minutes for extension, with a final hold temperature of 4^{o}C. Reaction mixtures were then purified for capillary electrophoresis using BigDye Xterminator; 45 µL SAM solution and 10 µL BigDye XTerminator bead solution were mixed with the reaction mixture, vortexed and centrifuged at 1,000 g for 2 minutes prior to storage at 4^{o}C. Capillary electrophoresis was performed using an ABI 3730 capillary sequencer (Applied Biosystems) at the Functional Genomics Facility, University of Birmingham.

Round 1			
number	name	sequence	n
101 short	Vδ1 Forward	CAAGCCCAGTCATCAGTATCC	21
101	Vδ1 Forward	ACTCAAGCCCAGTCATCAGTATCC	24
102	Cδ Reverse	GCAGGATCAAACTCTGTTATCTTC	24
103	Vγ1-5 Forward	GTCATCTGCTGAAATCACYTGYG	23
104	Vγ8 Forward	AATGCCGTCTACACCCACTG	20
105	Vγ9 Forward	AGAGAGACCTGGTGAAGTCATACA	24
106	Vγ10 Forward	GAGCACCTGATCTATATTGTCTCAAC	26
107	Vγ11 Forward	GCATCCATCCAAGGCTTTAG	20
108	Cγ Reverse	CTGACGATACATCTGTGTTCTTTG	24
Round 2A			
number	name	sequence	n
206	Vδ1 Forward	CAACTTCCCAGCAAAGAGATG	21
201	Cδ Reverse	TCCTTCACCAGACAAGCGAC	20
Round 2B			
number	name	sequence	n
103	Vγ1-5 Forward	GTCATCTGCTGAAATCACYTGYG	23
104	Vγ8 Forward	AATGCCGTCTACACCCACTG	20
202	Cγ Reverse	AATCGTGTTGCTCTTCTTTTCTT	23
Round 2C			
number	name	sequence	n
203	Vγ9 Forward	GGTGGATAGGATACCTGAAACG	22
204	Vγ10 Forward	AATTCTCAAACTCTCACTTCAATCC	25
205	Vγ11 Forward	ATGTCTTCTTGACAATCTCTGCTC	23
202	Cγ Reverse	AATCGTGTTGCTCTTCTTTTCTT	23

Table 2.1: Single cell PCR T cell receptor primers

Two round nested PCR to determine CDR3 sequence of gamma delta T cell TCR. First round PCR products were used as template for second round primers, grouped into three reactions depending on optimal annealing temperature

2.5 Statistical analysis

All compiled data were analysed in Graphpad PRISM 7 (Graphpad Software Inc, USA) and NGS-based TCR sequencing data by VDJTools. After assessing normality using Shapiro-Wilko tests, either two-tailed Student's T tests or Mann-Whitney U-tests were used to identify differences between groups of normally distributed or non-parametric data, respectively.

Where more than two groups were to be analysed simultaneously, one-way ANOVA with Holm-sidak's post-tests or with Kruskal–Wallis ANOVA and Dunn's post-tests were used to identify differences between normal and non-parametrically distributed data respectively. Two-way ANOVA was used when comparing groups with independent variables. *$p<0.05$, **$p<0.01$, ***$p<0.001$ and ****$p<0.0001$, as indicated in relevant figures. Normally distributed data were assessed for correlation with Pearson's correlation coefficient, while Spearman correlation was employed for non-parametric data.

3

Intrahepatic gamma delta T cells in health and disease: prevalence and localisation

3.1 Introduction

In healthy liver, oxygen-rich blood from the hepatic artery and nutrient-rich blood from the hepatic portal vein drains into the tissue in a series of evenly spaced arterioles that, together with the bile ducts, form the portal triads – the corners of the classically hexagonally shaped liver lobules. From these portal triads, very narrow specialised capillaries termed sinusoids carry efferent blood through the parenchyma of the liver towards central venules and eventual egress from the tissue via the hepatic vein. During this transit through the sinusoids, physical constriction reduces blood flow rate to ~100–400 μm s^{-1}, increases shear stress and forces cellular components of the blood into close contact with the parenchymal cells of the hepatic lobes (Sironi *et al*., 2014). These factors combine with the uniquely fenestrated structure of the hepatic sinusoidal endothelial cells (HSEC) to allow lingering and direct interactions between leucocytes and platelets of the blood and the primary component of the liver parenchyma, the hepatocytes, as well as the immunologically critical HSEC, hepatic stellate cells (HSC), and liver-resident leucocytes such as Kupffer cells and dendritic cells (Braet and Wisse, 2002). By this method gut-derived antigen can be sensed by liver parenchymal cells, either directly via cell surface receptors such as TLRs or indirectly via contact with blood derived myeloid cells. In the case of commonly encountered non-harmful antigen the antigen-presenting capability of the liver parenchymal cells will then normally tolerise local T cell populations through priming via MHC without signal 2 or in the presence of immunosuppressive cytokines such as TGF-β and IL-10 (Jenne and Kubes, 2013).

In chronically inflamed livers, irrespective of the initial cause of the injury, whether it be autoimmune, metabolic dysregulation or viral in nature, leucocytes are recruited from the blood via upregulation of pro-inflammatory chemotactic cues such as chemokine ligands CXCL9, 10 and 11 and accumulate in the liver at abnormally high frequencies (Borchers *et al*., 2009). Retention and positioning of these lymphocytes within the liver microanatomy is determined by further chemotactic signals and upregulation of activation associated adhesion molecules on both lymphocyte and stromal cells (Oo *et al*., 2010). Previous studies have demonstrated that this accumulation is particularly prevalent where chronic attempts to repair damaged tissue has resulted in the formation of excessive collagenous fibrous septa, which commonly occurs in the areas around the portal tracts and the along the boundaries between portal tracts that form the edges of the liver lobules (interface hepatitis) often driven by high expression of matrix protein binding integrins such as CD49d (Patsenker and Stickel, 2011).

Since the liver is composed of such a heterogeneous population of different cell types that normally work in harmony to ensure effective immune regulation, identifying precisely where in the microanatomy lymphocytes are localising, and therefore what other cells they are likely to be interacting with, can provide a valuable insight into the role of the lymphocytes in both health and progression of pathology. Accordingly, the aim of this chapter was to elucidate 1) the scale of γδ T cell infiltration in normal and diseased livers, and also 2) identify where liver-associated γδ T cells are found in the context of the liver microanatomy.

Although the general T cell population has been extensively researched in this context in many different disease settings, the only study to date on intrahepatic gamma delta T cell localisation focussed on Hepatitis C virus (HCV) infection (Kasper *et al.*, 2009). Using immunohistochemical analysis of frozen sections, the authors found no discernible difference in number of liver-infiltrating gamma delta T cells between HCV, HBV or autoimmune hepatitis cases and found that those cells that were infiltrating were predominantly associated with the portal inflammation and not in contact with hepatocytes. This study did not examine normal tissue infiltration however.

Two techniques enable localisation of specific subsets of cells within tissue sections, immunohistochemistry (IHC), which relies on antibody-based detection of proteins within the tissue sections, and in-situ hybridisation (ISH), which uses complementary nucleic acid probes for specific detection of RNA sequences within tissue. This study attempted to incorporate both methods.

3.2 Analysis of infiltration of liver tissue by gamma delta T cells by IHC

3.2.1 Method

Immunohistochemistry has been used as a technique to identify proteins in tissues since the 1940s. It relies on recognition of a specific target protein antigen by a primary antibody raised in an animal in response to that antigen administered exogenously. As long as the tissue section to be stained is correctly prepared, antibodies in solution will bind with exposed antigen in the tissue. Visualisation can take a number of forms, but all use a secondary antibody raised against the isotype of the primary antibody, and these

are usually conjugated, either to an enzyme that catalyses breakdown of a substrate to form a chromogen which can be visualised by light microscopy, or a fluorophore to allow visualisation by fluorescence microscopy.

Working within the Centre for Liver Research, a large depository of formalin-fixed paraffin embedded (FFPE) tissue blocks from all chronic liver disease aetiologies, as well as normal liver sections from unused donor livers was available for this study. FFPE sections exhibit superior tissue morphology and clarity compared with frozen sections, so for these reasons were chosen for this study.

IHC as a technique relies predominantly on the quality of the primary antibody. At the time these experiments were performed, there were only a handful of antibodies commercially available for identification of the human γδ TCR, and few of them had been convincingly validated in published work. After an initial pilot test performed using historical FFPE human tonsil sections, the H-20 clone supplied by Santa Cruz Biotechnology gave the most encouraging results (not shown), and so all further optimisation was performed using this primary. Tonsil was chosen as a positive control tissue throughout the localisation studies since relatively high frequencies of gamma delta T cells are found there, and the tissue is relatively easy to work with in that it contains few tissue specific elements that can cause non-specific signal, such as liver associated bile and auto-fluorescent hepatocytes. Representative examples of positive staining in the liver sections were verified by a senior pathologist at Queen Elizabeth Hospital, Birmingham, Prof. Stefan Hubscher, during the antibody validation phase of the study.

A critical element to successful IHC using FFPE sections is antigen retrieval – that is, unmasking of the protein epitopes from the cross-linked matrix that preserved the sample during FFPE fixation. There are a number of methods for this, which generally use heat, proteases or a combination of the two. During this study an antigen retrieval protocol developed in the Centre for Liver Research was followed with optimisation of heat pre-treatment time to maximise final staining while maintaining optimum tissue morphology, since over-treating the sections at this stage leads to degradation of the section.

Although using bright-field visualisation allows clear and relatively straightforward enumeration of one or two epitopes of interest in tissue sections, for example, using DAB and alkaline phosphatase for brown and red staining on a single section, it is not suitable for use imaging multiple targets and close cell-cell interactions. Confocal fluorescent microscopy allows simultaneous use of multiple colours due to the variety of fluorophores available, as well as enhanced optical resolution and contrast compared with bright-field. To identify possible important cellular interactions of intrahepatic gamma delta T cells, the H-20 clone antibody was used with a fluorescein isothiocyanate-conjugated secondary and photographed on a Leica DM6000 microscope (Figure 3.1). However, despite attempts to improve the signal to noise of the resulting images by varying the antibody concentration and incubation time/ temperature, consistent positive staining of liver tissue was not achieved. This was likely due to the combination of naturally high background auto-fluorescence of liver parenchymal cells and the fact that the primary antibody was a polyclonal goat-derived antibody with quite a high

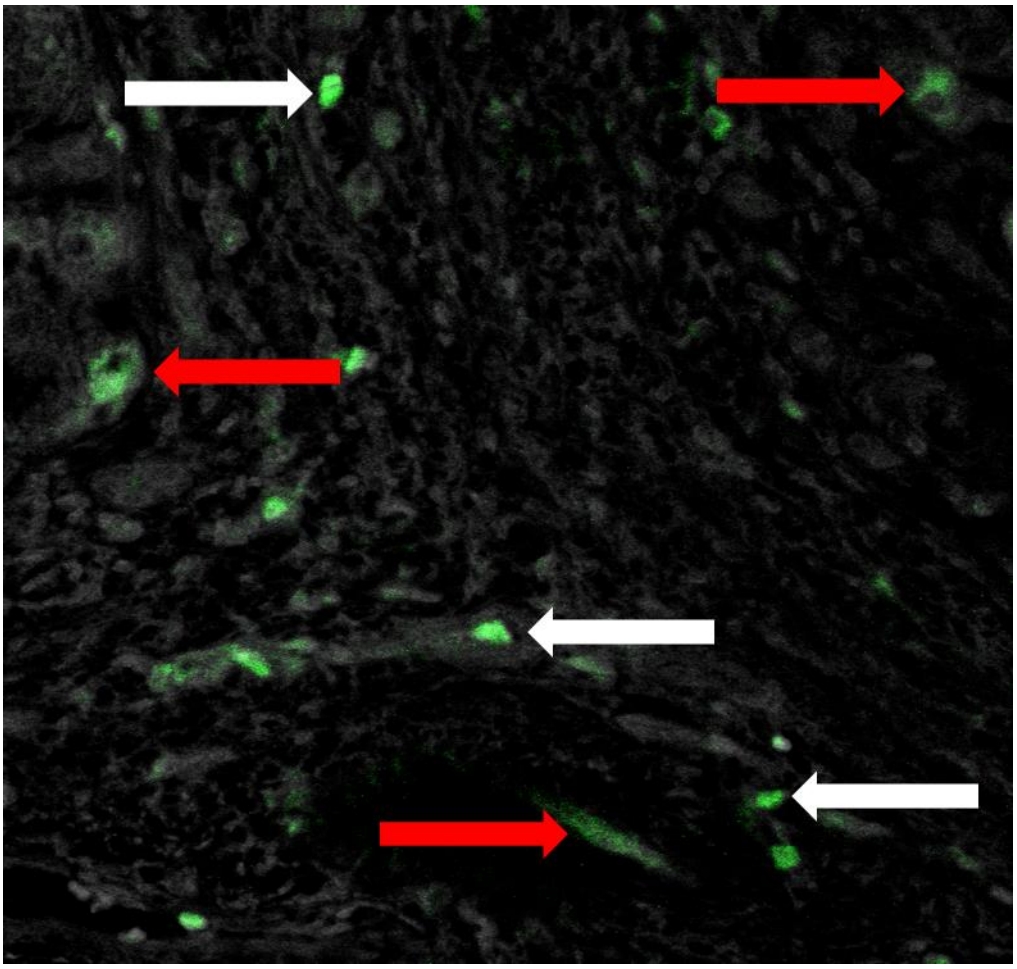

Figure 3.1: Fluorescent IHC staining of γδ T cells in human liver

FITC-conjugated γδ-TCR specific antibody labelling of portal area of liver from a patient with non-alcoholic steatotic hepatitis. Examples of positively stained (green) cells are highlighted with white arrows. Examples of non-specific non-cellular staining are highlighted with red arrows. Counterstaining was performed using DAPI. 40x magnification.

degree of non-specific staining, which while reasonable under bright-field visualisation became problematic when using the increased sensitivity of confocal imaging.

3.2.2 γδ T cell localisation in liver tissue

Two liver tissue sections isolated from explanted livers from five individuals from each of the following disease groups were stained using immunohistochemistry, visualised using the DAB method: ALD, NAFLD, PBC, PSC, AIH, HCV and HBV. Liver tissue sections from five normal donors were also analysed. The first section was incubated with a primary antibody specific for the delta-chain of the gamma delta TCR, while the second sequential section was incubated with a primary antibody specific for CD3, part of the T cell receptor complex. In all cases the same area of the section was identified on the two sections as accurately as possible to allow direct comparison of γδ TCR^+ and $CD3^+$ staining (Figure 3.2).

Previous studies have shown the human liver gamma delta T cell population is somewhere between 3% and 15% of the total $CD3^+$ T cell population (Kenna *et al*., 2004). By counting positively stained cells from three random high-power fields from each section stained and comparing the number of γδ TCR^+ to the number of $CD3^+$, in diseased livers taken as a whole, γδ TCR^+ cells represented 11.1% of the total T cell infiltration, whilst strikingly, in normal individuals this rose to 26.7% (Figure 3.3a). This represents a significant increase when compared with the disease group ($p<0.001$, Mann-Whitney U-test).

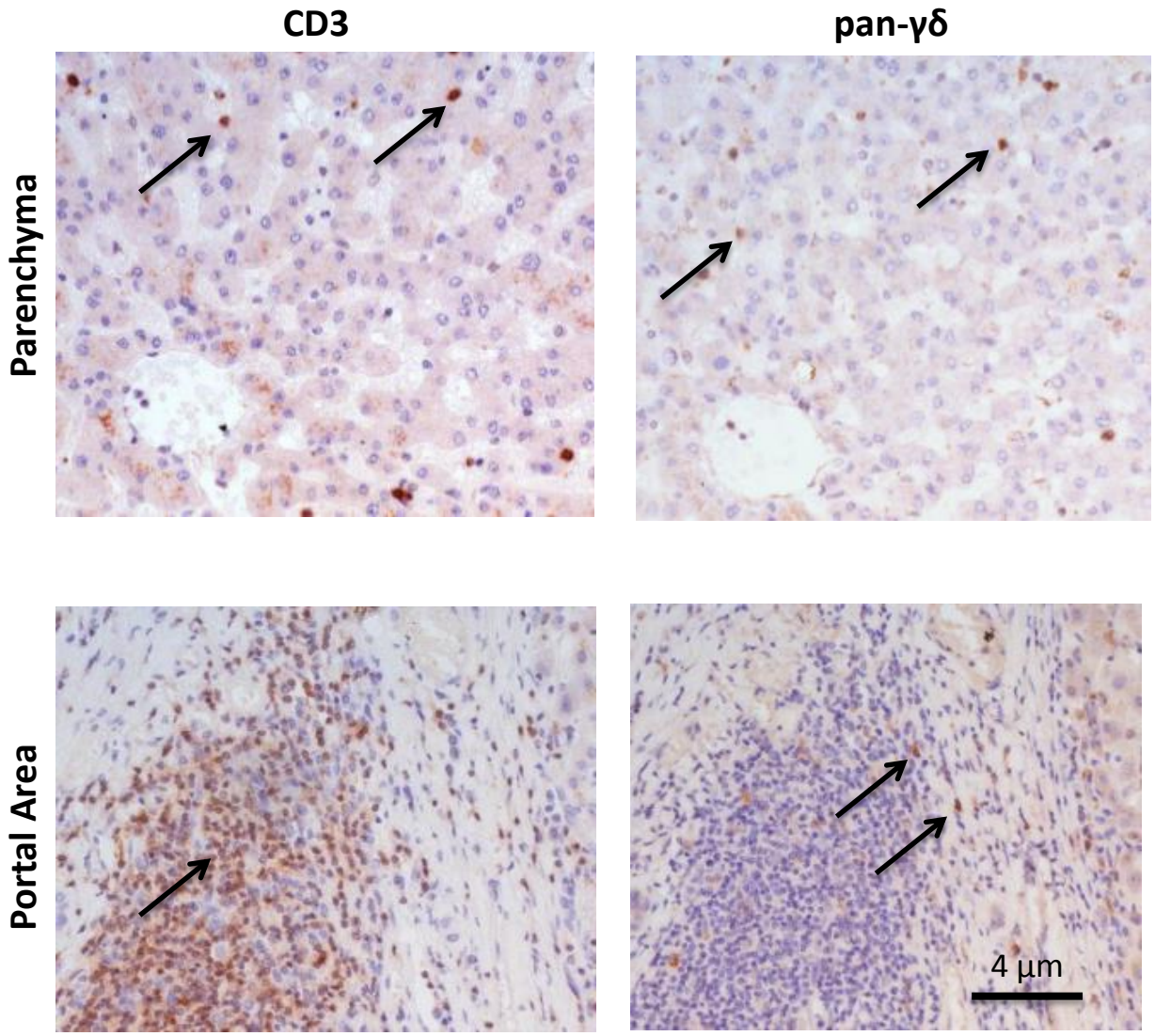

Figure 3.2: γδ T cells are enriched in parenchyma of human liver

Representative images of sequential FFPE sections from parenchymal (upper panels) and portal (lower panels) areas of liver explanted from a NASH patient, stained by IHC and visualised using DAB for γδ-TCR (right panels) and CD3 (left panels). Examples of positively stained (brown) cells are highlighted with black arrows. 40x magnification.

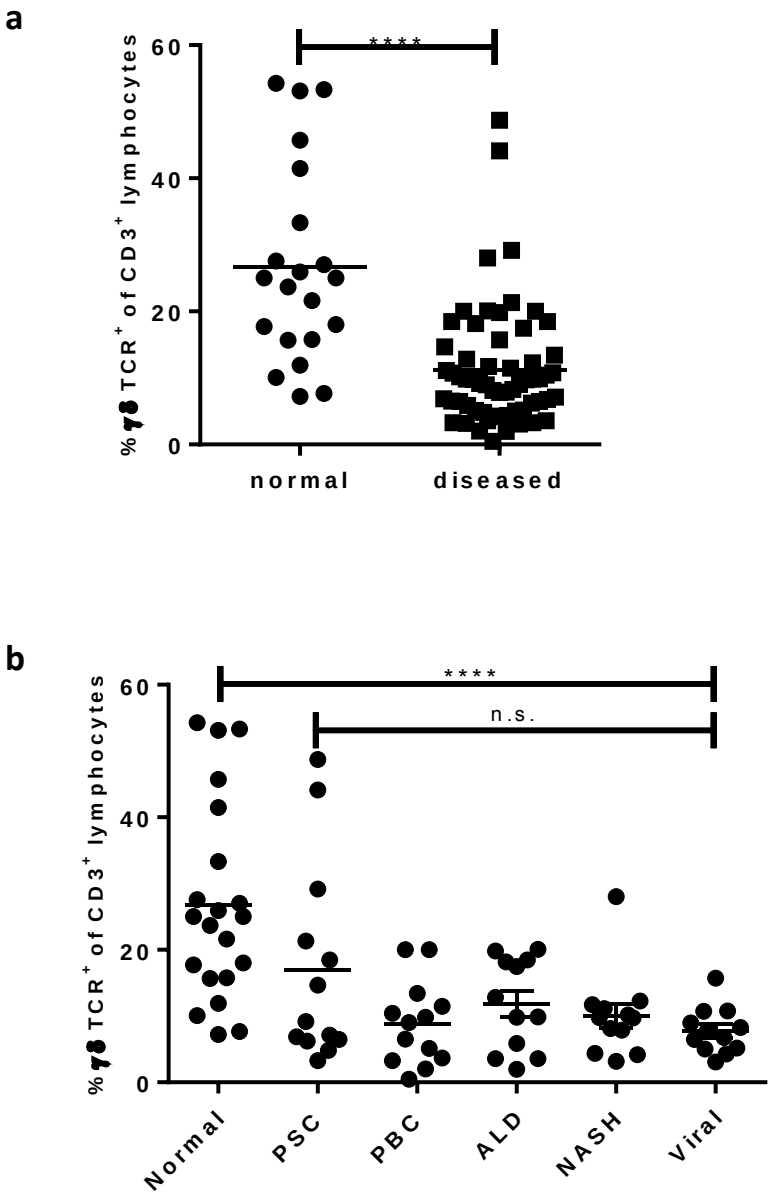

Figure 3.3: γδ T cells are enriched in normal liver

a) Proportion of γδ-TCR$^+$ cells identified as a ratio of CD3$^+$ cells from IHC staining of sequential FFPE sections using γδ-TCR and CD3 specific antibodies, from normal (n=21) and diseased (n= 62) livers. ($p<0.0001$, Mann-Whitney U-test)

b) Proportion of γδ-TCR$^+$ cells identified as a ratio of CD3$^+$ cells from IHC staining of sequential FFPE sections using γδ-TCR and CD3 specific antibodies, from normal (n=21) and various chronically diseased livers (n=12). ($p<0.0001$, 1way ANOVA, Kruskal Wallis test)

Figure 3.3b shows these data for each disease subtype, as well as normal liver. There was no significant difference in the average percentages of γδ TCR^+ cells between any of the inflammatory disease states compared with each other (PSC – 17.0%; PBC – 8,9%, ALD – 11.8%, NASH – 10.4%, HBV/ HCV - 7.6%, p=0.48, 1-way ANOVA, Kruskal Wallis test), although all are significantly reduced when compared with normal liver (p=0.0001, 1-way ANOVA, Kruskal Wallis test).

As well as measuring the frequency of γδ TCR^+ cells as a percentage of total $CD3^+$ cells, it was also possible to determine absolute numbers of infiltrating cells per field in normal and diseased livers. These data are illustrated in Figure 3.4a. In diseased livers, when examining the group as a whole, there was a greater than 5-fold increase in absolute numbers of infiltrating $CD3^+$ T cells in inflamed conditions compared with normal livers (213 cells/ field vs 41 cells/ field, p<0.001, Mann Whitney U test). However, a similar comparison for the γδ TCR^+ cells shows no such increase in inflamed conditions compared with normal liver (21 cells/ field vs 16 cells/ field, p>0.05). Additionally, no particular disease state showed any significant change from this paradigm, with $CD3^+$ enrichments of greater than 5-fold in autoimmune (PSC, PBC and AIH), fatty liver (ALD + NASH) and viral liver disease (HCV and HBV) patients compared with normal liver (Figure 3.4b). As a whole, these data were suggestive of a scenario where gamma delta T cells are relatively abundant in normal liver compared with the total number of T cells present, but that during the course of chronic inflammation, a large infiltration of non-gamma delta T cells occurs while the number of γδ T cells does not significantly change. This therefore results in a reduction in the observed percentage of gamma delta T cells compared with $CD3^+$ T cells in disease compared with normal livers.

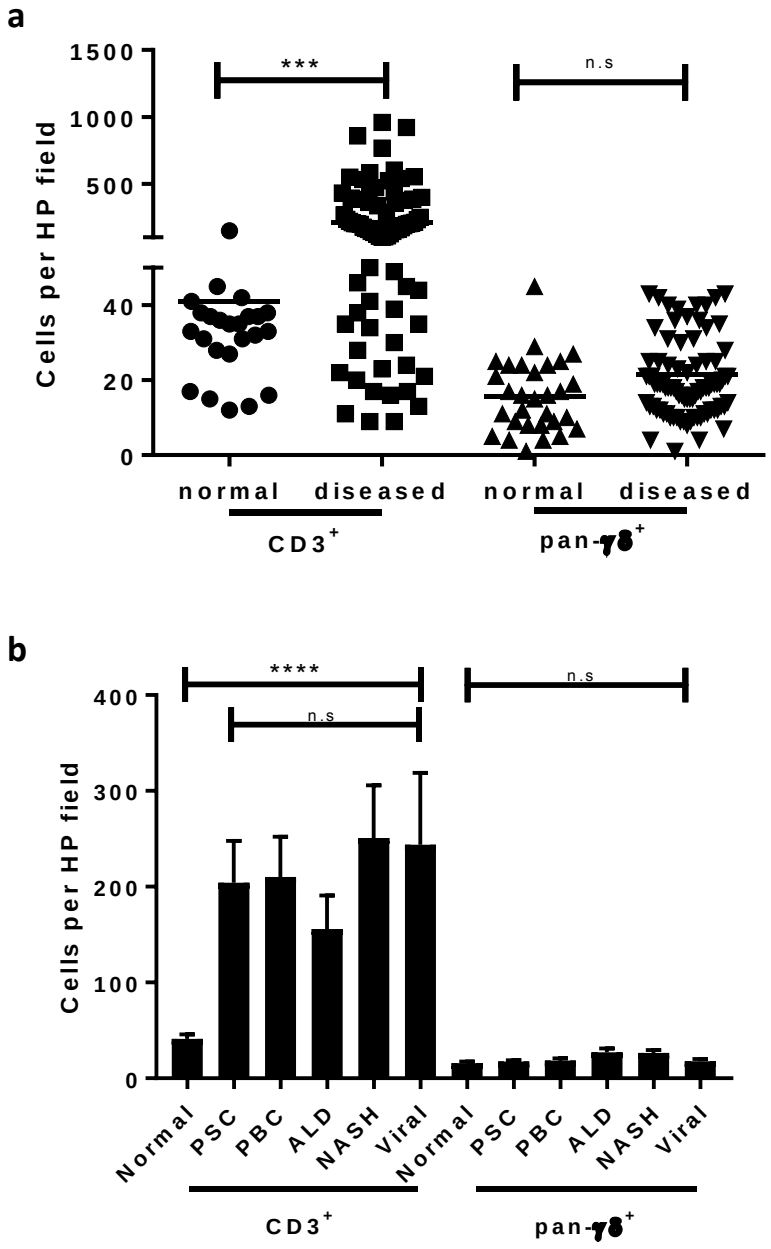

Figure 3.4: Liver disease is not associated with increased infiltration of γδ T cells

a) Liver infiltration of $CD3^+$ and γδ-TCR^+ cells identified as positively stained cells per high power field following IHC staining of sequential FFPE sections using γδ-TCR and CD3 specific antibodies, from normal (n=21) and diseased (n= 62) livers. ($p<0.0001$, 1-way ANOVA, Dunn's multiple comparison test)

b) Liver infiltration of $CD3^+$ and γδ-TCR^+ cells identified as positively stained cells per high power field following IHC staining of sequential FFPE sections using γδ-TCR and CD3 specific antibodies, from normal (n=21) and chronically diseased livers of varying aetiology (n=12). ($p<0.0001$, 1way ANOVA, Kruskal Wallis test)

In addition to determining the absolute frequencies of infiltrating γδ T cells in the liver, use of IHC allowed quantification of where in the liver microanatomy these cells were most abundant. Upon counting, the location of the positive cell was noted as either a) parenchymal, that is, in association with the hepatocytes or b) portal, that is, in association with the portal triad or area of fibrosis and interface hepatitis surrounding the triad (Figure 3.5). An average of 33.3 $CD3^+$ cells per field was present in the parenchyma of normal livers, with no significant difference in disease (35.5 cells/ field). 48.4 $CD3^+$ cells/ field were present in normal portal areas, rising to 301.7 cells/field in diseased livers, a 6.23-fold increase ($p<0.001$, Mann Whitney U test). γδ TCR^+ cells were not enriched in disease parenchyma (17.6 cells/ field vs 23.4 cells/ field, $p=0.057$ Mann Whitney U test) but, as for $CD3^+$ cells, were significantly enriched in portal areas (23.4 cells/ field vs 7.9 cells/ field, $p<0.001$). Interestingly, while $CD3^+$ cells were significantly enriched in diseased portal areas compared with diseased parenchyma ($p<0.001$), γδ TCR^+ cells were not, suggesting that the large increase in $CD3^+$ T cells in disease is mainly due to non-gamma delta T cells infiltrating the portal areas of the liver, while the parenchyma is relatively enriched for gamma delta T cells in both health and disease states.

The parenchymal enrichment of gamma delta T cells becomes strikingly apparent when the frequency of γδ T cells is viewed as a percentage of $CD3^+$ T cells present (Figure 3.6a). In normal liver, 66.2 ± 1.54% of $CD3^+$ were γδ TCR^+ in the parenchyma, dropping to 53.4 ± 2.54% in diseased livers ($p>0.05$). In the portal areas, 18.2 ± 1.43% of $CD3^+$ were γδ TCR^+ in normal liver, 8.3 ± 0.2% in diseased ($p<0.001$). As with overall infiltration, localisation of intrahepatic gamma delta T cells shows no discernible variation between individual

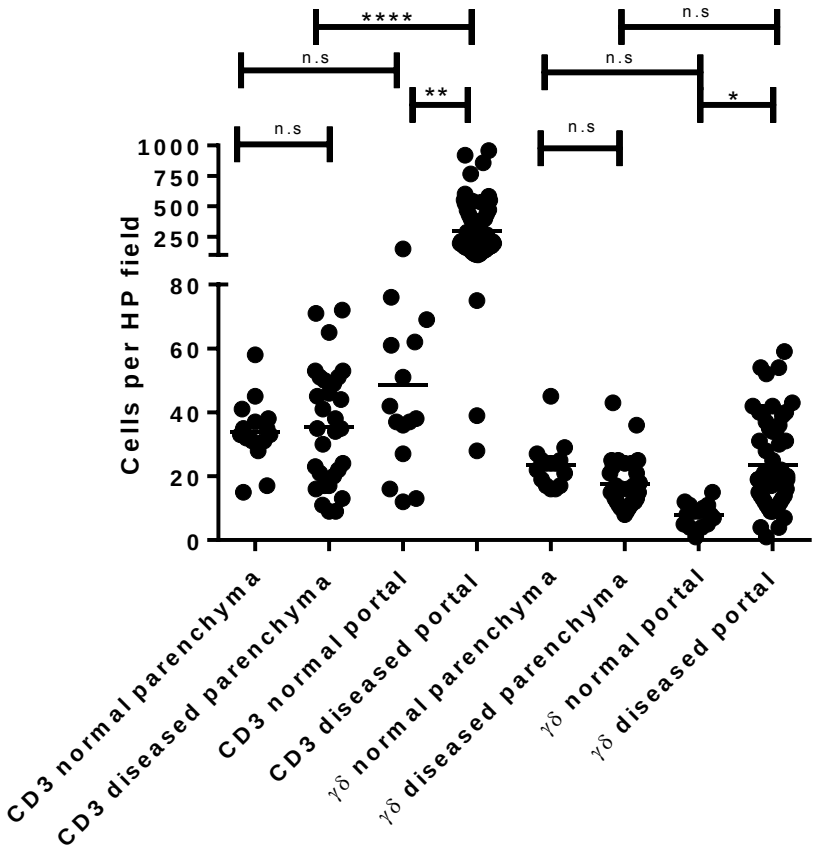

Figure 3.5: Portal regions are enriched for CD3$^+$ and γδ T cells in liver disease

Liver infiltration of CD3$^+$ and γδ-TCR$^+$ cells, identified as positively stained cells per high power field following IHC staining of sequential FFPE sections using γδ-TCR and CD3 specific antibodies, from normal (n=21) and diseased (n= 30) livers. Each cell counted was associated with either liver parenchyma or portal regions. *p<0.05, **p<0.01, ****p<0.0001, 1-way ANOVA, Dunn's multiple comparison test.

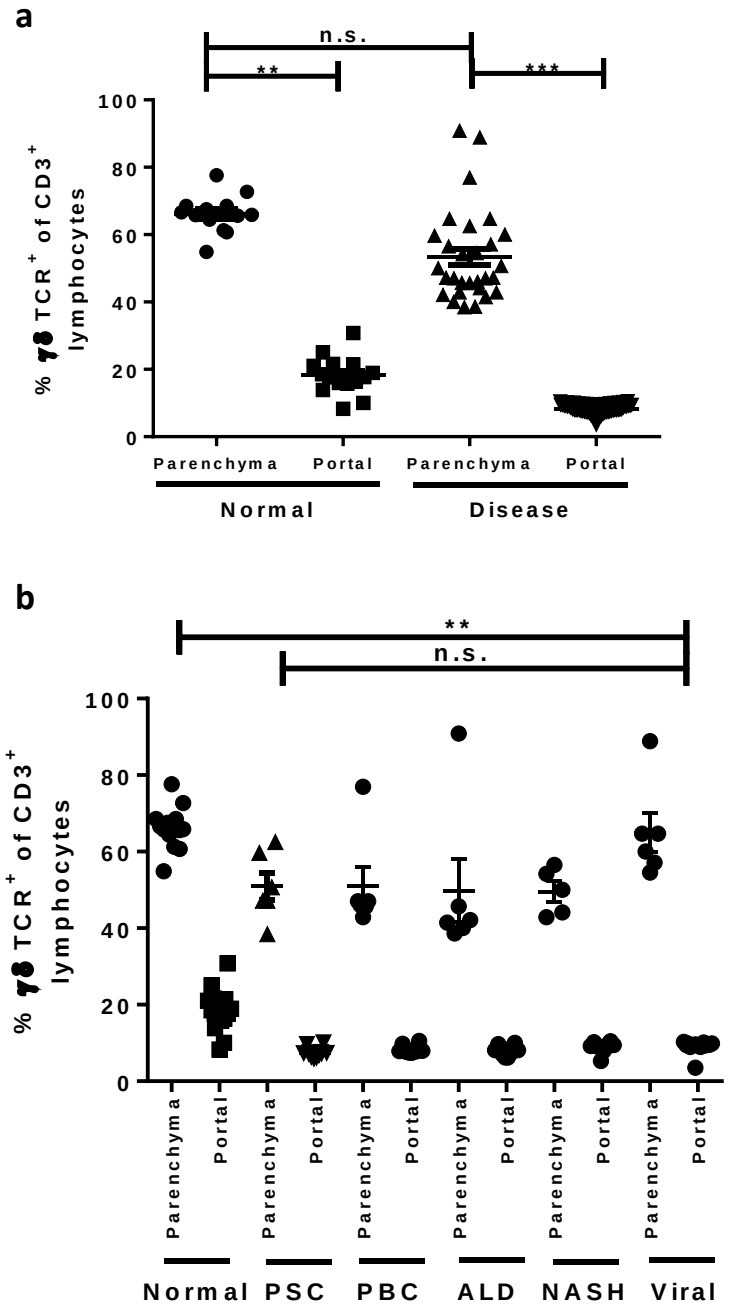

Figure 3.6: Localised γδ T cells proportion of liver infiltrating T cells by IHC analysis

a) Proportion of γδ-TCR$^+$ cells identified as a percentage of CD3$^+$ cells infiltrating either parenchymal or portal areas of normal (n=21) and diseased (n= 30) livers by IHC staining of sequential FFPE sections using γδ-TCR and CD3 specific antibodies.

b) Proportion of γδ-TCR$^+$ cells identified as a percentage of CD3$^+$ cells infiltrating either parenchymal or portal areas of normal (n=21) and diseased livers of various aetiologies (n=6) by IHC staining of sequential FFPE sections using γδ-TCR and CD3 specific antibodies. **p<0.01, ***p<0.001, 1-way ANOVA, Dunn's multiple comparison test.

disease groups, with the parenchymal areas being dominated by gamma delta T cells in all cases (Figure 3.6b).

3.3 Analysis of liver infiltrating gamma delta T cells by ISH

3.3.1 Background

A significant drawback to IHC as a technique is that it relies on antibody detection of target epitopes and therefore if no antibody is available for the target of interest, IHC is impossible. In-situ hybridisation (ISH) is an alternative technique for visualisation of targets within tissues that has been used since the late 1960s but has recently been refined as a commercial product by Affymetrix™ and Advanced Cell Diagnostics™. Instead of antibody detection of a protein epitope, ISH uses oligonucleotide probes complementary to the mRNA target sequence to provide initial target recognition and then a series of hybridisation steps to adjacent oligonucleotides to amplify the bound probes to produce a visible readout. As with IHC, visualisation can be either bright field or fluorescent, but in this case as long as the mRNA target sequence is known and there are sufficient intact lengths of sequence present in the tissue, ISH probes can be designed for any target without need to develop and validate specific antibodies, a costly and often difficult process.

The antibody used in the IHC-based study was specific for TCR delta-chain constant region and therefore can only be used to assess “pan-γδ”-positive T cells. However, this provided no information as to the TCR chain usage of the gamma delta T cells present.

Previous studies have suggested that the classically tissue-associated Vδ1$^+$ and Vδ3$^+$ γδ T cells are likely enriched in human liver (Kenna *et al*., 2004), and so to quantify these cells and assess whether they are localised differently to the classically blood-associated Vδ2$^+$ γδ T cells, an ISH-based method was employed using oligonucleotide probes specific to the variable delta-chain regions specific to each individual TCR subset (Vδ1, Vδ2 and Vδ3). Additionally, by using an ISH duplex kit developed for co-staining two markers of interest, it should be possible to probe for TCR Vδ mRNA transcripts on the same section as CD3, thereby negating the requirement to use sequential sections for pan-γδ TCR and CD3, and providing a more reliable quantification of γδ T cells and CD3$^+$ cells than the IHC dataset.

While proteins tend to be fairly robust and withstand the fixation, embedding and de-paraffinisation involved in pre-treatment, mRNA is a lot more sensitive to degradation, particularly at the point of tissue collection and initial fixation. While every effort is made to process explanted tissues as quickly as possible, there is always a delay between the organ being removed from the donor in theatre and the tissue being processed for fixation, either in the hospital pathology department or in the Centre for Liver Research laboratories. mRNA degradation can therefore be an issue for sensitivity, particularly for low copy number mRNA transcripts. Additionally, since it is mRNA that is targeted using ISH, the technique relies on expression of that mRNA at the time of fixation, which may not be the case for all targets. TCR mRNA expression is relatively stable but increases upon cell activation (Uppenkamp *et al*., 1993), meaning this method may not be as sensitive to resting T cells as IHC, where protein level expression generally decreases upon prolonged stimulation (Schrum *et al*., 2003).

3.3.2 Development of ISH protocol for Vδ1/ Vδ2/ Vδ3 visualisation

3.3.2.1 ViewRNA protocol

The first attempt to use ISH to visualise gamma delta TCR mRNA in liver tissue used Affymetrix' ViewRNA ISH Tissue 2-plex Assay. Probes were designed for CD3, the constant region of the TCR delta-chain (Cδ), Vδ1 and Vδ2. Probes for CD3 and Cδ already existed in the manufacturer's library but new probes were designed for the variable-chain regions of gamma delta TCRs.

Before using the gamma delta TCR probes however, the method was validated using positive control sections and probes supplied by the manufacturer, which ensured reagents and equipment used were capable of yielding positive results. These consisted of rat kidney FFPE sections mounted on positively charged slides with low expression rat osteopontin (Spp1) and highly expressed ubiquitin C (Ubc) probe sets. The test probe sets were also used on tonsil tissue, as with the IHC protocol, since the frequency of positive gamma delta staining in liver tissue was unknown, while tonsil contains a relatively high number of γδ T cells.

In brief, the protocol required baking slides to fully dry them out and remove the majority of the embedding wax, deparaffinisation in xylene followed by dehydration in ethanol. The next two steps, heat pre-treatment and protease digestion, equivalent to IHC antigen retrieval, were according to the manufacturers the only steps that require optimisation. For liver tissue, best results were achieved using a pretreatment time of 30 minutes and a

protease digestion of an hour – both longer than the time recommended by the manufacturer.

Following pre-treatment the sections were incubated with the relevant oligonucleotide probes, with both probes added simultaneously. Each probe set consisted of between 7 and 20 engineered nucleotide sequences that form a "Z" shape molecule. These probes hybridised along their "lower" region to corresponding lengths of target mRNA sequence. Since this was a duplex assay, each probe was designed with one of two signal amplification systems – either Type 1 or Type 6. This meant any probe with Type 1 amplification could be used with any other probe with Type 6, but two Type 1 or Type 6 probes could not be used simultaneously. The lower region of each Z-shaped probe is linked to an upper region specific to the Type 1 or Type 6 amplification system. Sections were then washed and incubated with a preamplifier. These preamplifiers hybridise to the "upper" region of the oligonucleotide probes and form a branched DNA framework for the amplifiers, added in the next incubation step. The amplifiers consisted of long DNA chains with multiple hybridisation sites for the alkaline phosphatase conjugated label probes, either Type 1, which catalysed Fast Red substrate to produce red staining, or Type 6, which catalysed Fast Blue substrate to produce blue staining (illustrated in Figure 3.7). Each red or blue dot formed on the tissue corresponds to probes binding to a single RNA molecule.

Each assay incorporated a negative control to determine the level of background staining – in each case a slide from the same case was stained in full but without the target probe set (Figure 3.8a). Positive controls used included GAPD and CD3 (Figure 3.8b). Before

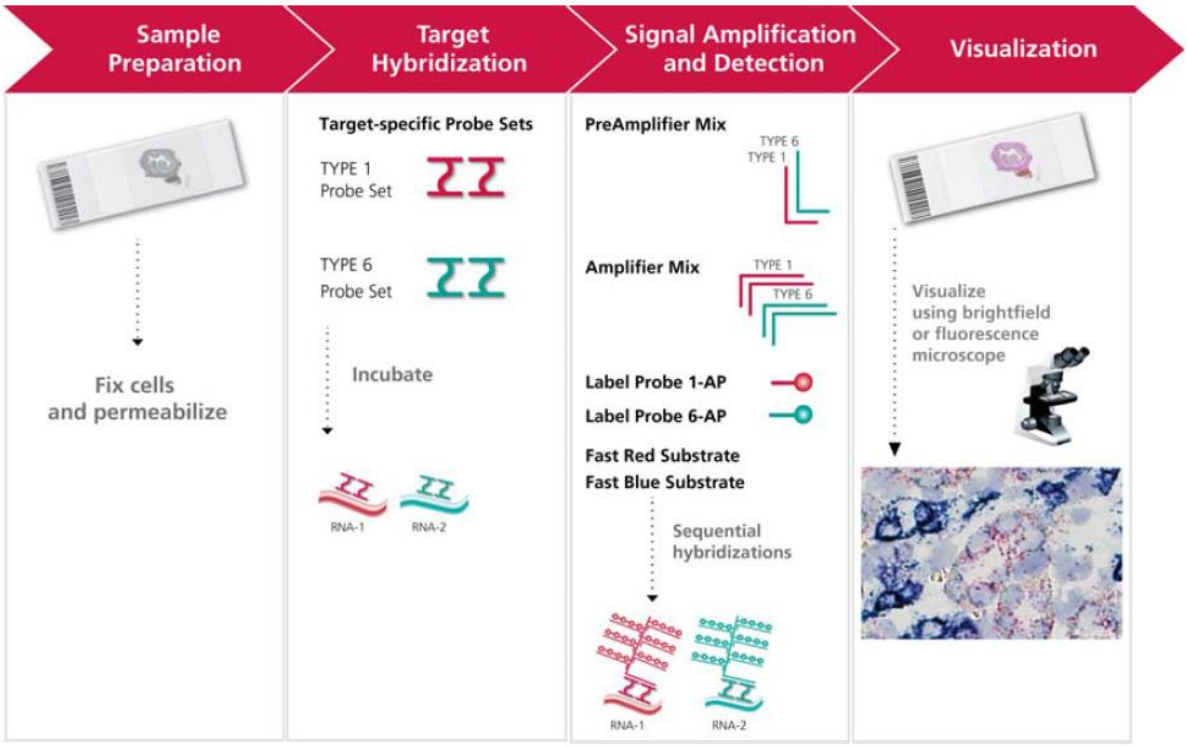

Figure 3.7: Illustration of Affymetrix ViewRNA Tissue 2-plex assay

duplex staining was attempted using gamma delta probes however, 1-plex staining was attempted for the Type 1 probes by omitting the Type 6 probes from the target probe mix. This was to ensure each probe worked consistently without the possibility of methodological issues involved in the visualisation step of the 2-plex assay causing problems. Since the Fast Blue and Fast Red substrates are sequentially developed in this assay, the Fast Blue precipitates that are formed first have the potential to partially block subsequent hybridization of the TYPE 1 Label Probe, by masking its binding sites on a nearby/co-localized target and consequently affecting the development of the Fast Red signal. Another issue discovered was that the Fast Blue was often difficult to distinguish from the haematoxylin counterstain, which is dark blue/ purple in colour. It was difficult to determine whether either potential issue may have been a problem in this experiment however, as single-plex staining did not prove satisfactory.

Results of 1-plex staining in tonsil tissue were generally in line expectations based on previous IHC of tonsil sections, with positive staining noted for GAPD, CD3, Vδ1 and Vδ2, although these results were not achieved every time (Figure 3.8c). In liver tissue, the success rate was considerably lower, even for the GAPD positive control, although positive results were achieved (Figure 3.9).

A number of factors could have contributed to this problem. The protocol had over 150 individual steps and took 2 days to perform and therefore is quite susceptible to variation in the multiple pipetting and washing stages of the protocol. A second issue that didn't become apparent until midway through the study was that when liver tissue was collected in the Centre for Liver Research and fixed in formalin, the length of time it was

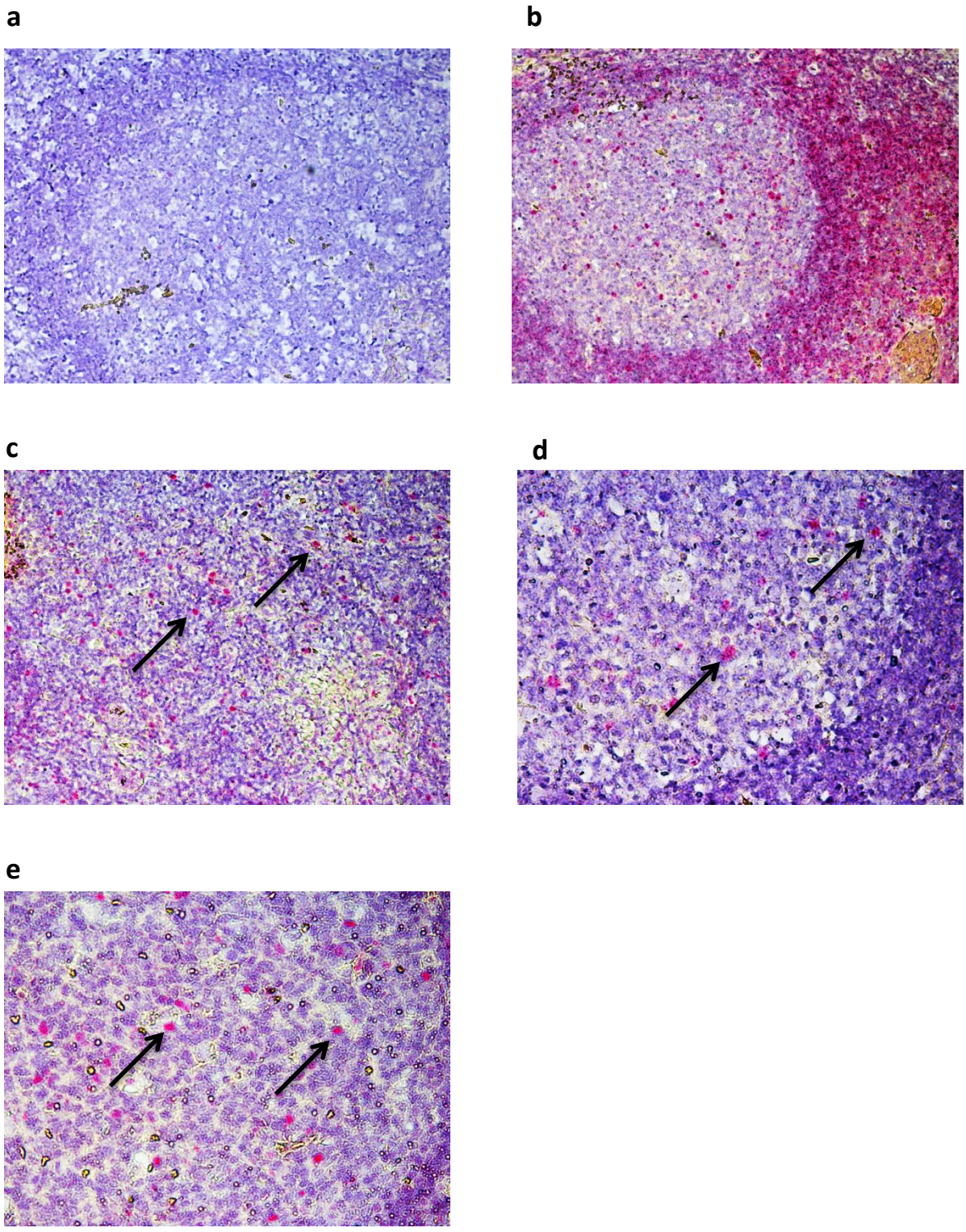

Figure 3.8: Single-plex staining of tonsil sections using Affymetrix ViewRNA in-situ hybridisation

Representative images of FFPE human tonsil sections stained using ISH probes specific for: a) negative control (no probe), b) GAPD, c) CD3, d) Vδ1 and e) Vδ2. Positively stained cells (red) are identified with black arrows. Sections were counter-stained using haematoxylin. Magnification for a-c, 40x and for d-e 20x.

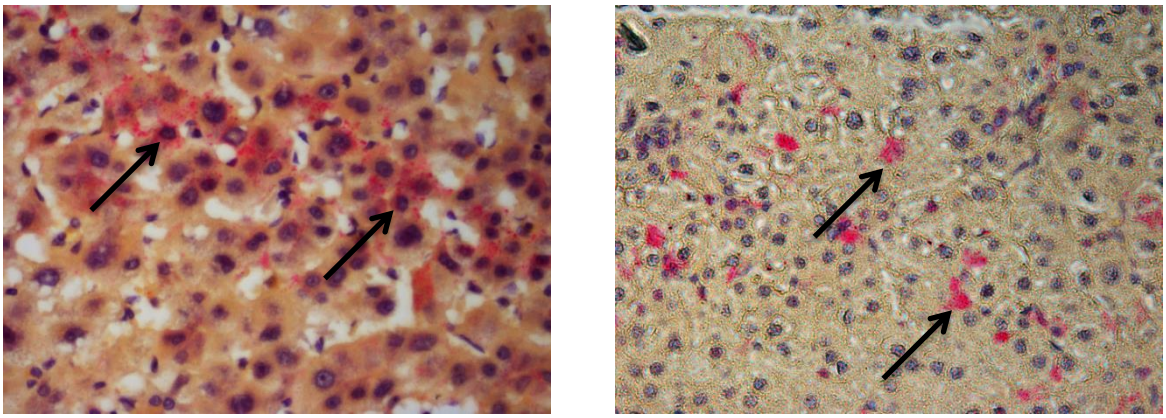

Figure 3.9: Single-plex staining of liver sections using Affymetrix ViewRNA in-situ hybridisation

Representative images of FFPE human liver derived sections stained using ISH probes specific for: GAPD (left) and Vδ2 (right). Positively staining (red) is identified with black arrows, however not all cells are stained positive for the GAPD control and the "cells" marked as positive in the Vδ2 image do not appear to have nuclei. Sections were counter-stained using haematoxylin. Magnification 40x.

fixed for often varied significantly – from 48 hours to over 3 weeks. That meant that each individual case would likely require differing pre-treatment for varying fixation times. While this is possible for IHC-based approaches, the significant cost and complexity of the ISH assay meant optimisation for individual cases became impractical. It did appear that some tissue blocks had been over-fixed, since the pre-treatment times were longer than those recommended and the tissue architecture generally remained good even at longer heat/ protease exposure. This issue could be addressed by using samples obtained from a set fixation period, such as QEHB pathology labs. Bile accumulation in chronic cholestatic disease also formed an unwanted source of interference in both the IHC and ISH-based protocols, forming non-specific "blobs" of staining that potentially masked areas of the section from being correctly stained.

3.3.2.2 RNAscope protocol

Results from the Affymetrix protocol were encouraging but consistency was proving a major challenge. To address this issue, an alternative kit was identified from Advanced Cell Diagnostics (ACD) that had been developed for use with a Leica Bond RX automated system – the RNAscope® 2.5 LS Automated Assay. Liver tissue samples were acquired from the Queen Elizabeth Hospital pathology department rather than the Centre for Liver Research, which would provide a more consistent fixation time, preventing over-fixation of tissue samples and standardising pre-treatment times.

The Bond RX staining protocol was supplied by ACD, and in essence was very similar to the ViewRNA protocol but all incubations and washes were performed by robot rather than by hand. As with the ViewRNA kit, a manufacturer supplied positive control kit was

used to validate the method on our equipment, and the results were in line with the manufacturer's criteria, with the low expression control peptidyl-prolyl cis-trans isomerase B (PPIB) and high expression control RNA polymerase II subunit A (Polr2A) visualised correctly in the brightly coloured red and DAB brown respectively (Figure 3.10a).

As before, the gamma delta probes were then tested on tonsil tissue as a positive control tissue (Figure 3.10b), with positive staining observed for the CD3 and Cδ probes. Each gamma delta TCR probe, in this case Vδ1, Vδ2, Vγ9 and Cδ, was then tested in duplex with CD3 in liver tissue sections. Three cases were selected to be stained based on previous flow cytometry-based frequency analysis from the same tissue, with all three having 5-10% of their $CD3^+$ T cell population represented by γδ T cells, of which roughly half were $V\delta1^+$ in each case. Of the three cases tested using the Bond RX autostainer, only one case had significant positive staining for all of the gamma delta TCR probes used, and would be used as a positive control tissue henceforth (Figure 3.11).

In order to elucidate close cell-cell interactions between γδ T cells and other cells in the hepatic microenvironment, a combination of ISH to stain the γδ T cells and fluorescence IHC was employed. To label the ISH probes with a fluorescent tag, the protocol was modified to include addition of a tyramide signal amplification (TSA) step. However, since this work was carried out, ACD have released their own Multiplex Fluorescent Assay kit that allows combination of ISH and IHC analysis on the same tissue, using a similar approach.

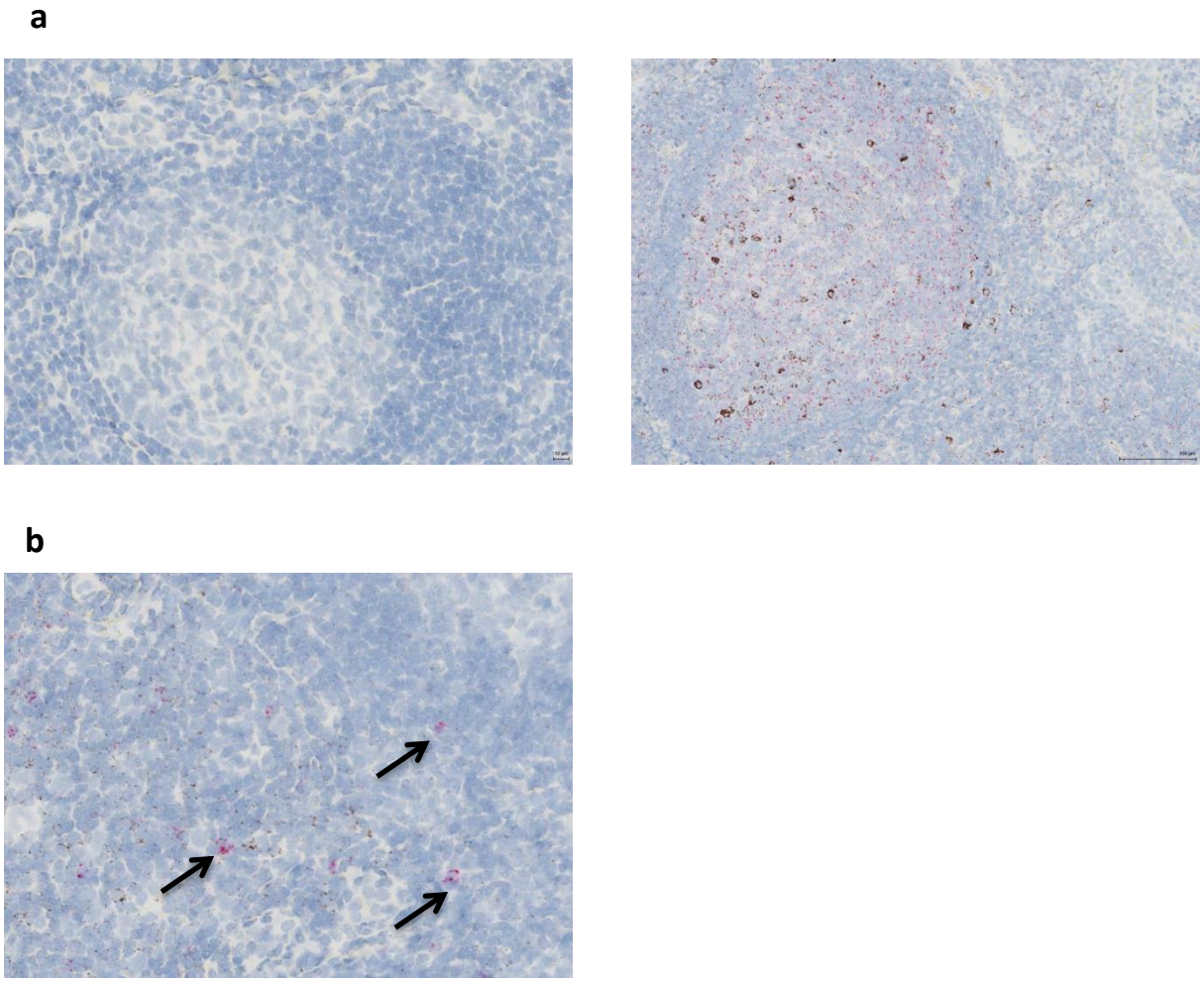

Figure 3.10: 2-plex staining of tonsil sections using ACD RNAscope in-situ hybridisation

a) Representative images of FFPE human tonsil derived sections stained using ISH probes specific for: negative control (left) and PPIB (red) + PolR2A (brown) (right). Sections were counter-stained using haematoxylin. Magnification 20x (left) 40x (right).

b) Representative image of FFPE human tonsil derived section stained using ISH probes specific for CD3 (brown) and constant-region δ chain (red – highlighted with arrows). Sections were counter-stained using haematoxylin. Magnification 40x.

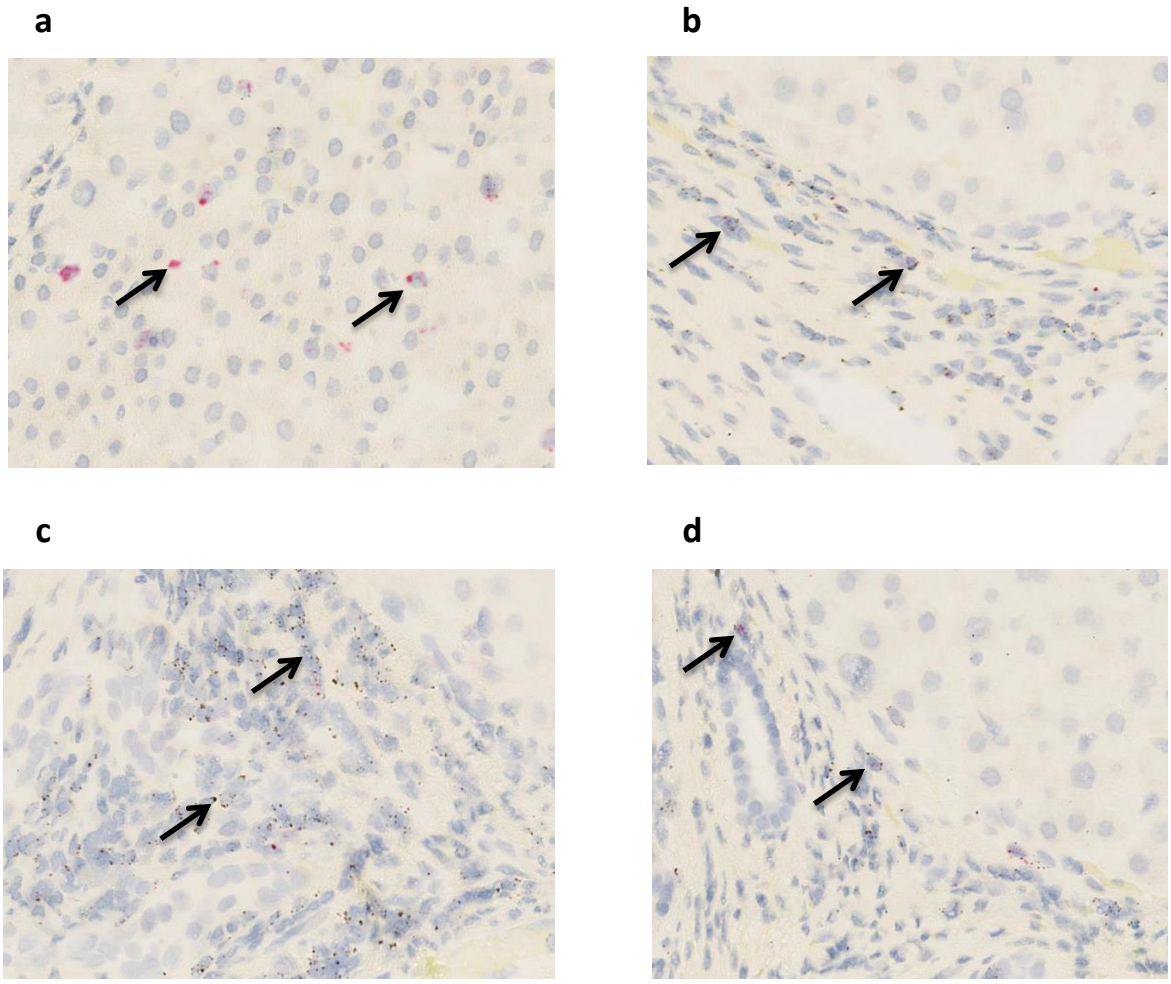

Figure 3.11: 2-plex staining of liver sections using ACD RNAscope in-situ hybridisation

Representative images of FFPE human liver derived sections stained using ISH probes specific for: in all cases CD3 (brown) + TRCD (a), Vδ1 (b), Vδ2 (c) and Vγ9 (d) (red). Positively staining of gamma delta TCR probes (red) is identified with black arrows. Sections were counter-stained using haematoxylin. Magnification 40x.

Firstly, to assess how good the ISH staining was for analysis of individual cells under high levels of magnification (40x), the CD3 ISH probe was stained in conjunction with a CD3 antibody on the same section (Figure 3.12). While a high level of co-staining was observed in $CD3^+$ cells, the punctate, intracellular nature of the ISH staining was clearly not as useful for staining cell-cell interactions as the cell surface IHC staining. Nevertheless, this did highlight the possibility of using a combination of ISH and IHC on the same sections, which would potentially allow for a wide variety of conventional cell surface protein targets to be stained in multiple fluorescent colours by IHC in combination with gamma delta T cell specific ISH probes, then visualised using multi-channel imaging technology such as the Vectra 3.0 Automated Imaging Platform (PerkinElmer). Additionally, since the number of fluorescent tags for ISH probes is much greater than the colours available for bright-field visualisation, this opened the possibility of combining more than two ISH targets in the same tissue, thereby allowing localisation analysis of the three main γδ T cell subsets; Vδ1, Vδ2 and Vδ3; in the same tissue.

Next, duplex staining of two ISH probes visualised in fluorescence was performed in tonsil sections and the slides were scanned digitally using the Vectra platform and analysed using the Definiens Tissue Studio software (Figure 3.13). Using this analysis $V\delta1^+$ cells were found to account for 2.52% of tonsil cells while $V\delta2^+$ cells accounted for 4.85%. While this was considered a successful attempt to use digital scoring to analyse ISH results, something that would be very important for this study going forward, there was some concern over the signal to background noise ratio. According to the manufacturer, as long as the washes are performed correctly, there should be no positive signalling if there is no hybridisation of the probes to their target. With the bright-field analysis,

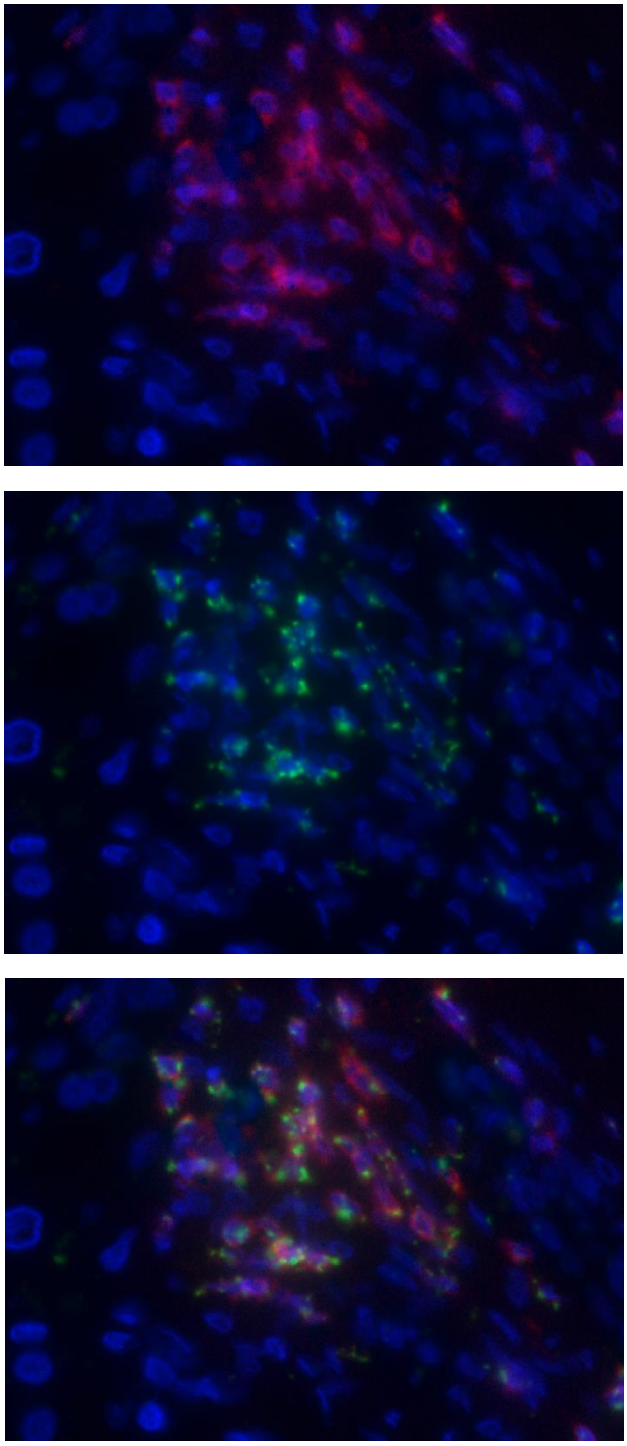

Figure 3.12: Dual IHC and ISH staining of liver sections

Representative images of FFPE human liver derived sections stained using IHC αCD3 antibody (upper) (red) and ISH probes specific for CD3 (centre) (green), and combined (lower). Sections were counter-stained using DAPI. Magnification 40x.

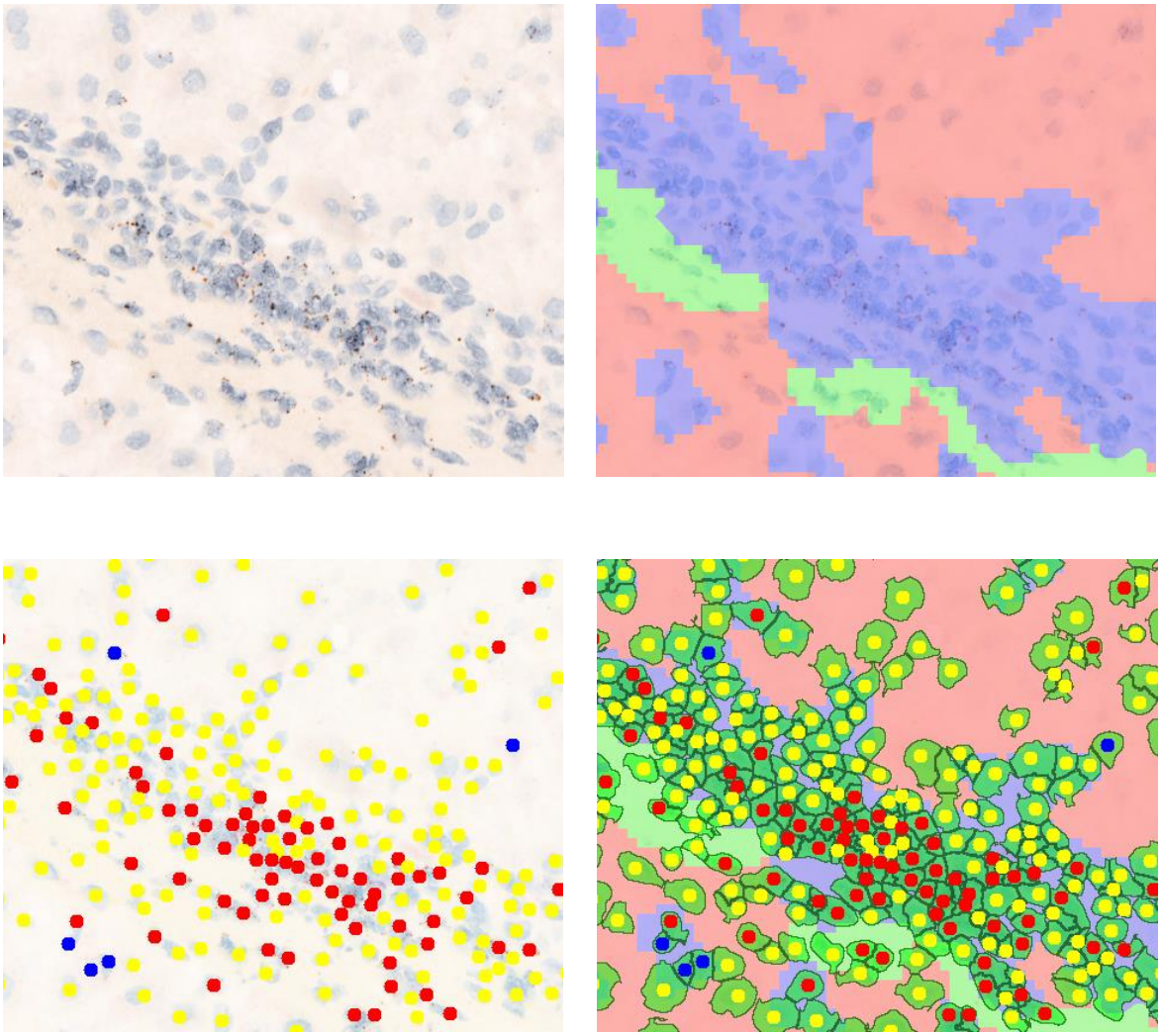

Figure 3.13: Definiens analysis of gamma delta T cell staining in human liver

Example of images generated using Definiens tissue analysis software. Top left: example field of liver section stained using RNAscope probes specific to CD3 (brown) and TRDC (red). Bottom left: the same field with staining scored using Definiens software – yellow dots are negatively stained cells, red dots are $CD3^+$ cells, blue dots are $TRDC^+$ and $CD3^+$ cells. Top right: liver tissue coloured according to histology – red areas are parenchyma, blue areas are portal and green areas are fibrous septa. Bottom right: Overlay image including histology, cell identification and cellar boundaries (indicated in dark green colour). Sections were counter-stained using haematoxylin. Magnification 40x.

background did generally seem low, so differing concentrations of the TSA tags were used in an attempt to reduce fluorescence background, which essentially seemed to consist of random dots of colour in areas that were clearly not positive, such as outside cell boundaries. However, no reduction in the number of false positive background dots could be achieved. Clearly non-specific "positive" dots, even at low level, would cause over estimation of staining by the scoring software. This was exacerbated by the generally low level of staining observed for the variable-δ and –γ chain probes, which were only 7 oligonucleotides in length rather than the manufacturer's preferred 20, which the strongly staining CD3 probe was.

To investigate whether the variable-region TCR probes were working effectively enough to raise positive staining above background noise, critical to the success of any scoring analysis, paraffin embedded tissue blocks were prepared from two T cell lines that had been transfected with either a $V\delta1^+$ TCR clone or a $V\delta2^+$ TCR clone. The blocks were sectioned and stained as per the RNAscope protocol. In addition to determining the level of staining, this would also provide a good control for probe specificity, since none of the assays performed thus far used tissue with precisely known frequencies of gamma delta T cells (Figure 3.14).

While there was no $V\delta2^+$ staining on the $V\delta1^+$ tissue block when the Vδ2 probes were used, and vice-versa, comparison of the CD3 staining and both Vδ1 and Vδ2 showed that while CD3 staining was clearly evident in all cells, many cells that were known to be positive for a given variable-region were often very dimly or negatively stained. Considering the mRNA levels in these transfected cells was likely to be higher than cells *in*

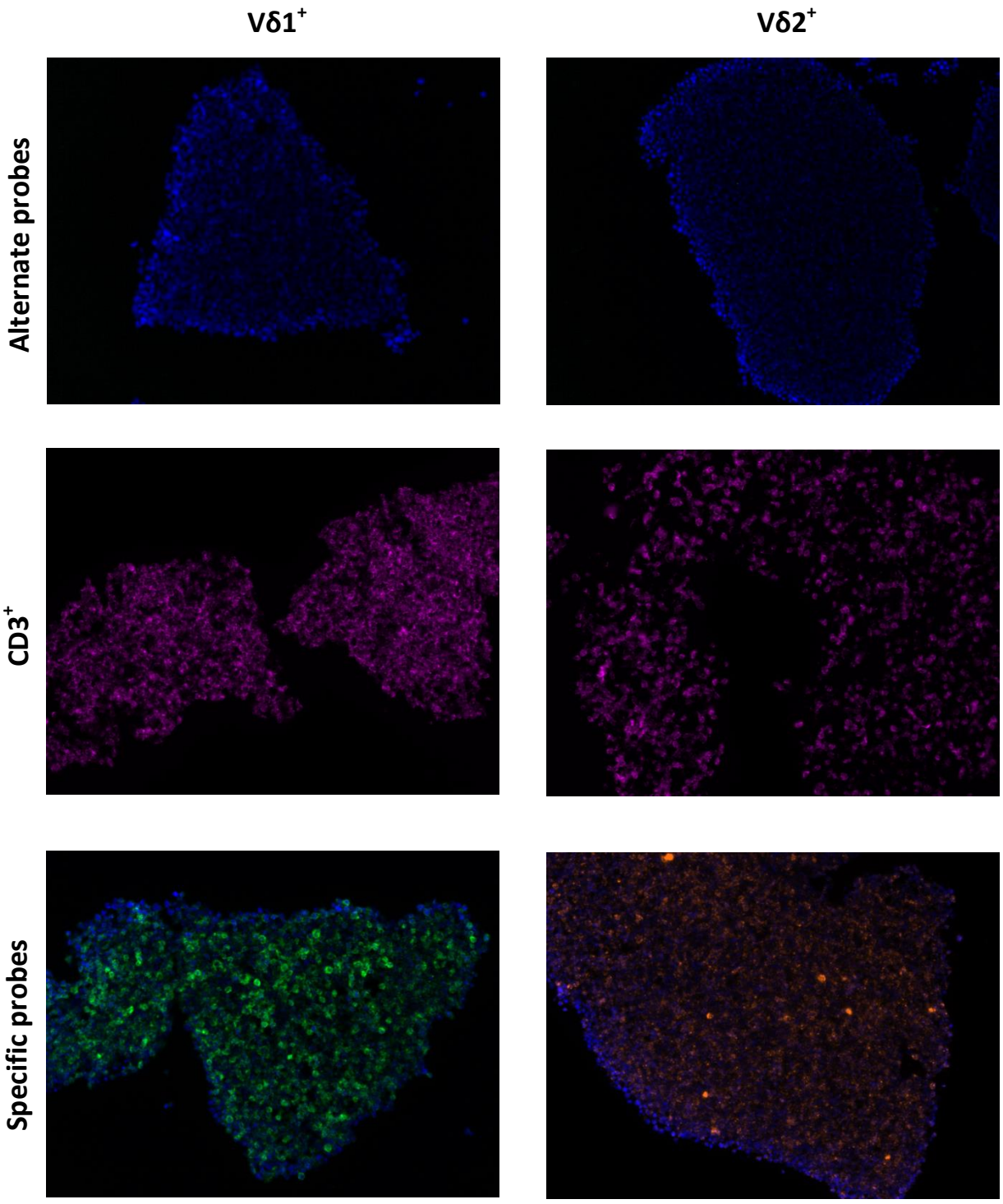

Figure 3.14: Fluorescent ISH assessment of Vδ1- and Vδ2-specific probes using transfected cell lines

Representative images of ISH staining of sectioned paraffin-embedded Jurkat cell lines transfected with either a Vδ1$^+$ TCR clone (left) or a Vδ2$^+$ TCR clone (right). Top: Probes specific to the alternate TCR were used to assess potential non-specific binding. Middle: CD3$^+$ staining using ISH probe. Lower: Vδ1$^+$ or Vδ2$^+$ positive staining, with image intensity increased by 300% in post-processing. Sections were counter-stained using DAPI. Magnification 20x.

vivo, and that the fixation of these cells was very quick after harvesting, minimising RNA degradation, it seems likely that these probes are not sensitive enough to stain enough of their targets to produce a reliable, quantifiable result. Since the CD3 probes did work consistently, it can be speculated that the reduced number of oligonucleotide sequences targeted by the variable-region probe sets, a necessity due to their short overall length, is the primary reason for this shortcoming. While this may not be an issue if the target cells were high in frequency, the relative paucity of them in liver tissue meant in the context of this study this technique would ultimately be flawed and not likely to yield useful results.

3.4 Gamma delta T cells interaction with HSEC *in vitro*

Through the use of IHC and ISH-based tissue visualisation methods, a high frequency of gamma delta T cells has been observed apparently localised in, our adjacent to, the hepatic sinusoids. Additionally, they represent a very high proportion of infiltrating $CD3^+$ T cells here. To determine whether interactions of gamma delta T cells with the dominant stromal subset of the sinusoids, the hepatic endothelium, may influence this apparent accumulation, adhesion and transmigration assays using primary human HSEC and PBMC-derived gamma delta T cells were performed.

3.4.1 Static adhesion assay

Firstly, a static adhesion assay was used to assess potential preferential adhesion of PBMC-derived gamma delta T cells to a monolayer of HSEC. This was performed using both unstimulated HSEC, to represent normal liver, and HSEC stimulated prior to the assay with pro-inflammatory TNF and IFNγ, exposure to both of which has been

demonstrated to upregulate expression of lymphotactic adhesion molecules in HSEC (Lalor *et al*., 2002) and a factor in chronic liver inflammation (Curbishley *et al*., 2005). Magnetically sorted $CD3^+$ cells were added to the monolayer and incubated for 15 minutes. In both stimulated and unstimulated conditions, the proportion of gamma delta T cells amongst adherent $CD3^+$ T cells increased (+16.1% ± 12.2% unstimulated, +58.5% ± 15.1% stimulated, n=3), suggestive of increased adherence to HSEC for these cells compared with non-gamma delta $CD3^+$ T cells, even in "non-inflamed" conditions where the HSEC are not activated by pro-inflammatory cytokines (Figure 3.15a). Interestingly, the $V\delta2^+$ population appeared to adhere better to HSEC than the $V\delta2^-$ gamma delta T cells in both conditions (+19.0% vs. +3.8% unstimulated, +61.8% vs. +45.0% stimulated), but this was not statistically significant.

3.4.2 Transmigration assay

Having demonstrated superior adhesion of gamma delta T cells to primary HSEC compared with non-gamma delta T cells, transmigration across an endothelial monolayer assessed using a transwell assay. Here, PBMC-derived T cells were added to the upper chamber of the transwell system cells and then were harvested from both upper and lower chambers of the transwell system following 48 hour incubation. The enrichment of gamma delta T cells in the lower chamber compared with the upper chamber following the assay was determined (Figure 3.15b). As with the static assay, in both stimulated and unstimulated conditions the proportion of gamma delta T cells in the lower well (i.e. having successfully transmigrated) increased relative to non-gamma delta

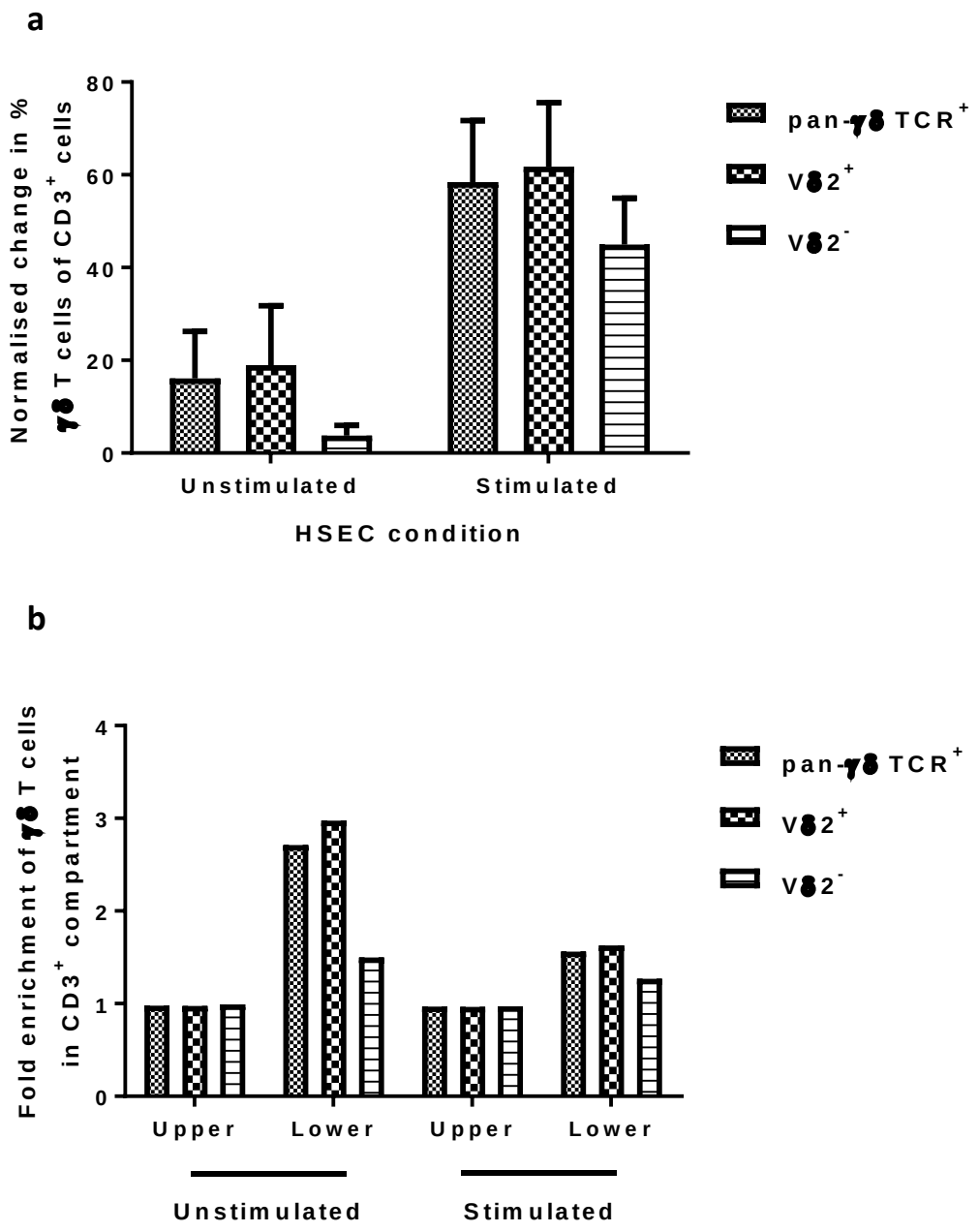

Figure 3.15: Interaction of γδ T cells with HSEC

a) Static adhesion of PBMC-derived γδ T cells to a monolayer of primary human unstimulated and stimulated hepatic sinusoidal endothelial cells (HSEC). Bars represent the increase in percentage of γδ T cell subsets as a proportion of $CD3^+$ cells in the HSEC-associated lymphocyte population after 15 minute incubation with HSEC (n=3 blood and 3 HSEC donors).

b) Transmigration of PBMC-derived γδ T cell subsets across an unstimulated and stimulated primary human HSEC monolayer in a transwell system. Bars represent the fold enrichment of γδ T cell subsets as a proportion of $CD3^+$ T cells in the upper (non-migrated) and lower (migrated) chamber of the transwell after 48 hours incubation (n=3 blood and 3 HSEC donors). Error bars = SEM.

T cells. Contrary to the static assay, in this experiment a significantly increased migration of gamma delta T cells was noted in unstimulated conditions (2.71-fold increase across unstimulated HSEC, 1.56-fold increase across stimulated HSEC, n=3, p=0.03). $V\delta2^+$ cells migrated more readily into the lower chamber than $V\delta2^-$, although this was more notable in unstimulated conditions (2.97-fold increase vs. 1.5-fold increase) than stimulated (1.63-fold vs. 1.27-fold).

3.4.3 Immunophenotyping of intrahepatic gamma delta T cells

To highlight potential molecular mechanisms that may explain these observations, surface expression of lymphocyte function-associated antigen-1 (LFA-1), platelet endothelial cell adhesion molecule (CD31) and killer cell lectin like receptor B1 (CD161) and α_E integrin (CD103) on intrahepatic $\alpha\beta$ TCR^+, $V\delta2^{neg}$ and $V\delta2^+$ T cells were analysed by flow cytometry. Expression of LFA-1 on $CD8^+$ liver infiltrating T cells has been implicated in association with HSEC (McNamara *et al*., 2017), while CD31 and CD161 have been implicated in endothelial transmigration of $V\delta1^+$ and $V\delta2^+$ cells respectively (Poggi *et al*., 2002, Poggi *et al*., 1999) and CD103 is expressed by memory $CD8^+$ T cells to retain them within tissues (Strauch *et al*., 2001). $V\delta2^{neg}$ cells had significantly increased surface expression of CD31 (68.7% ± 3.9%) compared with $\alpha\beta$ T cells (29.5% ± 3.0%, p=0.0004) and were slightly enriched for LFA-1 expression, which was very high in $V\delta2^{neg}$ T cells overall (91.5% ± 2.8%). $V\delta2^+$ cells expressed similarly high levels of CD161 (90.8% ± 2.8%), while gamma delta T cells did not express high levels of CD103 ($V\delta2^{neg}$: 6.96% ± 2.17%; $V\delta2^+$: 4.39% ± 0.88%). These data suggest that LFA-1 and/ or CD31

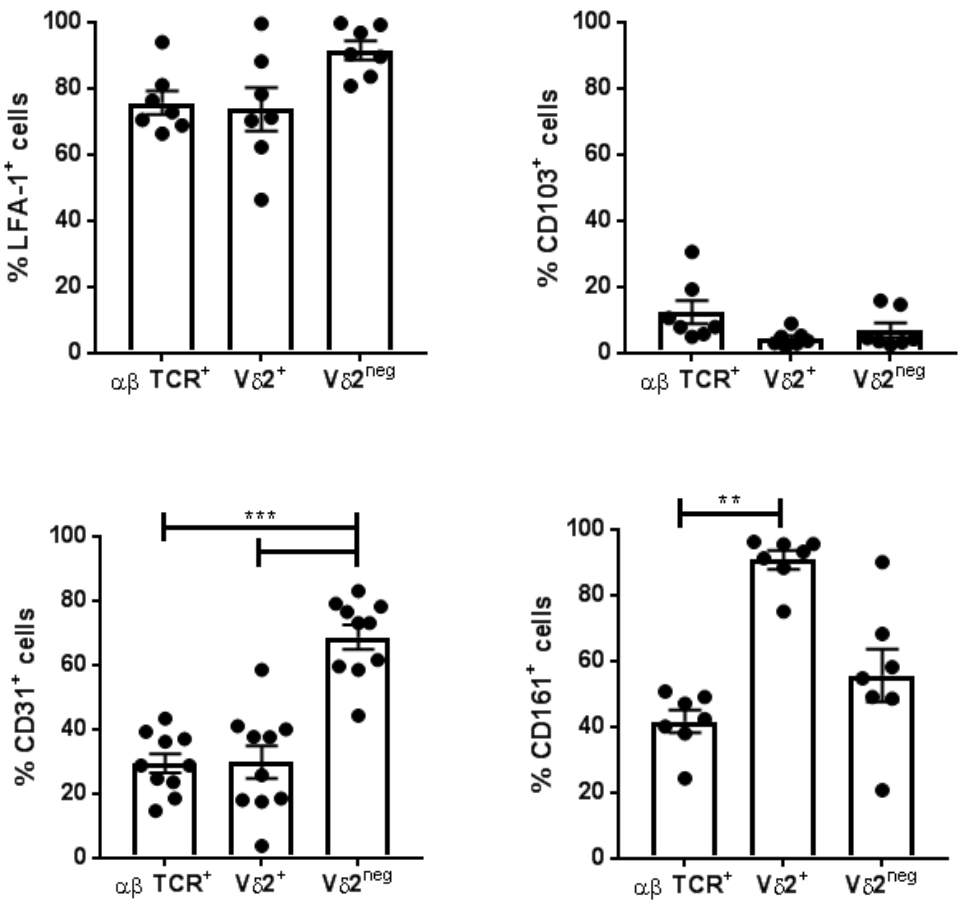

Figure 3.16: Intrahepatic gamma delta T cells are enriched for various adhesion/ transmigration molecules

Comparison of mean ± s.e.m expression of various surface markers previously implicated in cell adhesion and/or transmigration across endothelium in liver-derived αβ TCR^+, $V\delta2^+$ and $V\delta2^{neg}$ T cell subsets, measured by flow cytometry. n=7-10 ALD, NASH, PSC and PBC explants, **p<0.01, ***p<0.001, 1-way ANOVA

expression may be important factors in retention of Vδ2^{neg} T cells in the hepatic sinusoids.

3.5 Discussion

Despite several previous studies having highlighted the relative enrichment of gamma delta T cells in human liver compared with the periphery, few studies have investigated where within the liver microanatomy these cells are distributed. Since the role of gamma delta T cells in liver biology and chronic inflammation is poorly understood, knowledge of the localisation of these cells within the liver could be crucial in determining which cells will be interacting with these unconventional lymphocytes and therefore provide clues as to their function.

Two methods were adopted to investigate this question, IHC and ISH. Although a robust dataset was generated from the IHC in terms of infiltration and gross localisation, due to limitations with the primary antibody and the liver tissue itself, fluorescence based confocal IHC, which would have ideally allowed detailed co-localisation analysis using multiple fluorophores, was not possible, which does limit the scale of this study. Although convincing results were obtained, the polyclonal goat H-20 antibody used has since been discontinued by the manufacturer. A new monoclonal antibody has been made available in its stead, and it would be interesting to see if better results would be achievable with fluorescence IHC for future co-localisation studies. The problem with varying fixation times of the tissue blocks before sectioning, which was not realised until the ISH protocol was being used, may well have caused the not infrequent problems

encountered when using the H-20 clone. Additionally, it should be remembered that these data were obtained from staining of sequential sections, rather than simultaneous γδ and CD3 staining on the same section, and is therefore subject to some error. More extensive use of the ISH would solve this, although the cost involved was too high considering the IHC dataset was relatively robust.

The IHC dataset suggested a relatively high burden of gamma delta T cells as a percentage of total infiltrating $CD3^+$ T cells,. While these figures are in line with previously published data, it is important to assess whether there may be any systematic reasons for the high percentages noted here. Firstly, the majority of the frequency data published have been generated from flow cytometry analysis of bulk tissue that has been mechanically and/or enzymatically disrupted to isolate lymphocytes. Since many of the gamma delta T cells identified via IHC in this study were parenchymally associated, that is, either in the liver sinusoids or having migrated across the sinusoidal endothelium, it is possible that these cells are more firmly "tissue associated" than transiently passing "blood associated" cells of the portal tract areas. Therefore one could envisage these cells may be harder to extract from bulk liver tissue than portally associated αβ T cells when isolating cells for flow cytometry analysis, and therefore decreasing the apparent percentage of total T cells represented by gamma delta TCR^+ cells. This phenomenon has been reported in studies of tissue associated $CD8^+$ T cells in mice (Steinert *et al*., 2015).

Another potential possibility is that since the antibody used was specific for a δ-chain epitope, it was staining positive for αβT cells that also express δ-chain TCR. Cells expressing the constant δ-chain and an αβ TCR are rare, however (Pellicci *et al*., 2014).

This could be addressed by co-staining with an anti-αβ TCR antibody on the same section as the pan-γδ antibody, which would be possible using a two-stage protocol and visualising with two fluorophores, for example DAB and alkaline phosphatase.

Despite this, a clear finding from this study is that normal liver contains a higher frequency of gamma delta T cells than diseased liver. Why this occurs is not entirely clear. It is known that circulating gamma delta T cells, particularly those with the $V\delta2^{+}$ TCR, express high levels of inflammation associated chemokine receptors such as CXCR3 (Glatzel *et al*., 2002). One may expect that on instigation of a chronic inflammatory event, these cells would be more readily recruited to the site of inflammation, in this case the liver, than the more abundant circulating $CXCR3^{lo}$ naïve and memory αβ T cells, and thereby increase in relative numbers in disease. What was particularly interesting though was the suggestion that the overall number of infiltrating γδ lymphocytes did not numerically increase during disease, particularly in parenchymal areas, while non-γδ, assumed to be αβ TCR^{+} cells, did. This may hint at dilution of a pre-existing γδ T cell population present in parenchymal areas of the liver of healthy livers by infiltrating periphery-associated T cells in disease. Since the burden of gamma delta T cells in these regions is clearly much higher than in the periphery, where typical healthy adults may have 2-5% of their T cell population as γδ TCR^{+}, it would follow that non-selective recruitment and retention of all peripheral T cells in chronic inflammation would by its nature dilute the number of γδ T cells present in the liver, irrespective of inflammation induced cell recruitment. Whether this means the "pre-existing" parenchymal population is a resident population requires further study, and explored further in Chapter 5 of this thesis.

The data obtained from the *in vitro* migration assays is intriguing, as it suggests gamma delta T cells in circulation are likely to be better at both adhering to and transmigrating across the hepatic endothelium compared with other $CD3^+$ T cells. Additionally, this observation held whether the endothelium was inflamed using pro-inflammatory exogenous recombinant cytokines or not. It could be hypothesized that enhanced recruitment and/or retention of gamma delta T cells from the periphery to the hepatic endothelium may, at least in part, be responsible for the observed high levels of parenchymally associated liver-infiltrating gamma delta T cells in both health and disease, although the precise molecular mechanism behind such an observation is unclear. Previous research on lymphocyte adhesion and recruitment in the liver has highlighted a number of molecular interactions important to these processes, including LFA-1-ICAM and vascular adhesion protein-1 (VAP-1). Gamma delta T cells express high surface levels of CXCR3, CD31, LFA-1 and VLA-4, all of which have been implicated in trans-endothelial recruitment of lymphocytes into tissues (Chosay *et al*., 1998, Lalor *et al*., 2002, Tuncer *et al*., 2013). Further research using blocking antibodies and G-protein coupled receptor inhibitors could shed further light on this, as well as flow-based adhesion assays that would be more representative of physiological conditions and may be important in upregulation of certain adhesion molecules (Shetty *et al*., 2014, Lawrence *et al*., 1997). A critical observation from this study however, was that relative transmigration of gamma delta T cells was significantly higher in unstimulated conditions compared with across stimulated HSEC. This supports the hypothesis that inflammation may drive a general T cell recruitment upshift that ultimately may reduce the overall proportion of gamma delta T cells in the liver, compared with normal physiological conditions. Clearly, further efforts to distinguish between recruitment-based enrichment of intrahepatic gamma

delta T cells and potential tissue residency of these cells are required to more thoroughly assess the biology of these cells in the liver.

The parenchymally dominated distribution of the intrahepatic gamma delta T cell population is interesting, and has not previously been reported. Kupffer cells are located in the liver sinusoids, where they are capable of capturing bacteria directly from the blood flow (Jenne and Kubes, 2013). Lymphocytic cells such as $CD8^+$ αβ T cells and NKT cells have been demonstrated to remain within the sinusoids rather than extravasate into the parenchymal areas (Guidotti *et al*., 2015, Geissmann *et al*., 2005), where it is posited that contact with the parenchymal hepatocytes is enabled by the fenestrations in the sinusoidal endothelium. Although confocal fluorescence imaging of these tissue sections may have helped to determine whether the gamma delta T cells identified in the liver parenchyma had truly migrated across the endothelium or were still within the sinusoids, without a mouse model such as those used to image NKT and $CD8^+$ cells in previous studies, it is very hard to prove. Nevertheless, one could speculate that gamma delta T cells likely share a similar biology to these other T cell subsets, and via close proximity to both gut derived antigen in the portal blood flow and perhaps more pertinently close proximity to sinusoidal Kupffer cells and the cytokines they secrete, may form part of the liver associated "firewall", capable of responding quickly to gut associated antigen (Balmer *et al*., 2014). This scenario is given credence by the fact that healthy liver is heavily enriched for these cells, as this process is clearly a vital one in maintaining immunosurveillance in normal conditions.

While the results obtained with the ISH method were not ultimately successful here, the ability to distinguish between different subsets of gamma delta T cells based on V-chain usage in human tissue sections would represent a fundamental step forward in human γδ T cell biology, and should be pursued. Although the probe sets used here seemed insufficiently sensitive, the methods did prove to be fundamentally sound, with positive staining detected for each of the three most common variable-δ chain TCRs. It may be that ACD's new BaseScope^{TM} technology will prove a successful route to achieving this, being designed for detection of shorter RNA targets than RNAscope, with increased signal amplification. Indeed, the manufacturers claim to have used it to stain for specific CDR3 regions of TCR clonotypes. It will not be cheap but should prove more consistent than the poor quality IHC-based options available to the gamma delta T cell research community currently available.

4

TCR repertoire of intrahepatic gamma delta T cells

4.1 Introduction

One of the most significant unresolved questions concerning gamma delta T cell biology is the extent of the role of the T cell receptor (TCR) in the physiological function of these cells. Two primary issues are currently under investigation – firstly, what role does TCR signalling play in the function of gamma delta T cells, and secondly, what antigens are γδ TCRs capable of recognising? Through improved understanding of the nature of the TCR repertoire, particularly in the poorly understood context of human solid tissues, this study will attempt to shed light on this important issue.

Somatic recombination of the variable (V), diversity (D) and joining (J) gene segments of the TCR locus to form antigen receptors is a crucial feature of adaptive immunity. In addition to these recombination events, further diversity is generated through non-templated addition (n-addition) or exonuclease mediated deletion of nucleotides at the interface of segment recombinations. Upon successful recombination and, in the case of αβ T cells, positive selection from thymic epithelial cells, mature immunocompetent T cells enter the circulation and form part of that individual's T cell repertoire. The αβ TCR repertoire diversity has been demonstrated to be extremely large (Zarnitsyna *et al*., 2013), allowing potential recognition of a huge number of epitopes.

The recombined junction of V, D and J segments forms the complementarity determining region 3 (CDR3). This area comprises the main contact patch with antigenic epitopes, and therefore is crucial in directing specific antigen recognition by the TCR (Davis *et al*., 1998, Jorgensen *et al*., 1992). Some VDJ rearrangements are simpler to generate than others, potentially leading to convergent overlap in easily recombined CDR3 regions (Madi *et al*.,

2014), however the huge number of theoretical CDR3s in any naïve T cell repertoire means the vast majority are likely to be unique for each T cell. Proliferating T cells retain their clonotypic TCRs, therefore any expansion, whether due to TCR independent homeostasis or TCR dependent antigen driven response results in a clonal population of cells with identical CDR3s. Such clonal expansions can be detected in αβ T cell vaccine responses and lymphoproliferative disorders such as lymphoma (Gong *et al*., 2017), as well as in responses to viral infection, such as CMV (Butz and Bevan, 1998).

Human γδ T cells exhibit a more restricted repertoire of V and J gene segment use than αβ T cells, with just three conventional Vδ genes embedded in the α-TCR gene locus; Vδ1, Vδ2 and Vδ3 (Figure 4.1). A handful of Vα genes are occasionally recombined to form a δ-chain: Vδ4 (Vα14), Vδ5 (Vα29), Vδ6 (Vα23), Vδ7 (Vα36), and Vδ8 (Vα38). Similarly, the human Vγ repertoire consists of only 12 Vγ genes, and of these 5 are pseudogenes, leaving just seven functional. Additionally, gamma delta TCRs draw from a total of just nine J gene segments, contrasting with 72 from the α and β loci. The apparent lack of potential diversity of gamma delta TCRs compared with αβ T cells has been attributed to their recognition of conserved self-antigens (Janeway *et al*., 1988).

However, although there are few V and J gene segments used in the γδ TCR, unlike αβ TCRs, the γδ TCR often incorporates multiple D segments, which can recombine in forward or reverse frame and often without stop codons. This plasticity in D segment usage confers incredible diversity on to the amino acid sequence of the CDR3δ loop, indeed it is the most diverse loop found in any rearranged receptor (Davis and Bjorkman, 1988). Quite what the impact of this ultra-variable antigen binding loop in the γδ TCR is on the nature of its targets is currently unclear.

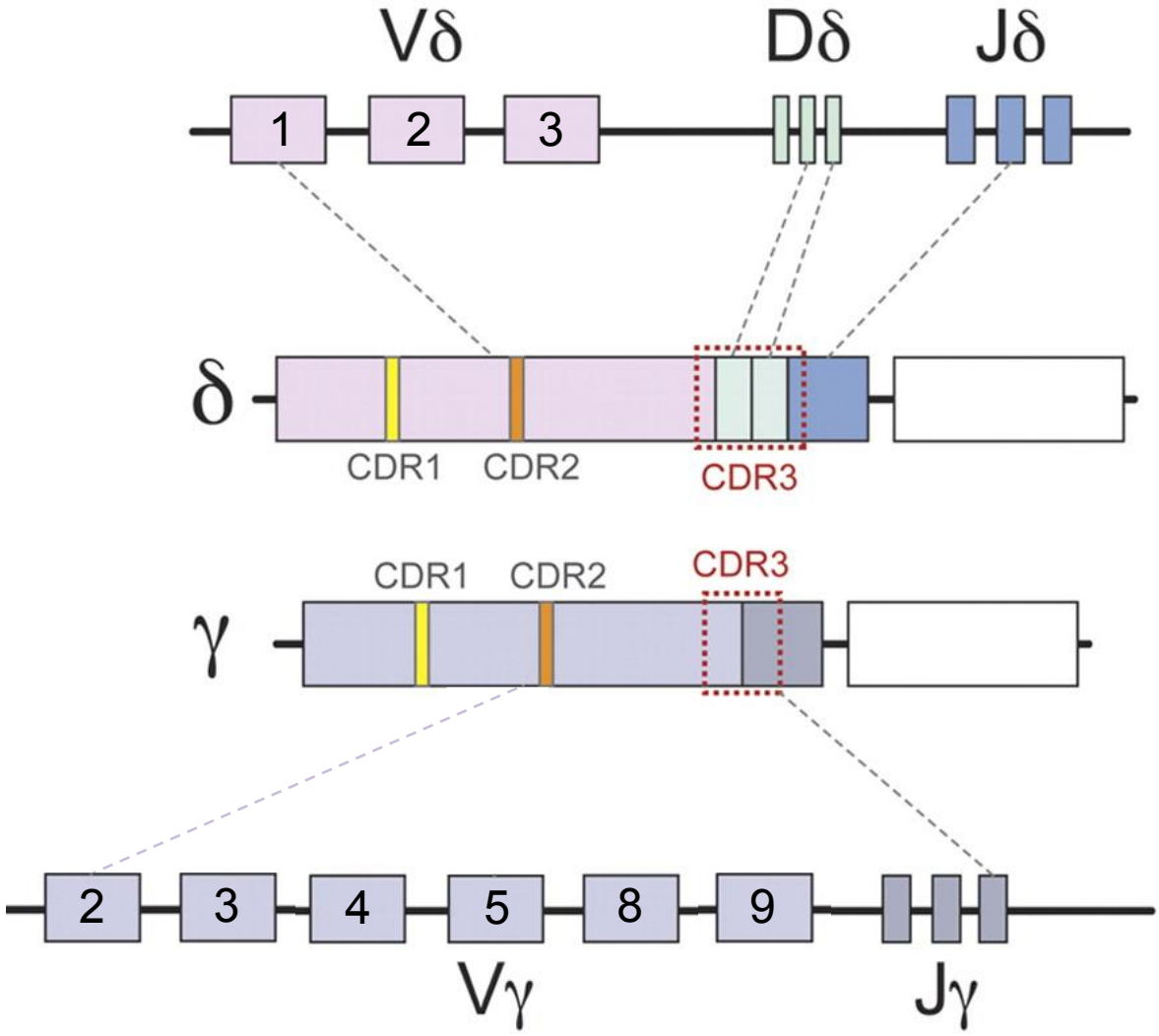

Figure 4.1: Rearrangement of V, D and J segments to form the γδ TCR

Representation of the V-D-J recombination to produce the δ-chain and V-J recombination to produce the γ-chain of the γδ TCR, with CDR1, 2 and 3 loops denoted. Adapted from (Kazen and Adams, 2011).

Despite the vast array of potential αβ TCRs, several subsets of T cells have been identified that express an invariant α-chain, including invariant natural killer T (iNKT) cells, which express Vα24-Jα18 paired with a limited range of β-chains in humans and recognise α-galactosylceramide presented by the monomorphic MHC-like CD1d (Lantz and Bendelac, 1994, Exley *et al*., 1997). Mucosal associated invariant T (MAIT) cells express a semi-invariant α-chain, *TRAV1-2/TRAJ12/20/33*, and recognise bacterial riboflavin metabolites presented by the MHC-like MR1 molecule (Treiner *et al*., 2005). As such, T cells such as these, which recognise conserved ligand via relatively non-polymorphic presentation machinery have been termed innate-like T cells, functioning via PAMP-like recognition in contrast to the stochastically recombined αβ TCR recognition of polymorphic MHC/ peptide complexes, or antibody recognition of polymorphic three-dimensional protein antigens.

Which paradigm gamma delta T cells fit into is currently debated. Although murine gamma delta T cell subsets are not homologous with human, a great deal of work has been performed using mouse models to investigate gamma delta T cell development and function. Early studies identified a VγJγ1Cγ-Vδ1 TCR bearing population of dendritic epidermal T cells (DETC) in the epidermis of mice (Asarnow *et al*., 1988, Havran *et al*., 1989). Other tissues in mice, including uterus, lamina propria and liver (Itohara *et al*., 1990, Sheridan *et al*., 2013, Hamada *et al*., 2008) are home to gamma delta T cells bearing the same Vδ1 chain as DETC, this time paired with an invariant Vγ6Jγ1Cγ1 TCR. Of relevance to the liver, an IL-4 producing subset has been identified in mice bearing a semi-invariant Vγ1Jγ4Cγ4 -Vδ6Dδ2Jδ1 TCR (Gerber *et al*., 1999). In many cases the use of specific γδ TCRs in murine tissues is linked with specific functional capability, such as

interferon-γ or IL-17 production (O'Brien and Born, 2010, Kashani *et al*., 2015). This restriction in diversity is highly suggestive of recognition of conserved, often self-encoded ligand and an essentially innate-like biology.

In humans, the traditionally blood-associated Vδ2^{+} gamma delta T cells appear to conform to an innate-like paradigm. Featuring a conserved chain pairing of Vδ2 and Vγ9, they also display restricted CDR3 region diversity with a common amino acid motif found in most cells (Sherwood *et al*., 2011) that is indicative of reactivity to pyrophosphate antigens. Universal activation by bacterially derived phosphoantigens, dependent on interaction with butyrophilin-like molecule BTN3A1 (Rhodes *et al*., 2016) is highly suggestive of a similar biology to the established innate-like T cell subsets.

In contrast, the non Vδ2^{+} gamma delta T cells in humans (Vδ2^{neg}) do not appear to exhibit the same degree of chain pairing restriction and to date no conserved family of antigen has been discovered, although following CMV infection in utero a germline encoded Vγ8Vδ1 TCR was identified in multiple individuals and has subsequently been identified in other donors (Vermijlen *et al*., 2010). Vδ2^{neg} gamma delta T cells have also been demonstrated to respond to other viruses including Epstein-Barr virus (Farnault *et al*., 2013), and cancer cell lines (Halary *et al*., 2005). Despite this, other work has determined that while functionally active Vδ2^{+} gamma delta T cells are dominant in the second trimester foetus (Dimova *et al*., 2015), Vδ2^{neg} T cells are present at very low frequencies at birth, suggestive of post-natal expansion in response to antigenic stimulation (Morita *et al*., 1994).

Previous studies of human liver-derived gamma delta T cells have indicated that the liver is enriched for both Vδ1^{+} and Vδ3^{+} TCRs compared with the periphery (Agrati *et al*., 2001,

Kenna *et al*., 2004). However, both these studies were conducted either in a specific inflammatory context, namely HCV infection, or on a relatively low number of donor livers. In addition, no detailed analysis of TCR repertoire beyond γ- and δ-chain use has been conducted. The aim of the study in this chapter was to assess human intrahepatic and peripheral gamma delta T cell TCR repertoire using next generation sequencing techniques, with the intention of shedding light not only on TCR chain usage but also specific CDR3 composition within these samples, allowing assessment of clonality and sample diversity, focussing on the tissue associated $V\delta2^{neg}$ population.

4.2 Method

4.2.1 Tissue acquisition

Throughout this study, comparison is made between "normal" and "diseased" liver. Genuinely normal liver tissue is challenging to obtain, since healthy functioning tissue is transplanted into an unwell recipient wherever possible. Occasionally livers are too big for their recipient, often in the case of children receiving livers from adult donors, in which case "cut-downs" are sometimes available for research purposes. On other occasions mis-handling of the donor liver during retrieval can leave it unsuitable for transplantation. Liver tissue obtained from hepatectomy for tumour removal was only used if no radio- or chemo-therapeutic regimen had been undertaken by the donor prior to resection, and if there was no chronic liver disease background. Since primary hepatocellular carcinoma (HCC) is fairly rare on a non-inflamed background, the primary source of resected liver material that was considered "normal" was from patients undergoing surgery to remove colorectal metastases. The most common reason for the

Centre for Liver Research to obtain “normal” liver, however, is if it was rejected for transplantation because it was deemed too steatotic. In these cases, which often may be undiagnosed fatty liver disease, the liver was inspected visually – if it was markedly discoloured or fatty it was not used in this study. At the time of processing, all patient data were fully anonymised in accordance with the ethics protocols established in the Centre for Liver Research.

4.2.2 Lymphocyte Isolation

Isolation of lymphocytes from human liver has been performed routinely in the Centre for Liver Research for many years (Eksteen *et al*., 2004) by mechanical digestion. Although use of collagenases to break down extracellular matrix has been employed elsewhere for intrahepatic lymphocyte isolation, some surface antigens are susceptible to enzymatic cleavage. Additionally, since a large mass of tissue is generally obtained from explanted livers, the superior cellular yield obtained from enzymatic digestion is not strictly needed to isolate enough lymphocytes for these studies. For studies requiring RNA isolation, samples needed to be processed as quickly as possible to prevent RNA degradation. Accordingly, the quicker and cheaper mechanical digestion approach was adopted here.

4.2.3 TCR Repertoire Analysis

T cell receptor characterisation in its most basic form can be performed using antibodies specific to TCR V-regions and analysed by flow cytometry. In the case of αβ T cells this

requires a large panel of antibodies, and even though the number of V-regions for delta- and gamma-chains is considerably smaller, commercial antibodies are currently only available for Vδ1, Vδ2 and Vγ9. This does cover a large percentage of human γδ TCRs and is most straightforward to perform, whilst also allowing assessment of cell surface protein expression, and accordingly was the first method used in this study. However, clearly this method provides limited information, both in terms of the number of V regions analysed and the lack of informational regarding individual clonotypes.

Therefore, a more fundamental analysis of the TCR repertoire was desired in order to shed light not only on the full diversity of V-regions present (particularly relevant for the liver, where populations using δ-chain V-regions other than Vδ1 and Vδ2 may be highly prevalent (Kenna *et al*., 2004), but also on clonotypic diversity. There are several molecular approaches that have been used to investigate TCR repertoire previously, which provide information on different clonotypes.

4.2.3.1 Spectratyping

Once RNA has been isolated from the cells of interest, cDNA can be generated by amplifying across the CDR3 regions using suitable PCR primers that anneal at fixed positions in the 5' and 3' ends. The sizes of the PCR products can then be determined using electrophoresis and plotted against signal intensity to yield a size distribution that reflects the varying CDR3 lengths in the sample – a technique referred to as spectratyping (Pannetier *et al*., 1993). Due to the highly varied nature of our T cell repertoire, and the stochastic recombination events that form it, most healthy donors tend to exhibit a normal bell-shaped distribution of CDR3 lengths in their αβ T cell repertoire. Any

significant deviation from this can be attributed to a more focussed repertoire with over-representation of CDR3s of specific lengths, likely driven by clonal expansion (Pannetier *et al*., 1995). Spectratyping has been conducted on Vδ2$^-$ gamma delta T cell populations in the context of reactivation of CMV infection (Knight *et al*., 2010).

Spectratyping does not yield the frequency of cells expressing a given V-region however. Multiplex PCR using a pool of V- and/or J-region specific primers can generate chain use data alongside CDR3 length analysis (Du *et al*., 2006), yielding greater resolution to spectratyping data, and has been performed to analyse murine gamma delta T cells responding to *M. tuberculosis* infection (Huang *et al*., 2012). This method still does not give a genuine insight into clonality however – to tackle this next generation sequencing (NGS) protocols have been developed.

4.3.2.2 High throughput/Next Generation Sequencing analyses

High throughput sequencing allows simultaneous sequencing of potentially millions of individual CDR3 region amplicons from a single sample (Voelkerding *et al*., 2009). Profiling of actual nucleotide sequences in this manner enables compilation of a huge quantity of high resolution information, allowing identification of large expanded clonotypes across samples in cases of disease or vaccination. TCR deep sequencing has been used in previous studies to estimate the repertoire size in human αβ T cell populations (Robins *et al*., 2009), as well as to define the effect of T cell differentiation from naïve to effector on the TCR diversity as a function of ageing (Qi *et al*., 2014). Additionally, the effect of disease on TCR repertoire has been assessed in an analysis of tumour-infiltrating T cells (Emerson *et al*., 2013). Examination of the TCR repertoire in

healthy individuals has furthered understanding of public clonotypes and convergent CDR3 recombination, brought about by a molecular bias in TCR formation (Dziubianau *et al*., 2013).

NGS TCR repertoire profiling can be performed using both DNA and RNA as a starting template. DNA-based approaches, such as the immunoSEQ platform marketed by Adaptive Biosystems, amplify recombined genomic DNA regions using V and J region specific primers (Robins *et al*., 2009). Resulting PCR products are then sequenced. RNA-based approaches include amplicon-rescued multiplex PCR (arm-PCR) wherein nested primers specific for each TCR V region are used in the initial PCR round. Then a second exponential phase round of PCR is performed with the addition of fresh communal primers recognizing the shared tag sequence already introduced during the first round of amplification (Wang *et al*., 2010, Han *et al*., 2006). Analysis of genomic DNA is methodologically simpler and can be performed from bulk tissue (Liaskou *et al*., 2016), and in addition gDNA results will not be skewed by expression levels within cells analysed – each cell should only contain one copy of the TCR of interest. However, after VDJ rearrangement, those V and J segments not involved in the recombination will still be in the genome and can serve as binding sites for the PCR primers. Binding at these sites may generate background amplifications, exhaust primers, and introduce bias. Additionally, the RNA reagent systems developed by iRepertoire to create the cDNA template from sample RNA is “immune-specific” –supposedly thereby minimising the amount of non-targeted RNA and gDNA in the template cDNA for the PCR reaction, thereby gaining a potentially improved read depth compared with DNA-based approaches. Additionally, the RNA-based deep sequencing approach can be combined elegantly with in-house

single cell TCR PCR for validation purposes and to confirm chain pairings. For this reason the RNA based TCR repertoire profiling used by iRepertoire was used in this study.

4.3.2.3 NGS Error Correction

In common with all NGS-based technology, dataset biases and errors caused by the PCR-based preparation of samples and the sequencing itself can be a major problem. iRepertoire's software did employ an error correction algorithm, but to investigate the quality of this and ensure a quality dataset, the MiXCR software was employed (in collaboration with the software's authors based in Russia), to ensure high quality sequencing data (Figure 4.2) (Bolotin *et al*., 2015). According to the authors, "MiXCR employs an advanced alignment algorithm that processes tens of millions of reads within minutes, with accurate alignment of gene segments even in a severely hypermutated context. In paired-end sequencing analysis, MiXCR aligns both reads and aggregates information from both alignments to achieve high V and J gene assignment accuracy. It handles mismatches and indels and thus is suitable even for sequences with many errors and hypermutations. MiXCR employs a built-in library of reference germline V, D, J and C gene sequences for human and mouse based on corresponding loci from GenBan" (Bolotin *et al*., 2015). The importance of this error correction was noted by pre- and post-analysis of the same dataset from this study, illustrated by an example in Figure 4.3. A high number of apparently Vδ3^{+} CDR3 sequences were removed from the iRepertoire dataset by the MiXCR software that, on closer inspection, are clearly sequencing errors, consisting of only single nucleotide differences in most cases (Table 4.1). This led to over-representation of Vδ3^{+} usage in the final plot, an important observation since identification of repeated TCR usage with very similar CDR3 composition could easily be mis-interpreted as conserved or semi-invariant TCR

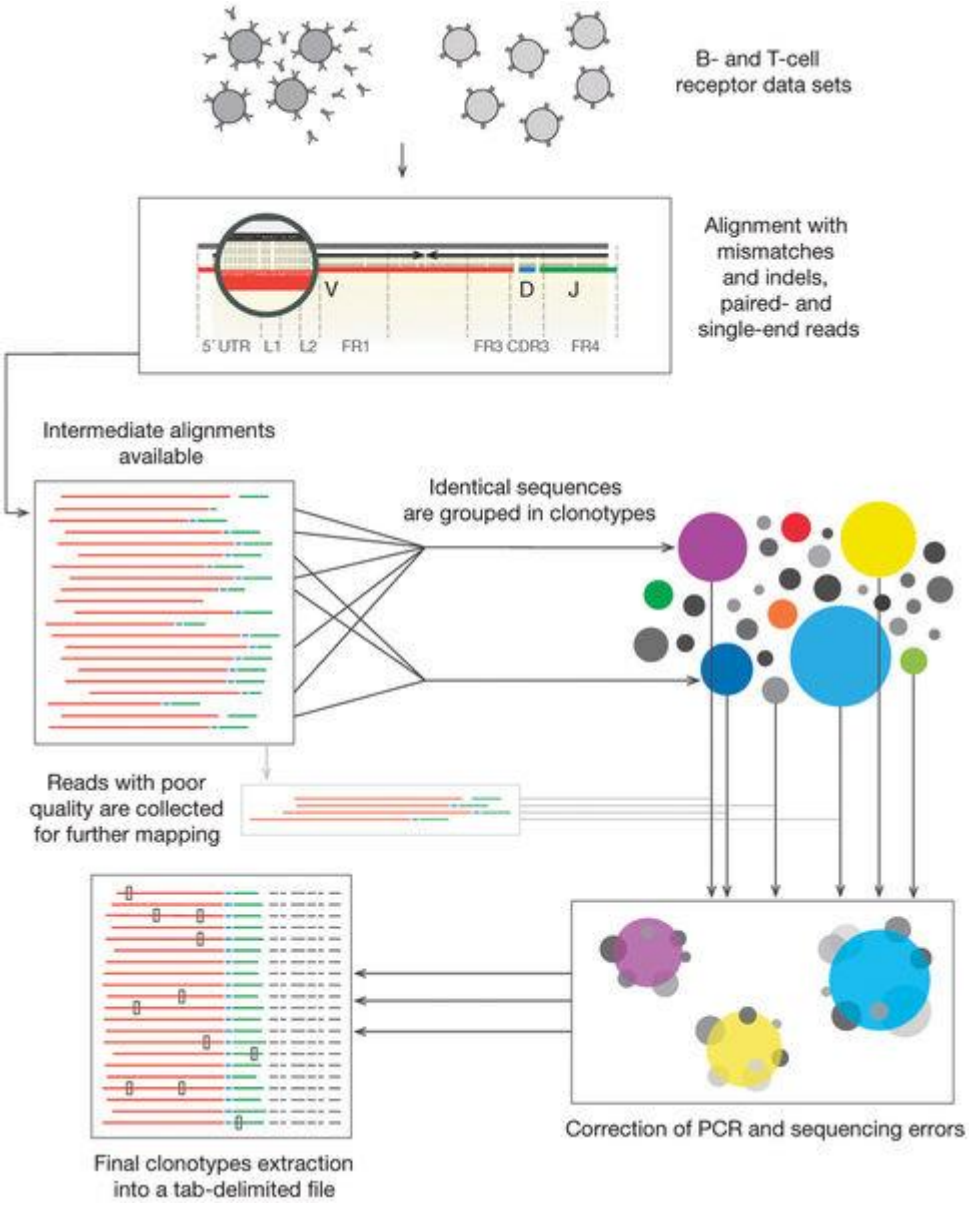

Figure 4.2: Illustration of MiXCR pipeline

From Bolotin *et al*, 2015

usage.

4.2.3.4 γδ T cell ontogeny and NGS sample preparation

Since γ-chain recombination occurs early in T cell development, concurrent with β- and δ-chain rearrangement, some αβ T cells also express a recombined γ-chain. To prevent contamination of the γ-chain dataset by γ-chain data from ostensibly αβ T cells, it is important to remove αβ T cells from the sample before isolating RNA. Additionally, an important facet of this study was to investigate intrahepatic $V\delta2^{neg}$ gamma delta T cells. Since the arm-PCR technology used by iRepertoire used primers for all V region sequences it was necessary to remove $V\delta2^{+}$ cells prior to cDNA formation, especially since the data obtained from this technique does not give matched γ- and δ- chain pairings. This means that although it is simple to remove $V\delta2^{+}$ sequences from the final dataset, the corresponding γ-chains are considerably harder to remove post-processing. To isolate $V\delta2^{neg}$ gamma delta T cells, samples were cell sorted by FACS, using a $CD3^{+}$, pan-γδ TCR^{+}, $V\delta2^{neg}$ strategy (Figure 4.3). In some samples, Vδ2 TCR contamination was noted. Subsequent to these sorts being performed, it was noted that certain Vδ2-specific antibodies "clash" with the pan-γδ TCR antibody if incubated simultaneously. Possibly due to steric hindrance, pan-γδ and Vδ2 antibodies would not bind some TCRs together, and therefore some $V\delta2^{+}$ cells may have remained unstained and been included in the $V\delta2^{neg}$ gate for sorting and subsequent repertoire analysis. This problem was reduced by incubating with the anti-Vδ2 antibody first and then adding the pan-γδ TCR antibody to the incubation mix later, however, $V\delta2^{+}$ contamination was not completely abrogated, for reasons that will be investigated later in this thesis.

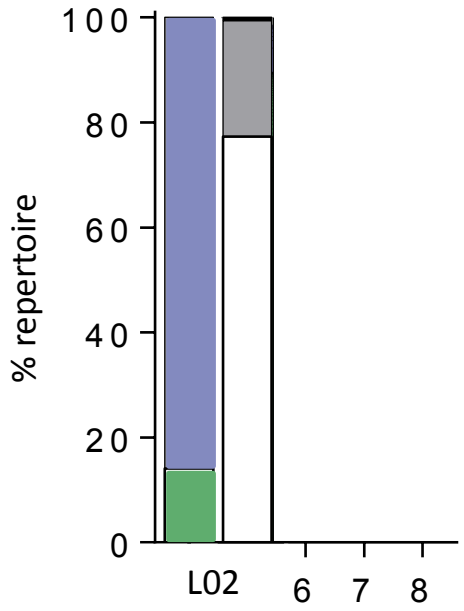

Figure 4.3: MiXCR error correction

Liver sample L02 Vδ chain usage determined by iRepertoire (left) and MiXCR (right) error correction algorithms. Vδ1 = green Vδ3 = blue Vδ4 = yellow.

CDR3δ amino acid sequence	
ACRFGYWGSTDKLI	hTRDV3*01
ASLGLPTGLGEKLI	hTRDV3*01
ALINLHPGGGAGYTDKLI	hTRDV3*01
AYRFGYWGSTDKLI	hTRDV3*01
ACRFGYWGPTDKLI	hTRDV3*01
ASLGLPTRLGEKLI	hTRDV3*01
ACRFGY*GSTDKLI	hTRDV3*01
ACRFGYWGSADKLI	hTRDV3*01
ACRFGYRGSTDKLI	hTRDV3*01
ACRFGYWGSTDKLI	hTRDV3*01
ASLGPPTGLGEKLI	hTRDV3*01
ACRFGHWGSTDKLI	hTRDV3*01
ACRFGCWGSTDKLI	hTRDV3*01

Table 4.1: L02 Top 13 CDR3δ amino acid sequences determined by iRepertoire deep sequencing

The 13 highest frequency CDR3 amino acid sequences for sample L02 as determined by iRepertoire algorithms following NGS TCR sequencing. The three highest frequency sequences, (red box) are distinct, but the following 10 sequences are all likely derived from sequencing errors of one of the "parent" top three sequences. Homology is indicated by grey shading.

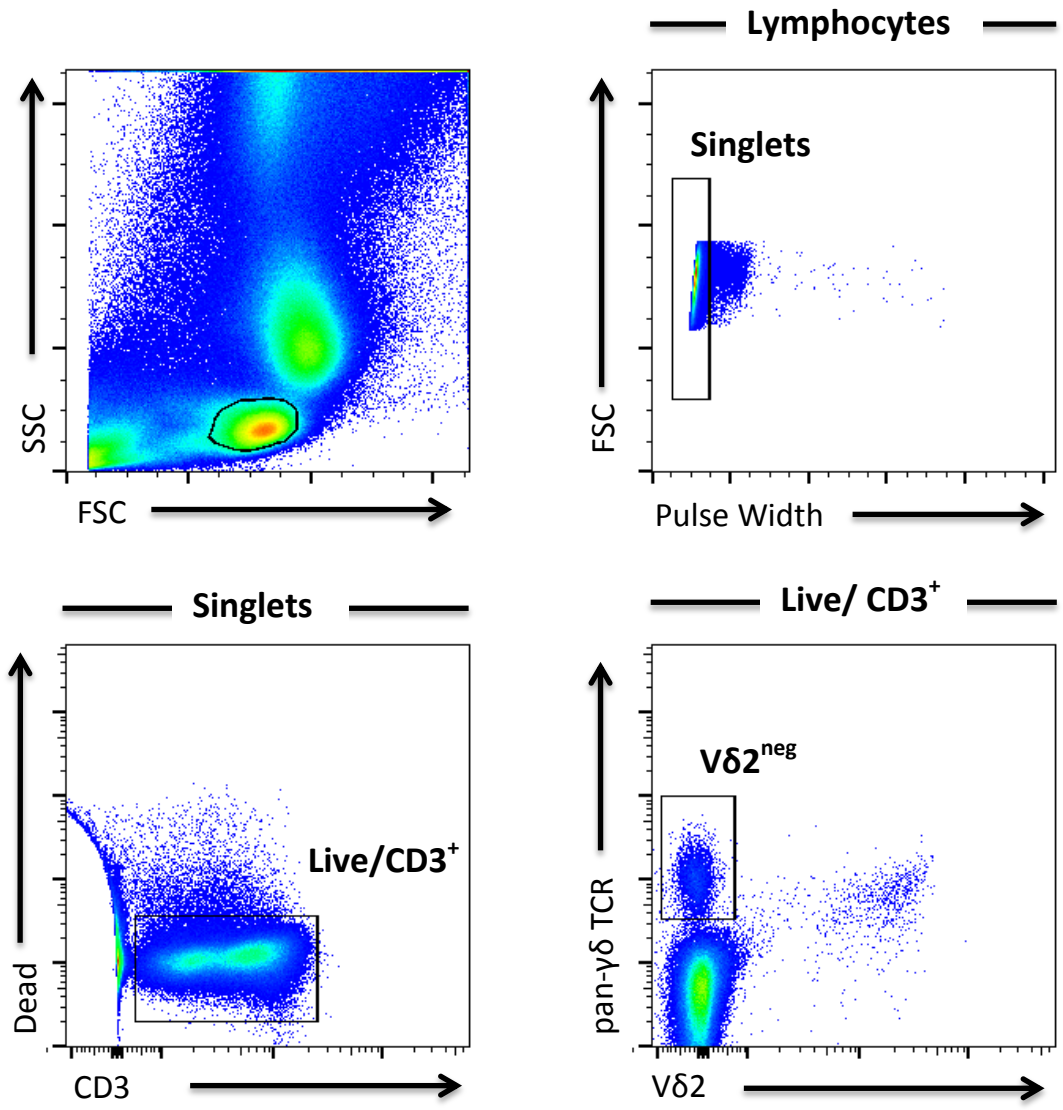

Figure 4.4: Gating strategy for identifying and sorting Vδ2^{neg} gamma delta TCR sequencing

Representative flow cytometry plots show the gating strategy used to identify single live lymphocytes and CD3^{+} γδ^{+} TCR Vδ2^{neg} cells for TCR repertoire sequencing. Plots representative of 10 liver donors and 8 blood donors.

4.3 Results

4.3.1 Flow cytometry repertoire analysis

To examine the frequencies of the liver infiltrating γδ T cell population, human explanted liver from healthy donors (n=15) and diseased donors (n=45) was analysed by flow cytometry . An antibody specific to a constant region of the δ-chain was used, as well as a live dead marker and CD3 to confirm T cell status. Corroborating the immunohistochemistry data displayed in the previous chapter, a significantly higher proportion of the $CD3^+$ T cell compartment was comprised of γδ T cells in healthy liver (12.5% ± 2.6% SEM) compared with diseased liver (4.6% ± 0.62% SEM, p=0.007, student's T test) (Figure 4.5a). When the diseased liver cohort was separated into specific disease subtypes (PSC, PBC, ALD, NASH and virally originating disease (HCV and HBV)) no significant difference between γδ TCR^+ frequencies as a percentage of $CD3^+$ T cells was observed, other than for PBC, which was significantly reduced compared with PSC derived intrahepatic lymphocytes (Figure 4.5b).

To assess the impact of chronic liver disease on circulating gamma delta T cell burden, blood from patients with autoimmune hepatitis (AIH) (n=19) was also analysed by flow cytometry, and compared with blood obtained from a cohort of patients undergoing venesection to treat ongoing haemochromatosis (HFE) (n=13). This HFE cohort was selected as they were likely to be age matched with both the liver and blood donors and HFE is not an immune mediated disorder. Studies have suggested that HFE may have an impact on circulating T cells however, specifically $CD8^+$ T cells (Macedo *et al*., 2010, Costa *et al*., 2015).

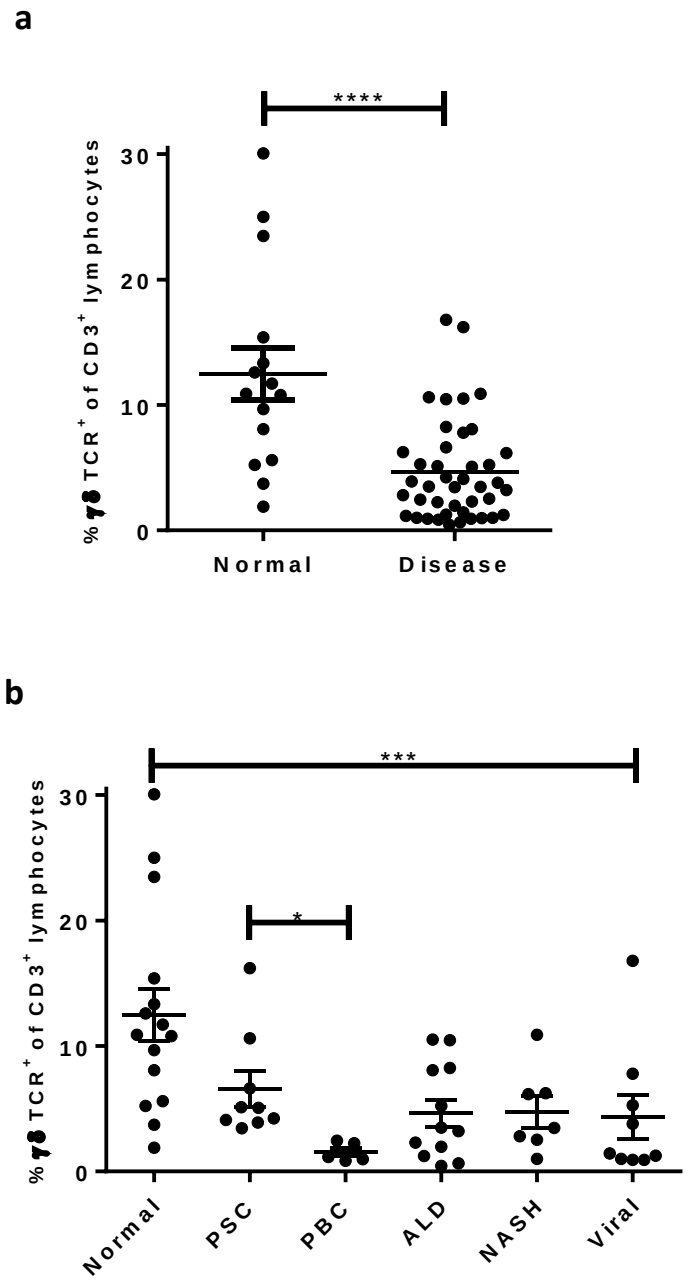

Figure 4.5: Gamma delta T cell proportions in human normal and diseased liver explants.

a) Proportion of gamma delta T cells in intrahepatic T cell populations determined by flow cytometry. n = 15 normal liver, 45 diseased liver, ****p<0.0001, Mann-Whitney U test.

b) Proportion of gamma delta T cells in intrahepatic T cell populations determined by flow cytometry. n = 15 normal liver, 6-12 each diseased liver, ***p<0.001 1-way ANOVA, Kruskal-Wallis test.

Accordingly, circulating gamma delta T cell burden was also analysed in a healthy cohort (n=20), although the mean age of this group (donors ranged from 20 – 30 years in age) was likely lower than that of the explanted liver cohort.

Healthy liver was significantly enriched for gamma delta T cells compared with aged matched HFE blood (12.5% ± 2.1% vs. 3.1% ± 0.6%, p=0.002), and the AIH liver disease group (4.9% ± 1.2% p=0.0014) but not younger healthy blood donors (7.2% ± 0.8%, p>0.99) (Figure 4.6). Diseased liver was not significantly enriched with gamma delta T cells compared with any blood donor cohorts. In our cohort, young healthy donors had significantly higher frequencies of gamma delta T cells than the older HFE cohort (p=0.02), in line with previous observations (Roux *et al*., 2013). No significant differences in peripheral gamma delta T cell frequencies were determined between AIH and HFE blood donors.

Commercial antibodies are available that are specific for Vδ1, Vδ2 and Vγ9 TCR chains, allowing limited repertoire analysis by flow cytometry. First, the percentage of $V\delta2^{neg}$ cells was analysed as a percentage of the total gamma delta T cell population (Figure 4.7). These were found to be in the majority in both normal and diseased livers (66.4% ± 4.7% normal, 72.62% ± 3.5% diseased, p>0.05). Healthy blood was dominated by $V\delta2^{+}$ gamma delta T cells as expected from previous studies, with 21.8% ± 3.3% $V\delta2^{neg}$, and a similar result was observed for the HFE patient derived cohort (18.9% ± 3.4%). Interestingly however, AIH-derived blood, despite not having higher overall frequencies of gamma delta T cells, was dominated by the $V\delta2^{neg}$ compartment (63.0% ± 6.5%), a similar distribution to that observed in the intrahepatic gamma delta T cell population.

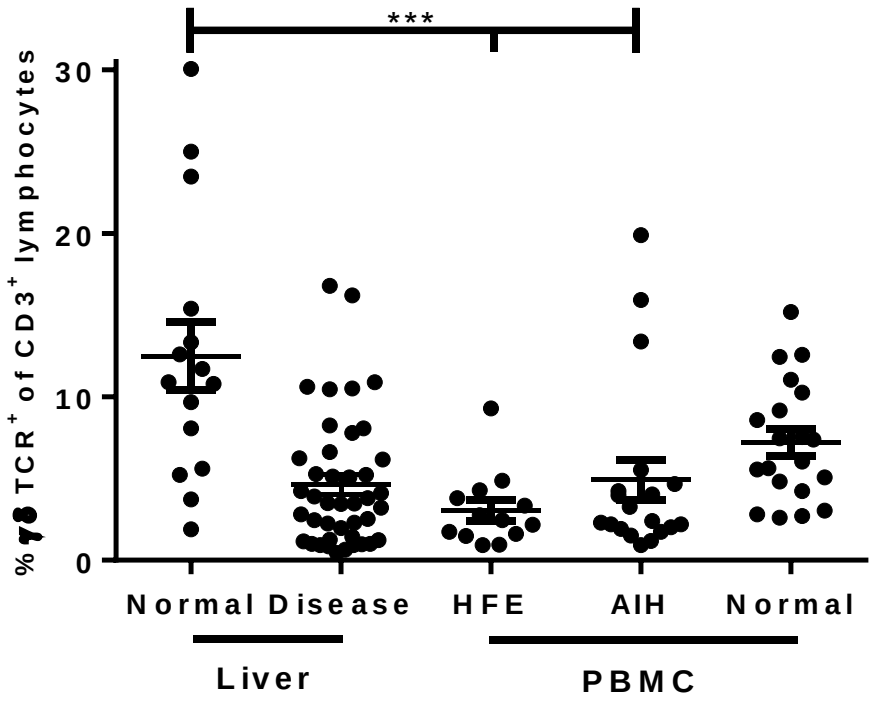

Figure 4.6: Gamma delta T cell proportion in liver and the periphery

Proportion of gamma delta T cells in intrahepatic and peripheral blood derived T cell populations determined by flow cytometry. n = 15 normal liver, 45 diseased liver, 13 HFE, 19 AIH, 20 normal blood. ***p<0.001, 1-way ANOVA)

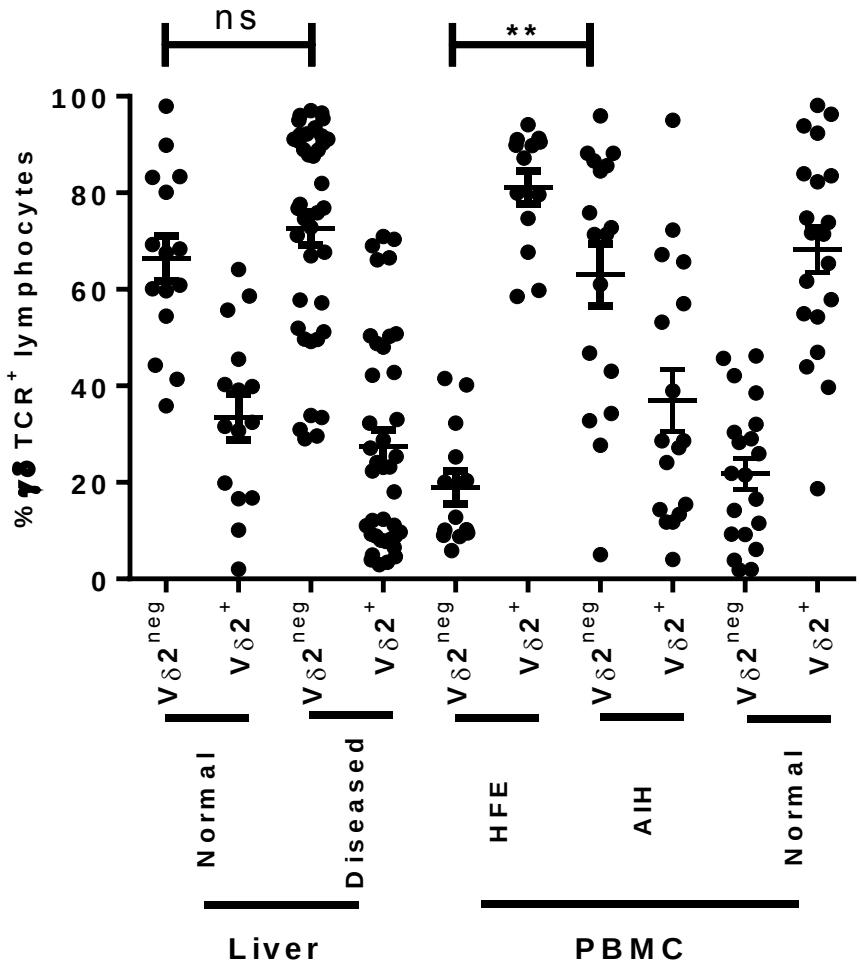

Figure 4.7: Vδ2^{+} proportion among γδ T cells in liver and the periphery

Proportion of Vδ2^{neg} and Vδ2^{+} T cells of total gamma delta T cells determined by flow cytometry.

n = 15 normal liver, 45 diseased liver, 13 HFE, 19 AIH, 20 normal blood. **p<0.01, 1-way ANOVA)

In the explanted liver cohort, of the $V\delta2^{neg}$ population the dominant TCR chain usage was Vδ1 in all sample groups analysed with appropriate antibodies, with between 10.2% and 32.7% comprised of other TCR-δ chains with no available antibody (Figure 4.8a). The largest $V\delta2^{neg}V\delta1^{neg}$ population was observed in diseased livers (32.7% ± 5.7%), compared with normal liver (24.4% ± 5.6%) although the number of normal livers stained in this manner was low (n=5). In healthy blood donors this percentage dropped to 21.6% ± 3.5%, (p=0.65 vs. diseased liver), 17.9% ± 3.5% in AIH donors and 10.2% ± 5.0% in HFE donors (n=8). Although no significant difference was observed between any of these groups, when analysed as a whole, liver was significantly enriched for $V\delta2^{neg}V\delta1^{neg}$ gamma delta T cells compared with blood (30.7% ± 4.6% vs 18.8% ± 23.%, p=0.03, Mann-Whitney U test) (Figure 4.8b).

Of the $V\delta1^{+}$ population, 17.2% ± 4.7% of intrahepatic gamma delta T cells also expressed the Vγ9 TCR chain (Figure 4.9). This was significantly lower than the frequency of $V\gamma9^{+}V\delta1^{+}$ cells in the healthy blood cohort (38.1% ± 6.6%, p=0.008), although there was a wide range of expression of this chain pairing in both groups.

Autoimmune hepatitis is a chronic auto-inflammatory disease with an undefined cause. Patients often have a number of autoantibodies present in serum, including α-smooth muscle antibody (SMA) and α-mitochondrial antibody (AMA), although several subtypes of the disease have been identified. No cure is currently available, with standard therapy consisting of life-long immunosuppressive agents such as the glucocorticoid prednisone, azathioprine, tacrolimus and mycophenalate (Liberal *et al*., 2016). Although remission rates are reasonably high, relapse often occurs. The majority of samples in this study were obtained from patients undergoing immunosuppression therapy and in remission

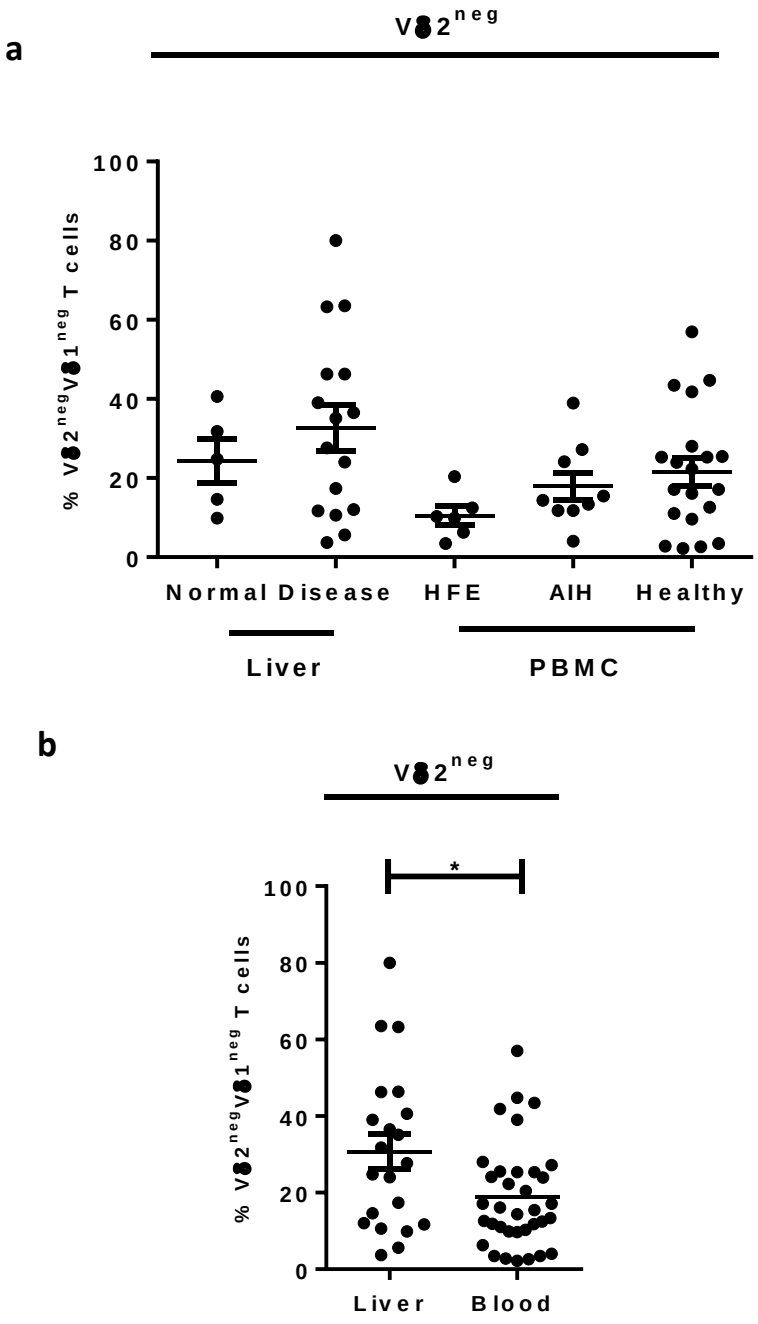

Figure 4.8: Vδ2^{neg}Vδ1^{neg} gamma delta T cells in liver and the periphery

a) Proportion of Vδ2^{neg}Vδ1^{neg} as a percentage of liver and blood-derived Vδ2^{neg} gamma delta T cells determined by flow cytometry, n=5-20

b) Grouped proportion of Vδ2^{neg}Vδ1^{neg} as a percentage of liver and blood-derived Vδ2^{neg} gamma delta T cells determined by flow cytometry, n=21 – 36, *p<0.05, Stundent's T test

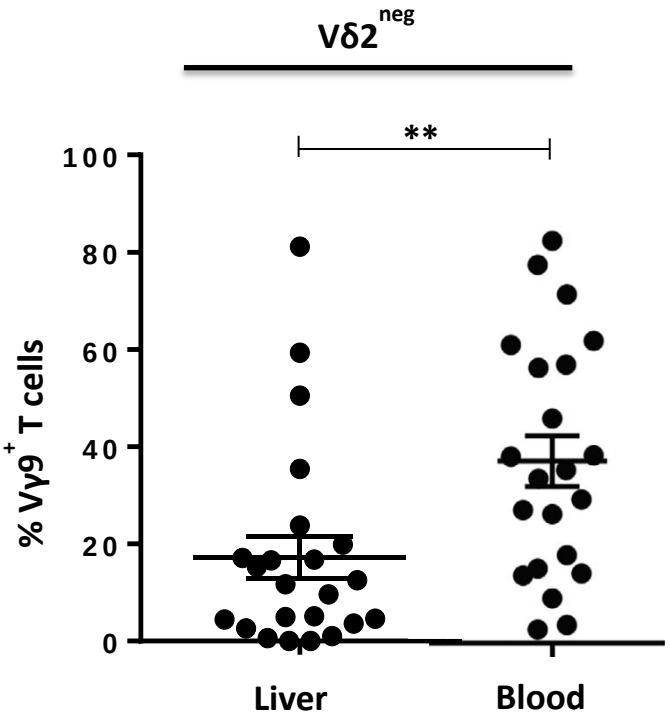

Figure 4.9: Vδ2^{neg}Vγ9^{+} gamma delta T cells are enriched in healthy peripheral blood compared with liver

Proportion of Vγ9^{+} cells as a percentage of liver and blood-derived Vδ2^{neg} gamma delta T cells determined by flow cytometry, n=25 **p<0.01, Mann-Whitney U test

for the disease, however, several were in relapse, with active disease. When split into the two groups (remission and active disease), the active disease group had a significantly higher overall proportion of circulating gamma delta T cells than both the remission group and HFE group (8.3% ± 2.5% vs. 2.4% ± 0.39%) (Figure 4.10a), and slightly higher proportion of $V\delta2^{neg}$ than the remission group (Figure 4.10b). Flow cytometry analysis of surface differentiation and activation markers CD27 and CD69 from these AIH remission (n=14) and active disease (n=8) groups was then performed. In contrast to autologous αβ T cells and $V\delta2^{+}$ gamma delta T cells, both AIH patient group's $V\delta2^{neg}$ populations exhibited significantly higher surface expression of early activation marker CD69 when compared with age-matched healthy donors (Remission: 26.1% ± 5.1%; Active Disease: 31.3% ± 4.5% vs. Healthy 8.1% ± 3.8%, p= 0.01 Kruskal Wallis) (Figure 4.10c). In addition, $V\delta2^{neg}$ gamma delta T cells isolated from the AIH active disease cohort demonstrated a significant loss of CD27, an indicator of gain of effector function, in comparison with HFE age-matched donors ($CD27^{+}$ 15.0% ± 4.44% vs. 89.5% ±2.9%, p=0.0004). This is strongly indicative of an activated phenotype for these numerically increased $V\delta2^{neg}$ gamma delta T cells in the periphery of AIH patients (Figure 4.10d).

4.3.2 Deep sequencing repertoire analysis

Having established a V-region level repertoire analysis of human liver and blood by flow cytometry, a deeper insight of both TCR chain usage and CDR3 composition was gained through next generation sequencing analysis of selected samples, performed by iRepertoire Inc. 10,000 – 50,000 $V\delta2^{neg}$ gamma delta T cells were sorted from 10 explanted livers and 4 autoimmune hepatitis blood samples by fluorescence activated cell

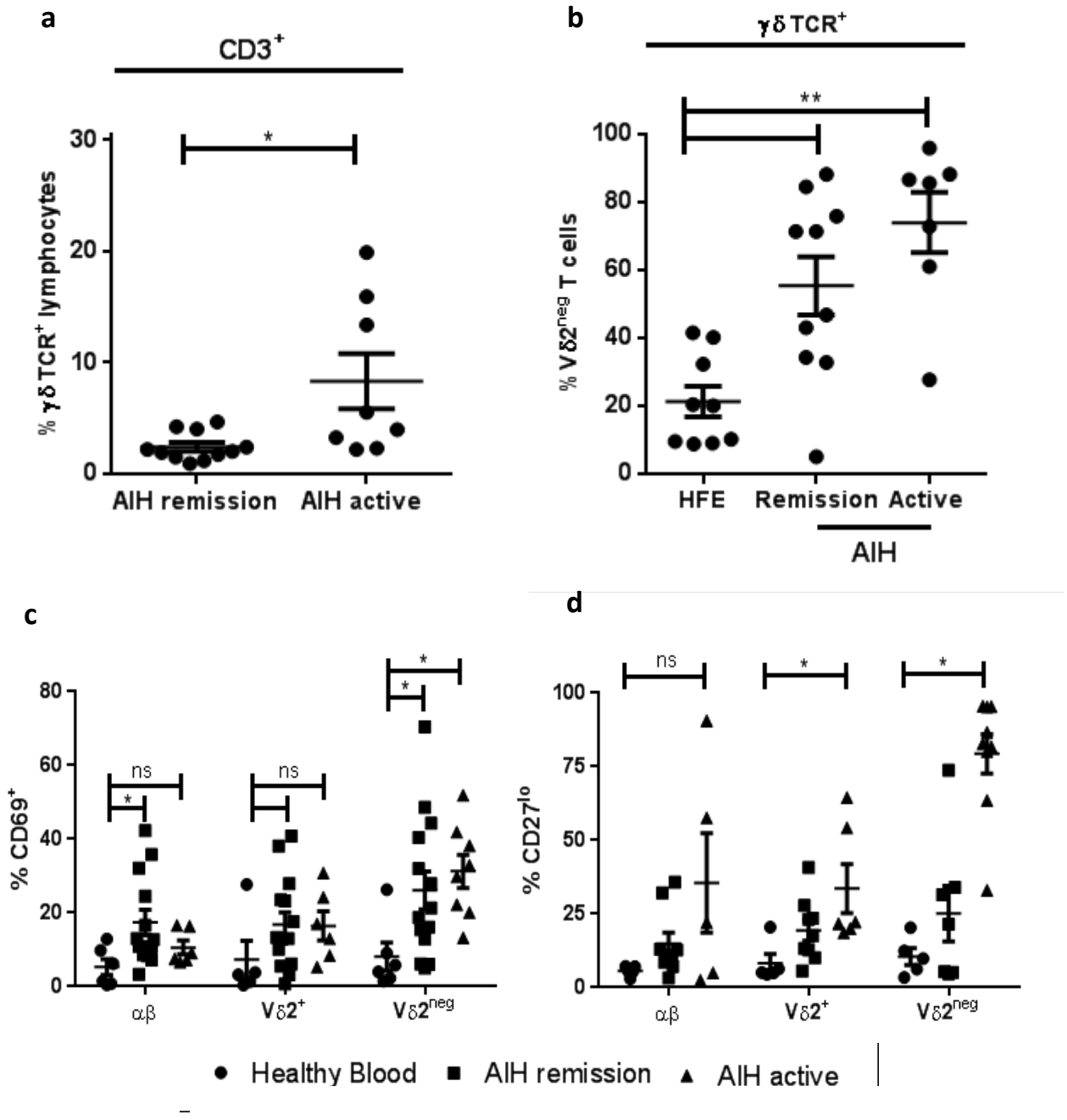

Figure 4.10: AIH patient's blood is enriched for activated, effector phenotype Vδ2^{neg} gamma delta T cells

- **a)** Proportion of γδ TCR^{+} cells as a percentage of blood-derived CD3^{+} T cells from AIH patients, determined by flow cytometry, n=8-11, *p<0.05
- **b)** Proportion of Vδ2^{neg} T cells as a percentage of blood-derived γδ TCR^{+} T cells from AIH and HFE patients, determined by flow cytometry, **p<0.01
- **c)** Proportion of cells with positive surface expression of CD69 for various T cell subsets among three donor groups, n=6-14, *p<0.05
- **d)** Proportion of cells with negative surface expression of CD27 (CD27^{lo}) for various T cell subsets among three donor groups, n=6-14, *p<0.05

sorting into RNA*later* according to the strategy denoted in section 4.2.3.4. Total RNA was then extracted from these cells before shipping to iRepertoire for cDNA synthesis, amplification, NGS library preparation and sequencing. V, D and J gene usage was identified using iRepertoire's in house software; iRweb tools (Yang *et al*., 2015).

A mean sequencing depth of 455307 ± 52273 reads per sample was achieved with an average of 676 ± 189 unique CDR3 sequences for TCRδ and TCRγ from the liver samples (Table 4.2). However, there were significantly fewer reads obtained from the AIH blood cohort (Figure 4.11a). Despite this, no correlation was observed between sequencing depth and the number of unique CDR3s assigned in any group (overall, r=0.33 p=0.08 Spearman correlation) (Figure 4.11b). This is important as it suggests that the diversity of the repertoire, in terms of unique CDR3s sequenced, did not depend on sequencing depth, which in turn can be dependent on the number of cells and/or quality of the RNA isolated from the cells, thereby suggesting that no obvious methodological bias may be skewing this dataset.

To investigate the potential effect of chronic disease on TCR repertoire, 5 samples were obtained from normal livers and 5 from chronically diseased liver (2 PBC, 2 NASH, 1 PSC). Several samples contained varying quantities of TCR sequences using Vδ2. Since these were considered to be contaminants from poor $V\delta2^{+}$ antibody staining during the cell sorting, these sequences were removed from the dataset post-processing. Additionally, TCRγ9 sequences containing the JγP joining region were also removed post-processing as these are almost exclusively used by Vδ2Vγ9 phosphoantigen-reactive gamma delta T cells (Borst *et al*., 1989) and should not therefore be encountered in a $V\delta2^{neg}$ selected

Donor	TCR chain	Sequencing Reads	Total CDR3	Unique CDR3	Cell Number
L01	TRD	557760	546240	1009	25
Healthy	TRG	860902	815056	357	25
L02	TRD	634718	631791	266	25
NASH	TRG	604316	557532	113	25
L03	TRD	489938	452517	993	20
Healthy	TRG	785366	618012	305	20
L04	TRD	547244	534933	969	20
PSC	TRG	854254	831961	885	20
L05	TRD	265300	262093	84	50
Healthy	TRG	92176	83410	103	50
L06	TRD	423150	389541	472	10
PBC	TRG	185020	171971	283	10
L07	TRD	61576	55269	210	10
ALD	TRG	175619	159579	240	10
L08	TRD	464215	456542	388	23
NASH	TRG	556388	484058	242	23
L09	TRD	365394	362765	450	50
Healthy	TRG	512875	478983	263	50
L10	TRD	283825	255658	3450	25
Healthy	TRG	386109	351065	2433	25
L0106	TRD	49738	49459	178	15
AIH Blood	TRG	145535	134257	200	15
L0107	TRD	61046	57705	215	31
AIH Blood	TRG	137275	84014	304	31
L0109	TRD	66364	60450	1394	15
AIH Blood	TRG	137269	117064	824	15
L0111	TRD	59353	56126	273	50
AIH Blood	TRG	85917	61097	110	50

Table 4.2: Raw TCR sequencing data

Total sequencing reads, total CDR3s determined, unique CDR3s determined and cell number for each sample. L0106 – L0111 were derived from PBMCs of AIH patients.

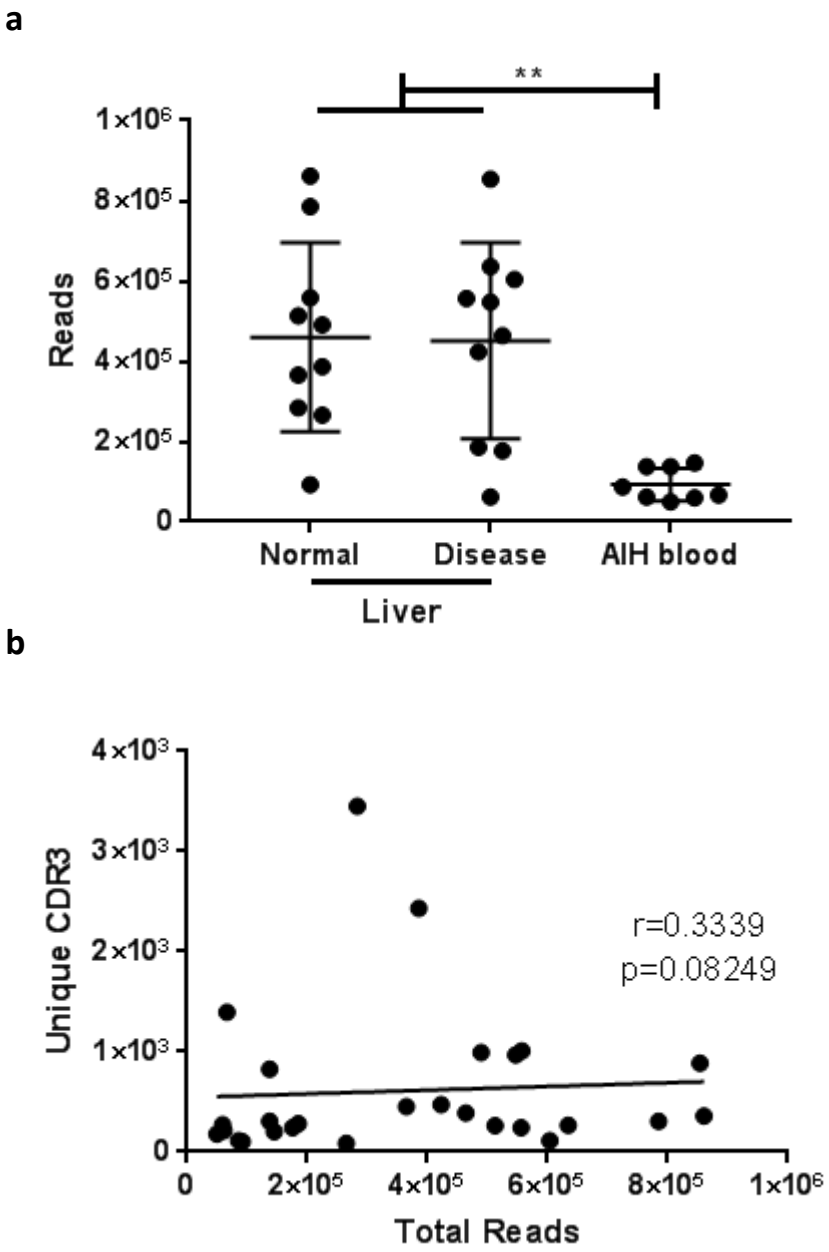

Figure 4.11: NGS read depth did not alter unique CDR3 sequences obtained

a) Mean ± s.e.m. read depth of NGS samples of total sequencing reads for each donor grouping, n=8-10, **p<0.01

b) Comparison of total sequencing reads against the number of unique CDR3s determined for each donor in this study, Spearman correlation

population. Consistent with the flow cytometry analysis (section 4.3.1), in 8 of the 10 samples, Vδ1 was the dominant δ-chain, with 76.1% ± 9.8% of the total δ-chain repertoire represented by Vδ1 (Figure 4.12a), significantly higher than any other chain ($p<0.0001$, 1-way ANOVA Friedman test). Significant usage of the Vδ3 chain was observed, with $V\delta3^{+}$ clonotypes comprising the dominant δ-chain in 2 of the 10 samples and accounting for 22.7% ± 10.0% of the total Vδ repertoire overall. Use of Vδ4 (0.78% ± 0.64%) and Vδ8 (0.35% ± 0.24%) was also observed in some individuals. There was no statistically significant difference in use of any δ-chain between the healthy and diseased sample groups ($p>0.99$) (Figure 4.12b). Interestingly, highly consistent Vδ-region usage was observed across all liver samples when plotted unweighted by clonotype proportion – i.e. each individual sequence was only counted once, irrespective of how many times in occurred in the repertoire (Figure 4.13).

As for $V\delta2^{+}$ sequences, TCRγ9 sequences containing the JγP joining region and the glutamate-leucine-glycine amino acid CDR3 motif were also removed post-processing as these are almost exclusively used by Vδ2Vγ9 phosphoantigen-reactive gamma delta T cells and should not therefore be encountered in a $V\delta2^{neg}$ selected population. Unlike for the delta-chain, there was no predominant Vγ chain usage ($p=0.18$, 1-way ANOVA, Friedman test), with the liver samples demonstrating a wide range of Vγ9 expression, from 0.2% in sample L05 to 80.7% in sample L02, representing the largest represented Vγ chain across all samples, with 22.4% (Figure 4.14a). All other functional γ-chains were identified in at least one sample and expression levels were highly heterogeneous: Vγ2 - 15.1%, Vγ3 – 9.7%, Vγ4 - 20.3%, Vγ5 - 14.7% and Vγ8 – 17.4% overall. As with δ-chain usage, no significant difference in γ-chain usage was observed between healthy and

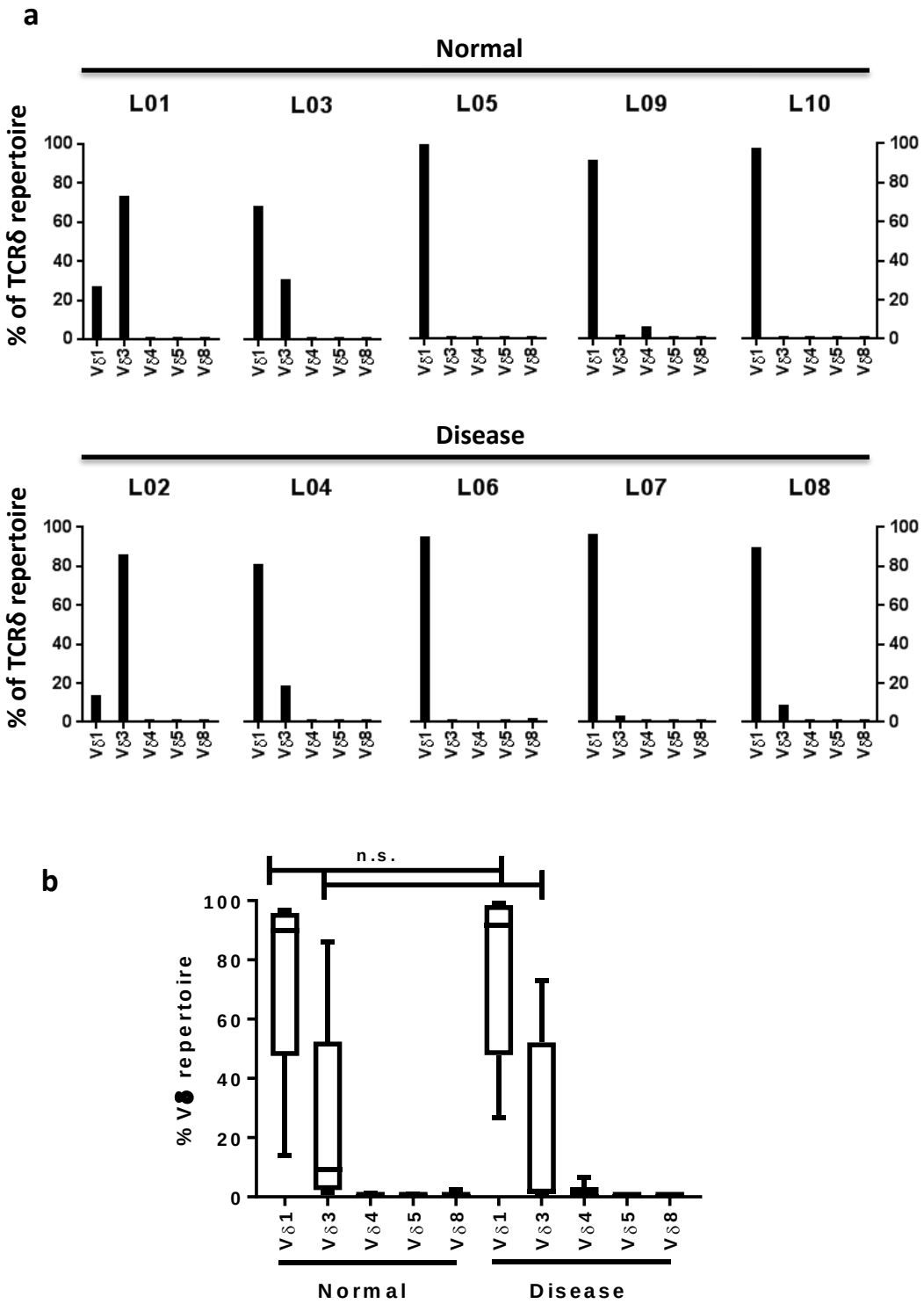

Figure 4.12: TCRδ repertoire of intrahepatic Vδ2^{neg} gamma delta T cells

a) Vδ chain usage by gamma delta TCR sequences from Vδ2^{neg} sorted T cells from human liver

b) Summary of TCRδ chain usage amongst intrahepatic Vδ2^{neg} samples (n=5 normal, 5 disease, p>0.99, 1-way ANOVA, Dunn's multiple comparisons test)

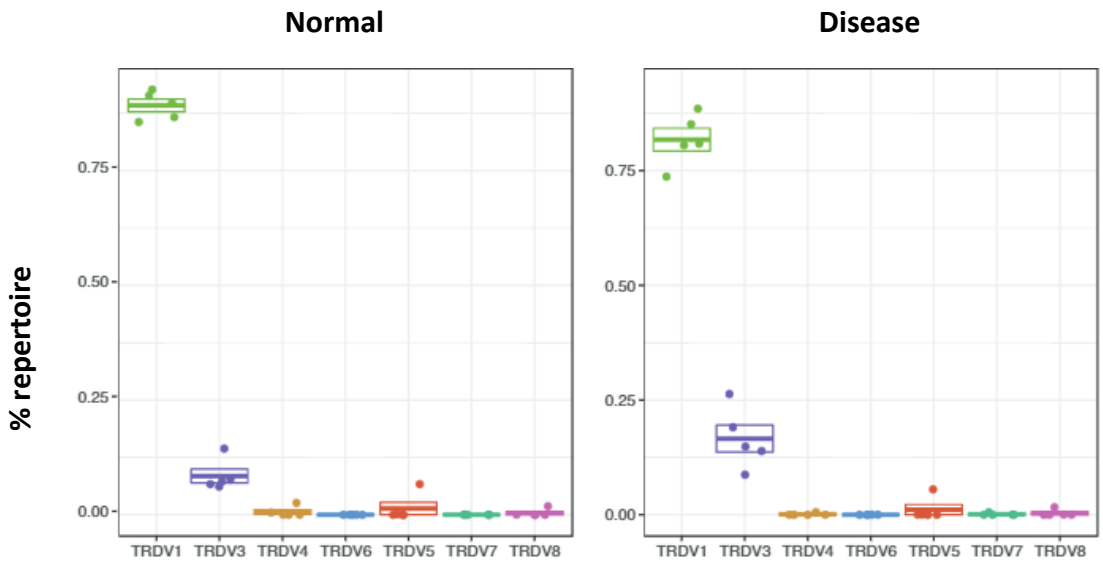

Figure 4.13: Normalised TCRδ chain usage for liver samples

TCRδ chain usage for normal and diseased liver cohorts normalised to remove weighting by clonal size (n=5)

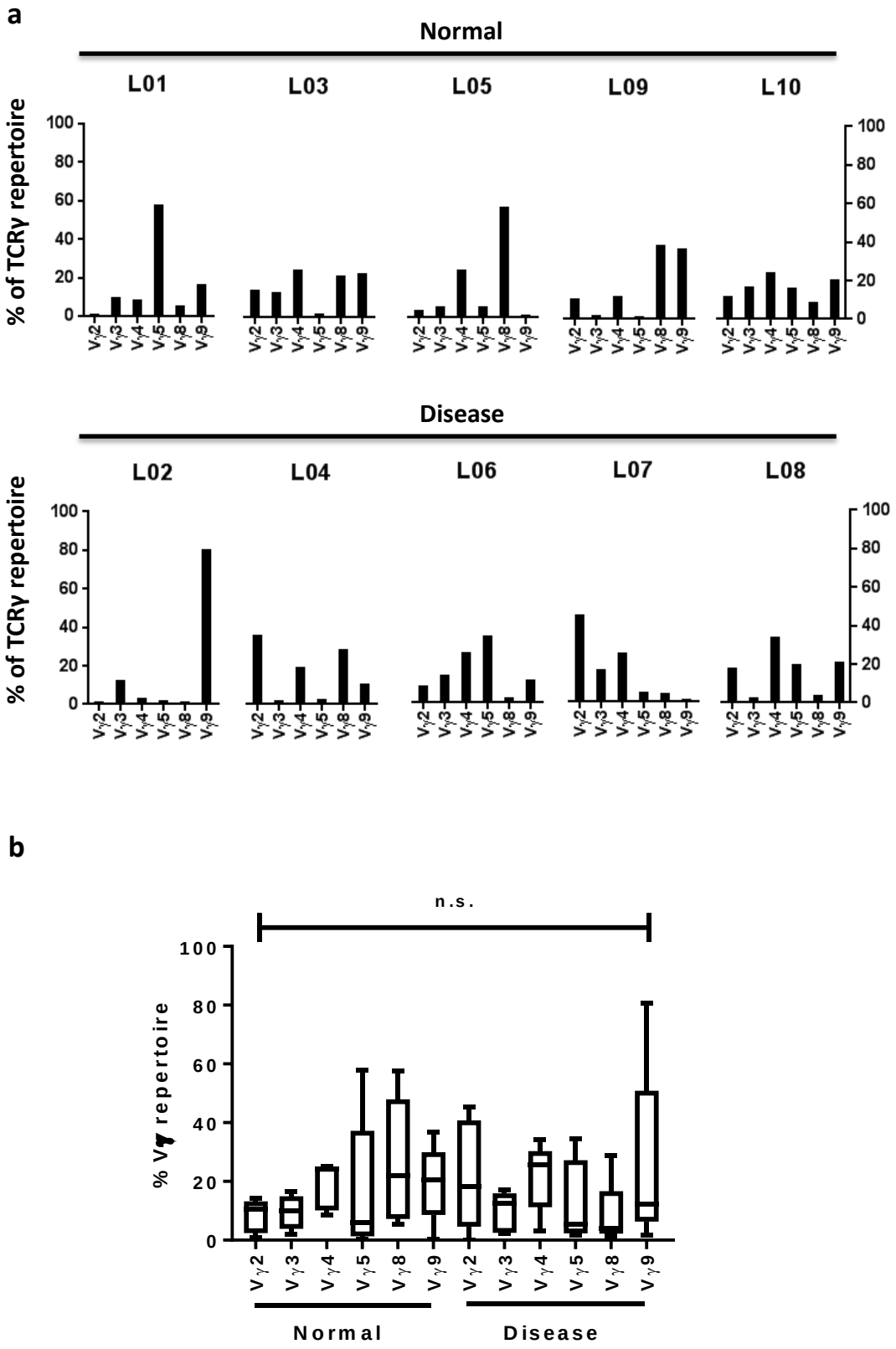

Figure 4.14: TCRγ repertoire of intrahepatic Vδ2^{neg} gamma delta T cells

a) Vγ chain usage in gamma delta TCR sequences from Vδ2^{neg} sorted T cells from human liver

b) Summary of TCRγ chain usage amongst intrahepatic Vδ2^{neg} samples (n=5 normal, 5 disease, p>0.99, 1-way ANOVA, Dunn's multiple comparisons test)

diseased sample groups (p>0.99) (Figure 4.14b).

For TCRδ, the dominant J region usage was Jδ1 (91.4%) although some samples did have δ-chains that incorporated Jδ2, Jδ3 and Jδ4 (Figure 4.15a). TCRγ J region usage was a little more heterogeneous, with the dominant J region being Jγ1 in all samples (83.6%) but with a significant number of Jγ2, JγP1 and JγP2 also being detected in several samples (Figure 4.15b).

Flow cytometry analysis had previously shown that many AIH patients have an increased percentage of their T cell population occupied by $V\delta2^{neg}$ gamma delta T cells compared with healthy donors, and that these cells had a more activated phenotype. To investigate whether these cells expressed a different TCR repertoire to healthy donors and to compare with the repertoire identified in liver samples, 4 AIH patient blood samples were analysed by deep sequencing; 3 patients were in remission and one was undergoing active disease (Figure 4.16a). TCRδ usage was, as with liver, dominated by Vδ1 which occupied 68.6% ± 4.5% of the repertoire across all the samples, while $V\delta3^{+}$ TCRs were also present in 24.9% ± 5.5% of the sequences read and Vδ4, Vδ5 and Vδ8 also represented at low levels (4.4%, 9.7% and 11.5% respectively). TCRγ was again more heterogeneous than δ-chain usage, with both Vγ4 (37.3% ± 4.1%) and Vγ9 (24.4% ± 6.1%) strongly represented with all other chains also observed (Vγ2 - 10.23% Vγ3 - 9.375% Vγ5 - 9.475%Vγ8 - 9.25%) (Figure 4.16b). To assess whether there was a difference in TCR chain usage compared with healthy blood donors, this data was compared with four PBMC-derived samples that were sorted using the same $V\delta2^{neg}$ strategy (Davey *et al*., 2017), which all exhibited very low frequencies of $V\delta3^{+}$ chain usage (Figure 4.16c). Although the sample size was too small to make any direct implications, this is

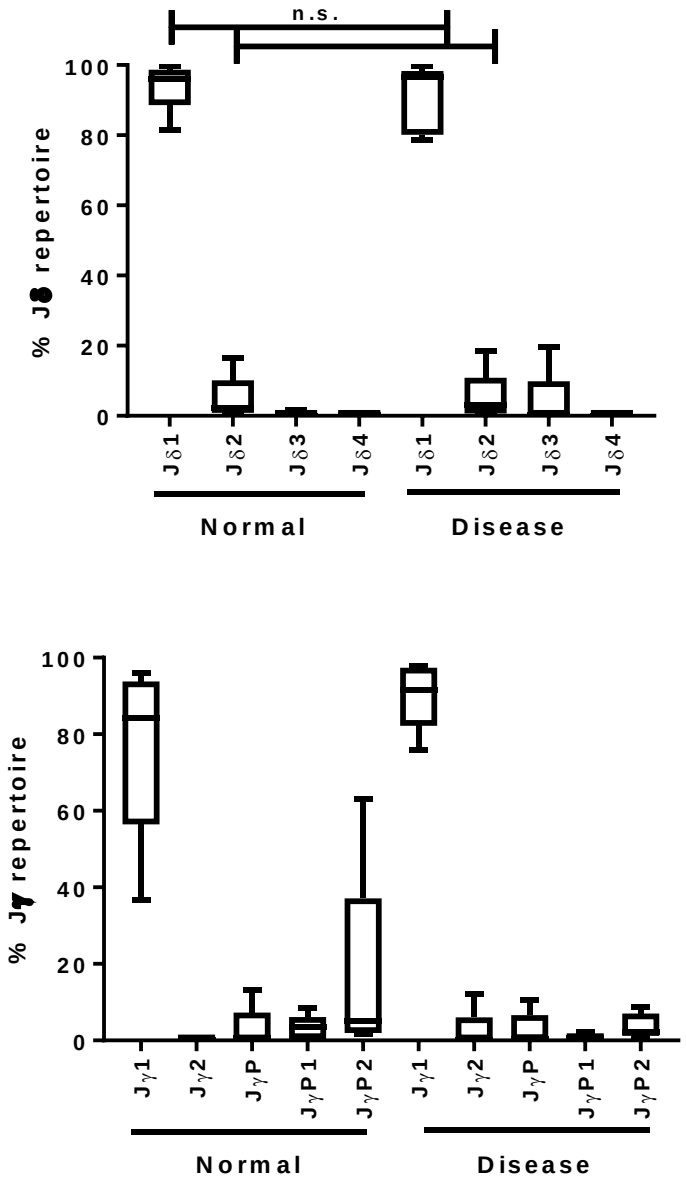

Figure 4.15: J-region usage of intrahepatic Vδ2^{neg} gamma delta T cells

Comparison of J-region usage for both TCRδ (top) and TCRγ (lower) for intrahepatic Vδ2^{neg} gamma delta T cells isolated from normal and chronically diseased explanted human liver. n=5 normal, 5 disease, p>0.99 1-way ANOVA, Kruskal-Wallis test.

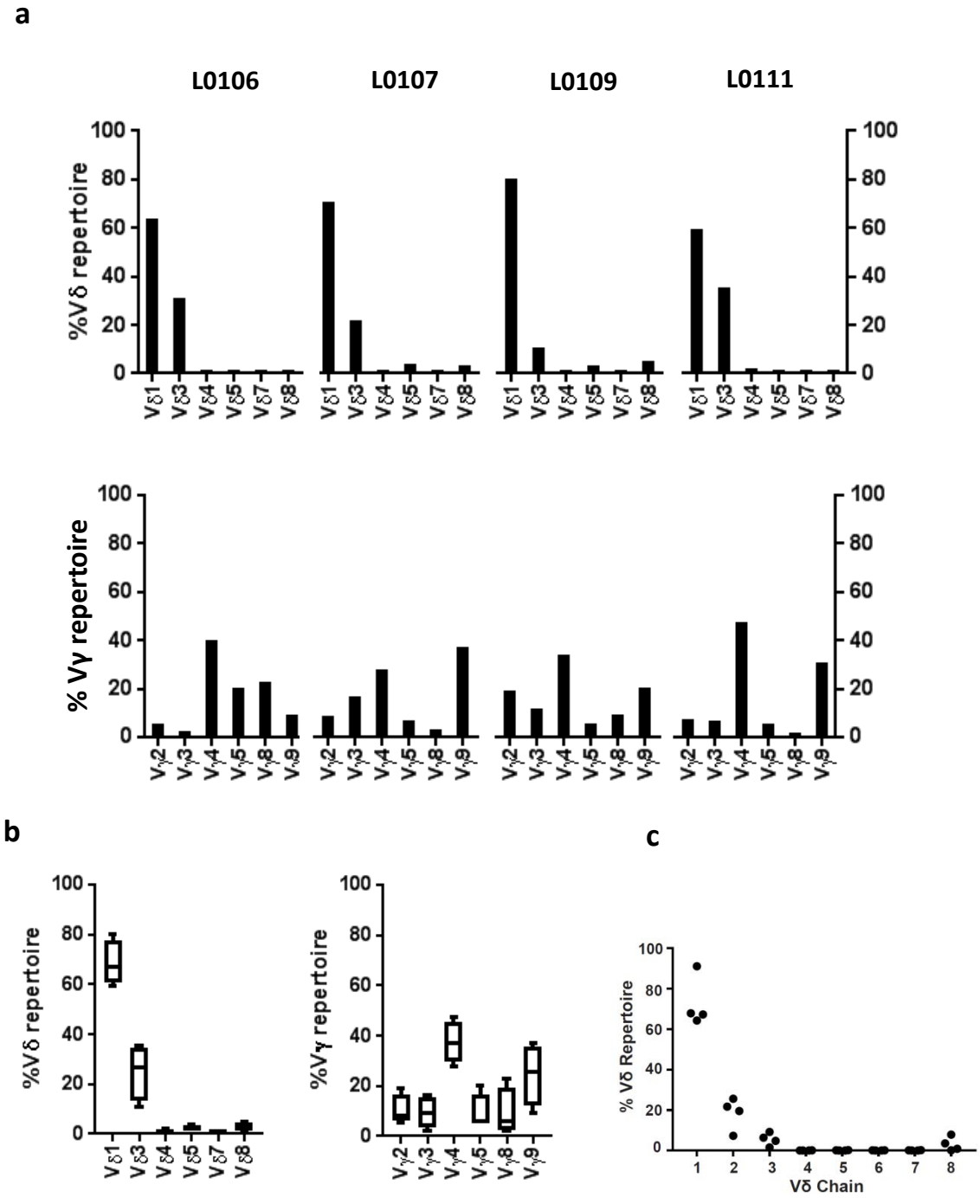

Figure 4.16: V-region usage of AIH patient PBMC –derived Vδ2^{neg} gamma delta T cells

a) Vδ (upper) and Vγ (lower) chain usage in gamma delta TCR sequences from Vδ2^{neg} sorted T cells from PBMCs of autoimmune hepatitis patients

b) Summary of TCRδ (left) and TCRγ (right) chain usage amongst AIH patient PBMC-derived Vδ2^{neg} samples (n=4)

c) Vδ chain usage in Vδ2^{neg} sorted cells from healthy donors (n=4) (from Davey *et al*, 2017)

suggestive of an enrichment of $V\delta3^+$ clonotypes in the periphery of patients with AIH to similar proportions as that found in the liver.

4.3.3 CDR3 analysis

The key research advantage that can be gained by deep sequencing-based TCR repertoire profiling compared with any other method is full exploration of the nature of the complementarity determining region 3 sequences present in the population of cells being analysed. Each individual CDR3 represents a different clonotype, so the number and variety of CDR3s obtained from a population informs on the size and scope of the TCR repertoire. Since CDR3 regions are critical in defining T cell antigen specificities, knowledge of CDR3 sequences can yield insight into the nature of the antigenic influence on the repertoire of the population analysed, and possibly, the nature of the antigen itself.

The iRweb Tools software developed by iRepertoire generates “tree maps” to visualise the CDR3 repertoire for each sample. Tree maps show each unique CDR3 as a coloured rectangle, where the size of each rectangle corresponds to the abundance of each CDR3 within the repertoire. The positioning of each rectangle is then grouped according to the V region usage. Figure 4.17 shows tree maps for the 10 liver samples analysed in this study for both the γ- and δ-chains. Strikingly apparent from these plots is the very large contribution of a small number of clonotypes to the repertoire in the majority of the samples.

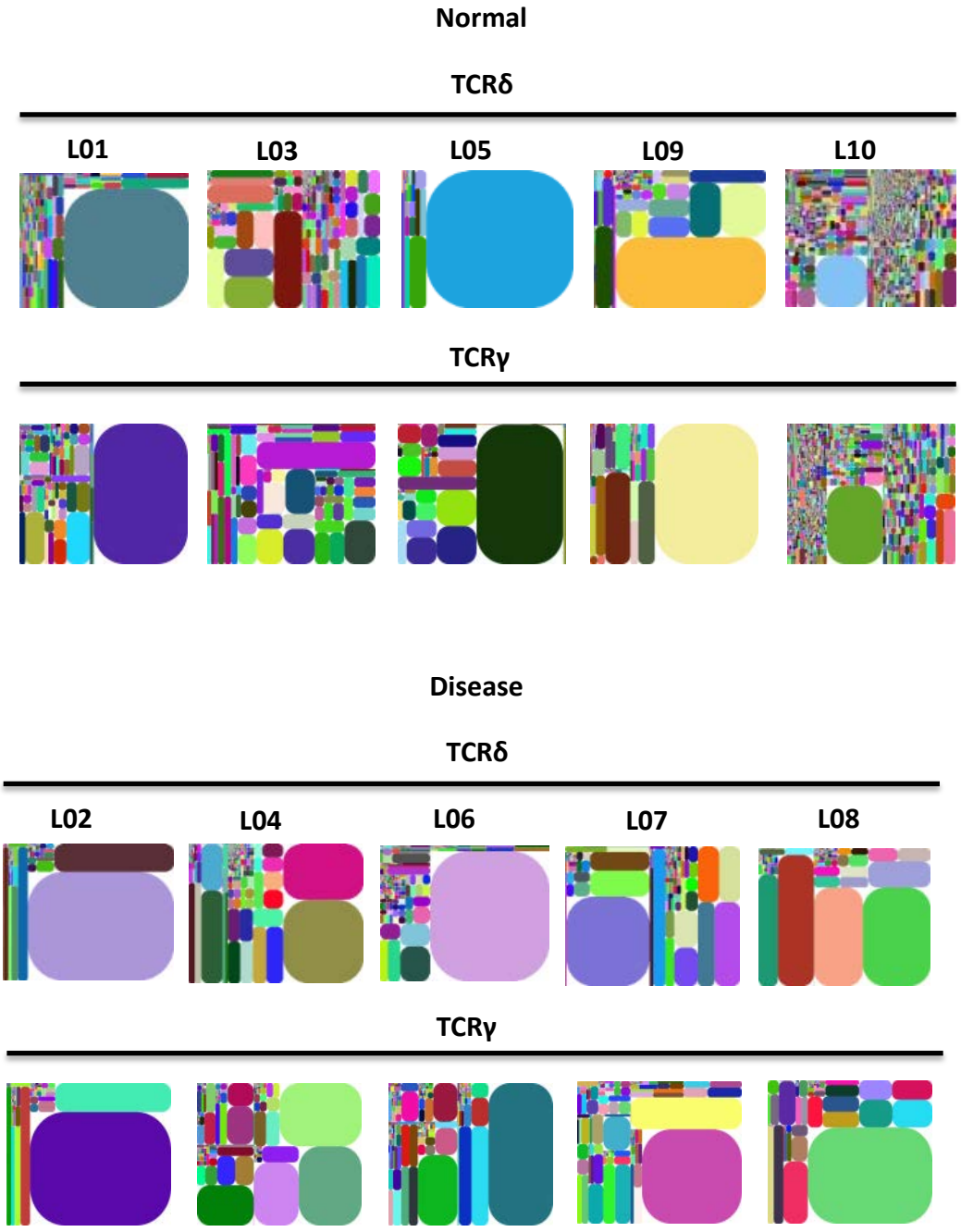

Figure 4.17: The intrahepatic Vδ2^{neg} TCR repertoire is dominated by clonal expansions

Tree maps show CDR3 clonotype usage in relation to total repertoire size (each CDR3 colour is chosen randomly and does not match between plots). This data is representative of the raw iRepertoire data and has not undergone MiXCR error correction.

The contribution to the total repertoire of just the top ten most frequent clonotypes was plotted post error correction, cumulatively, for each sample for both TCRγ and TCRδ (Figure 4.18). In 8 of the 10 samples the most prevalent CDR3s accounted for at least 50% of the entire repertoire sequenced, with one dominant clone representing in excess of 50% of the entire repertoire in 4 of the 10 donors. This was evident for both TCRγ and TCRδ chains. 7 of the 10 samples included a single clonotype that represented over 3 times the number of copies represented by any other clonotype. The 2 samples where the 10 most prevalent CDR3s did not account for over 50% of the repertoire were both from normal livers, but both normal and diseased liver cohorts contained samples with a high degree of clonal focussing.

While these samples were dominated by $V\delta1^{+}$ TCRs, there was also a significant proportion of $V\delta3^{+}$ cells present. Cumulative frequency plots generated using only $V\delta3^{+}$ sequences demonstrated that $V\delta3^{+}$ cells also exhibited strong clonal focussing, as for the total $V\delta2^{neg}$ population (Figure 4.19a). The repertoire focussing present in the top 10 $V\delta1^{+}$ and $V\delta3^{+}$ clonotypes from liver was equivalent to that observed in "focussed" individuals' healthy blood but much greater than that observed for $V\delta1^{+}$ T cells isolated from cord blood in a study conducted previously by this group (Figure 4.19b) (Davey *et al*., 2017).

In addition to clear strong clonal focussing, the total number of clonotypes identified in these samples was in general very low. In Figure 4.20a, δ- and γ-chain frequencies are plotted for the top 100 clonotypes found in each sample. As predicted from Figure 4.18, in 9/10 samples liver-derived samples, 100% of the repertoire is represented by the top 100 TCRδ clonotypes determined, but of note in 4/10 samples there were fewer than 100

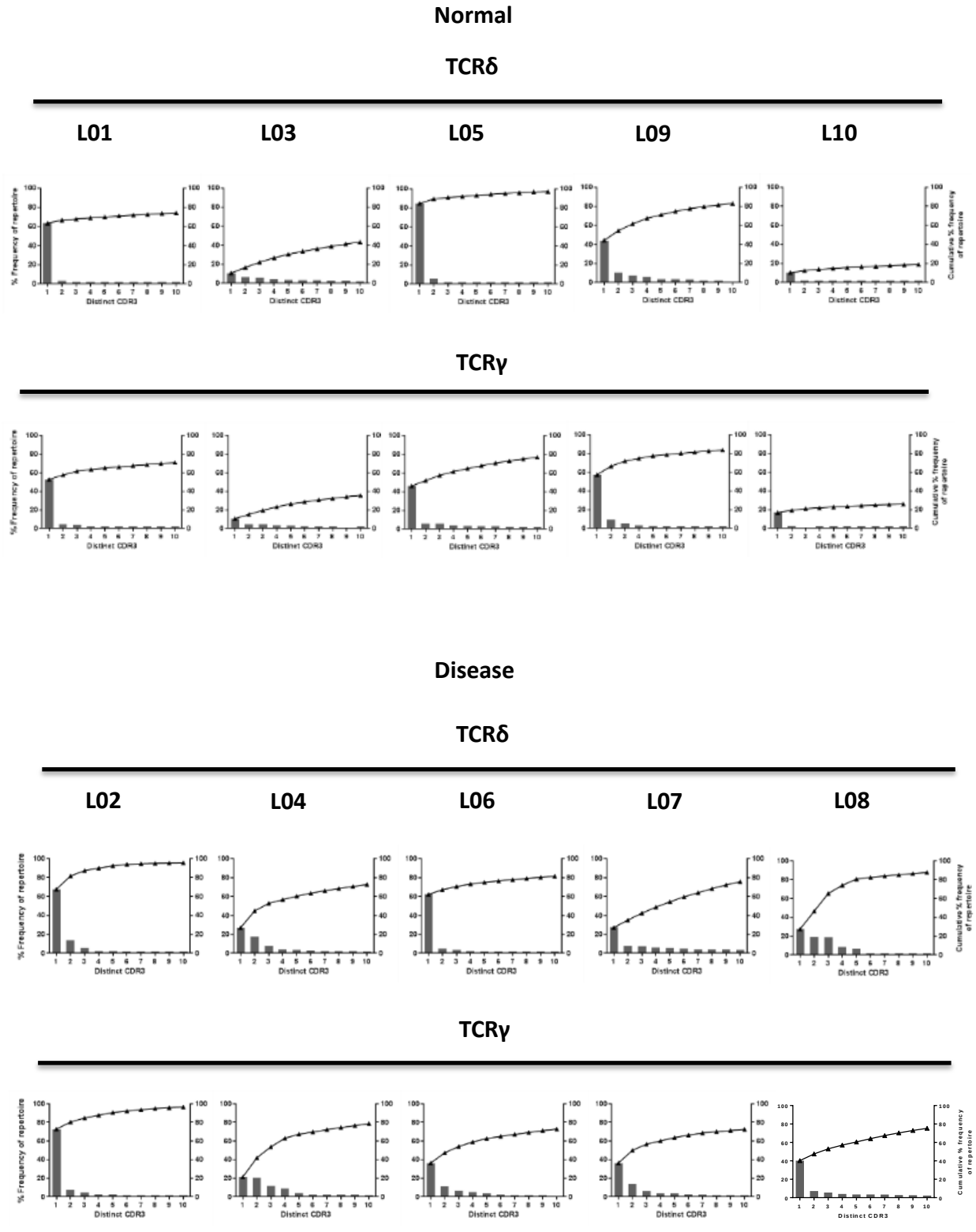

Figure 4.18: Clonal focussing of intrahepatic Vδ2^{neg} gamma delta T cells

Individual clone frequency (left y axis) and accumulated frequency (right y axis) for the first 10 most prevalent clonotypes identified by deep sequencing of Vδ2^{neg} intrahepatic gamma delta T cells in normal and chronically diseased explanted livers.

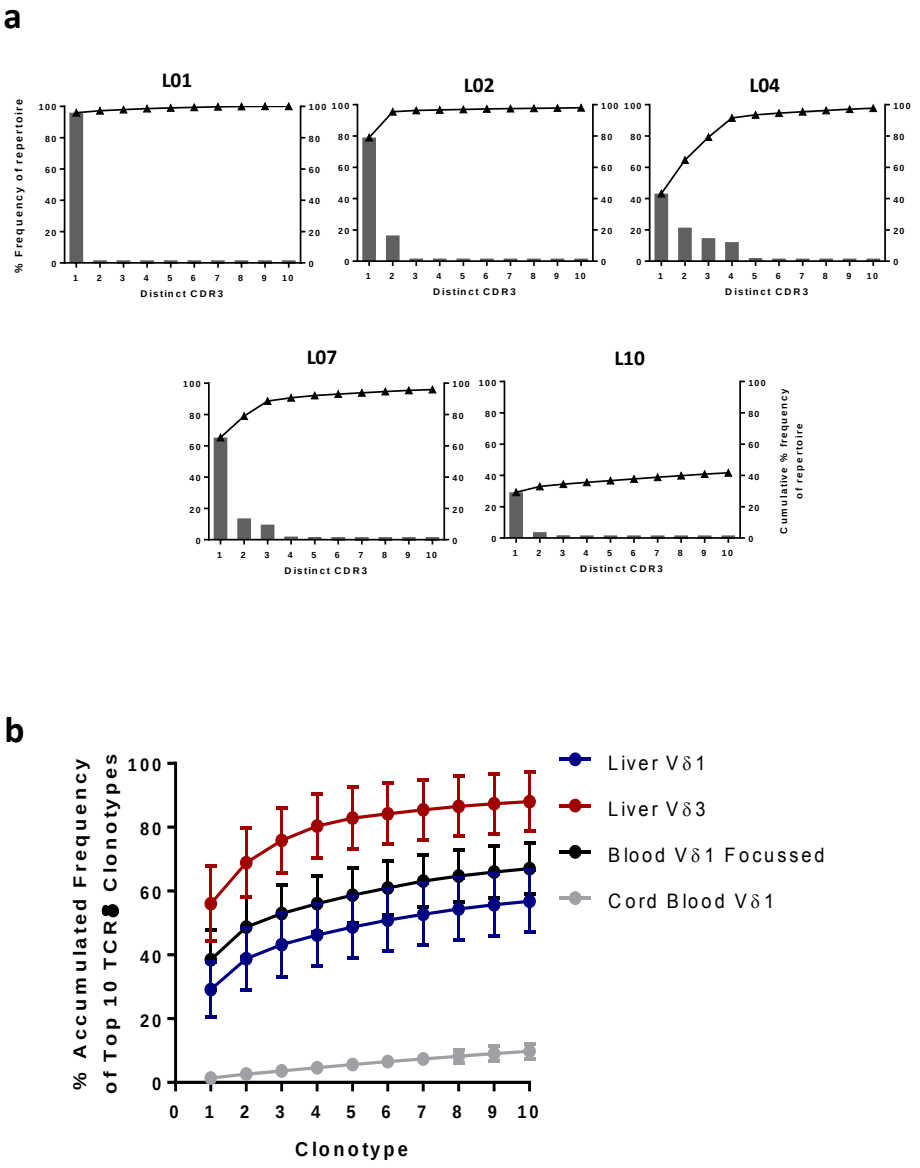

Figure 4.19: Clonal focussing of intrahepatic Vδ3^{+} gamma delta T cells

a) Individual clone frequency (left y axis) and accumulated frequency (right y axis) for the first 10 most prevalent Vδ3^{+} clonotypes identified by deep sequencing of intrahepatic gamma delta T cells in normal and chronically diseased explanted livers, where the Vδ3^{+} population represented greater than 5% of the total Vδ2^{neg} population.

b) Comparison of frequency of top 10 most prevalent clonotypes across all liver samples for Vδ1^{+} (blue) Vδ3^{+} (red), as well as "focussed" healthy adult blood donors (black) and cord blood (grey) (from Davey *et al*, 2017).

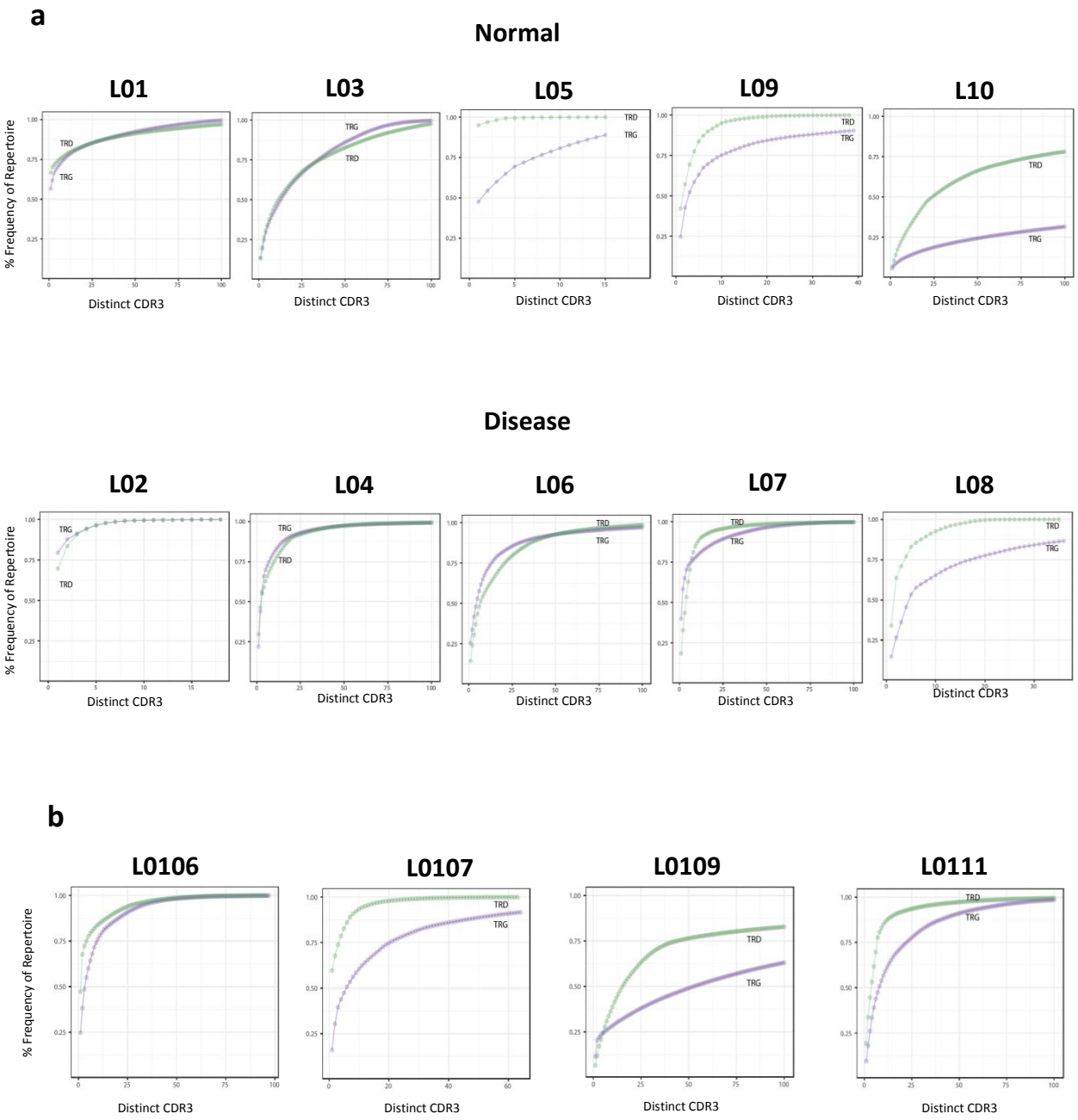

Figure 4.20: Clonal focussing of intrahepatic and diseased blood Vδ2^{neg} gamma delta T cells

a) Accumulated frequency for the first 100 most prevalent clonotypes identified by deep sequencing of intrahepatic Vδ2^{neg} gamma delta T cells in normal and chronically diseased explanted livers, for TCRδ (green) and TCRγ (blue).

b) Accumulated frequency for the first 100 most prevalent clonotypes identified by deep sequencing of diseased blood Vδ2^{neg} gamma delta T cells for TCRδ (green) and TCRγ (blue).

clonotypes identified in total (L02, L05, L08 and L09). While only one of the blood-derived samples demonstrated this, the repertoire was also strongly focussed in these samples, with 100% of the TCRδ repertoire being composed of the top 100 clonotypes by frequency observed in 3 of the 4 AIH-patient samples (Figure 4.20b). To further investigate the potential size of the repertoire, the non-parametric abundance based Chao1 index was used. This metric is based on the work of biodiversity researchers but can be applied to any population to extrapolate estimated population sizes (Chao, 1984), and uses the following equation:

$$S_1 = S_{obs} + \frac{F_1^2}{2F_2}$$

where S_{obs} is the number of species in the sample, F1 is the number of singly-occurring sequences in the sample and F2 is the number of doubly-occurring sequences. Rarefaction of the TCR sequence dataset was conducted computationally using randomly selected batches of sequences using the VDJtools software developed by Chudakov *et al*, where it has been demonstrated to be a robust metric for TCR repertoire size analysis (Shugay *et al*., 2015). The Chao1 estimated population (S_1) from the TCR δ-chain liver- and blood-derived sample groups normalised by read depth is shown in Figure 4.21. The diseased liver population had a mean Chao1 of just 201.5, compared with 397 in healthy liver, 420 in AIH-derived blood and 1,583 in healthy blood. While this metric should not be used as a direct measurement of population size, and no statistically significant differences in Chao1 were observed between any the sample groups, it is clear that for $V\delta2^{neg}$ cells in general there are strikingly few different clonotypes observed even

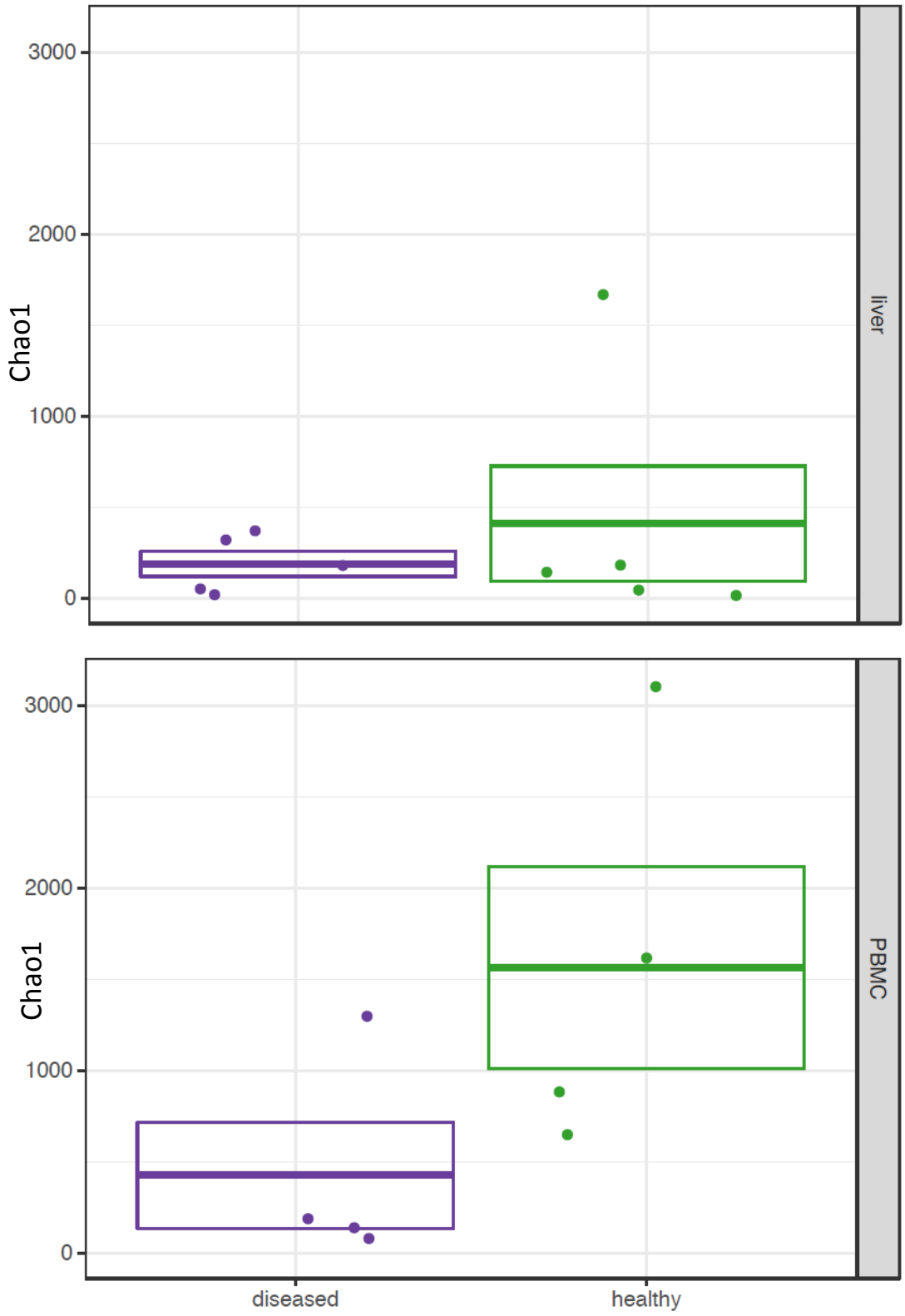

Figure 4.21: Intrahepatic and peripheral Vδ2^{neg} population size estimation

Chao1 estimated population size from TCRδ sequencing of Vδ2^{neg} gamma delta T cell subset for normal and diseased liver (n=5) (upper) and AIH patient and healthy donor blood (n=4) (lower).

in healthy blood, and that the liver may contain fewer still. By comparison, analysis of a human blood-derived TCRβ sequence dataset (Putintseva *et al*., 2013) using the Chao1-based algorithm determined the TCRβ population to be between 1.2×10^7 and 5.4×10^7 unique amino acid CDR3s (Shugay *et al*., 2013).

To assess the diversity of the TCR repertoire identified in these samples, two diversity metrics were used; the Shannon-Weiner index and the D75 metric. The Shannon-Weiner index accounts for both the abundance and "evenness" of the sequences identified – that is, how frequently each sequence is encountered relative to one another. The proportion of sequences (i) relative to the total number of sequences (p_i) is calculated, and then multiplied by the natural logarithm of this proportion ($\ln p_i$). The resulting product is summed across sequences identified, and multiplied by -1:

$$H' = \sum_{i=1}^{s} (p_i)(\ln p_i)$$

The Shannon Wiener diversity (H) scores, normalised to read depth for each sample, are plotted for the liver and blood TCRδ sequences in Figure 4.22. Again, no significant difference was observed between any of the populations, although the diseased liver cohort did trend towards a lower Shannon diversity than the healthy liver, AIH blood and healthy blood cohorts, which were all equivalent.

An additional method of calculating diversity is to use D75, that is, the percentage of unique sequences required to account for 75% of total reads. This method highlights the effect of large clonal expansions on the overall diversity of the population, since the lowest frequency quarter of the repertoire is effectively ignored, and was used in a recent

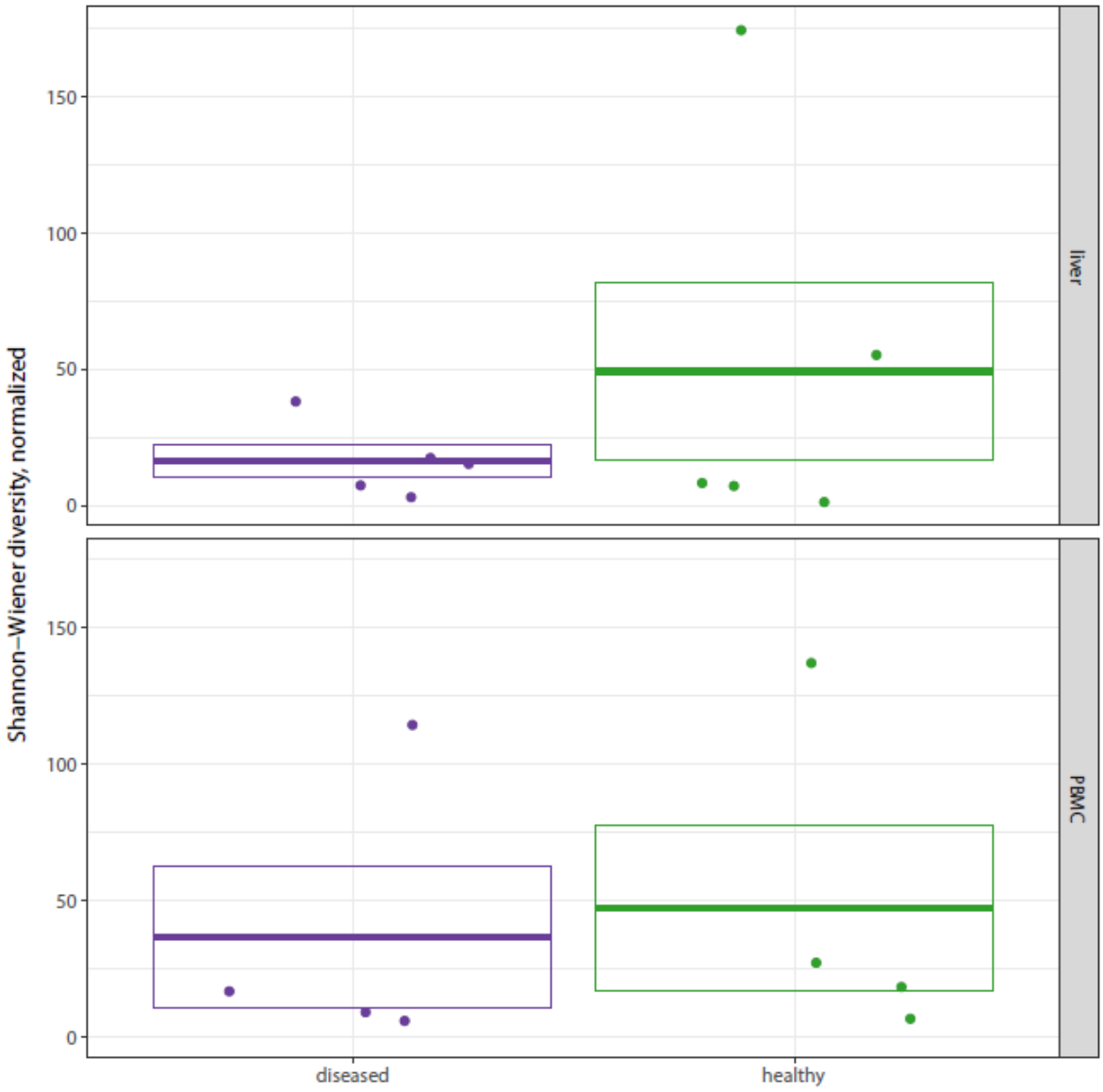

Figure 4.22: Intrahepatic and peripheral Vδ2^{neg} population diversity estimation

Shannon-Weiner diversity estimation for TCRδ sequences from Vδ2^{neg} gamma delta T cell subset for normal and diseased liver (n=5) (upper) and AIH patient and healthy donor blood (n=4) (lower) normalised by read count.

study investigating the repertoire of Vδ1^{+} T cells in adult and cord blood (Davey *et al*., 2017). Here, average D75 for the diseased livers was 2.1%, healthy liver 3.0%, AIH blood 6.8% and healthy blood 5.6% (Figure 4.23a). No significant difference was observed between any group, but these data again highlight the clonotypic focussing present in this population, since only 2-3% of all the CDR3s identified accounted for at least 75% of the total repertoire. Interestingly, one sample (L10) exhibited a much higher D75 (10.7) than observed in any other liver sample. Similarly, a proportion of adults also appear to exhibit a more diverse CDRδ1^{+} TCR repertoire in peripheral blood than commonly observed (Davey *et al*., 2017). Although absence of CMV infection did not appear to be a driving factor in this scenario, in as much as CMV positivity did not always induce a "focussed" repertoire in otherwise healthy adult donors, it is unclear what does drive the Vδ2^{neg} repertoire focussing observed in most blood and liver donors. However, this does suggest that the liver may not be populated by large clonotypic expansions by default, and that perhaps whatever drives the expansions in the periphery may also contribute to the expansions present in most adult livers.

Although no statistically significant difference in diversity was observed between blood and liver using both Shannon and D75 metrics, an alternative analysis using only Vδ1^{+} sequences identified in this study combined with that of Davey *et al*, 2017 did display a significant difference in the number of unique CDR3 regions identified by deep sequencing in liver and blood per 10,000 CDR3s sequenced (Figure 4.23b). Combined blood samples contained an average of 622 Vδ1^{+} CDR3 sequences per 10,000 sequences while liver samples averaged only 135 unique CDR3s per 10,000 sequences (p=0.0005).

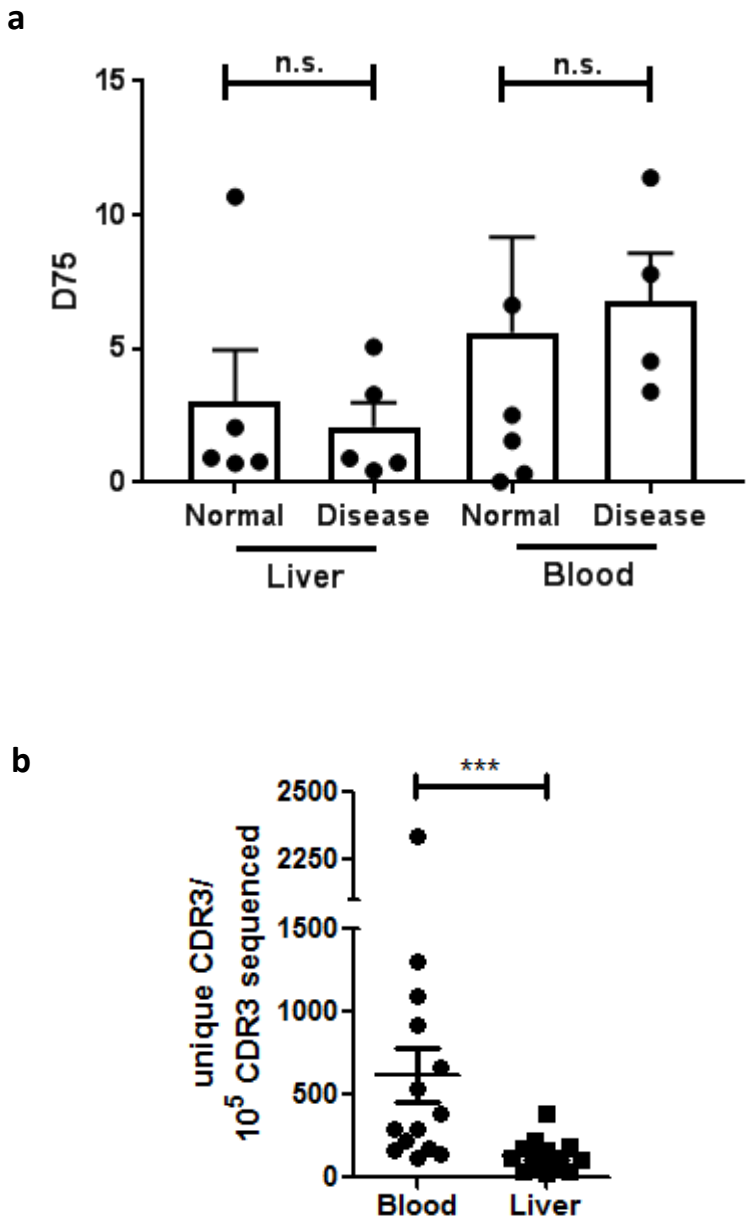

Figure 4.23: Intrahepatic and peripheral Vδ2^{neg} population diversity estimation

a) D75 diversity estimation for TCRδ sequences from Vδ2^{neg} gamma delta T cell subset for normal and diseased liver (n=5) and AIH patient and healthy donor blood (n=4) ($p>0.05$, student's T test)

b) Number of unique CDR3 sequences identified for each liver (n=10) and blood sample (n=14) per 10^5 sequences obtained. Blood data includes Vδ1$^+$ sequences identified in Davey *et al*, 2017. ($p=0.0005$, student's T test).

This suggests that while both compartments are dominated by large clonotypes the periphery has a greater pool of non-expanded clonotypes than the liver.

Next, the composition of the CDR3 itself was analysed. When the frequency of individual clonotypes was accounted for, all liver samples, perhaps with the exception of L10, displayed highly skewed CDR3δ spectratypes (Figure 4.24a). This is indicative of non-stochastic expansion of certain clonotypes of varying CDR3 length. However, there was no specific CDR3δ length favoured across all samples, with each being dominated by clonotypes of differing CDRδ length. This suggests that the expanded clonotypes observed are specific to each individual, i.e. the CDR3δ repertoire is private. Additionally, when the spectratypes were combined there was no significant CDR3 length profile observed for healthy donor cohort compared with diseased donor cohort, suggesting that chronic liver disease does not alter the CDR3δ repertoire, at least in terms of CDR3 length (Figure 4.24b). Interestingly, when segregated by Vδ-region, $V\delta1^+$ CDR3s were significantly longer than $V\delta3^+$ $V\delta5^+$ and $V\delta8^+$ CDR3s, at 54 nucleotides vs. 45 nucleotides ($p<0.0001$) (Figure 4.24c).

The most expanded $V\delta1^+$ and $V\delta3^+$ clonotype from each donor exhibited significant divergence from germline CDR3δ sequences, with most including extensive n-and p-nucleotide addition, resulting from rare recombination events (Table 4.3). Analysis of the entire CDR3δ dataset from all donors sequenced revealed just 3 shared CDR3δ - CACRFGYWGSTDKLIF (liver samples L02 and L06), CALGELPDKLIF (blood samples donor22 and L0109) and CALGELRLGDTFTDKLIF (blood samples donor012 and L0109). All three sequences were present at low frequencies in both donors and exhibited extensive

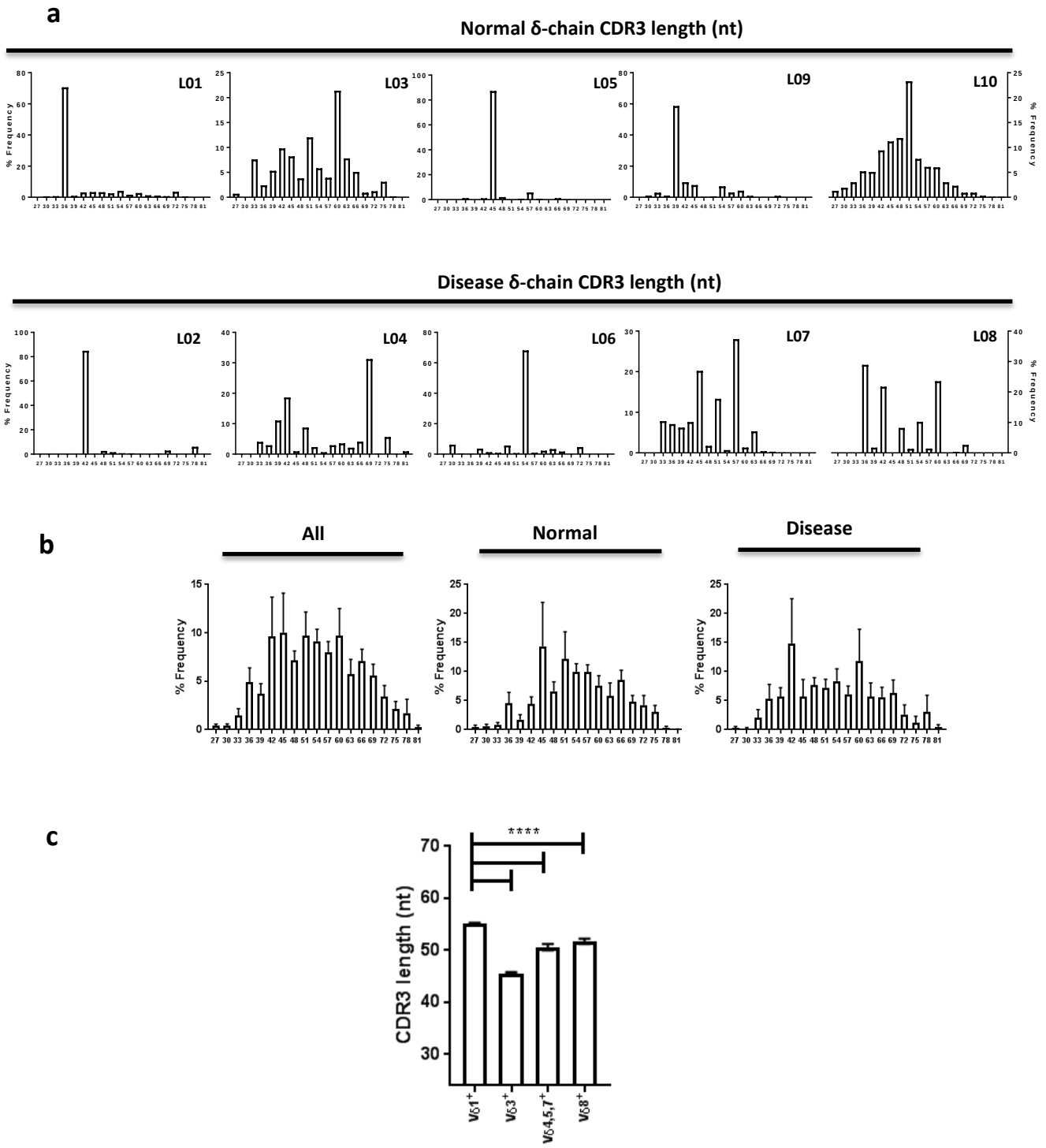

Figure 4.24: Skewed distribution of CDR3δ lengths in intrahepatic Vδ2^{neg} T cells

a) An NGS based approach was used to determine CDR3 length of intrahepatic Vδ2^{neg} T cells. Comparison of non-normalized CDR3δ length spectratyping is displayed here for healthy (n=5) and diseased (n=5) liver donors
b) Comparison of mean + s.e.m. CDR3δ spectratypes of Vδ2^{neg} T cells from all (left), normal (centre) and diseased livers (right)
c) Comparison of mean + s.e.m. CDR3 lengths for all liver samples based on V-region usage, ****p<0.0001

germline		TRDV					N/P	TRDD1	TRDD2	N/P	TRDD3	N/P			TRDJ								
	TRDV1	GCT	CTT	GGG	GAA	CT		GAAATAGT	CCTTCCTAC		ACTGGGGGATACG					AC	ACC	GAT	AAA	CTC	ATC	TRJD1			
															CT	TTG	ACA	GCA	CAA	CTC	TTC	TRJD2			
													C	TCC	TGG	GAC	ACC	CGA	CAG	ATG	TTT	TRJD3			
																							CDR3	N/P nt	
donor																							length	added	protein sequence
L01	TRDV1	GCT	CTT	GGG	GAA	C	GTCAGGCGTTAGGTA		CTTCC	CTCCGAA	ACTGGGGGATA	GTAAAAAT					C	GAT	AAA	CTC	ATC	TRJD1	72	30	CALGERQALGTSLRNWGIVKIDKLIF
L02	TRDV1	GCT	CTT	GGG	GAA	C	GTTC		CCTTCCT	GCCAAACGATATGGGGTGCT	GGGGATA	AGCCTCCCTT				AC	ACC	GAT	AAA	CTC	ATC	TRJD1	78	34	CALGERSLPAKRYGVLGISLPYTDKLIF
L03	TRDV1	GCT	CTT	GGG	GAA	C	ATAT		CTTCCTAC	GT	CTGG	ATCCGGCGCTAGA			T	TTG	ACA	GCA	CAA	CTC	TTC	TRJD2	60	19	CALGEHFLRLDPALDLTAQLFF
L04	TRDV1	GCT	CTT	GGG			ACCGTCCTA	GAAAT		CTTCAGT	ACTGGGGGATA	TAGGGGTATGGG				C	ACC	GAT	AAA	CTC	ATC	TRJD1	69	28	CALGTVLEIFSTGGYRGMGTDKLIF
L05	TRDV1	GCT	CTT	GGG			CCCCTGAG				CTGGGGG	TCTC				AC	ACC	GAT	AAA	CTC	ATC	TRJD1	45	12	CALGPLSWGSHTDKLIF
L06	TRDV1	GCT	CT	GGG	GA		CCCCGG		CCTTCC	CCGGAGGTGTACT	CTGGGGGATACG	CGATGTGTTG					CC	GAT	AAA	CTC	ATC	TRJD1	72	29	CALGDPGLPRRCTLGDTRCVADKLIF
L07	TRDV1	GCT	CTT	GGG	GAA	CT	GACGACT				ACTGGGGG					C	ACC	GAT	AAA	CTC	ATC	TRJD1	45	7	CALGELTTTGGTDKLIF
L08	TRDV1	GCT	CTT	G			CAAT				TGGGG	CATGGGACGT						T	AAA	CTC	ATC	TRJD1	36	14	CALAIGAWDVKLIF
L09	TRDV1	GCT	CTT	GGG	GAA		GGTTGTGGTC				GGGAT	TGTACGT				AC	ACC	GAT	AAA	CTC	ATC	TRJD1	51	17	CALGEGCGRDCTYTDKLIF
L10	TRDV1	GCT	CTT	GGG	GAA	C	CGGGCCCGGG				CTGGGGGAT	GCAA					ACC	GAT	AAA	CTC	ATC	TRJD1	51	14	CALGEPGPGWGMQTDKLIF
0860-1	TRDV1	GCT	CTT	GGG	GA		CCGA		TTCC	CGGACAGT							ACC	GAT	AAA	CTC	ATC	TRJD1	42	12	CALGDRFPDSTDKLIF
0860-2	TRDV1	GCT	CTT	GGG	GAA	CT	ACGA				TGGGGGATA	AT					C	GAT	AAA	CTC	ATC	TRJD1	42	6	CALGELRWGIIDKLIF
1410	TRDV1	GCT	CTT	GGG	G		TCT		TTCC			CGCCAGGT				AC	ACC	GAT	AAA	CTC	ATC	TRJD1	42	11	CALGVFPARYTDKLIF
1445	TRDV1	GCT	CTT	GGG	GA		G		CTAC	GT	TGGGGGA	AAAT					C	GAT	AAA	CTC	ATC	TRJD1	42	7	CALGELRWGKIDKLIF
888	TRDV1	GCT	CTT	GGG	G		GGGGGGG		CTTCC	CCCAAAAACCC	GGGGG	GGCCGGGCCCCCAACAGCC							CAA	CTC	TTC	TRJD2	66	37	CALGGGGFPQKPGGAGPPTAQLFF
1421	TRDV1	GCT	CTT	GGG	GAA	C	CCCA		CTTCCTAC	ATCTCAT	TGGG	ACGAT						T	AAA	CTC	ATC	TRJD1	51	16	CALGEPHFLHLIGTIKLIF
0802-1	TRDV1	GCT	CTT	GGG	GAA	CT	ATAT		CTTCCT	CCTAACTCCAATATATTATTCTTCCTACC	ACTGGGGGA	CG				AC	ACC	GAT	AAA	CTC	ATC	TRJD1	81	35	CALGELYLPPNSNILFFLPLGDDTDKLIF
0802-2	TRDV1	GCT	CTT	GGG	G		CCAGTCTT		CCTTCCT	TAAT	ACTGGGGG	CTATACAAAAAAGATTCT				AC	ACC	GAT	AAA	CTC	ATC	TRJD1	72	30	CALGASLPSLILGAIQKRFYTDKLIF
618	TRDV1	GCT	CTT	GGG	G		TACCGACTC				GGGGGATACG	CTCTAGGG				TG	ACA	GCA	CAA	CTC	TTC	TRJD2	54	17	CALGVPTRGIRSRVTAQLFF
464	TRDV1	GCT	CTT	GGG	GAA	CT	TTA		TTCC	CCTCCCCTCCCCTGGTTGG	TGGGGGAT	CCGTGG					ACC	GAT	AAA	CTC	ATC	TRJD1	69	28	CALGELYSPPLPWLVGDPWTDKLIF
																					average		57	20.15	
																					range		36-81nt	6-37nt	

Table 4.3: Dominant clonotypes have complex, private CDR3 regions

Table includes the CDR3δ of the most dominant clonotype for each of the liver samples that underwent NGS TCR sequencing at iRepertoire (L01-L10), as well as single cell PCR TCR sequencing (see Chapter 5). V, D and J segment usage is identified, as well as n- and p-nucleotide addition, highlighted in red and blue respectively. CDR3 length, n/p addition and amino acid sequence for each clonotype is shown.

modification from germ-line encoding in the case of the first and last noted above. The highly private and complex nature of the Vδ2^{neg} CDR3δ repertoire in human liver is suggestive of non-stochastic selection of specific clonotypes unique in each individual, consistent with antigenic stimulation.

In the CDR3γ repertoire however, some evidence of sequence commonality both within and between individuals was observed across the combined liver and blood derived dataset. The D metric represents the number of shared sequences divided by (diversity of clonotypes in sample 1 * diversity of clonotypes in sample 2) to normalize for sequencing depth. D values, allowing for one amino acid mismatch, for each sample amongst liver- and blood-derived samples is plotted in Figure 4.25a, as well as clonotypes identified shared, with up to one amino acid mismatch, among both compartments. The liver displayed significantly fewer overlapping CDR3γ clonotypes than blood although in both compartments this represented a very small percentage of the total repertoire (D=0.0017% vs. 0.0038%). Analysis of the overlapping sequences in both liver and blood revealed that the shared clonotypes were less variable in CDR3 length than private sequences in both compartments, and in liver were significantly shorter in amino acid (aa) sequence (12 aa vs. 14 aa) (Figure 4.25b). Furthermore, analysis of the shared CDR3γ specific amino acid sequence revealed a relatively constant structure over 12 amino acids with only aa at position 6 and 7 displaying significant divergence across the population (Figure 4.25c). This suggests that shared CDRγ sequences are likely simple to rearrange "germline"-like in nature with few if any n- and p-nucleotide additions which are more prevalent in the periphery than the liver. This is consistent with the putative existence of a non-antigenically selected "naïve" population of Vδ2^{neg} cells that possess easily

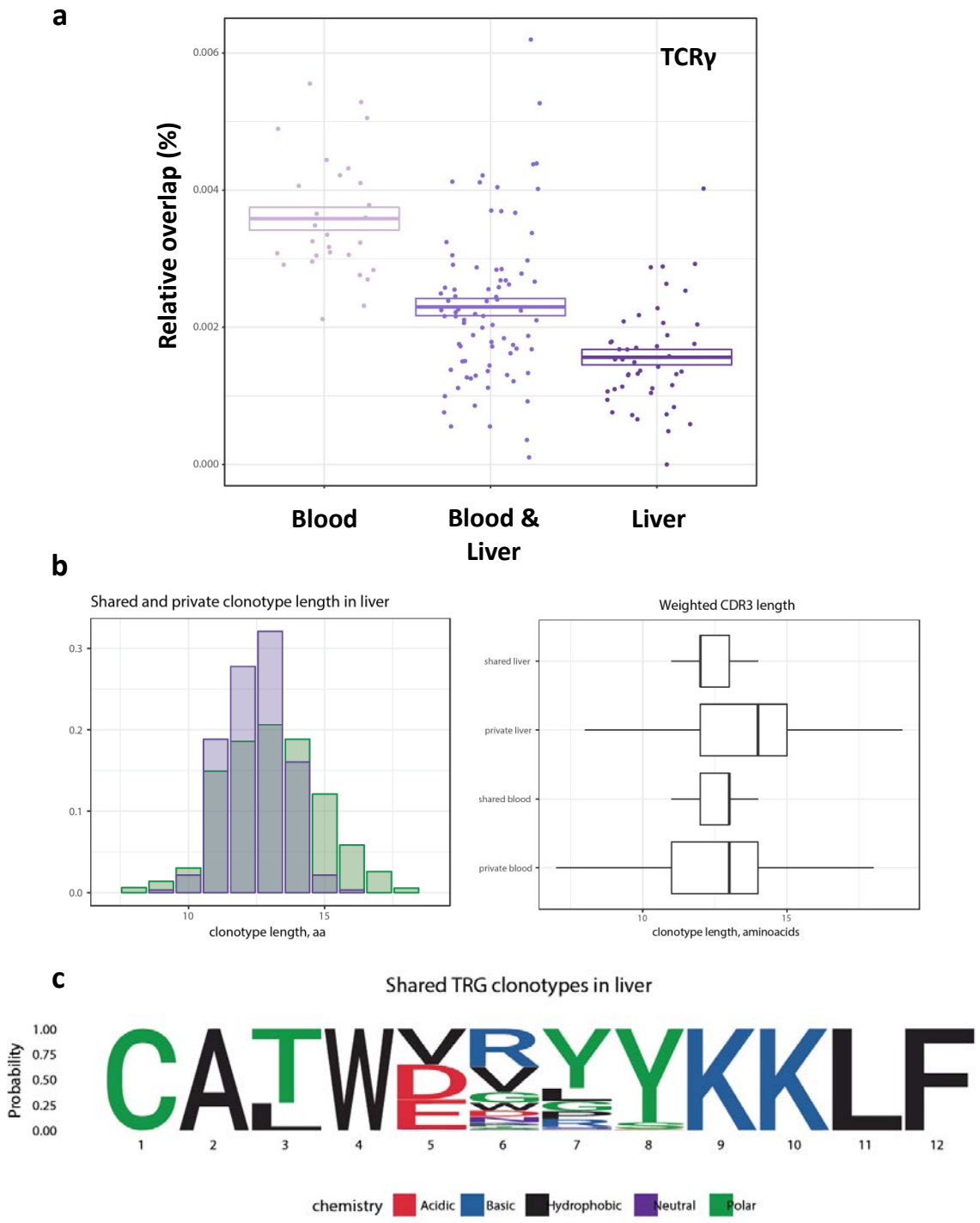

Figure 4.25: Clonal overlap in CDRγ sequences in liver and blood derived Vδ2^{neg} T cells

a) Extent of clonal overlap in CDR3γ sequences within liver, blood and between the two compartments. Each dot corresponds to a specific sequence identified in more than one sample, and what proportion of the repertoire said sequence occupies in each sample it is found in

b) Comparison of shared (blue) and private (green) clonotype CDR3γ lengths in liver and blood

c) Visual representation of amino acid enrichment at each position in shared sequence CDR3γ in liver

recombined CDR3γ chains common to multiple individuals. Such a population has been identified in Vδ1^{+} gamma delta T cells in healthy blood donors (Davey *et al*, 2017).

4.3.4 Single cell TCR PCR analysis

To confirm that the large clonal expansions identified by deep sequencing were genuine and not simply a reflection of disproportionate amplification of overexpressed TCR mRNA transcripts, single cell TCR sequencing was performed on Vδ1^{+} and Vδ3^{+} cells isolated from explanted human liver (n=3). In the samples analysed, clear dominance of specific TCR CDR3δ chains was observed for both Vδ1 and Vδ3 bearing cells, with between 56% and 94% of Vδ1^{+} cells sorted and between 83% and 100% of Vδ3^{+} cells sharing CDR3δ sequences with at least one other sorted cell (Figure 4.26). This data also confirms the strong clonal expansions present in the Vδ3^{+} subset within the liver.

In summary, these results are consistent with the selective retention and/or expansion of Vδ2^{neg} gamma delta T cells in the liver of both chronically inflamed but also healthy donors. These populations are generally composed of massively expanded clonotypes, concomitant with a focussed repertoire lacking in overall diversity. The expanded TCRs identified are highly private in nature, with no significant overlap between individuals and exhibiting extensive recombinational modification, consistent with non-stochastic antigen-specific expansion. While chronic inflammation did not appear to alter the overall shape of the observed Vδ2^{neg} repertoire in liver, patients undergoing therapy for autoimmune hepatitis did exhibit perturbed expansions of phenotypically activated clonotypically focussed Vδ2^{neg} T cells in the periphery.

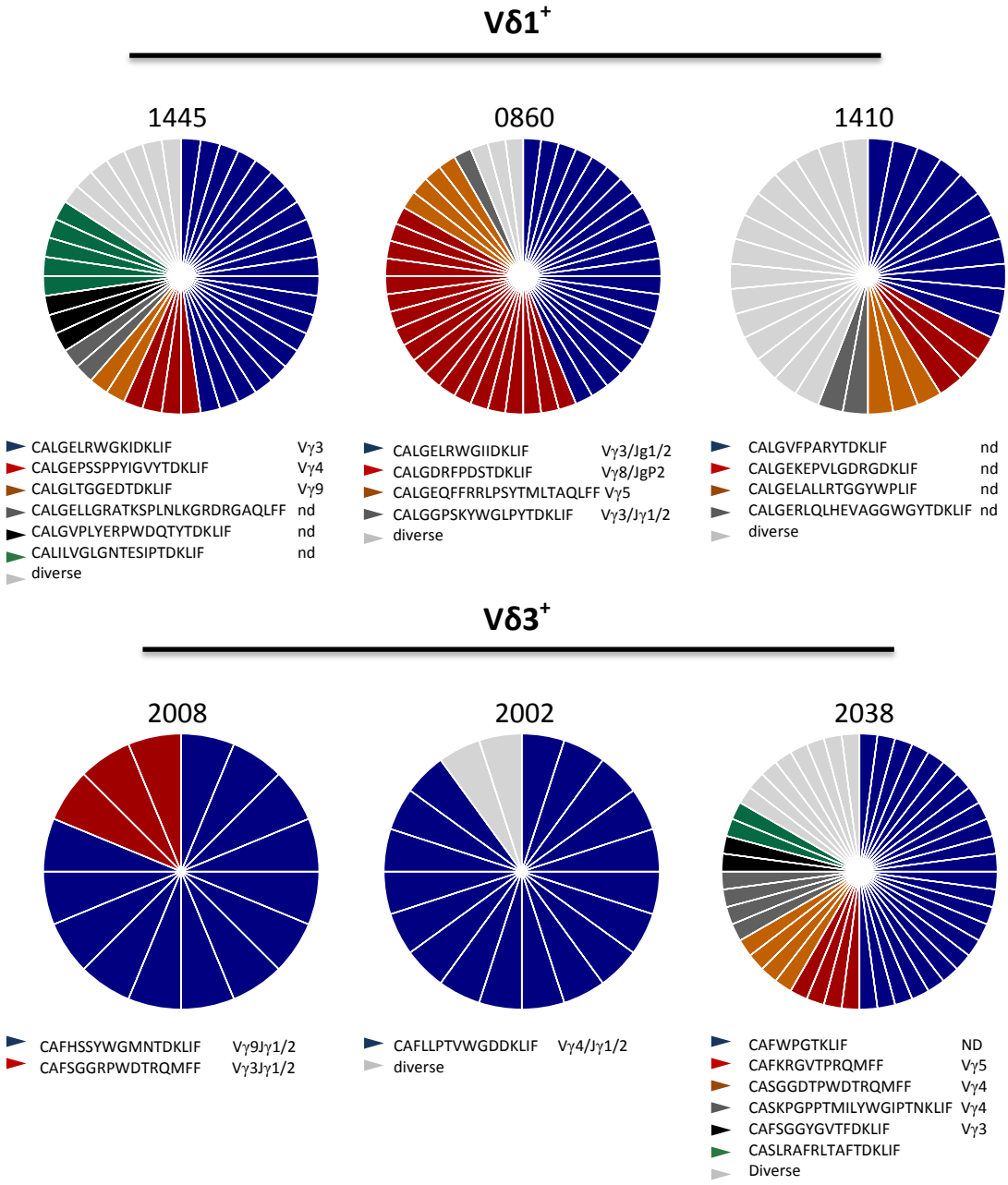

Figure 4.26: Single cell PCR TCR sequencing of intrahepatic Vδ2^{neg} T cells

Vδ1^{+} (upper) and Vδ3^{+} (lower) cells were singly sorted and the CDR3 sequenced by single cell PCR (n= 16 – 44). Each colour represents a unique CDR3δ sequence, listed below each chart with corresponding Vγ-chain usage. "Diverse" notation corresponds to cells with CDR3δ not identified in any other cell.

4.4 Discussion

This chapter focussed on the assessment of human intrahepatic and peripheral gamma delta T cell TCR chain usage, composition of the CDR3 and analysis of clonality in health and chronic liver disease. This was achieved using a combination of flow cytometry and NGS-based TCR sequencing. The $V\delta2^{neg}$ repertoire elucidated from the samples in this study suggested highly clonally focussed expanded clonotypes constructed from highly variable, private CDR3 regions for both CDR3γ and CDR3δ. This presents a stark contrast to the repertoire determined for two innate like T cells populations in humans; MAIT cells, which exhibited a high degree of publicity and distinct bias in CDR3β length distribution (Lepore *et al*., 2014) and $V\delta2^{+}$ gamma delta T cells, which are also highly public and restricted in CDR3 composition (Davey *et al*, unpublished).

Interestingly, although δ-chain usage strongly favoured Vδ1 in the majority of samples analysed, γ-chain use was highly heterogeneous in all patient cohorts analysed. This throws these cells into sharp contrast with murine gamma delta T cells, where specific tissues, including the liver, are associated with accumulation of γ-chain restricted TCRs. Recent work from Hayday *et al* suggested that gut resident $V\delta2^{neg}$ T cells favoured expression of Vγ4, and that these cells could be selectively regulated by intestinal epithelium expression of butyrophilin-like family members 3 and 8 (Di Marco Barros *et al*., 2016). Contrary to these findings, no Vγ-chain specific enrichment was observed in human livers, although the potential for regulation of $V\delta2^{neg}$ cells by BTNL family molecules in humans remains an intriguing prospect. It is also possible that the more significant physical compartmentalisation of intra-epithelial gamma delta lymphocytes in

the gut by the lamina propria may promote an accumulation of enriched Vγ-chain specific populations in the gut that is not observed in the less physically restrained liver-tissue associated gamma delta T cell population.

The analysis of clonotypic cumulative frequency primarily supported the observation that very few clonotypes contributed to the overwhelming majority of the entire repertoire in most of the donors. However, in several donors the cumulative frequency of the TCRγ did not match that of the TCRδ. Later analysis of shared clonotypes suggested that there was a greater publicity of TCRγ sequences than TCRδ, which contained just three overlapping clonotypes amongst all 18 donors. These data seem to be slightly contradictory, since in order for there to be shared gamma-chain clonotypes but not delta-chain, "psuedoclonotypes" must exist with common TCRγ paired with diverse TCRδ sequences. However, if that were the case, one may expect the diversity of the CDR3γ to be less than CDR3δ, which is contrary to the slower accumulation of TCRγ clonotypes in the cumulative frequency plots. It is unclear what the reason for this is, but further analysis of this and other datasets may help provide answers.

One possible explanation for the increased publicity within the CDRγ sequences compared with the CDR3δ sequences is the presence of contaminating Vγ9JγP region sequences specifically used by the semi-invariant Vδ2Vγ9 phosphoantigen-reactive gamma delta T cells, and despite post-processing removal of these sequences it is still possible that some CDRγ sequences expressed by contaminating $V\delta2^{+}$ cells may have been present in the population analysed, since paired chain data is not available from these analyses. However, analysis of CDR3 length and amino acid sequence suggested that CDR3γ public clonotypes were very similar and relatively simple compared with

private sequences, as well as representing a very low proportion of the repertoire. An attractive explanatory hypothesis may be that this represents the use of simple gamma-chain recombinations that have yet to undergo antigenic stimulation and expansion, consistent with their low overall frequency. Further study of the impact of clonal selection by specific stimuli such as CMV infection is warranted to establish whether $V\delta2^{neg}$ gamma delta T cells genuinely act in an adaptive manner.

What implications this research has for the field of chronic liver disease research is perhaps debatable. No significant differences between healthy and diseased livers were observed in chain usages, CDR3 lengths or complexity. Additionally no disease-related clonotypes were identified. Clearly, the pathologies of the various chronic liver diseases are highly diverse, with some diseases associated with antigen specific responses, and other yet to be. For example, in PBC patients $CD4^{+}$ αβ T cells specific for the E2 component of the pyruvate dehydrogenase complex have been discovered (Van de Water *et al*., 1995), while PSC has been linked with HLA haplotype (Schrumpf *et al*., 1982), suggesting a specific T cell related contribution to disease progression. An NGS-based study of TCRβ repertoire in PBC and PSC livers discovered several apparently disease-specific clonotypes (Liaskou *et al*., 2016), although whether these are reactive to disease specific antigens is unclear as many of them have also been identified as public TCRβ sequences in other studies (Britanova *et al*., 2014). Accordingly, the grouping of livers of multiple disease aetiologies as a "disease liver" cohort was unlikely to highlight any disease specific clonotypes, but it did suggest that there was no significant contribution of general chronic inflammation to the repertoire of intrahepatic $V\delta2^{neg}$ T cells, consistent with the findings of the previous chapter that suggested chronic disease

did not significantly impact gamma delta T cell infiltration into livers. In order to ascertain the genuine potential for disease related Vδ2^{neg} expansions, one would need to analyse considerably more samples than used in this study, but based on the findings here and in previous work conducted on peripheral Vδ1^{+} cells, it seems highly likely that the tremendously diverse focussing of the Vδ2^{neg} repertoire in many adults may preclude the possibility of ever identifying common sequences present at high frequencies in response to disease-specific stimuli in a setting such as the liver.

This being said, there is a clear perturbation in the frequencies and phenotype of circulating Vδ2^{neg} T cells in autoimmune hepatitis patients. Similar perturbations have been described in PSC (Martins *et al*., 1996) and PBC (Hua *et al*., 2016). In addition to an inversion of the usual Vδ1/Vδ2 ratio observed in most healthy adults, the frequency of Vδ1^{neg}Vδ^{neg} cells was also increased in these samples compared with healthy donor blood. In addition, they expressed higher CD69 and lower CD27, suggestive of induced effector function, which is indicative of potential TCR engagement. Once more, no significant differences were observed in the nature of the repertoire between diseased and healthy donors, providing no evidence of disease-specific reaction within the repertoire to AIH. However, since even healthy individuals often possess highly focussed Vδ2^{neg} repertoires, it cannot be ruled out that a change in the frequency of specific disease-related clonotypes has not taken place in these individuals. Longitudinal study of AIH patients before, during and after therapy, perhaps also including relapse, may help address this question, although there is an obvious difficulty in getting blood samples from patients pre-diagnosis. In the case of AIH, it is also difficult to distinguish whether it is the disease or the treatment that leads to the observed fluctuations in circulating

gamma delta T cells, as many immunosuppressive regimens will impact circulating T cell populations, as has been demonstrated with azathioprine and Vδ2$^+$ cells (McCarthy *et al*., 2015). A full study using patients undergoing different immunosuppression and perhaps including a cohort of blood donors from non-immunosuppressed chronic liver disease patients (such as NASH) may start to unpick the apparent complexities of this scenario. Additionally, further examination of a cohort of this nature could provide insight into whether the observations made in this study and others are related to a general systemic response of gamma delta T cells to the increased permeability of the gut to microbes and microbial antigen, often associated with non-viral chronic liver inflammation (Martinez-Esparza *et al*., 2015, Szabo, 2015).

Vδ3$^+$ gamma delta T cells have been associated with the human liver by studies performed over the last 15 years (Kenna *et al*., 2004, Mangan *et al*., 2013) and also comprised the most frequent gamma delta T cell subset in a study of healthy human colon (Dunne *et al*., 2013). Here, enrichment of liver with these cells was confirmed indirectly by flow cytometry and directly by deep sequencing. Additionally, isolation of Vδ3$^+$ sequences from repertoire data and single cell PCR of Vδ3$^+$ cells demonstrated that these cells are equally as dominated by clonal expansions as Vδ1$^+$ cells. It is unclear whether these cells are responsive to liver associated antigen, but the parallels between these cells and Vδ1$^+$ gamma delta T cells, in terms of repertoire at least, are clear, suggestive of an adaptive-like immunobiology for Vδ3$^+$ cells also. *Ex vivo* expanded human blood derived Vδ3$^+$ cells have been demonstrated to kill CD1d-expressing cells in a CD1d non-αGalCer dependent fashion (Mangan *et al*., 2013). Whether the liver derived Vδ3$^+$ populations described in this study were CD1d reactive is unclear, but the strong

clonotypic expansions of diverse complex CDR3 region bearing Vδ3$^+$ cells is unlike the TCR composition exhibited by other generally innate like CD1d-reactive T cells. Unlike in rodents that have high constitutive expression of CD1d and large intrahepatic iNKT populations, healthy human hepatocytes express CD1d intracellularly only at very low levels, although it is upregulated in certain chronic liver diseases, such as HCV (Yanagisawa *et al*., 2013) and PBC (Tsuneyama *et al*., 1998). Despite this, it is possible that the enrichment of these cells in the liver may be driven by recognition of stress-induced CD1d upregulation and subsequent TCR-mediated binding of CD1d presented glycolipids, however, considerably more work would be required to prove the biological significance of such an interaction.

While the iRepertoire approach was chosen for several reasons, it was not perfect in some aspects, such as repertoire size estimation. In a comparison of various non-parametric population estimators, Asquith *et al* showed that TCR repertoire size estimators are biased by sample size, which would likely change the results based on the number of cells sequenced or the quality of the RNA and subsequent sequencing itself (Laydon *et al*., 2014). They also strongly suggested that these estimates, including Chao1 used in this study, underestimate diversity. The Chao1 results obtained here were indeed very low, and while it is clear that they do reflect a genuinely focussed repertoire, the use of molecular barcoding of samples such as MIGEC (molecular identifier groups–based error correction) (Shugay *et al*., 2014) during sequencing has been proposed to eliminate sequencing errors and hugely improve the accuracy of diversity assessments. Future analyses such as this would therefore benefit from being performed in house using barcoding protocols such as this.

In summary, the work presented in this chapter represents, to the author's knowledge, the first detailed repertoire analysis of $V\delta2^{neg}$ gamma delta T cells in any human solid tissue, and has highlighted the remarkably private and clonally focussed repertoire that bears the hallmarks of association with an adaptive-like immune response.

5

Intrahepatic gamma delta T cells: the relationship between phenotype, clonotype and function

5.1 Introduction

5.1.1 Tissue-resident T cells

In the previous chapters, evidence for the presence of $V\delta2^{neg}$ gamma delta T cells enriched with large, complex and private TCR clonotypes in the liver was presented. Immunohistochemical analysis highlighted the predominantly parenchymal localisation of gamma delta T cells, and combined with flow cytometry analysis of *ex vivo* lymphocytes, suggested that $V\delta2^{neg}$ T cells were present at high proportion in normal liver tissue. A question that arose from this is whether these intrahepatic $V\delta2^{neg}$ T cells were enriched due to enhanced recruitment from the periphery or whether a pool of these cells may be genuinely liver resident.

The topic of tissue residency of lymphocytes has received a lot of attention in the scientific literature over recent years. Once naïve T cells have recognised cognate antigen they proliferate and upregulate homing receptors that allow re-distribution of these cells from the periphery and into tissues, where they mount an effective localised response. While some clonal daughter cells remain in circulation as memory cells, others remain at the site of response as tissue resident memory cells (T_{RM}) and do not re-enter circulation. First identified using mouse models (Masopust *et al*., 2001), T_{RM} have since been demonstrated to exist throughout the human body (Thome and Farber, 2015).

Naïve αβ T cells express CCR7, which facilitates migration into lymph nodes from the periphery (Bromley *et al*., 2005). A study by Lanzavecchia's group determined that expression of this surface molecule is a defining element of T cell naivety (Sallusto *et al*., 1999), and definitively linked migrational capability with memory status. Other surface

proteins have since also been ascribed to differentiation status, including isoforms of CD45, CD62L, the TCR co-stimulatory CD27 and CD28 and CD127, the IL-7 receptor. Naïve T cells (T_N) express CD45RA, which is lost in circulating central memory T cells (T_{CM}). Effector memory cells (T_{EM}) lose expression of lymph node associated CCR7, CD62L and homeostasis associated CD127, as well as CD27 and CD28 (Obar and Lefrancois, 2010). Terminally differentiated T cells (T_{EMRA}) re-acquire expression of CD45RA, with each step in differentiation controlled by a variety of transcription factors including TCF7, Tbet (Szabo *et al*., 2000), Eomes and Blimp-1 (Kallies, 2008). Regulation of the transcription factors is not fully understood, but a dominant factor is clearly TCR-mediated T cell activation, as well as cytokine exposure and other stimuli. In general, naïve and central memory T cells have a higher proliferative capacity and produce IL-2, while effector T cells have a low proliferative capacity and produce effector cytokines such as interferon-γ (IFNγ) and tumour necrosis factor α (TNFα).

The question of whether memory cells continue to circulate through blood and lymphatics while surveying tissues or are retained within tissues was initially addressed using murine models of infection and monitoring antigen-specific T cell responses following procedures such as adoptive T cell transfer (Masopust *et al*., 2004) and parabiosis – surgical splicing of two mouse circulatory systems (Klonowski *et al*., 2004). Local infection generated a non-migratory site-specific T cell response in a number of tissues that, importantly, was capable of mounting a quick response to re-challenge by the same initial pathogen. These studies also highlighted a degree of phenotypic commonality amongst T_{RM}, specifically expression of the early-activation marker CD69 and epithelial α_E integrin CD103.

In human studies, these markers have also been attributed with populations of memory cells that do not recirculate, although the level of expression does vary somewhat depending on tissue and T cell subset. $CD4^+$ T cells rarely express CD103, but $CD8^+$ T cells do, especially in epithelial and mucosal tissues such as skin, lung and intestine (Mackay *et al*., 2012). Both subsets express CD69, although again $CD4^+$ T cells not as highly as $CD8^+$. As well as being upregulated swiftly after TCR and cytokine stimulation, CD69 has been demonstrated to sequester the sphingosine-1-phosphate receptor (S1PR1), which in turn is a vital requirement in lymphocyte egress from tissues (Matloubian *et al*., 2004) 2004). Therefore CD69 may be involved in retention of memory cells in tissues (Mackay *et al*., 2015).

Although no experimental system in humans can be quite as conclusive as murine models, several studies have implicated the presence of local memory T cell populations capable of withstanding circulatory T cell depletion during organ transplantation (Watanabe *et al*., 2015, Turner *et al*., 2014). In addition, sites including lung and bone marrow have been demonstrated to be enriched for memory phenotype T cells specific toward pathogens such as influenza (Purwar *et al*., 2011) and other chronic viruses (Okhrimenko *et al*., 2014) that are not present in peripheral blood. Although these studies utilised pathogen specific epitope tetramers, NGS based αβT cell TCR sequencing has also revealed clonal expansions present in colorectal tumours that are not found in adjacent tissue, suggestive of tumour-specific expansions (Sherwood *et al*., 2013) and cerebrospinal fluid-specific clones not shared with blood in multiple sclerosis patients (Lossius *et al*., 2014). Combined, this research not only demonstrates tissue localised

memory T cells that are distinct from circulatory populations, but also the potential power of TCR sequencing in furthering our understanding of this field.

5.1.2 Lymphocyte residency in the liver

The liver is an interesting organ physiologically as there is no basement membrane to physically separate the tissue from the peripheral blood supply, and the endothelium that permeates the liver is highly fenestrated, allowing relatively free movement of blood- and tissue-associated cells between the two compartments (Racanelli and Rehermann, 2006). Nevertheless, an expanding body of work suggests that the liver is home to a number of resident lymphocyte populations (Peng and Tian, 2015, McNamara and Cockburn, 2016).

Murine parabiosis experiments have highlighted several lymphocyte populations that, when joined with the circulation of another mouse, stay within the liver of the original mouse, thereby providing clear evidence that they are truly resident. Liver resident NKT cells in mice do not express high surface levels of CD103 but instead appear to be anchored in the tissue by high expression of lymphocyte functional antigen-1 (LFA-1) and interaction of this molecule with tissue-expressed intercellular cellular adhesion molecule-1 (ICAM-1) (Thomas *et al*., 2011). Additionally, the surface expression of the chemokine receptor CXCR6 has been demonstrated to be involved in mediating murine NKT recruitment, a feature apparently shared by many intrahepatic lymphocyte subsets in both mice and humans (Geissmann *et al*., 2005, Hudspeth *et al*., 2016, Stegmann *et al*., 2016).

As with NKT cells, murine liver NK cells have been demonstrated not to recirculate in parabiosis experiments (Peng *et al*., 2013). A $CD56^{hi}$ $CD16^{neg}$ population of intrahepatic

NK cells that express the integrin CD49a, which pairs with CD29 to form very late antigen-1 (VLA-1), has been demonstrated to be resident in humans by analysis of afferent and efferent blood sampling simultaneously with liver biopsy (Marquardt *et al*., 2015). These cells displayed distinctive functional aspects, with low degranulation and high cytokine production compared with the non-resident populations.

Both NKT and NK cells are enriched in the human liver compared with the periphery. Another lymphocyte subset enriched in the liver is $CD8^+$ T cells (Norris *et al*., 1998). Using a mouse model of vaccination, Heath and colleagues identified by parabiosis liver resident $CD8^+$ T cells which displayed a T_{RM} gene expression signature when analysed by microarray analysis (Fernandez-Ruiz *et al*., 2016). A number of genes form this signature, including CXCR3, CXCR6, BTLA, CD25, CD31, & CD127 amongst others. A recently published study on human liver corroborated the existence of a $CD45RA^{neg}$ $CD69^+$ $CD103^+$ $CD8^+$ T cell population that is seemingly liver resident (Pallett *et al*., 2017). Analysis of transcription factors expressed by this population suggested that the liver resident $CD8^+$ population identified was T-bet^{lo} $Eomes^{lo}$ Blimp-1^{hi} $Hobit^{lo}$, consistent with previous findings in mice (Mackay *et al*., 2016) and human tonsil (Vieira Braga *et al*., 2015). Additionally, these cells were generally less cytotoxic than non-resident effector $CD8^+$ cells and seemed to play a role in controlling HBV infection through non-cytotoxic cytokine production (Pallett *et al*., 2017).

5.1.3 Tissue Resident Gamma Delta T cells

Although tissue residency, as defined in the previous section, has been demonstrated in humans for $CD4^+$ and $CD8^+$ αβ T cells to occur in many tissues (Zaid *et al*., 2014), the

picture for gamma delta T cells is less clear. This is because in mice, gamma delta T cells have been demonstrated to home to tissues as a result of a hard-wired developmental process (Bandeira *et al*., 1990, Haas *et al*., 2012), where the role of the TCR and extra-thymic ligand recognition is unclear (Munoz-Ruiz *et al*., 2016) other than in the case of DETC selection by Skint-1 (Salim *et al*., 2016). Accordingly, much of the research into tissue-associated gamma delta T cells has focussed on mice in attempts to understand these processes and discover what relevance they may have in the human system. Combined with the difficulty in accessing human solid tissue for many labs, there is a distinct paucity of human data on this topic in the literature.

The aim of this chapter was therefore to investigate differences between liver- and periphery-associated gamma delta T cell populations, focussing on frequencies, phenotype and TCR repertoire. Any populations considered liver-specific would then be characterised functionally to attempt to discern the potential role for these cells within the liver. To do this, matched blood from patients undergoing liver transplant was taken and lymphocyte populations from both blood and liver analysed.

5.2 Results

5.2.1 Frequencies of Vδ1$^+$ T cells in donor matched blood and liver

Sampling peripheral blood from individuals undergoing liver transplantation allowed a comprehensive comparison of intrahepatic and peripheral gamma delta T cells populations from within the same donor. Since autoimmune liver disorders have been associated with perturbations in circulating gamma delta T cell frequencies (Martins *et al*., 1996, Hua *et al*., 2016), as well as in this study, perhaps due to therapy regimes

(McCarthy *et al*., 2015), samples were taken from 8 individuals undergoing transplantation for non-autoimmune based chronic liver disease, including ALD, NASH and polycystic liver disease. To corroborate the findings in Chapter 3, frequencies of lymphocyte populations of interest were analysed by flow cytometry. Firstly, the frequency of circulating gamma delta T cells amongst $CD3^+$ cells was increased in liver compared with blood, from 3.4% ± 1.8% in blood to 7.77% ± 4.2% in liver (p=0.04) (Figure 5.1a & 5.1b). Within this subset, both $V\delta1^+$ and $V\delta2^{neg}V\delta1^{neg}$ cells increased as a proportion of $CD3^+$ lymphocytes, from 1.13% to 3.31% (p=0.008) and 0.23% to 1.59% (p=0.005) respectively (Figure 5.2a), representing a 2.9-fold increase of $V\delta1^+$ and a 6.9-fold increase in $V\delta2^{neg}V\delta1^{neg}$ cells in the liver. Interestingly, $V\delta2^+$ cells were not significantly increased in liver as a proportion of $CD3^+$ T cells, but neither did they decrease (2.04% to 2.87%, p=0.38), suggestive of a slight preferential tissue retention of these cells that form the dominant subset in the periphery. The samples in this cohort also demonstrated the enrichment of liver for $CD8^+$ αβ T cells, which formed the dominant T cell subset in the liver (25.6% ± 6.1% of $CD3^+$ in blood, 50.5% ± 5.2% of $CD3^+$ in liver, p=0.011), which is in line with previous studies (Benechet and Iannacone, 2017) (Figure 5.1c). As a proportion of infiltrating gamma delta T cells, $V\delta1^+$ formed the majority (50.7% ± 7.25%), with $V\delta2^{neg}V\delta1^{neg}$ cells the second largest group (27.1% ± 5.7%) and $V\delta2^+$ in the minority (21.3 ±6.1%), contrasting with the blood where $V\delta2^+$ cells were the largest subset present (64.4 ± 5.3%) (Figure 5.2b). Since they represented the largest subset present in the liver, and were easily classified due to the availability of a specific monoclonal antibody, subsequent phenotypic analysis focussed on the $V\delta1^+$ subset of gamma delta T cells. The similarly tissue-enriched $CD8^+$ αβ T cells represented a point of

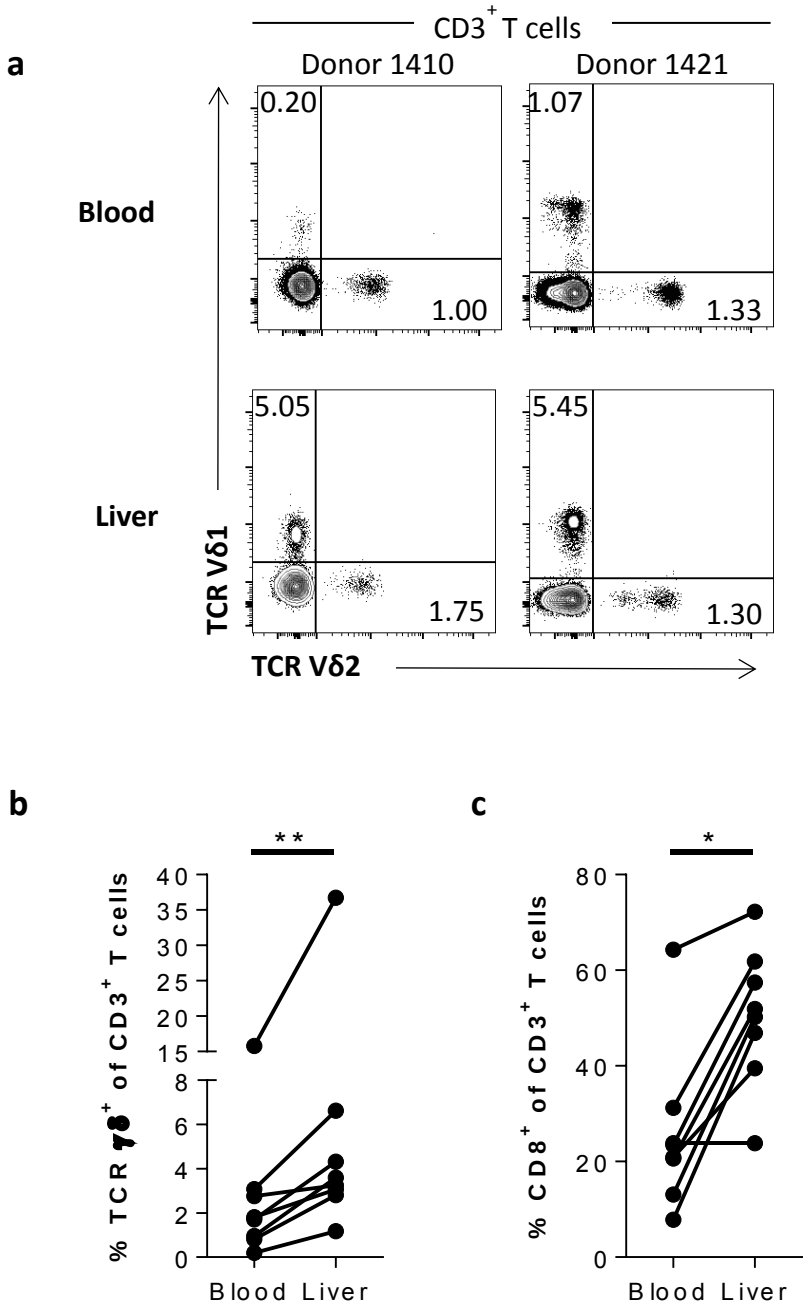

Figure 5.1: Matched blood and liver lymphocyte frequencies

- **a)** Representative flow cytometry plots gated on $CD3^+$ cells showing typical distribution of $V\delta1^+$ and $V\delta2^+$ cells in matched blood and liver from two donors
- **b)** Frequency of pan-γδ TCR^+ cells as a proportion of all $CD3^+$ T cells in blood and matched donor liver (n=8, p=0.04 Wilcoxon test)
- **c)** Frequency of $CD8^+$ T cells as a proportion of all $CD3^+$ T cells in blood and matched donor liver (n=8, p=0.01 Wilcoxon test) (2 NASH, 2 ALD, 2 PSC, 2 non-inflammatory)

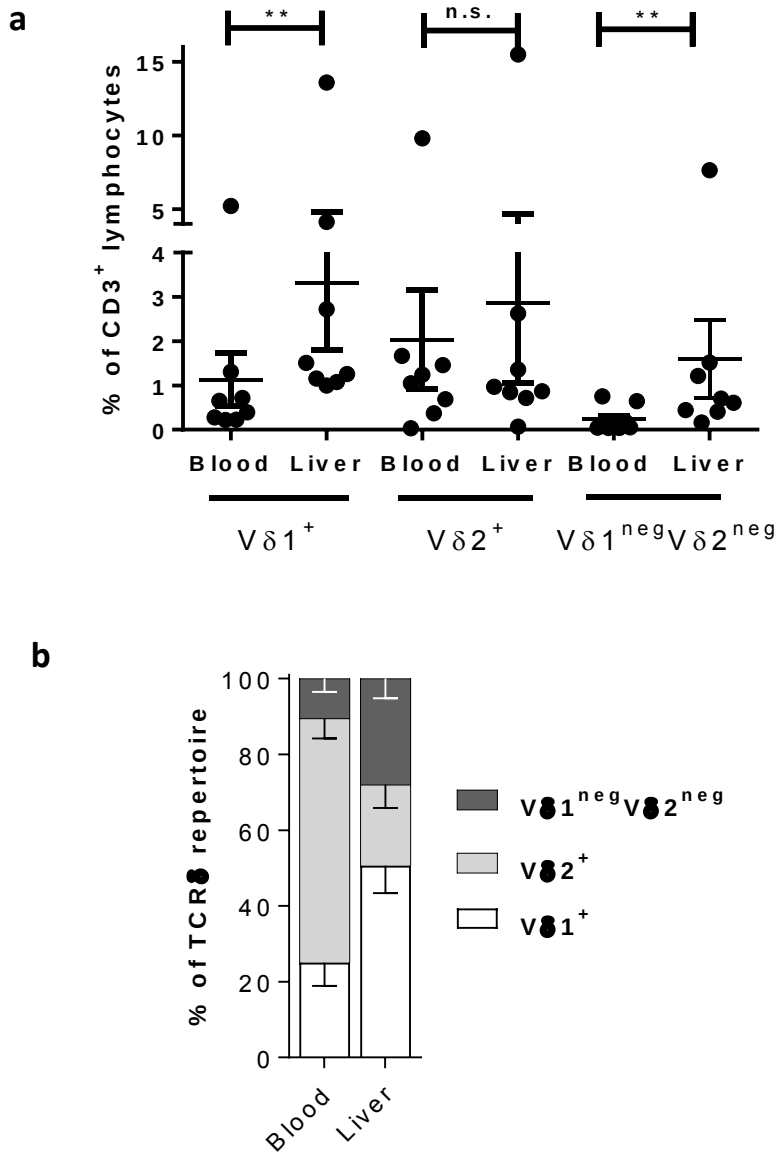

Figure 5.2: Matched blood and liver TCRδ chain usage

a) Frequency of Vδ1^{+}, Vδ2^{+} and Vδ1^{neg}Vδ2^{neg} gamma delta T cells as a proportion of CD3^{+} T cells in blood and matched liver donors with mean + s.e.m. (n=8, p=0.08 1-way ANOVA)

b) Frequency of all Vδ1^{+}, Vδ2^{+} and Vδ1^{neg}Vδ2^{neg} gamma delta T cells as a proportion of the total TCRδ repertoire in blood and matched liver donors with s.e.m. (n=8) (2 NASH, 2 ALD, 2 PSC, 2 non-inflammatory)

comparison during this study.

5.2.2 Differentiation of Vδ1$^+$ T cells in donor matched blood and liver

A critical step in the development of tissue resident T cells is antigen recognition and concomitant transcriptional re-profiling of clonal daughter cells to adopt a memory phenotype and track into tissues to mount an effective response to subsequent antigenic exposure. Recent work from this laboratory has correlated clonal expansion with loss of naïve status in Vδ1$^+$ blood-derived T cells (Davey *et al*., 2017). Accordingly, classical surface markers of T cell naivety were analysed by flow cytometry. CD27, a TNF receptor superfamily member, is involved in co-stimulation of the TCR and surface expression is lost after TCR engagement. Loss of expression of CD27 has been associated with gain of effector memory status for both gamma delta and αβ T cells in previous studies (Dieli *et al*., 2003, Fritsch *et al*., 2005, Wirth *et al*., 2010). CD62L (L-selectin) is a cell adhesion molecule that mediates interaction with endothelium, particularly important in the entry of naïve and central memory lymphocytes into lymphoid organs via the high endothelial venules (Stamenkovic, 1995). Loss of expression of CD62L prevents this and therefore forms part of the expression pattern of non-circulatory effector memory T cells. CCR7 is a chemokine receptor expressed by naïve T cells and used to home to lymphoid structures due to local secretion of its ligands CCL19 and CCL21 by stromal lymphoid cells with expression of CCR7 also lost in non-circulatory cells (Ebert *et al*., 2005).

When analysing CD27 expression in both blood and liver by flow cytometry, a distinction became apparent based on the level of expression, with some cells exhibiting a CD27^{hi} phenotype, others a CD27^{int} phenotype, and others truly CD27^{neg} (Figure 5.3a). Previous

work from the Willcox group has demonstrated that the $CD27^{hi}$ population of $V\delta1^+$ cells in blood are in fact highly polyclonal and resemble genuinely naïve conventional T cells phenotypically and functionally (Davey *et al*., 2017). Accordingly, the proportion of $CD27^{hi}$ $V\delta1^+$ T cells was focussed on here as a potential marker of true naivety.

The percentage of cells with $CD27^{hi}$ expression was significantly higher in blood-derived $V\delta1^+$ gamma delta T cells than liver (27% ± 7.1% vs. 4.7% ± 1.1%, p=0.008) (Figure 5.3b and Figure 5.3c). In addition, co-expression of CD62L and CCR7 reduced from 21.5% ± 7.6% in blood to 1.5% ± 0.5% in matched liver (p=0.004) (Figure 5.3d). These results are consistent with a loss of the naïve and central memory compartments, present in circulating $V\delta1^+$ T cells, in liver tissue.

Analysis of peripheral gamma delta T cells in previous studies has used co-expression of CD27 and CD45RA as an indicator of differentiation status. Cells expressing both CD27 ($CD27^{hi}$) and CD45RA are phenotypically and functionally equivalent to naïve αβ T cells, while cells lacking CD27 expression become phenotypically and functionally equivalent to effector αβ T cells. Finally, in $V\delta1^+$ cells lacking expression of CD27 but also expressing CD45RA, the high cytotoxicity and phenotype of terminally differentiated (T_{EMRA}) αβ T cells was noted (Davey *et al*., 2017). While this paradigm has also been demonstrated for αβ T cells, higher expression of CCR7 and CD28 in αβ T cells has led most studies of these cells to use these as typical surface markers of naivety in combination with either CD45RA or CD45RO. Historically, the picture has been muddied for gamma delta T cell research by the lack of distinction between $V\delta1^+$ and $V\delta2^+$ cells, as $V\delta2^+$ cells do not appear to conform to this differentiation pathway in quite as distinct a way as $V\delta1^+$ cells (DeBarros *et al*., 2011).

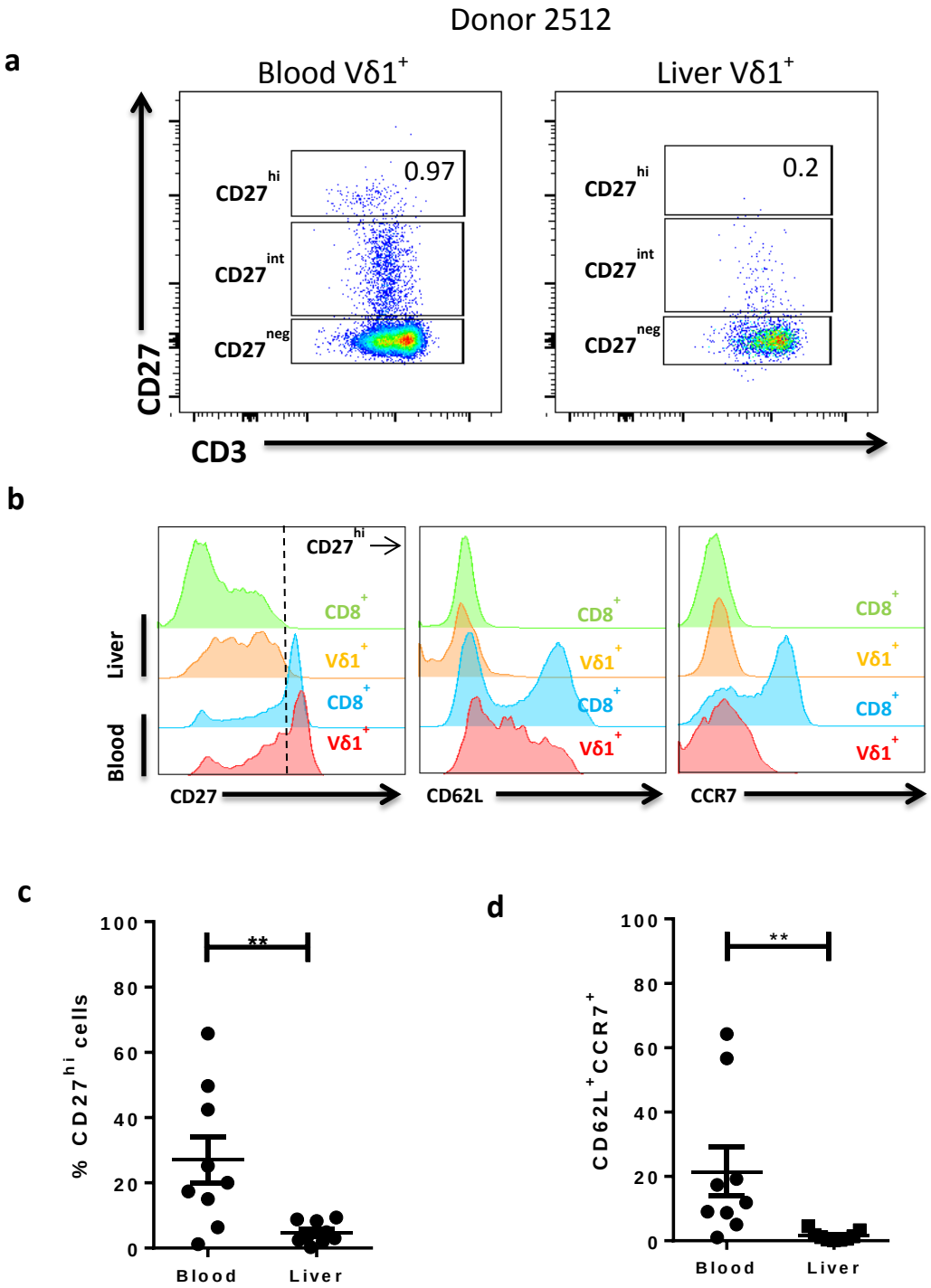

Figure 5.3: Blood has a higher frequency of phenotypically naïve Vδ1$^+$ cells than matched liver

- **a)** Representative flow cytometry plots of CD27 expression by Vδ1$^+$ gamma delta T cells, showing CD27$^{hi, int}$ and ^{lo} populations in blood and matched donor liver
- **b)** Comparison of CD27, CD62L and CCR7 expression for blood and liver derived Vδ1$^+$ T cells and CD8$^+$ T cells. Histograms from one representative donor
- **c)** CD27^{hi} Vδ1$^+$ cells in blood and matched liver with mean + s.e.m., n=9, p=0.008, Wilcoxon test
- **d)** CD62L$^+$CCR7$^+$ Vδ1$^+$ cells in blood and matched liver with mean + s.e.m., n=9, p=0.004, Wilcoxon test

As with CD27 expression, CD45RA expression seemed to categorise three sub-populations; $CD45RA^{+}$, $CD45RA^{int}$ and $CD45RA^{neg}$ (Figure 5.4a). For the rest of this study, cells both negative and intermediate for CD27 expression will be termed $CD27^{lo/neg}$ and cells negative and intermediate for CD45RA expression will be termed $CD45RA^{lo/neg}$. The majority of $V\delta1^{+}$ T cells in both blood and liver were $CD27^{lo/neg}$ and also $CD45RA^{+}$, and therefore by αβ T cell convention would be classified as T_{EMRA} (77.0% ± 7.2% in blood, 73.1% ± 5.7% in liver, p=0.65) (Figure 5.4b and Figure 5.4c). This is in contrast to $CD8^{+}$ αβ T cells, where the largest subset in liver was $CD27^{lo/neg}CD45RA^{lo/neg}$ T_{EM}-like (51.7% ± 3.4%), a subset significantly enriched compared with matched blood, where they comprised only 11.8% ± 4.3% (p=0.03, Wilcoxon test) (Figure 5.4c). As with $V\delta1^{+}$ T cells, there was only a minor, statistically insignificant, change in the proportion of $CD8^{+}$ $CD27^{lo/neg}CD45RA^{+}$ cells between the periphery and liver (9.5% ± 3.0% vs. 16.5% ± 5.9%, p=0.44). Interestingly, the $CD27^{lo/neg}CD45RA^{lo/neg}$ subset was also significantly enriched in $V\delta1^{+}$ T cells despite not forming the majority population, going from 3.58% ± 1.1% of PBMC-derived Vδ1+ T cells to 21.3% ± 5.0% in liver (p=0.004, Wilcoxon test) (Figure 5.4c), and has been demonstrated to comprise tissue-resident $CD8^{+}$ T cells in previous studies of the liver (Pallett *et al*., 2017).

To summarise, peripheral blood $V\delta1^{+}$ gamma delta T cells contain a proportion of $CD27^{hi}$ cells that are not present in the liver, while both compartments exhibit a dominant proportion of $V\delta1^{+}$ cells with a $CD27^{lo/neg}CD45RA^{+}$ phenotype. However, the liver $V\delta1^{+}$ population also contains a phenotypically distinct $CD27^{lo/neg}CD45RA^{lo/neg}$ population that is not observed in the periphery.

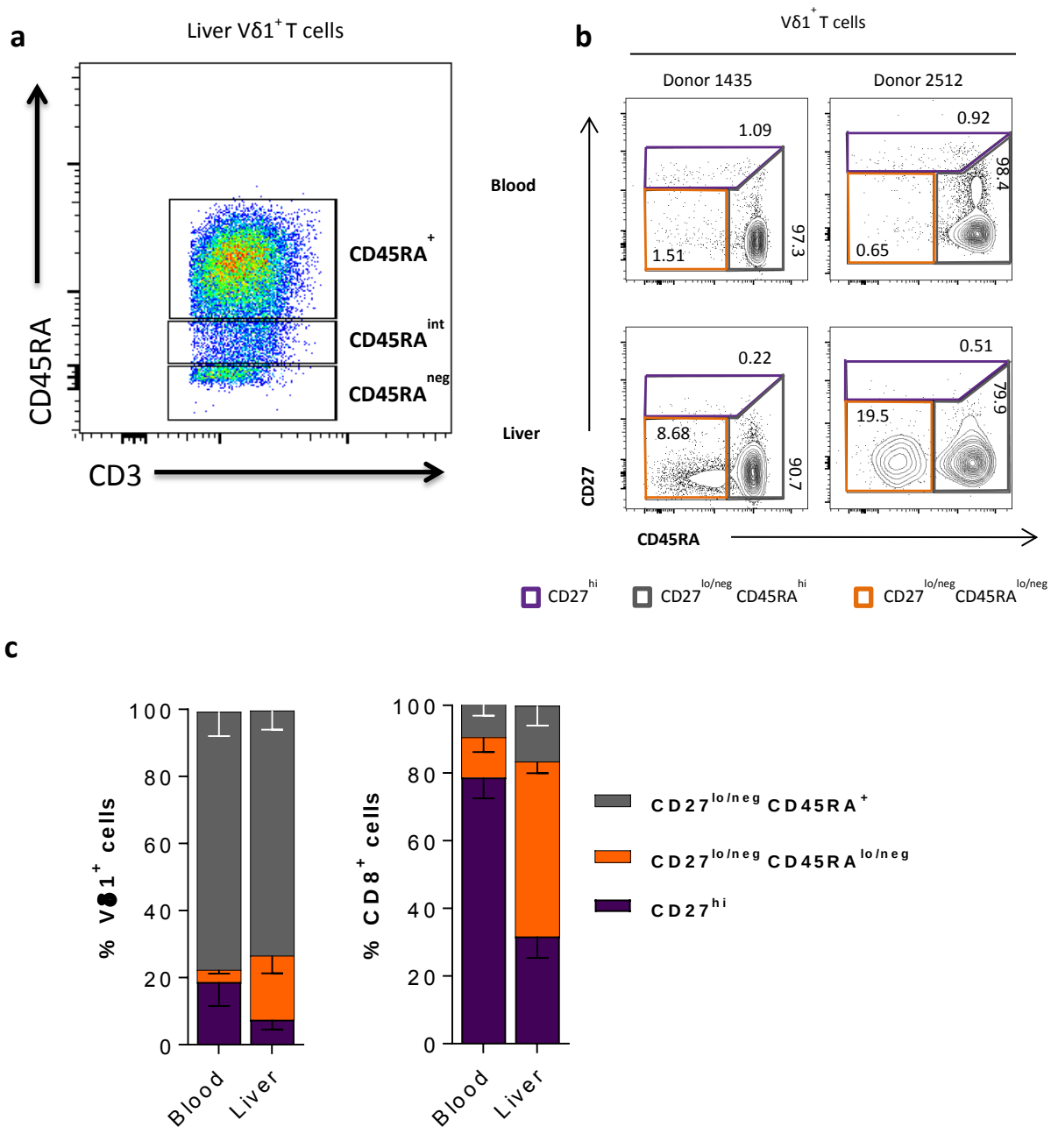

Figure 5.4: Liver has a higher frequency of T_{EM}-like Vδ1$^+$ and CD8$^+$ cells compared with the periphery

- **a)** Representative flow cytometry plots of CD45RA expression by Vδ1$^+$ gamma delta T cells, showing CD45RA$^{hi, int}$ and ^{lo} populations in liver
- **b)** Representative flow cytometry plots gated on Vδ1$^+$ showing typical distribution of CD27 and CD45RA expression in cells isolated from matched blood and liver from two donors
- **c)** Frequency of CD27^{hi}, CD27$^{lo/neg}$CD45RA$^{lo/neg}$ and CD27$^{lo/neg}$CD45RA$^+$ populations as a proportion of total Vδ1$^+$ (left) and CD8$^+$ (right) cells from blood and donor matched livers, with s.e.m. (2 NASH, 2 ALD, 2 PSC, 2 non-inflammatory)

5.2.3 The relationship between differentiation and clonality in donor matched blood and liver Vδ1^{+} T cells.

Having established the loss of a phenotypically naïve population between transition from the periphery into liver tissue and the formation of a minor but significantly enriched CD27$^{lo/neg}$CD45RA$^{lo/neg}$ population in intrahepatic Vδ1^{+} T cells, we wanted to explore how the high degree of clonal focussing observed in Chapter 4 mapped onto these phenotypically distinct populations. To do this, single cell polymerase chain reaction (sc-PCR) techniques were used on individual cells sorted from blood and liver-derived Vδ1^{+} T cells, using primers specific to both delta- and gamma-chains to sequence the complete CDR3 region of the TCR expressed by each cell. Although the number of cells analysed using this method is orders of magnitude lower than the deep sequencing approach adopted in Chapter 4, it had the advantage of being considerably cheaper, performed in-house and is able to generate complete CDR3 sequences including both gamma- and delta-chains of the TCR, important for both stringent identification of clonality and also potentially useful in future ligand identification processes. In addition, the data from the deep-sequencing suggested that the dominant clonotypes would be frequent enough to be identified in even a small number of sampled cells, allowing identification of dominant clonotypes common to both liver and blood, should they be present. The key research advantage of the sc-PCR technique however was the ability to link the TCR sequence with phenotype by index sorting.

To ensure that sampling as few as 30 Vδ1^{+}cells would allow identification of clonal expansions, cells were sorted initially from a normal liver donor. Critical to this technique was index sorting, that is, using conjugated antibody staining to not only define the cell

population of interest for sorting purposes but to also to phenotype relevant surface markers that could later be used to identify distinct sub-populations of the sorted cells. In this case, sorted cells were indexed with CD27 and CD45RA specific antibodies, allowing correlation of differentiation phenotype with TCR clonotype. Figure 5.5 shows the results of this experiment, including the phenotypic differentiation of the bulk population of $V\delta1^{+}$ cells in this sample. As observed in the matched liver and blood samples, there was very little expression of CD27, with approximately equal distribution of cells between the $CD45RA^{+}$ and $CD45RA^{lo/neg}$ populations. There were a total of four clonotypes identified from the 30 cells sequenced, representative of a strikingly focussed repertoire, and critically both the $CD45RA^{+}$ and $CD45RA^{lo/neg}$ compartments were almost completely monoclonal and clonotypically distinct. This was consistent with previous deep sequencing data that demonstrated strong clonal focussing in the liver (Chapter 4).

When this pilot study was extended to the matched blood and liver samples, both the $CD27^{lo/neg}CD45RA^{+}$ and $CD27^{lo/neg}CD45RA^{lo/neg}$ compartments predominantly consisted of expanded clonotypes – that is, clonotypes exhibited by more than one cell within the same sample (68.5% ± 6.4% and 56.9% ± 9.2% respectively) (Figure 5.6a). Considering the relatively small sample sizes (between 10 and 36 cells per compartment per sample) the degree of clonality exhibited here is striking. Within the blood derived cells, the $CD45RA^{+}$ subset was equally as clonally dominated as the liver, 75.4% ± 5.8% of cells sharing CDR3 sequence with at least one other cell, while the $CD27^{hi}$ subset, not present within the liver, had only 5.7% ± 2.6% of cells sharing CDR3 regions, suggestive of a distinctly more polyclonal nature (Figure 5.6b).

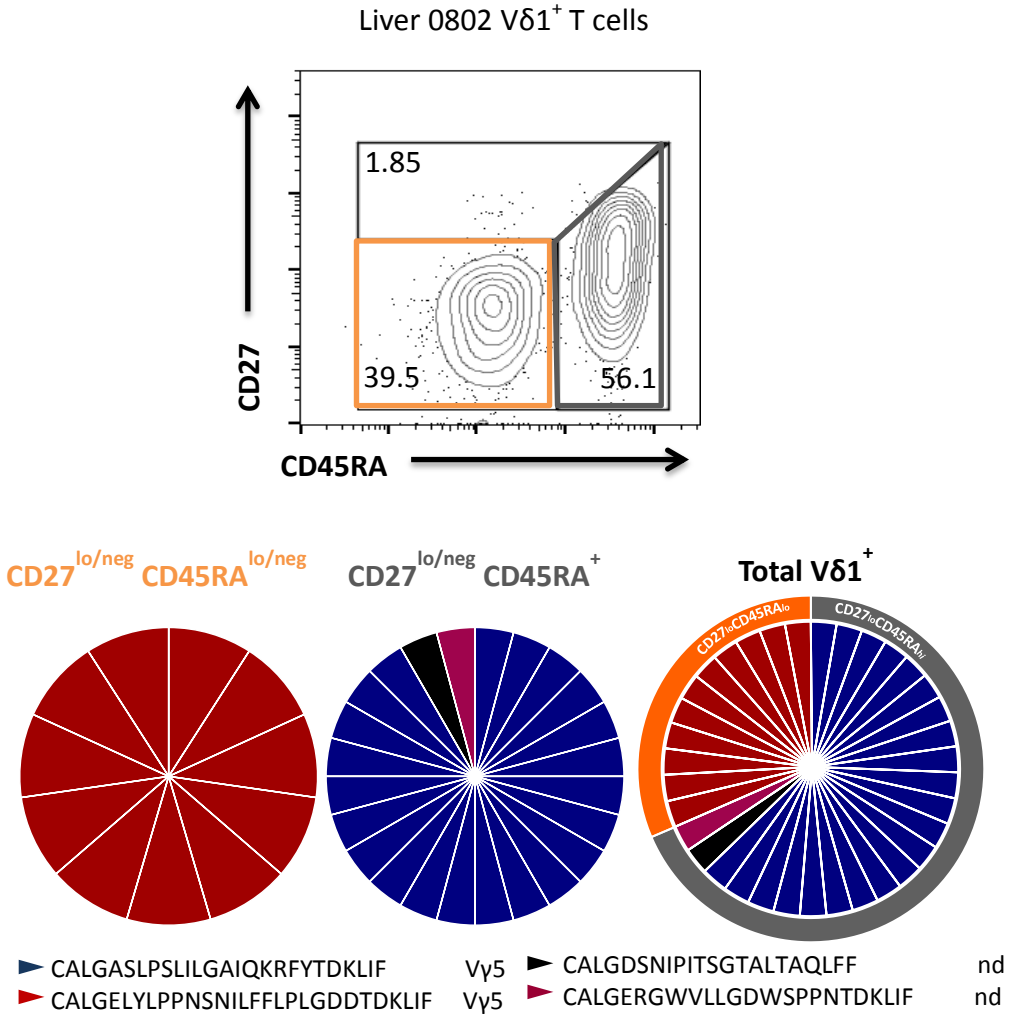

Figure 5.5: Highly focused clonal expansions in liver 0802 revealed by sc-PCR

Donor liver 0802 was index sorted for single cell PCR analysis of TCR sequences. Distribution of bulk Vδ1$^+$ cells according to surface expression of CD27 and CD45RA is shown (upper). Identified clonotypes were grouped according to classification as CD27$^{lo/neg}$CD45RA$^{lo/neg}$ (orange), CD27$^{lo/neg}$CD45RA$^+$ (grey) (lower) or total Vδ1$^+$. CDR3 sequence for each TCRδ clonotype determined is shown below with γ-chain pairing.

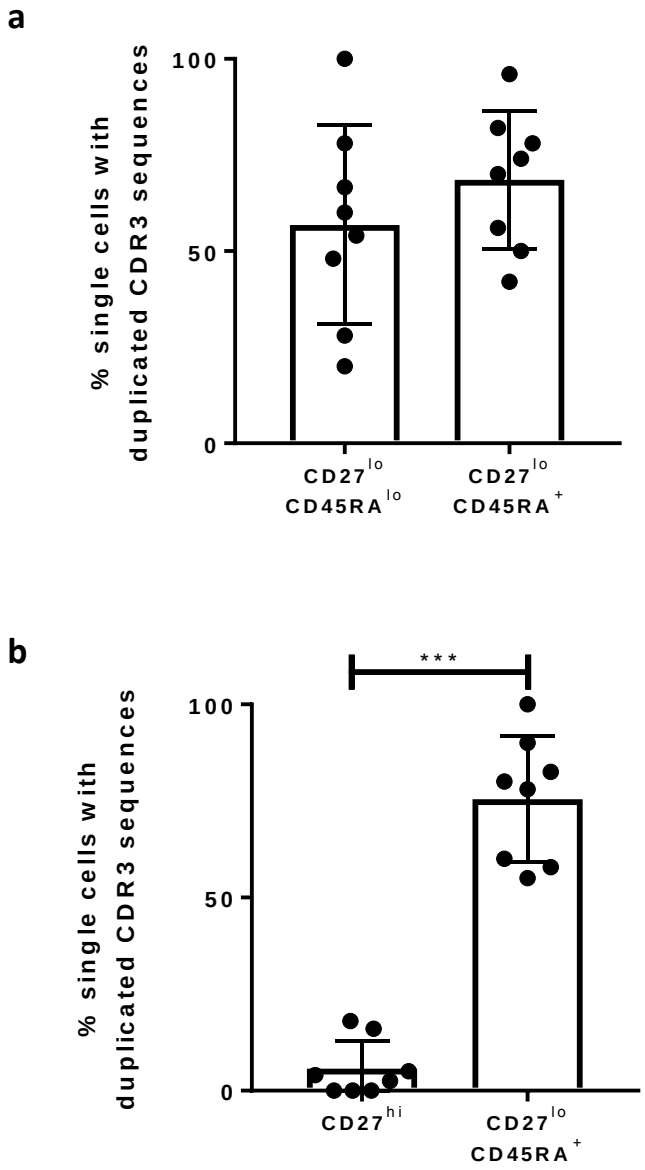

Figure 5.6: A high degree of clonal focussing is present in all $CD27^{lo/neg}CD45RA^{lo/neg}$ and $CD27^{lo/neg}CD45RA^{+}$ Vδ1^{+} populations

a) Intrahepatic Vδ1^{+} T cells were single cell sorted and TCR sequenced by PCR. Clonotypes were phenotyped by indexing of the sort and the proportion of the total cell number within that phenotype that share specific CDR3δ with other cells is plotted here, with mean and s.e.m. (n=8)

b) Peripheral blood Vδ1^{+} T cells were single cell sorted and TCR sequenced by PCR. Clonotypes were phenotyped by indexing of the sort and the proportion of the total cell number within that phenotype that share specific CDR3δ with other cells is plotted here, with mean and s.e.m. (n=8, ***p<0.001, Wilcoxon test)

Next, the degree of clonal overlap between liver and blood was assessed. The samples analysed contained a varying degree of clonotypic sharing between blood and liver. In blood, across all the samples, an average of 57.6% ± 11.0% of cells analysed had identical TCR CDR3 also present in the liver (Figure 5.7). In liver, 39.1% ± 11.0% of cells analysed had identical TCR CDR3 also present in the blood. While not statistically significant ($p=0.26$), likely due to the high degree of variation between samples, the reduction of overlapping clonotypes present in the liver is perhaps suggestive of the presence of a tissue associated CDR3 repertoire, at least in some individuals. Within the cohort, 23.4% of all liver-derived $V\delta1^+$ cells expressed a TCR not also represented in the blood derived sample whilst simultaneously represented by more than one cell within the liver (Figure 5.7), although it is important to note that 2 of the 8 samples actually had no liver-specific clonal populations. This compares to the blood where unique expanded clonotypes comprised only 12.4% of the cells sequenced across all samples, where no blood-specific clonal expansions were detected in 3 of the 8 samples. In both liver and blood, around 30% of all the cells sequenced had single copy CDR3s not observed in any other cell (individual clonotypes), which could represent $CD27^{hi}$ naïve clonotypes in blood or may merely reflect the low resolution of the sc-PCR technique in identifying low frequency expanded clonotypes in the liver.

As well as demonstrating the high degree of oligoclonality amongst both $CD27^{lo/neg}CD45RA^{lo/neg}$ and $CD27^{lo/neg}CD45RA^{+}$ subsets of intrahepatic $V\delta1^+$ T cells, the pilot sc-PCR study (Figure 5.5) suggested another intriguing possibility. Not only was the

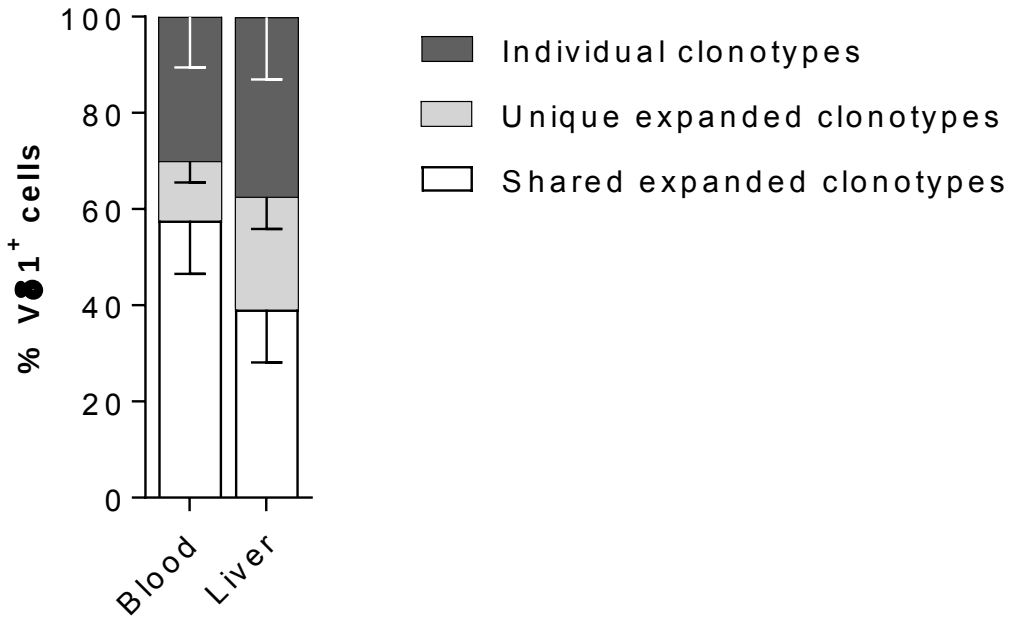

Figure 5.7: A high degree of clonal overlap between blood and liver Vδ1$^+$ cells

Analysis of clonality in blood and matched donor liver by sc-PCR. Each cell was assigned one of three categories depending on whether they expressed an individual clonotype not expressed by any other cell (dark grey), expressed a clonotype shared only by other cells within that tissue (light grey) or expressed clonotypes shared by other cells in both tissues (white). n=8 with mean and s.e.m.

CD45RA$^{lo/neg}$ population monoclonal in the normal liver sample analysed, it consisted of an entirely distinct clonotype from the CD45RA^{+} cells (δ-chain CDR3 – CALGASLPSLILGAIQKRFYTDKLIF vs. CALGELYLPPNSNILFFLPLGDDTDKLIF). Of note here is the very long CDR3 sequence (78 and 87 base pairs respectively) which is in concordance with the overall long delta-chain CDR3 regions identified amongst this population in Chapter 4. This represents the first suggestion from this study that γδ TCR clonotype and cell differentiation, at least on a phenotypic level, may be linked for tissue associated Vδ1^{+} cells. In addition, it is possible that this CD45RA$^{lo/neg}$ population may be liver-specific, since although blood was not obtained from this individual, from analysis of the matched samples it is clear that the CD45RA$^{lo/neg}$ population is very small or entirely absent in peripheral blood.

Interestingly, when the percentage of all liver-restricted Vδ1^{+} clonotypes (cells sharing CDR3 regions with at least one other cell in only the liver) was plotted against the proportion of cells from the sample with the CD27$^{lo/neg}$CD45RA$^{lo/neg}$ phenotype, a strong correlation was noted (R^2=0.71, p=0.008 Pearson correlation) (Figure 5.8a). Conversely, when the percentage of liver derived Vδ1^{+} cells with CDR3 regions found in both blood and liver was plotted against the proportion of cells from the sample with the CD27$^{lo/neg}$CD45RA^{+} phenotype, a significant correlation was also noted (R^2=0.53, p=0.04 Pearson correlation) (Figure 5.8b). This suggests that the greater the number of cells present in the blood-dominant CD45RA^{+} group, the more overlap there was between clonotypes in blood and liver, and the greater the number of cells in the liver-enriched CD45RA$^{lo/neg}$ group, the greater the number of liver-specific clonal expansions.

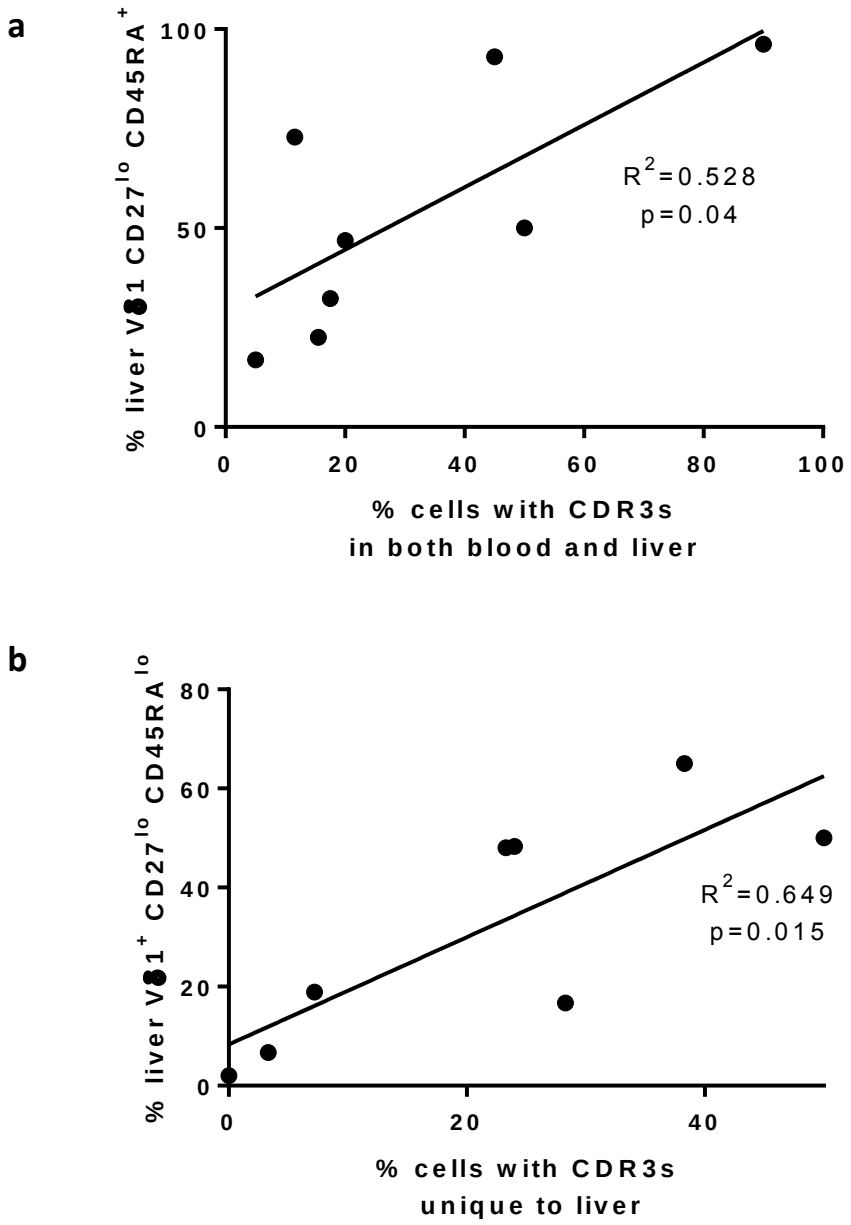

Figure 5.8: Correlations between clonality and phenotype in matched blood and liver Vδ1$^+$ cells

a) Proportion of intrahepatic CD27$^{lo/neg}$CD45RA$^+$ Vδ1$^+$ T cells plotted as a function of the percentage of cells with CDR3δ sequences found in both liver and blood for each sample, n=8, Pearson correlation

b) Proportion of intrahepatic CD27$^{lo/neg}$CD45RA$^{lo/neg}$ Vδ1$^+$ T cells plotted as a function of the percentage of cells with CDR3δ sequences found at least twice but only in the liver for each sample, n=8, Pearson correlation

To determine whether the liver enriched, clonally dominated CD45RA$^{lo/neg}$ populations of intrahepatic Vδ1^{+} cells were indeed liver specific, the indexed cell sorting data was used in conjunction with the CDR3 sequences determined by sc-PCR. Since the well number of each cell in the PCR was tracked, the position of each cell, and therefore each clonotype, during sorting could be determined on the flow cytometry dot plot, specifically in regards to its expression of CD27 and CD45RA. This way, all the cells with the same clonotype, or with clonotypes found in both blood and liver could be assigned a phenotypic differentiation status. An example of such plots is shown in Figure 5.9.

The left hand side of each plot shows the CD27 vs CD45RA dot plot for both the blood and liver derived cells sorted for sc-PCR TCR sequencing. As previously observed, the blood derived Vδ1^{+} cells are predominantly CD45RA^{+} in both samples, with a minority of cells falling into the CD27^{hi} gate. In the liver, the CD45RA$^{lo/neg}$ population is enriched. The CD27 vs CD45RA dot plot of cells with only the most frequent clonotype observed in both blood and liver is displayed in the middle panels. Here, the CD27^{hi} population has virtually disappeared, as expected since this is likely predominantly polyclonal in nature and there are unlikely to be expanded clonotypes with this phenotype considering the small number of cells sampled. Strikingly however, the phenotype of these cells is very similar in both blood and liver, localising within the CD45RA^{+} T_{EMRA} population. However, when only the dots representing the liver-specific clonally expanded cells (i.e. liver-derived cells sharing a CDR3 region with at least one other cell and not with a cell found in the blood) were plotted, they almost uniformly cluster in the CD27$^{lo/neg}$CD45RA$^{lo/neg}$ T_{EM}-like population. These data are summarised as a multi-layer pie chart for multiple donors in Figure 5.10a.

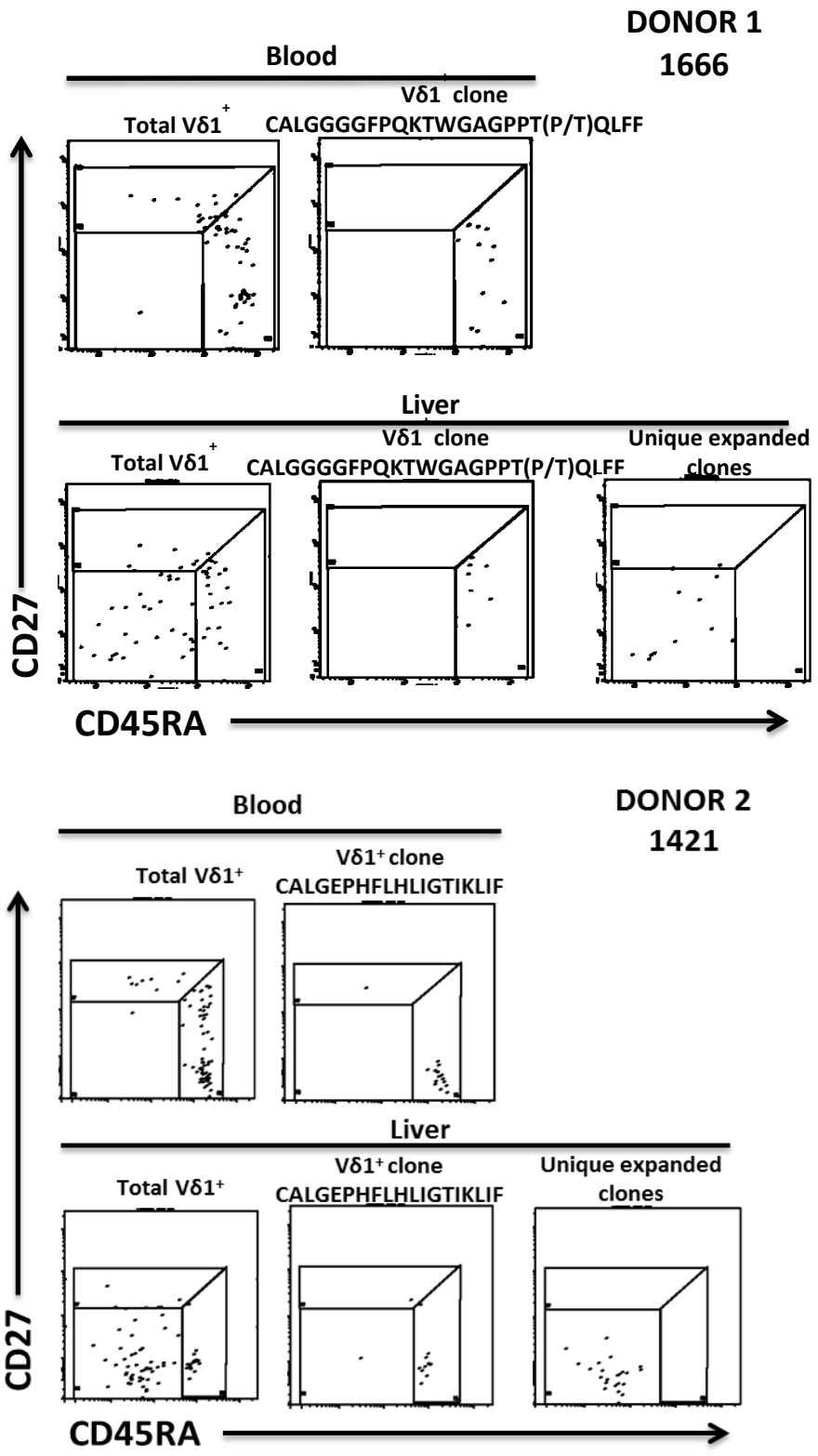

Figure 5.9: Single cell index sorting of blood and donor matched liver Vδ1$^+$ T cells

Representative flow cytometry plots showing distribution of Vδ1$^+$ T cells single cell sorted and TCR sequenced by sc-PCR according to expression of CD27 and CD45RA from two donors. Left hand panels show total Vδ1$^+$ population, middle panels show only largest expanded clonotype observed in both blood and liver, right hand panel shows all expanded clonotypes identified in liver only.

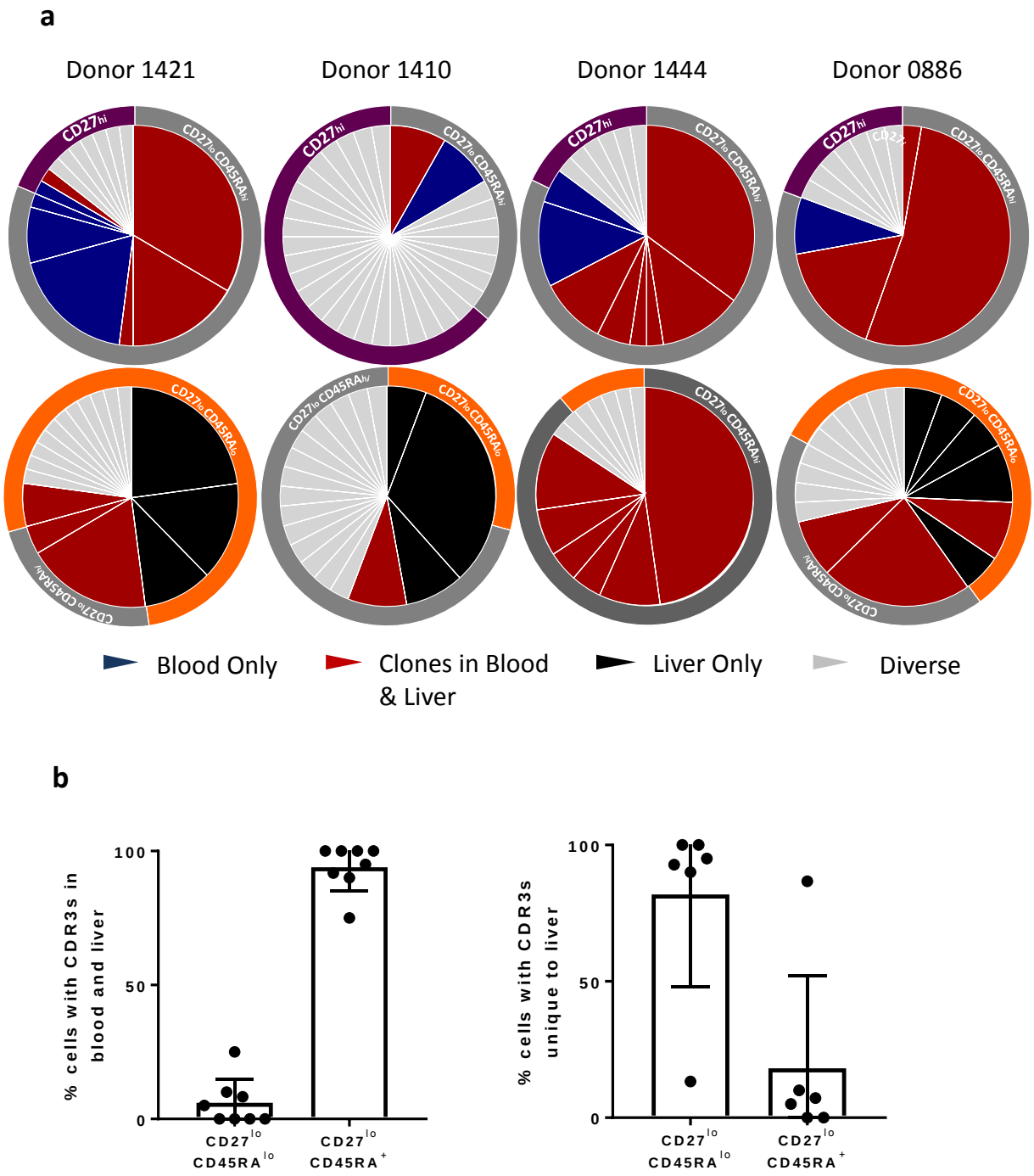

Figure 5.10: Clonotypic expansions, phenotype and extent of sharing in blood and matched liver Vδ1^{+} cells

a) Inner pies display extent of clonotypic expansion (size of slice) and extent of sharing amongst expanded clonotypes – expansions identified in both liver and blood (red), only in blood (blue) and only in liver (black). Single clonotypes are shaded in light grey. Outer pies display phenotype of corresponding cells, according to CD27 and CD45RA expression. Data shows 4 donors of 8 in total.

b) The proportion of all cells with identical CDR3δ found in both blood and liver (left) and only in liver (right) as a percentage of all cells of CD45RA$^{lo/neg}$ or CD45RA^{+} phenotype, mean + s.e.m. (n=8)

The same pattern of large clonal expansions either unique to blood or shared between blood and liver being $CD27^{lo/neg}CD45RA^{+}$ while clonal expansions unique to liver are $CD27^{lo/neg}CD45RA^{lo/neg}$ is observed across all the donors analysed in this study. 94.0% ± 3.1% of all the cells sampled with shared clonotypes were $CD27^{lo/neg}CD45RA^{+}$, while 81.9% ± 13.8% of all cells sampled with liver-specific expansions were $CD27^{lo/neg}CD45RA^{lo/neg}$ (Figure 5.10b). This is compelling evidence that the liver harbours a clonally-distinct $CD27^{lo/neg}CD45RA^{lo/neg}$ T_{EM}-like population of $V\delta1^{+}$ T cells, and that there is considerable enrichment of blood-associated $CD27^{lo/neg}CD45RA^{+}$ T_{EMRA}-like clonally expanded cells also present within this tissue.

5.2.4 Clonally distinct $V\delta1^{+}$ cells exhibit a liver-associated or a vasculature-associated immunophenotype

Considerable research efforts have been conducted on the nature and significance of tissue resident cells in many human tissues including the liver. Based on findings from murine studies and lacking similar model systems in humans, many of the studies conducted in humans have used surface markers such as CD69 as surrogates of tissue-association and/or residency. Often this has been performed successfully, particularly in studies with associated transcriptomic analysis that allow in-depth characterisation of tissue-associated phenotype. Having identified, via TCR sequencing, a likely population of tissue-restricted $V\delta1^{+}$ T cells in human liver and ascribed a general $CD27^{lo/neg}CD45RA^{lo/neg}$ differentiation phenotype to these cells, further characterisation would allow comparison of these cells with previous non-gamma delta T cell datasets to see how they relate to the emerging paradigms of human tissue resident lymphocytes.

To begin, expression of CD69 a protein intrinsically linked with human lymphocyte residency in tissues, was determined. CD69 expression in general was relatively high amongst liver-derived $V\delta1^+$ cells (mean 60.7%), and significantly increased compared with the periphery in matched donors (n=10, $p<0.0001$, 2-way ANOVA) (Figure 5.11a). Since the liver-associated $V\delta1^+$ clonotypes often adopted a $CD27^{lo/neg}CD45RA^{lo/neg}$ phenotype, the expression of CD69 was determined as a function of CD45RA expression, here gated on intrahepatic $CD27^{lo/neg}$ cells (Figure 5.11b). For the $CD45RA^{lo/neg}$ $V\delta1^+$ cells, 90.0% ± 4.6% expressed CD69, while for $CD45RA^+$ cells this figure dropped significantly to 47.2% ± 8.1% ($p=0.007$). Similar results were obtained for the intrahepatic $CD8^+$ αβ T cell population where CD69 expression in T_{EM} $CD8^+$ cells has been demonstrated to be a characteristic of liver residency in humans. Since there was a high degree of clonal overlap between liver and blood derived cells with the $CD45RA^+$ phenotypes, it is possible that this may represent genuine blood-associated cells ($CD69^{neg}$) and another population of cells that may have been transiently activated by local factors within the liver and upregulated CD69 accordingly. To investigate this further, index sorting was again used in conjunction with sc-PCR TCR sequencing. In several samples, CD69 expression was high on cells also expressing expanded liver-specific clonotypes, while CD69 expression was predominantly low or negative on expanded clonotypes shared between liver and blood (Figure 5.12). Due to cell sampling and methodological restraints, potentially corroborative observations from enough donors to prove the hypothesis were not obtained. Nevertheless, these data provide a clear link between TCR clonotype, differentiation status and the tissue association marker CD69.

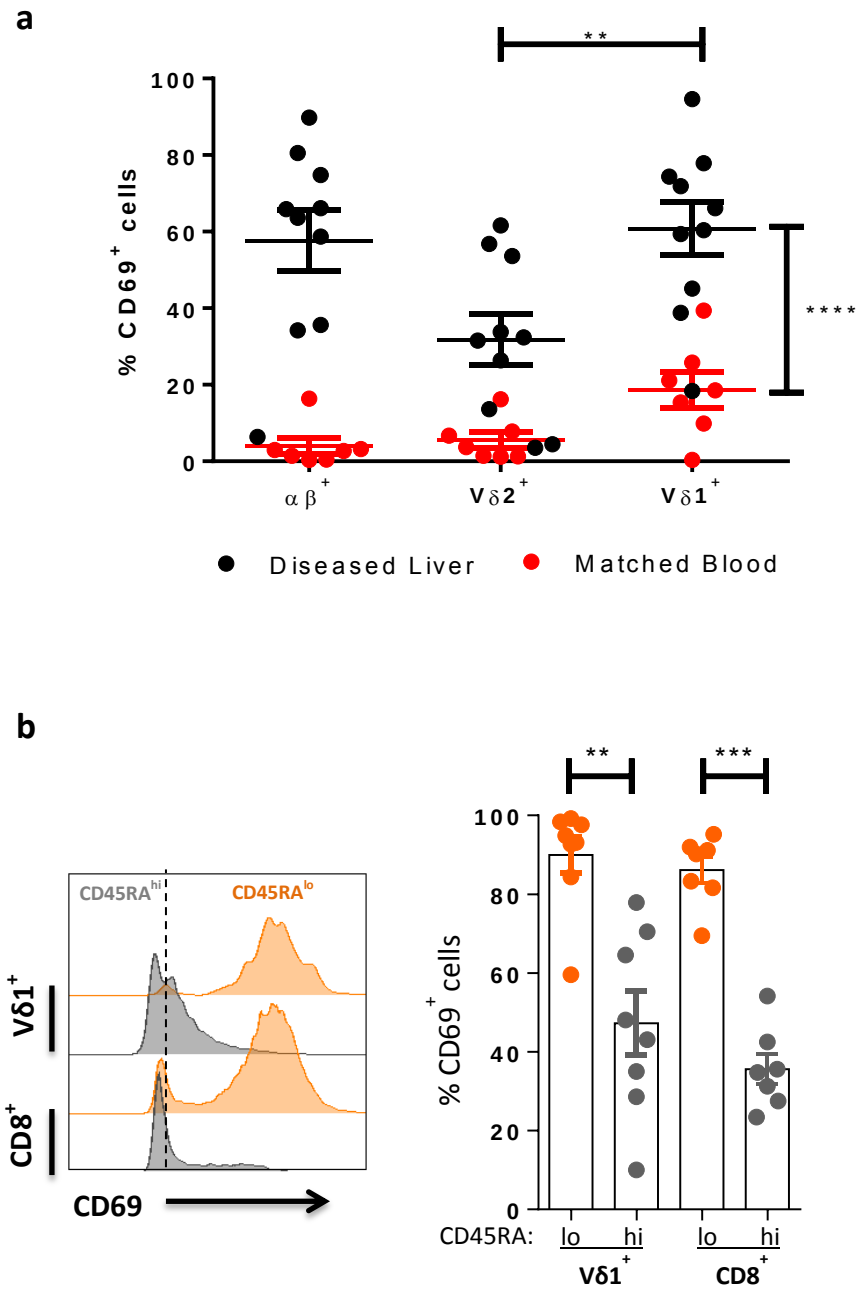

Figure 5.11: Tissue-association cell marker expression in intrahepatic T cells

a) Mean ± s.e.m. surface expression of tissue-association marker CD69 on intrahepatic (red) and matched donor peripheral blood (black) T cell subsets (n=10, **p<0.01,****p<0.0001, 2-way ANOVA)

b) Representative histogram of CD69 expression according to co-expression CD45RA (left). Mean ± s.e.m. expression of CD69 on intrahepatic Vδ1$^+$ and CD8$^+$ αβ T cells according to co-expression of CD45RA (n=8, **p<0.01, ***p<0.001, 1-way ANOVA, Dunn's comparison) (right)

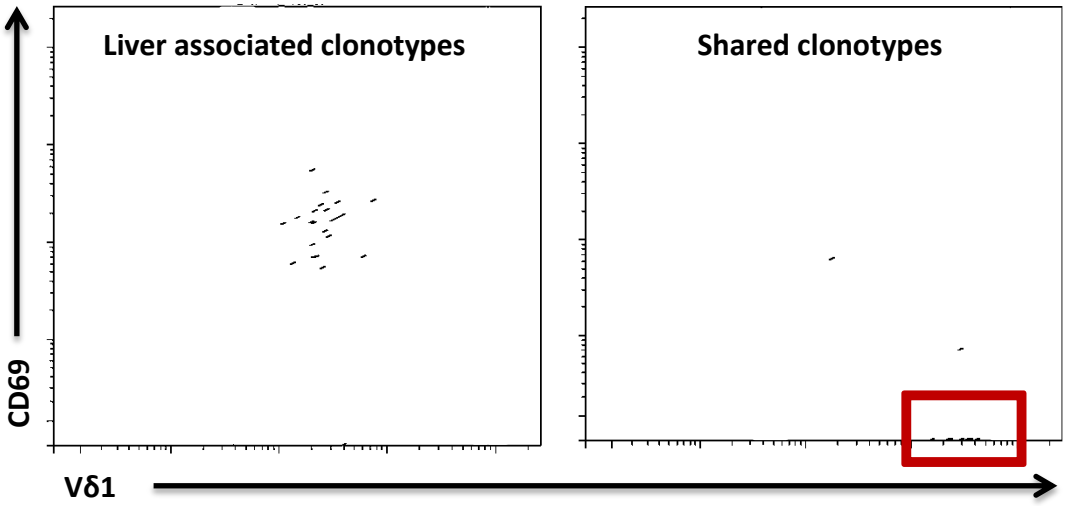

Figure 5.12: Vδ1^{+} liver specific clonotypes are CD69^{hi}

Representative flow cytometry dot plot from single cell sorting of one donor showing CD69 expression of expanded clonotypes found only in liver (left) and expanded clonotypes found in both liver and blood (right), highlighted in red as most cells appear on the x-axis.

In Chapter 3, surface expression of LFA-1 and CD31, was shown to be constitutively elevated in both circulating and intrahepatic Vδ1$^+$ T cells compared with αβ T cells, and it was hypothesised that these proteins may be involved in the increased adhesion of gamma delta T cells to HSEC *in vitro* compared with αβ T cells. However, as well as CD69, several other surface proteins involved with cell trafficking have been established to be involved in the tissue resident phenotype of lymphocytes. Surface expression of CXCR3, CXCR6 and CX_3CR1 was quantified according to CD45RA co-expression by flow cytometry (Figure 5.13). CXCR3 expression was significantly elevated in both Vδ1$^+$ and CD8$^+$ αβ CD45RA$^{lo/neg}$ T cells compared with CD45RA$^+$ cells - Vδ1; 87.2% ± 4.0% vs. 29.5% ± 4.8% (p=0.007): CD8; 67.0% ± 9.2% vs. 28.0% ± 4.4% (p=0.009). CXCR6 expression was likewise elevated in the CD45RA$^{lo/neg}$ population in both Vδ1$^+$ and CD8$^+$ αβ T cells – Vδ1; 63.8% ± 9.3% vs. 18.3% ± 8.2% (p=0.009): CD8; 55.2% ± 5.9% vs 18.1% ± 3.2% (p=0.002). CX_3CR1 is the receptor for fractalkine, a chemokine secreted by endothelial cells that mediates adhesion and migration of lymphocytes. The significance of CX_3CR1 expression in human chronic virus-specific T_{EMRA} cells has recently come under scrutiny in CD8$^+$ (Bottcher *et al*., 2015) and CD4$^+$ (Pachnio *et al*., 2016) populations, where it is linked with endothelial homing and vasculature residency (Remmerswaal *et al*., 2012). Here, it is the CD45RA$^+$ population of both Vδ1$^+$ and CD8$^+$ αβ T cells that expresses higher CX_3CR1, compared with the CD45RA$^{lo/neg}$ cells – Vδ1; 58.6% ± 8.0% vs. 18.5% ± 6.0% (p=0.009): CD8; 65.5% ± 8.7% vs. 12.3% ± 7.4% (p=0.002). Low affinity immunoglobulin gamma Fc region receptor III-A (FcγRIIIA/ CD16) is critical for monocyte and NK cell mediated antibody dependent cell-mediated cytotoxicity (ADCC) as it binds the Fc portion of IgG antibodies. Upregulation of CD16 has been associated with adoption of a cytotoxic phenotype in human NK cells (Lanier *et al*., 1986), while low CD16 expression is

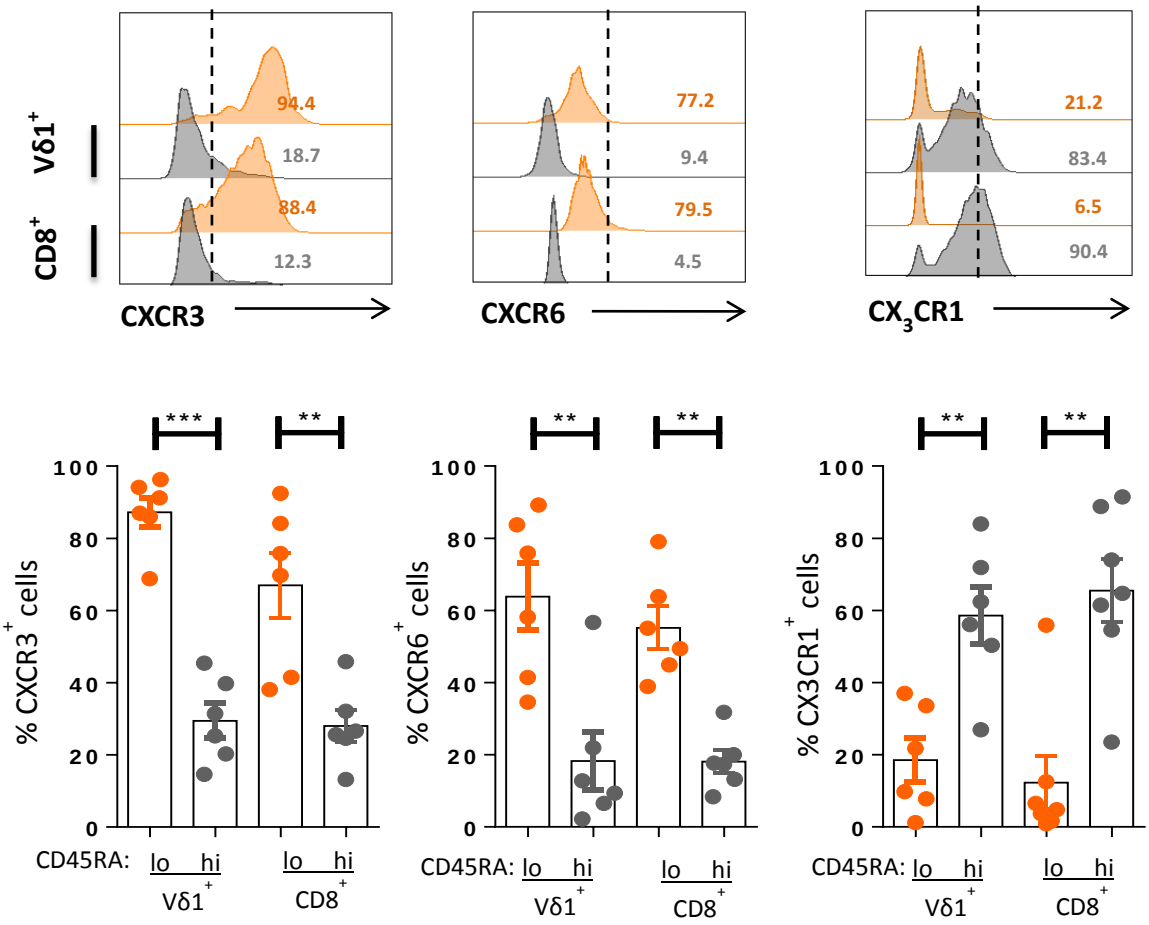

Figure 5.13: Chemokine receptor expression in intrahepatic Vδ1$^+$ T cells is associated with differentiation status

Comparison of CXCR3, CXCR6 and CX_3CR1 surface expression within Vδ1$^+$ and CD8$^+$ CD45RA$^{lo/neg}$ (orange) and CD45RA$^+$ (grey) T cells. Histograms from one representative donor and graphs show mean ± s.e.m. from 6 different donors. Data analysed by Kruskal–Wallis ANOVA with Dunn's post-test comparisons, *p<0.05, **p<0.01 and ***p<0.001.

attributed with poor cytotoxicity and high cytokine production in CD8 αβ T cells (Bjorkstrom *et al*., 2008). The same pattern of high CD16 expression has been observed in $CD8^+$ "innate-like" lymphocytes (Barbarin *et al*., 2017). Comparison of CD16 expression between the $CD45RA^{lo}$ and $CD45RA^+$ $V\delta1^+$ T cells demonstrated a significant increase in surface expression of this protein in the $CD45RA^+$ population, from 21.5% ± 7.2% to 67.4% ± 9.4% (n=6, p=0.012 Kruskal-Wallis ANOVA) (Figure 5.14a), which was also reflected in the $CD8^+$ αβ T cell population.

Certain transcription factors have been implicated in the differentiation and effector function of T cells. T-box expressed in T cells (Tbet) has been demonstrated to direct naïve T cells toward theT_H1, classically anti-viral, subset (Szabo *et al*., 2000) and is important in regulating the function of cytotoxic lymphocytes including NK cells and gamma delta T cells. Eomesodermin (Eomes) is important to the maintenance of CD8 T cell effector function, particularly in virus-specific cells (Simonetta *et al*., 2014), and these two transcription factors have a high degree of functional overlap in co-ordinating T cell development. Blimp-1 has been demonstrated to effect cytotoxic development of $CD8^+$ T cells (Kallies *et al*., 2009, Xin *et al*., 2016), and in conjunction with homologue of Blimp-1 in T cells (Hobit) has been implicated in formation of quiescent effector T and NK cell populations in tissues, including the liver (Vieira Braga *et al*., 2015, Stelma *et al*., 2017). Analysis of Tbet, Eomes and Hobit in the $CD45RA^{lo/neg}$ intrahepatic $V\delta1^+$ T cell groups highlighted generally low expression of these transcription factors, with a trend toward an increase in expression in the $CD45RA^+$ population (Figure 5.14b). This is consistent with the findings of Maini's group in human liver of low expression of these transcription factors in the "liver-resident" $CD8^+$ αβ T cell populations (Pallett *et al*., 2017).

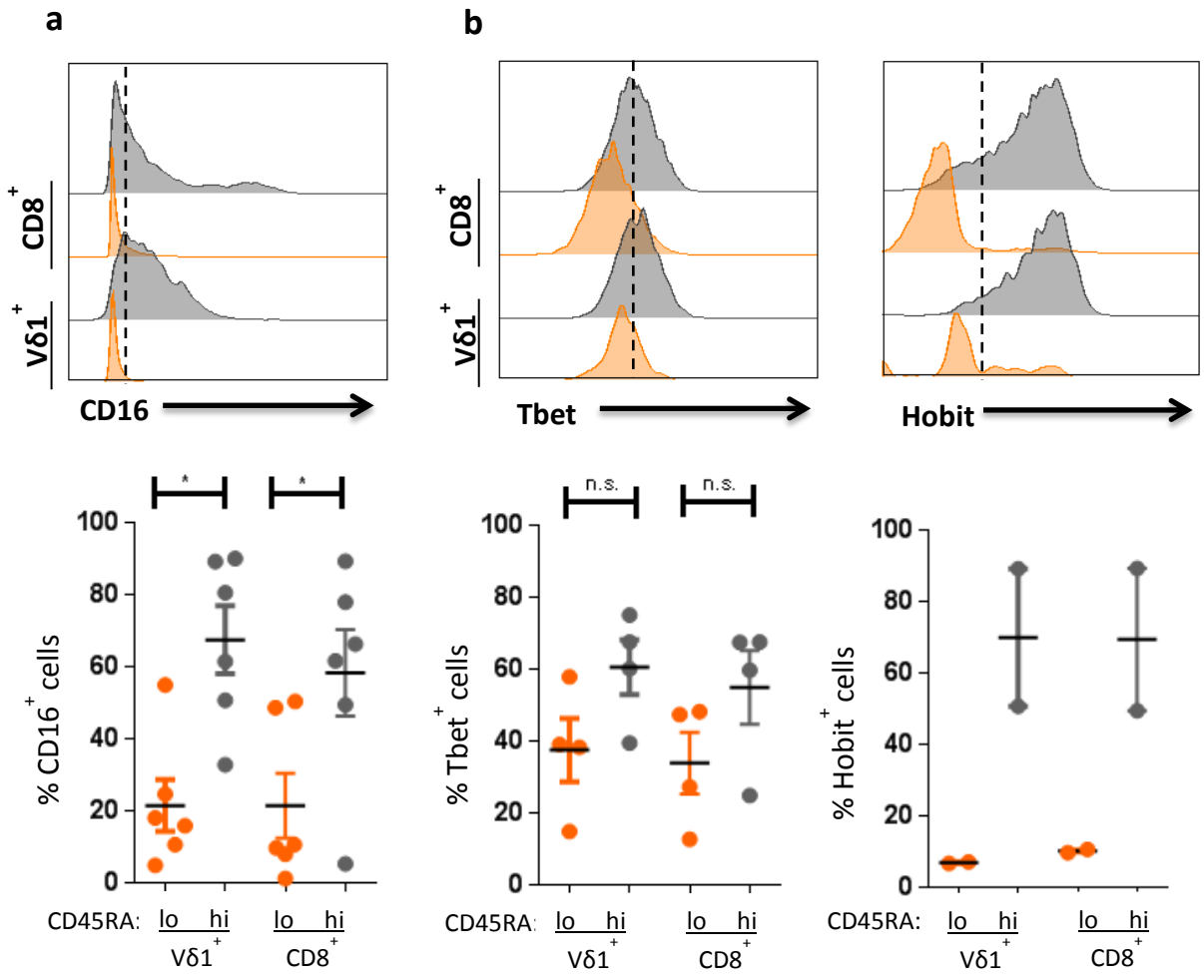

Figure 5.14: CD16 and transcription factor expression in intrahepatic Vδ1$^+$ T cells is associated with differentiation status

a) CD16 surface expression within Vδ1$^+$ and CD8$^+$ CD45RA$^{lo/neg}$ (orange) and CD45RA$^+$ (grey) T cells. Histograms from one representative donor and graphs show mean ± s.e.m. from 6 different donors. Data analysed by Kruskal–Wallis ANOVA with Dunn's post-test comparisons, *p<0.05.

b) Intracellular transcription factor expression within Vδ1$^+$ and CD8$^+$ CD45RA$^{lo/neg}$ (orange) and CD45RA$^+$ (grey) T cells. Histograms from one representative donor and graphs show mean ± s.e.m. from 2-4 different donors. Data analysed by Kruskal–Wallis ANOVA with Dunn's post-test comparisons, p>0.05.

These distinct patterns of chemokine receptor and transcription factor use between the CD45RA^{+} and CD45RA$^{lo/neg}$ populations is consistent with previous findings for tissue resident CD8^{+} T cells in the liver and other tissues.

5.2.5 The function of liver-associated and vasculature-associated intrahepatic Vδ1^{+} T cells

Having established a clonal and phenotypic difference between CD45RA^{+} and CD45RA$^{lo/neg}$ populations of intrahepatic Vδ1^{+} T cells, functional responses of these cells was investigated. Firstly, T cells were isolated from explanted livers and after magnetic sorting were cultured for 72 hours in cell media with various stimuli, including recombinant cytokines and TCR-stimulating αCD3/ CD28 beads. Since the majority of these cells expressed CD69 *ex vivo*, while CD25 was generally poorly expressed, CD25 was selected as an activation marker that could be simply analysed via flow cytometry. Initially, Vδ1, Vδ2 and CD8^{+} αβ T cells were analysed in bulk to investigate general responses to the stimulation conditions and activation compared with the same subsets in non-matched blood-derived cells, where CD69 and CD54 upregulation was measured (Figure 5.15). For blood derived cells, all three subsets responded strongly to TCR stimulation via αCD3/ CD28 beads (Vδ1; 77.4% ± 3.2%: Vδ2; 81.6% ± 7.8%: CD8^{+}; 74.9% ± 4.8%), with varying responses to IL-15 stimulation (Vδ1; 36.6% ± 8.4%: Vδ2; 80.5% ± 4.2%; CD8^{+}; 20.0% ± 4.9%). Interestingly, the only subset to respond strongly to combined stimulation with IL-12 and IL-18 was the Vδ2^{+} gamma delta T cells, (66.6% ± 7.1%), while Vδ1^{+} cells and CD8^{+} αβ cells did not (8.8% ± 2.0% and 9.1% ± 2.7% respectively). In the liver, the general pattern of responsivity changed, most significantly for the Vδ1^{+} and CD8^{+} subsets, although this may have been a reflection of the difference in read-out for

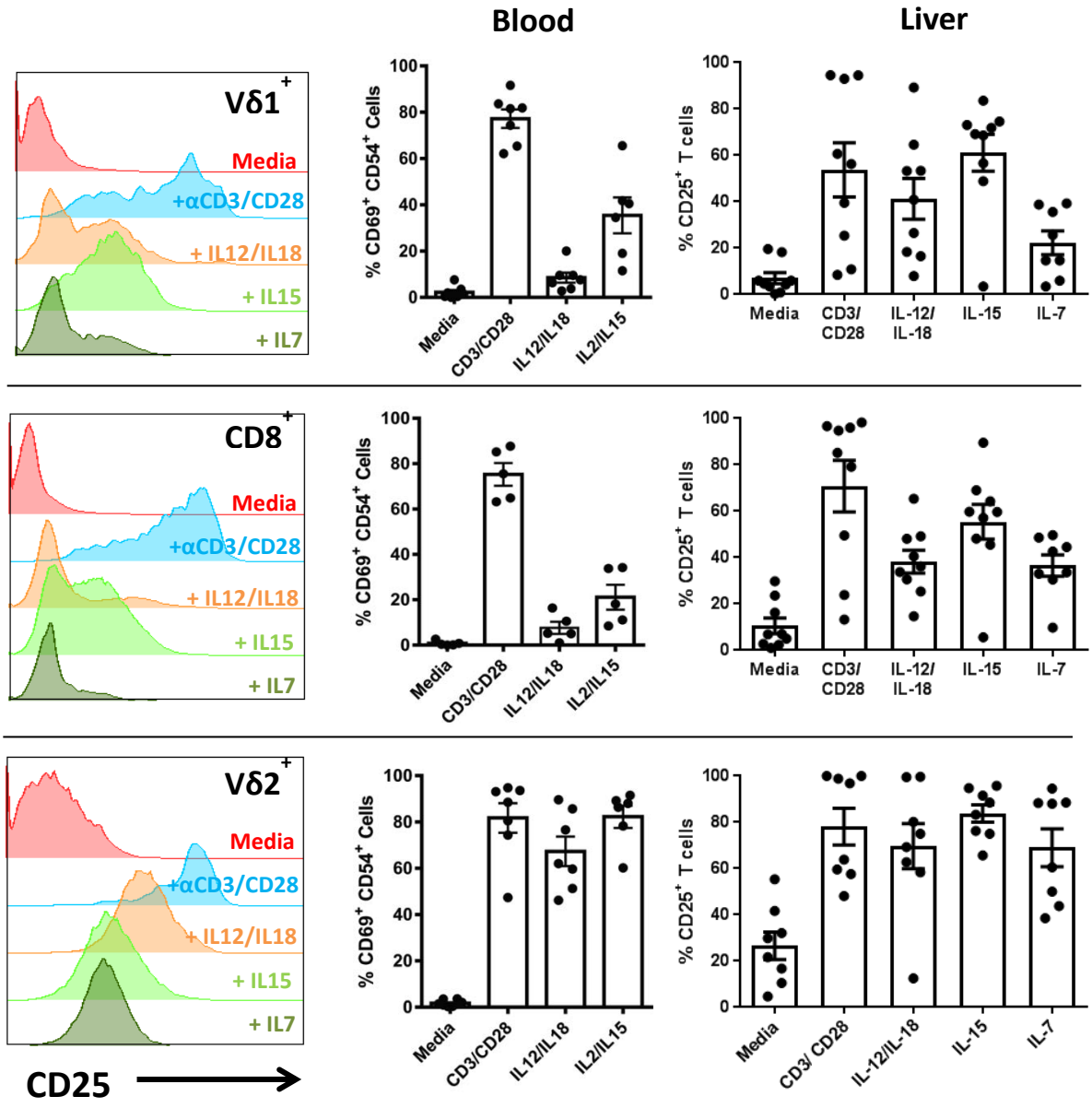

Figure 5.15: Activation of intrahepatic and peripheral T cells by exogenous stimulation

Peripheral and intrahepatic magnetically sorted $CD3^+$ T cells from non-matched donors were incubated for 72 hours with cytokines or anti-CD3/CD28 beads. $V\delta1^+$, $CD8^+$ αβ and $V\delta2^+$ T cells were then assessed for the upregulation of CD69 and CD54 (blood) or CD25 (liver). Histograms from one representative donor and graphs show mean ± s.e.m. for media control, CD3/CD28, IL-12/IL-18, IL-15 and IL-7 stimulation (liver only) (n=6-9).

the assay between the two compartments. Cell activation by αCD3/ CD28 beads was significantly reduced overall for intrahepatic Vδ1^{+} cells compared with blood Vδ1^{+} cells, to 53.7% ± 11.7% (p=0.035), but there was no significant change in the response of CD8^{+} cells (70.8% ± 11.1%) or Vδ2^{+} cells (78.1% ± 8.0%). Response to both IL-15 and IL-12/IL-18 stimulation increased significantly in liver-derived Vδ1^{+} T cells. 61.1% ± 8.0% of Vδ1^{+} cells upregulated CD25 post incubation with IL-15 (p=0.025 compared with blood), while 41.2% ± 8.8% were activated after incubation with IL-12 and IL-18 (p=0.008 compared with blood). The same findings were observed for the CD8^{+} T cells, where 55.4% ± 7.5% of cells were activated by IL-15, while 38.2% ± 4.2% were activated by IL-12/IL-18. Intrahepatic Vδ2^{+} cells displayed an equally vigorous response to blood-derived cells under both stimulatory conditions (IL-15; 83.9% ± 3.8%: IL-12/IL-18; 69.7% ± 7.8%).

Since phenotyping using putative differentiation markers had previously determined a reduction in liver-associated CD27^{hi} Vδ1^{+} cells and a substantial increase, from virtually zero, of CD45RA$^{lo/neg}$ Vδ1^{+} cells compared with peripheral blood, it is possible to speculate that the changes in response to activatory stimuli may be linked with these changes in differentiation. IL-15 has been demonstrated to be involved in the homeostatic maintenance of effector T cells, accompanied by increased expression of the IL-15R in effector CD8^{+} T cells (Geginat *et al*., 2003). Therefore increased response to this cytokine may simply reflect a greater proportion of effector cells within the liver-infiltrating population compared with blood. However, while the same may be possible for IL-12 and IL-18 responsivity, the blood exhibits a very weak response to these cytokines and yet has a large proportion of Vδ1^{+} cells that are CD27$^{lo/neg}$ (Davey *et al*., 2017). Therefore, the response of Vδ1^{+} cells to IL-12 and IL-18 was assessed in conjunction with their expression

of CD45RA. Since a decrease in TCR-mediated activation was also detected, the same was done with αCD3/ CD28 beads as a stimulus (Figure 5.16).

No significant difference for stimulation with αCD3/ CD28 beads was detected, with an average of 52.8% ± 14.0% of $CD45RA^{lo/neg}$ $V\delta1^{+}$ cells activated, compared with 60.2% ± 13.5% of $CD45RA^{+}$ cells. The same was true for $CD8^{+}$ T cells, with 70.0% ± 11.5% of $CD45RA^{lo/neg}$ cells activating and 62.1% ± 14.2% of $CD45RA^{+}$ cells. Interestingly, however, for $V\delta1^{+}$ T cells a significant increase in response to exogenous IL-12 and IL-18 was noted between $CD45RA^{+}$ and $CD45RA^{lo/neg}$ populations, rising from 34.9% ± 6.55 to 73.4% ± 5.1% (p=0.004, Mann-Whitney U test). Although there was also a rise in activation between $CD45RA^{+}$ and $CD45RA^{lo/neg}$ $CD8^{+}$ populations (27.3% ± 9.3% to 51.8% ± 9.3%, p=0.18, Mann-Whitney U test) this was not statistically significant. These data is highly suggestive of increased IL-12 and IL-18 response in the clonally and phenotypically distinct $CD45RA^{lo/neg}$ liver-associated $V\delta1^{+}$ cells.

Lastly, the cytotoxic potential and cytokine production of intrahepatic $V\delta1^{+}$ cells was assessed with respect to their differentiation status. Perforin and granzyme B are two proteins expressed by cytotoxic killer cells capable of lysing other cells. Intracellular expression of these proteins was therefore analysed using flow cytometry (Figure 5.17). For granzyme B, an average of 14.4% ± 3.0% of $V\delta1^{+}$ $CD45RA^{lo}$ cells were positive for expression, significantly decreased from the $CD45RA^{+}$ cells (50.9% ± 6.9%, p=0.002). This reflected the data for $CD8^{+}$ αβ T cells, where 22.6% ± 7.4% of $CD45RA^{lo}$ cells expressed Granzyme B, compared with 64.7% ± 7.1% of $CD45RA^{+}$ cells (p=0.01). A similar pattern was observed with perforin expression, with $CD45RA^{+}$ cells exhibiting higher expression for both $V\delta1^{+}$ and $CD8^{+}$ αβ cells ($V\delta1^{+}$ $CD45RA^{lo}$ 23.6% ± 4.2% vs. $CD45RA^{+}$ 66.0% ± 5.4%:

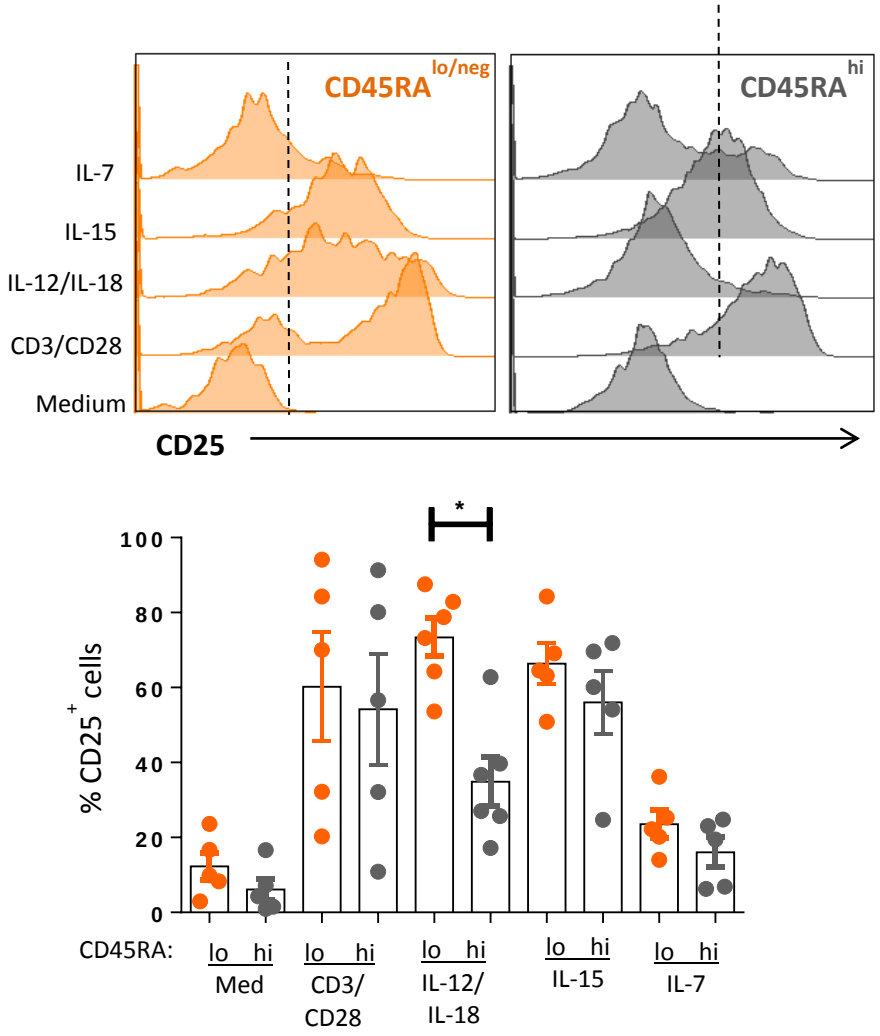

Figure 5.16: CD45RA$^{lo/neg}$ intrahepatic Vδ1^{+} T cells are responsive to exogenous IL-12 & IL-18 cytokines

Intrahepatic magnetically sorted CD3^{+} T cells from non-matched donors were incubated for 72 hours with cytokines or anti-CD3/CD28 beads. Vδ1^{+} T cells were then assessed for the upregulation of CD25 as a function of CD45RA expression. Histograms from one representative donor and graphs show mean ± s.e.m. for media control, CD3/CD28, IL-12/IL-18, IL-15 and IL-7 stimulation (n=5). Data analysed by Mann-Whitney U test, *p<0.05.

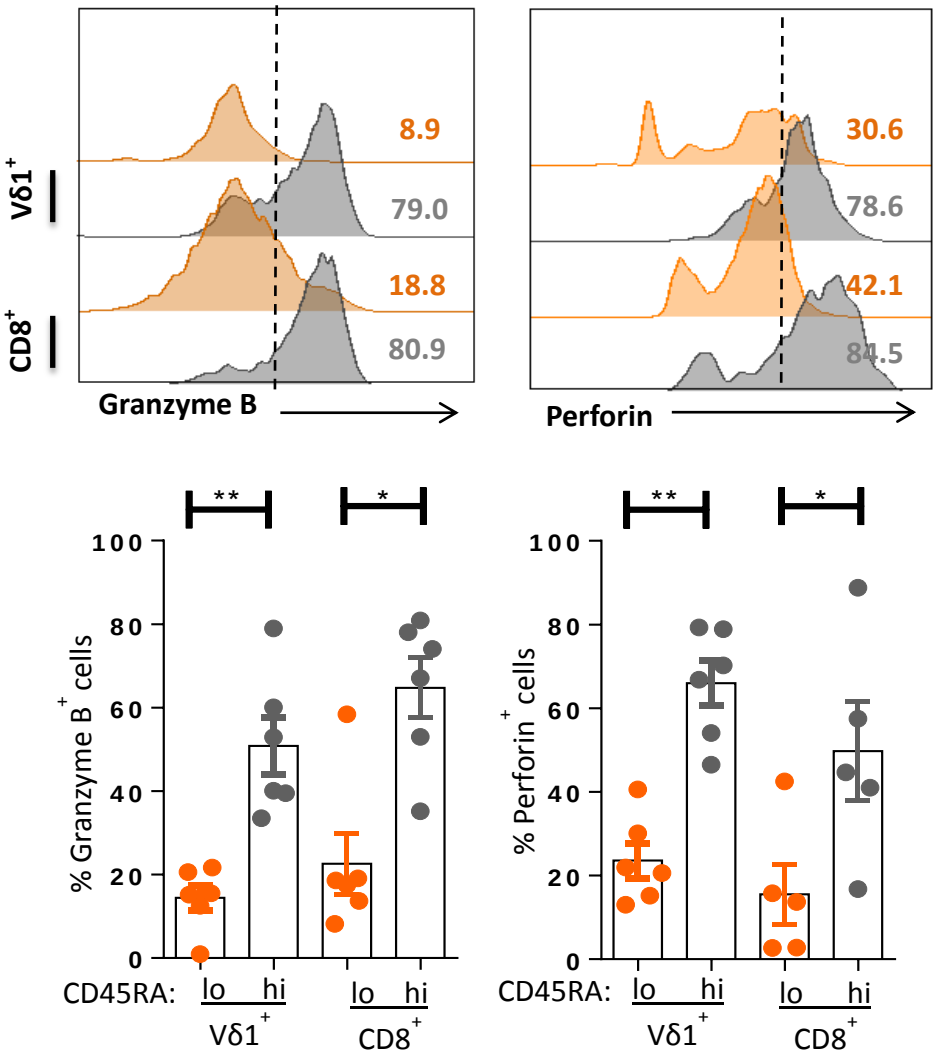

Figure 5.17: CD45RA$^{lo/neg}$ intrahepatic Vδ1^{+} and CD8 T cells are have less cytotoxic potential than CD45RA^{+} cells

Comparison of intracellular granzyme B and perforin expression within Vδ1^{+} and CD8^{+} CD45RA$^{lo/neg}$ (orange) and CD45RA^{+} (grey) T cells. Histograms from one representative donor and graphs show mean ± s.e.m. from 5-6 different donors. Data analysed by Kruskal–Wallis ANOVA with Dunn's post-test comparisons, *p<0.05, **p<0.01.

$CD8^+$ $CD45RA^{lo}$ 15.5% ± 7.3% vs. $CD45RA^+$ 49.8% ± 11.8%). This suggests the blood-associated $CD45RA^+$ $V\delta1^+$ cells may have higher cytotoxic potential, which is consistent with previous findings in peripheral blood (Davey *et al*., 2017), but that the liver-associated $CD45RA^{lo}$ cells have relatively lower cytotoxic potential.

To assess cytokine production, *ex vivo* magnetically labelled T cells were sorted and cultured overnight before addition of PMA and ionomycin with brefeldin-A to inhibit Golgi transport and secretion. The proinflammatory cytokines interferon-γ (IFN-γ) and tumour necrosis factor α (TNFα) were then detected intracellularly by flow cytometry, once again with respect to CD45RA expression (Figure 5.18). For $V\delta1^+$ cells, IFN-γ expression was marginally higher overall than TNFα, but expression of both cytokines was significantly higher in the $CD45RA^{lo}$ population than the $CD45RA^+$ (IFN-γ; 71.8% ± 9.0% vs. 37.5% ± 3.5% (p=0.026): TNFα; 64.1% ± 7.1% vs. 34.2% ± 5.2% (p=0.015)). Cytokine expression among the $CD8^+$ cells was consistently around 70% of all cells, regardless of phenotype. IFN-γ was expressed by 74.1% ± 6.3% and 74.3% ± 5.2% of $CD45RA^{lo}$ and $CD45RA^+$ cells respectively, while TNFα was expressed by 64.5% ± 8.4% and 72.6% ± 8.1% of $CD45RA^{lo}$ and $CD45RA^+$ cells respectively, with no significant difference between sub-populations.

Overall, these data suggests that a significant population of clonotypically, phenotypically and functionally distinct $V\delta1^+$ T cells exists in human liver that are phenotypically and functionally similar to the $CD8^+$ αβ T cells that have previously been described as liver resident.

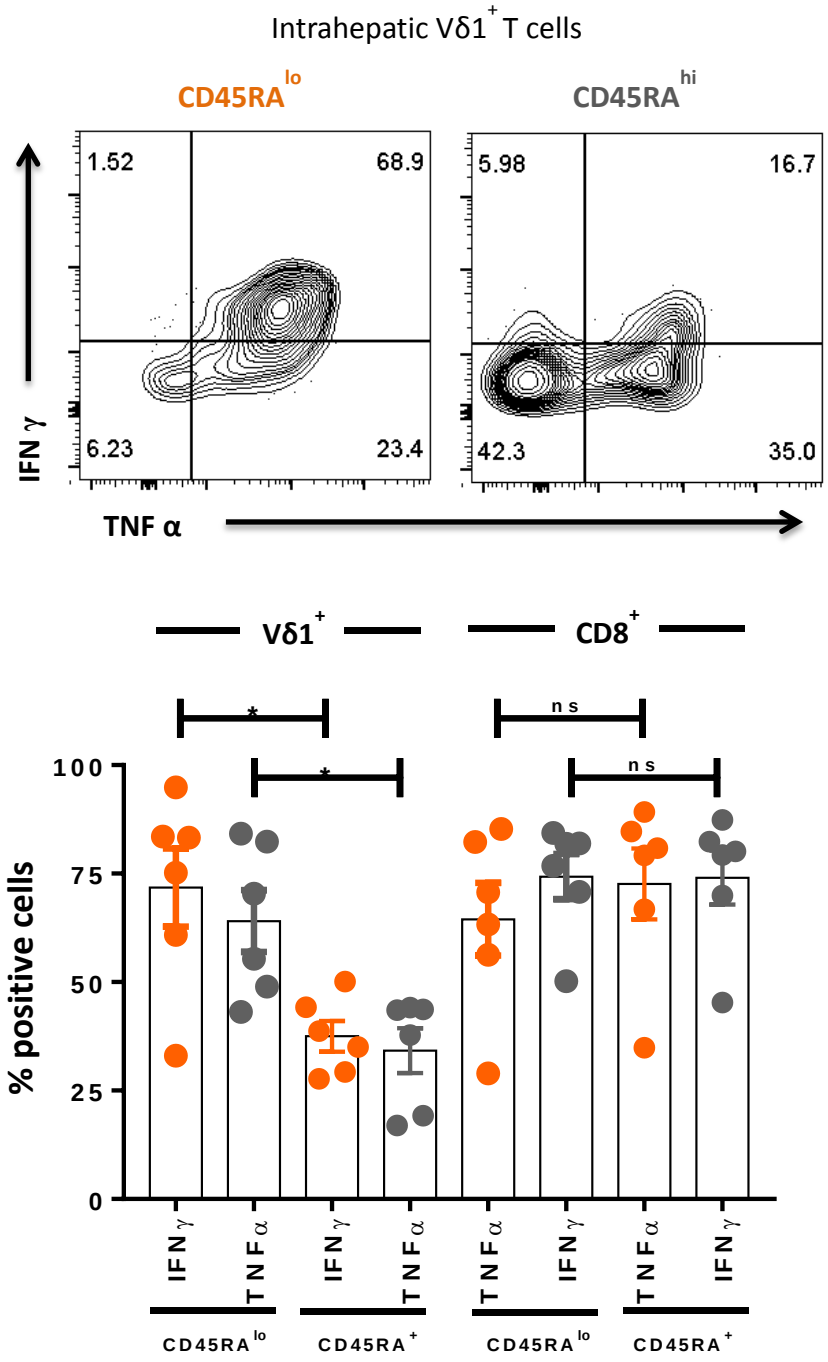

Figure 5.18: CD45RA$^{lo/neg}$ intrahepatic Vδ1^{+} T cells are higher producers of inflammatory cytokines than CD45RA^{+} cells

Intrahepatic magnetically sorted CD3^{+} T cells were stimulated for 4 hours with PMA, ionomycin and brefeldin-A. Vδ1^{+} T cells were then assessed for the upregulation of intracellular IFN-γ and TNFα as a function of CD45RA expression. Histograms from one representative donor and graphs show mean ± s.e.m. (n=5-6). Data analysed by Kruskal–Wallis ANOVA with Dunn's post-test comparisons, *p<0.05.

5.3 Discussion

Although a considerable amount of work has recently gone in to characterising murine and human tissue resident T cells, the nature of tissue-associated gamma delta T cells has remained unclear. This is perhaps due to the fact that in mice, where the bulk of gamma delta T cell biology research has been conducted, the majority of these cells are programmed to track into specific tissues based on thymic TCR recognition, where they adopt a generally innate-like function. In Chapter 4, the TCR repertoire of human intrahepatic gamma deltas was found to be highly variable between individuals, in terms of both CDR3 regions and chain usage, with highly private, apparently motif-free CDR3s and a diverse spectrum of chain usage and pairings, perhaps suggestive of an adaptive-like repertoire formation. This is somewhat at odds with the data from mouse studies that suggest most tissues in mice have a distinct, restricted chain usage and CDR3 lengths in their gamma delta T cell population, more reflective of an innate-like repertoire formation (Asarnow *et al*., 1989) and consistent with innate T cell populations such as MAITS (Lepore *et al*., 2014). Since previous studies on canonically tissue-associated Vδ1 T cells were based exclusively on peripheral blood Vδ1 cells (Davey *et al*., 2017), understanding the immunobiology of solid tissue-associated Vδ1s, often assumed to be innate-like, is particularly important.

Based on this, we wanted to investigate the nature of the human intrahepatic gamma delta T cell population and its relationship with the peripheral population, in an attempt to define whether or not these cells are indeed tissue associated and potentially resident. To do this, peripheral blood was sampled from patients undergoing liver transplant for

non-autoimmune chronic liver diseases. These were chosen as data from this study and others has suggested that either autoimmune liver diseases, including AIH, PBC and PSC, or the treatment thereof, may induce perturbations of the peripheral gamma delta T cell populations. With only one previous study of gamma delta T cells from matched blood and liver from human donors (Kenna *et al*., 2004), it was important to establish that the frequency of gamma delta subsets from these matched donors was consistent with previous observations from non-matched liver and blood, which was indeed the case. Both $V\delta1^{+}$ and $V\delta2^{neg}V\delta1^{neg}$ gamma delta T cells were enriched in liver, both as a proportion of the total $CD3^{+}$ T cell number and of the total pan-γδ TCR^{+} number. Interestingly, $V\delta2^{+}$ cells, classically associated with the periphery, were also mildly enriched in the liver compared with blood as a proportion of $CD3^{+}$ T cells.

Comparison of matched liver and blood samples indicated the differentiation status of the $V\delta2^{neg}$ T cell subset was distinct in each compartment. Strikingly, liver $V\delta2^{neg}$ T cells were uniformly $CD27^{lo/neg}$, a phenotype previously linked to a clonally expanded effector subset present in peripheral blood, and essentially entirely lacked the $CD27^{hi}$ subset, even when such populations were relatively prevalent in matched blood. Previously $CD27^{hi}$ $V\delta1^{+}$ T cells in peripheral blood have been demonstrated as TCR-diverse and naïve in phenotype, possessing CCR7 and CD62L required for recirculation between blood and lymph. Consistent with selective exclusion of this clonally diverse $CD27^{hi}$ naive population, liver $V\delta1^{+}$ cells lacked CCR7, CD62L and CD27 present on such naïve populations. Critically, substantial clonotypic overlap between these two populations was observed. While the possibility that such hepatic $CD27^{lo/neg}$ cells originated in the liver cannot be excluded, these results support the alternative concept that at least some

hepatic $CD27^{lo/neg}$ cells may derive from those present in peripheral blood. Such a scenario would fit an adaptive model whereby naive peripheral blood $V\delta2^{neg}$ $CD27^{hi}$ cells, which express secondary lymphoid homing markers but are devoid of peripheral homing markers, recirculate between blood and lymph, whereas the peripheral blood $CD27^{lo/neg}$ population, which is clonally expanded and likely antigen-experienced, is capable of accessing solid tissues, consistent with its expression of peripheral homing markers such as CXCR6 and constitutive expression of integrins such as LFA-1 and VLA-4.

A second indication of compartmentalisation was that in addition to being devoid of $CD27^{hi}$ naïve cells, the hepatic $V\delta2^{neg}$ T cell compartment comprised both $CD45RA^{+}$ and $CD45RA^{lo/neg}$ subsets. By contrast, the peripheral blood $CD27^{lo/neg}$ $V\delta1^{+}$ cells are almost entirely $CD45RA^{+}$. Importantly, single cell PCR and phenotyping of paired blood and liver samples revealed a striking degree of overlap in $CD45RA^{+}$ clonotypes between blood and liver. Such cells in the periphery express a high level of the endothelial homing receptor CX_3CR1 (fractalkine receptor) as well as increased CD16, low CD27/28, low CD127, and enhanced levels of adhesion molecules relative to naïve $CD27^{hi}$ cells (Davey *et al*., 2017). Studies conducted on cytomegalovirus (CMV)-infected individuals post kidney-transplant determined a CMV-specific expansion of $V\delta2^{-}$ T_{EMRA} cells expressing high levels of CX_3CR1 and critically CD16 in the periphery (Couzi *et al*., 2015), however, other studies have confirmed the expansion of such a subset in the periphery of CMV^{-} healthy donors also (Davey *et al*., 2017), and no commonality in TCR repertoire has yet been identified, so the antigenic origin of such clonal populations is unclear. Unfortunately, the CMV status of the individuals sampled could not be obtained for liver donors for ethical reasons. There was a wide variety in the proportion of the $CD45RA^{lo/neg}$ population in the liver – from less

than 5% of intrahepatic Vδ1^{+} cells to greater than 50%, and it is tempting to speculate that CMV^{+} individuals may have a lower proportion of CD45RA$^{lo/neg}$ cells than CMV^{-}, perhaps due to the CMV-associated CX_3CR1^{+} T_{EMRA} Vδ1^{+} cells accumulating in the endothelium-rich sinusoids post-CMV related expansion. Since fractalkine has been demonstrated to be expressed more highly by virally-infected liver cells (Kondo *et al*., 2015) and other chronic liver diseases (Shimoda *et al*., 2010) one may also predict an increase in this subset in diseased livers compared with normal livers, but this was not the case in this study, suggesting fractalkine-mediated recruitment of T_{EMRA} Vδ1^{+} cells may not be the sole driving factor in their accumulation in the liver.

Nevertheless, the concept of 'vascular residency', as has been suggested for αβ T cells exhibiting the CD27$^{lo/neg}$CD45RA^{+} CX_3CR1^{+} phenotype, is intriguing. Demonstrated for virus-specific CD8^{+} (Remmerswaal *et al*., 2012) and CD4^{+} (Pachnio *et al*., 2016) T cell subsets, this is not a concept that has been associated with gamma delta T cells previously, but the data presented here does give weight to the idea. The predominantly sinusoidal localisation of gamma delta T cells identified in Chapter 3 is consistent with this possibility, as is the striking level of clonal overlap between CD45RA^{+} cells in the blood and the liver, itself a large and complex network of endothelial vasculature. Although the antigenic targets of such Vδ2^{neg} subsets is unclear, the recent report that these include clonotypes expanding in response to CMV infection is consistent with a role of the unconventional T cell in response to chronic viral infection (Ravens *et al*., 2017).

In contrast to CD45RA^{+} clonotypes and consistent with a reduced proportion of CD45RA^{+} Vδ1^{+} cells in liver compared to peripheral blood, the same analyses of matched blood/liver samples revealed CD45RA$^{lo/neg}$ clonotypes that were typically identified only

in the liver samples. In addition, this liver CD45RA$^{lo/neg}$ compartment frequently contained highly clonal expansions. These cells demonstrate striking phenotypic correlation with liver resident lymphocytes identified in previous studies, including enhanced expression of CD69, CXCR6 and CXCR3, which has been noted in liver resident NK populations (Hudspeth *et al*., 2016, Stegmann *et al*., 2016) and CD8^{+} αβ populations (Pallett *et al*., 2017, Stelma *et al*., 2017). Additionally these cells had low expression of Tbet, Hobit and Eomes, in contrast with blood- and liver-derived naïve and T_{EMRA}-like Vδ1^{+} cells. Despite not expressing CD103, which is a defining element of epithelium-resident CD8^{+} cells, CD69 expression was clearly high in the liver-associated Vδ1^{+} populations. However, it was also upregulated in a smaller fraction of the T_{EMRA}-like Vδ1^{+} cells that were clonally identical to blood-derived cells. Whether this was due to a systemic upregulation of lymphocytic CD69 due to the chronic liver injury, reflective of local transient activation by liver-specific factors or whether some of these clonotypes shared with blood were in fact resident in the liver, is unclear. While Vδ1^{+} CD69 upregulation was demonstrated for patients undergoing reactivation of AIH in Chapter 3, in the matched cohort peripheral CD69 expression was not high for the majority of donors. Incubation of healthy PBMC-derived T cells in liver-derived supernatants did induce marked CD69 upregulation (data not shown) but the physiological relevance of such supernatants is perhaps dubious since they are highly concentrated and lack the homeostatic cellular processing of metabolites, toxins and extracellular proteins. Additionally, if due to transient activation, CD69 expression would have to be lost very rapidly on exiting the tissue as the liver receives a very large volume of blood every hour and one may expect this to raise peripheral expression of CD69.

$CD27^{lo/neg}CD45RA^{lo/neg}$ $V\delta1^+$ T cells may therefore represent a liver-resident subset, although conceivably they may be able to access other solid tissues. As such clonotypes are not present within the blood, their origin is unclear. One possibility is that they originate from a subset of blood $CD45RA^+$ cells that alter phenotype once in tissues and are retained there, perhaps following activation in the hepatic microenvironment. Recent work from the Maini group highlighted the potential for a liver resident phenotype to be induced independent of exogenous TCR stimulation in $CD8^+$ αβ T cells via IL-15 followed by TGF-β signalling (Pallett *et al*., 2017), and based on the parallels between $V\delta1^+$ and $CD8^+$ αβ T cells identified in this study, a similar mechanism may be at work here. The liver is rich in IL-15 (Golden-Mason *et al*., 2004) and the contribution of this cytokine to induction of tissue residency in NK cells has been proposed (Cuff *et al*., 2016). Activation of all intrahepatic $CD27^{lo/neg}$ $V\delta1^+$ cells by IL-15 was demonstrated in this study, and yet it is hard to evaluate the contribution of this cytokine to induction of residency in $CD45RA^{lo/neg}$ $V\delta1^+$ cells since they are so highly clonally focussed, with such a mechanism presumably being TCR-independent. An alternative is that they develop extra-thymically in response to tissue-specific TCR-mediated cues, potentially even from foetal liver cells (Wucherpfennig *et al*., 1993) although these are predominantly $V\delta2^+$ (Carding *et al*., 1990). Whatever the origin of these cells, the high degree of repertoire focussing and clonality is strongly suggestive of an important role for the TCR in shaping this population.

These results highlight that hepatic γδ T cells are not only phenotypically but also functionally distinct from equivalent subsets in peripheral blood. While overall still responsive to TCR stimulation/costimulation, unlike blood $V\delta2^{neg}$ T cells they displayed

increased responsiveness to IL-12/IL-18 in line with $CD8^+$ T cells isolated from the same tissue. A previous study of peripheral human $V\delta1^+$ T cells has demonstrated sensitization of these cells to IL-18 following TCR ligation (Guerville *et al*., 2015), and these findings were also demonstrated in mice with concomitant TCR hyporesponsivity (Wencker *et al*., 2014). This paradigm of TCR-driven "switching" from adaptive to innate-like responses cannot be ruled out here, although evidence of response to TCR stimulation here clearly rules out a full switch to innate-like response. Activation through TCR mediated stimulation was considerably more variable for intrahepatic $V\delta1^+$ cells compared with PBMC-derived, although whether this was a transcriptionally controlled re-programming of the cells or merely exhaustion from the isolation protocol, which is more stressful for the liver-derived cells than the blood-derived, is unclear. Additionally, this paradigm doesn't fit if the large blood-associated clonal expansions are considered TCR-mediated, as seems likely, as they remain IL-12 and IL-18 insensate, even within the liver, so TCR-mediated expansion and indeed liver microenvironment cannot be the sole driving influences on cytokine sensitisation. Other factors, possibly microenvironmental in nature or possibly developmentally imprinted, must be at play in this scenario, and hopefully techniques such as single cell transcriptomic analysis may lead to an answer in future studies.

In addition to increased sensitivity to exogenous activatory cytokines, the $CD45RA^{lo/neg}$ subset also appeared to display enhanced production of pro-inflammatory cytokines and decreased potential cytotoxicity compared with $CD45RA^+$ cells. This observation has been made in both liver-resident intrahepatic NK cells (Marquardt *et al*., 2015, Harmon *et al*., 2016) and $CD8^+$ αβ T cells (Pallett *et al*., 2017, Stelma *et al*., 2017), and certainly gives

credence to these cells being genuinely liver resident. Further examination of cellular function with a direct link to clonotype via indexed single cell sorting would help establish whether it is truly the liver-associated clonotypes that account for the differences observed between the CD45RA^{+} and CD45RA$^{lo/neg}$ Vδ1^{+} cells. One may even be able to extend such a study to include αβ T cells, where the influence of clonality has not been linked with liver-residency in human studies to date.

Overall, these observations suggest CD45RA^{+} and CD45RA$^{lo/neg}$ subsets may have significantly different roles, the former more vascular focussed and cytotoxic, the latter an immunoregulatory tissue-associated subset more focussed on cytokine production and potential induction of a wider T cell response to stress challenges. Since liver-resident Kupffer cells represent a potent source of IL-12 and IL-18, one can speculate on the biological significance of liver-associated Vδ1^{+} cells being activated by these cytokines. Activation of KC via TLR would induce IL-12 (Takahashi *et al*., 1996) and, via the caspase-1 inflammasome, IL-18 expression (Shrivastava *et al*., 2013), which could then activate pro-inflammatory cytokine release by liver-associated Vδ1^{+} gamma delta T cells, thereby forming part of the liver associated "firewall" against microbial gut-associated antigen. Whether or not this is the case, it is unclear if the distinct features of the CD45RA$^{lo/neg}$ populations of Vδ1^{+} T cells stem directly from expansion in response to tissue-specific TCR-mediated antigenic cues or whether they reflect the preferential homing and/ or retention of certain non-tissue restricted clonotypes, perhaps according to response to hepatic microenvironmental factors.

This study establishes that in humans, clonally expanded γδ T cell effector subsets can be selectively deployed to at least some solid tissues, thereby providing ongoing immune

surveillance against previously encountered infectious or non-infectious challenges. Moreover, the finding that such subsets can be phenotypically, functionally and most importantly clonotypically distinct from those in peripheral blood provides a basis for future investigation of tissue-resident γδ T cell populations.

6

A novel subset of Vδ2^{+} gamma delta T cells are enriched in liver

6.1 Introduction

Previous chapters have highlighted the enrichment of clonally expanded effector gamma delta T cells in human liver, focussing mainly on the historically tissue associated $V\delta1^+$ subset. However, evidence from matched donor liver and peripheral blood samples suggests that, as a percentage of the total infiltrating T cell population, the liver is also slightly enriched for the $V\delta2^+$ subset of gamma delta T cells, normally thought of as blood associated. Additionally, experiments detailed in Chapter 3 also demonstrated the enhanced adhesion and transmigration of $V\delta2^+$ cells across primary human liver endothelial cells compared with both αβ T cells and $V\delta2^{neg}$ gamma delta T cells, suggesting these cells may be capable of enhanced recruitment to the liver in both inflammatory and non-inflammatory conditions. In this chapter, a closer examination of this relatively well studied population of cells is performed, but in the previously undocumented context of human liver.

Perhaps the prototypic unconventional T cell, $V\delta2^+$ T cells typically co-express Vγ9 TCR chains and represent the major γδ subset in adult peripheral blood. This common chain pairing is made when Vγ9 rearranges with the JγP joining segment, and splices to C1 to form the Vγ9JγPC1 chain (Tribel *et al*., 1988). Despite there being no clear restriction in pairing, the rearranged Vγ9JγP chain pairs mainly with Vδ2 chains (Borst *et al*., 1989).

Whether the formation of the strongly $V\delta2^+V\gamma9^+$JγP dominant repertoire is the result of a molecular bias in TCR recombination, or driven by antigenic selection during development and maturation of these cells is not yet clear, although research in this area is still underway. Interestingly, the pre-thymic (<8 weeks) human liver gamma delta T cell

population is uniformly composed of functional Vδ2^{+}Vγ9^{+} cells (McVay and Carding, 1996). A more recent study of the gamma delta TCR repertoire at different stages of foetal development in humans described a sharp increase in the population of Vδ2^{+}Vγ9^{+} T cells with limited junctional diversity in blood at around 23 weeks of gestation (Dimova *et al*., 2015). While forming the dominant population at this time point, the frequency of these cells steadily declined until birth and was at very low frequency in cord blood and neonatal venous blood.

This high enrichment of Vδ2^{+}Vγ9^{+} T cells at an early stage of development, both in the foetal liver and blood, as well as the restricted CDR3γ9 usage early in gestation, is consistent with an innate-like ontogeny for Vδ2^{+}Vγ9^{+} T cells, at least pre-natally. However, post-natally, a dramatic expansion of Vδ2^{+}Vγ9^{+} T cells has been observed in the blood, which does occur extrathymically (Casorati *et al*., 1989). In addition, this expansion appears to occur clonotypically (Kalyan and Kabelitz, 2013, Carding and Egan, 2002, Pauza and Cairo, 2015), which naturally is suggestive of an adaptive immunobiology for these cells (Shen *et al*., 2002).

As described in Chapter 1, Vδ2^{+}Vγ9^{+} T cells respond to prenyl-pyrophosphate metabolites (phosphoantigens, or P-Ag) produced either by the microbial non-mevalonate pathway ((E)-4-Hydroxy-3-methyl-but-2-enyl pyrophosphate, or HMB-PP) or the host mevalonate pathway (isopentenyl pyrophosphate, or IPP) . In this way, they are capable of recognising both exogenous antigen as well as endogenous antigen associated with stressed-self. The expansion of Vδ2^{+}Vγ9^{+} T cells observed in adult peripheral blood has been attributed to post-natal exposure to P-Ag producing pathogens (De Libero *et al*., 1991, Davodeau *et al*., 1993), reflective of an adaptive-like mechanism, although the

basis of these expansions appears to occur polyclonally (M. Davey, unpublished). Consistent with this, primate models highlight improved Vδ2$^+$ responses to *Mycobacterium tuberculosis* upon secondary challenge (Chen *et al*., 2005). Indeed, the importance of the role of Vδ2$^+$ gamma delta T cells has been demonstrated in many anti-microbial immune responses, including against *Mycobacterium tuberculosis* (Chen *et al*., 2013) and *plasmodium falciparum*, where they target red blood cell-invasive extracellular plasmodium merozoites in a TCR specific manner *(Costa et al., 2011)*, although the basis for recognition is unclear .

Vδ2$^+$Vγ9$^+$ T cells have been demonstrated to increase numerically both systemically and at the site of many microbial infections (Davey *et al*., 2011), and can reach frequencies of over half of all peripheral T cells in a remarkably short time period during infection (Morita *et al*., 2007), revealing a fundamental role of this unconventional T cell population in acute disease. Despite these dynamics however, the limited diversity of the Vδ2 TCR and pattern recognition receptor-like MHC-independent recognition of P-Ag is more suggestive of an innate-like biology.

As for all gamma delta T cells, recognition of P-Ag appears to occur independently of both classical and non-classical MHC molecules (Morita *et al*., 1995, Lang *et al*., 1995). More recent studies have highlighted the role of a member of the B7 family of costimulatory molecules, butyrophilin 3A (BTN3A1/ CD277) in sensing of IPP/ HMB-PP by Vδ2$^+$ gamma delta T cells (Harly *et al*., 2012). While both intracellular and extracellular domains of BTN3A have been demonstrated to interact with P-Ag, suggestive of an innate pattern recognition receptor, it is unclear exactly how this binding leads to Vδ2$^+$ TCR-mediated cell activation. Further to this, monocytes are required for the activation of Vδ2$^+$ cells by

the P-Ag pamidronate (Miyagawa *et al*., 2001), and it is thought that internalisation of P-Ag by endocytic monocytes is involved in subsequent activation of Vδ2^{+} cells (Eberl *et al*., 2009).

Irrespective of the exact activation mechanism, Vδ2^{+}Vγ9^{+} T cells are capable of exerting a wide range of effector functions upon activation. These include cytolysis of infected and stressed cells, driving inflammatory and wound healing processes, inducing dendritic cell maturation and interestingly, they appear to have a significant role as antigen presentation cells, providing B cell help and priming αβ T cells (Tyler *et al*., 2015).

Accordingly, the aim of this chapter was to investigate the frequency, phenotype and function of a classically blood-associated subset of gamma delta T cells in the context of human liver and compare this with the periphery. To do this, a combination of TCR repertoire profiling, flow cytometry and immunological assays was combined, which unexpectedly also revealed the presence of a novel tissue-tropic subset of Vδ2^{+}Vγ9^{neg} cells that may play a role in liver immunosurveillance.

6.2 Results

6.2.1 TCR repertoire sequencing of Vδ2^{+} gamma delta T cells

6.2.1.1 Choice of Ab-based Vδ2^{+} T cell purification strategy

Previously in this study, next generation sequencing of TCR repertoires from 10 explanted human livers was conducted to investigate the degree of clonality and publicity of the repertoire of the intrahepatic Vδ2^{neg} gamma delta T cell population (Chapter 4). These cells were sorted using a MoFlo Astrios cell sorter according to fluorophore -conjugated

antibody directed labelling of CD3, pan-γδ TCR and Vδ2 TCR (Figure 4.3). Initial analysis of antibody performance conducted on peripheral blood established that one commonly used commercial antibody for the Vδ2 TCR (clone B6) does not stain all $V\delta2^{+}$ gamma delta T cells (Figure 6.1a & b), with the Miltenyi 123R3 $V\delta2^{+}$ antibody staining a higher frequency by comparison of the same donor sample. The 123R3 clone was therefore used in both negative sort selection of $V\delta2^{neg}$ gamma delta T cells (Chapter 4) but also positive selection of $V\delta2^{+}$ gamma delta T cells here.

A puzzling outcome of the $V\delta2^{neg}$ sorting strategy used in Chapter 4 was the presence of $V\delta2^{+}$ CDR3 sequences in the supposedly $V\delta2^{neg}$ population, despite use of the 123R3 antibody. In human blood, Vδ2 conventionally pairs with Vγ9 to form the phosphoantigen reactive Vδ2Vγ9 TCR. This pairing also includes the JγP joining region. However, when the iRepertoire next generation TCR sequencing dataset was analysed, despite the presence of $V\delta2^{+}$ CDR3δ sequences there were very few Vγ9JγP CDR3γ sequences - within shared CDR3γ clones across all samples only 20 Vγ9JγP clones were identified versus ~6000 shared CDR3γ clonotypes in total. This finding was suggestive of the existence of a $V\delta2^{+}V\gamma9J\gamma P^{neg}$ gamma delta T cell subset present at significant levels in the liver-derived $V\delta2^{neg}$ samples analysed in this study. Such a subset has never previously been highlighted in human solid tissue or blood, and so accordingly further investigation of such a putative subset was carried out as part of this study.

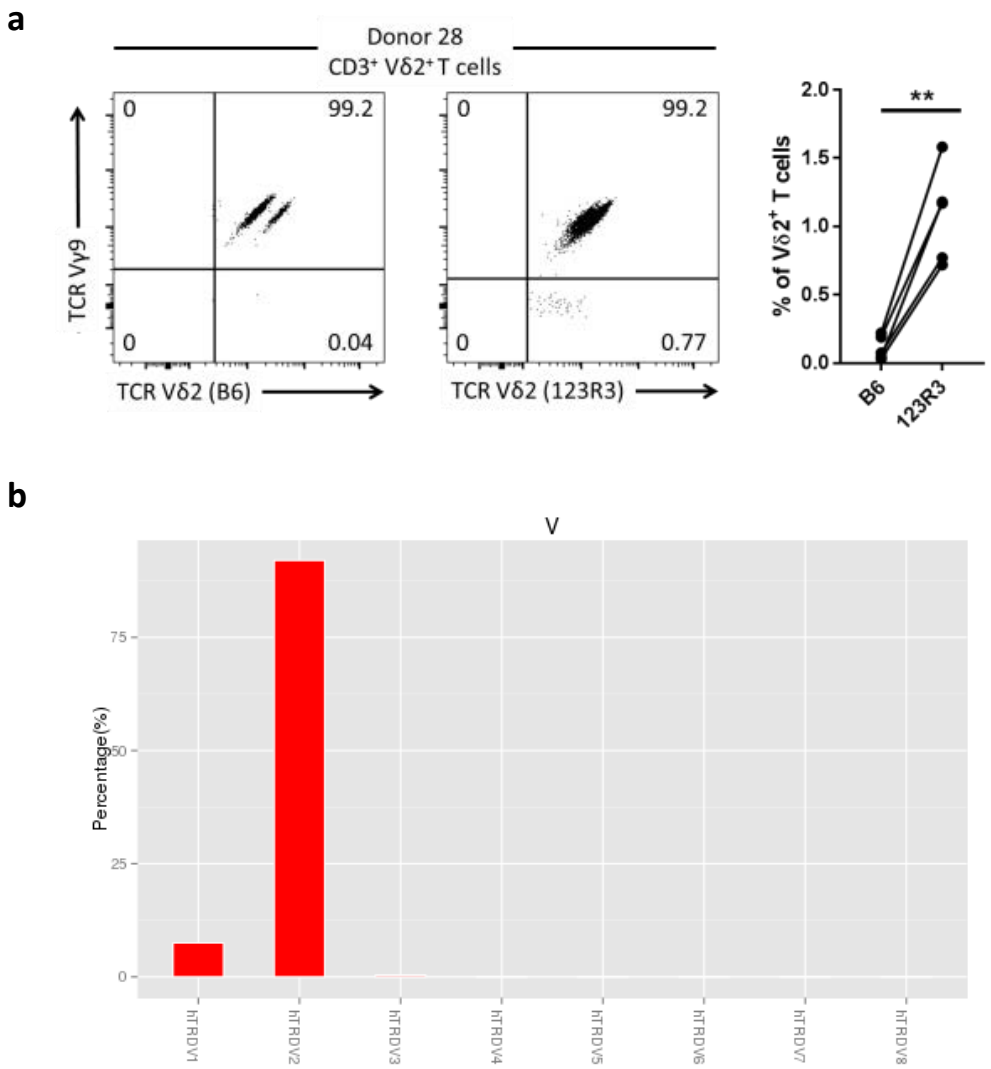

Figure 6.1: Vδ2^{+} TCR antibody clone 123R3 is necessary for correct Vδ2^{neg} γδ cell sorting

a) Representative flow cytometry plots of Vδ2^{+} staining for B6 and 123R3 clones in healthy donor peripheral blood sample. Right: comparison of Vδ2^{+} proportion in CD3^{+} T cells with antibody clones B6 and 123R3, n=4, **p<0.01, Student's T test. Taken from Davey *et al*, 2017.

b) Example of Vδ2^{+} contamination in Vδ2^{neg} sorted cell population determined by deep sequencing following sorting using B6 antibody clone, visualised using iRepertoire iRtools.

6.2.1.2 Analysis of Vδ2$^+$ CDR3 sequences

While no liver-derived Vδ2$^+$ samples were sorted for TCR repertoire deep sequencing, next generation TCR sequencing was performed on healthy donor PBMC-derived Vδ2$^+$ cells as part of a study conducted by this group (n=7), using a Vδ2$^+$ sorting strategy with the 123R3 Vδ2 antibody. Consistent with previous findings (McVay *et al*., 1991) and their categorisation as semi-invariant innate-like T cells, Vδ2$^+$ TCRγ repertoires were predominantly composed of Vγ9 chains and the joining region JγP (Figure 6.2). However, the presence of non-Vγ9 (i.e. Vγ2-8) sequences in the TCRγ repertoires was detected (mean 4.46% $\pm$ 0.78%) even in these PBMC derived samples.

Like the intrahepatic Vδ2^{neg} population, there was evidence of repertoire focussing and clonotypic expansion in the PBMC Vδ2$^+$ subset, illustrated by tree plots in Figure 6.3. When compared with liver-derived Vδ1$^+$ and Vδ3$^+$ cells (Figure 4.18), the 10 most prevalent PBMC-derived Vδ2$^+$ cells displayed shallower cumulative frequency curves, suggesting an intermediate level of repertoire focussing present in these populations (Figure 6.4a) in comparison with Vδ1$^+$ T cells from "focussed" donors or cord blood. Analysis of the D75 metrics (the percentage of clonotypes required to occupy 75% of TCR repertoire) from PBMC-derived Vδ2$^+$ cells suggested they were generally not composed of as many expanded clonotypes as the intrahepatic Vδ2^{neg} populations, particular in the δ-chain repertoire, with a mean δ-chain D75 of 9.8% compared with 2.6% for the intrahepatic Vδ2^{neg} δ-chain repertoire. In comparison, the γ-chain D75 was lower at 5.8% compared with 3.4% for intrahepatic Vδ2^{neg}, suggestive of greater focussing of this chain in the Vδ2$^+$ TCR (Figure 6.4b). Analysis of the CDR3 length for PBMC-derived

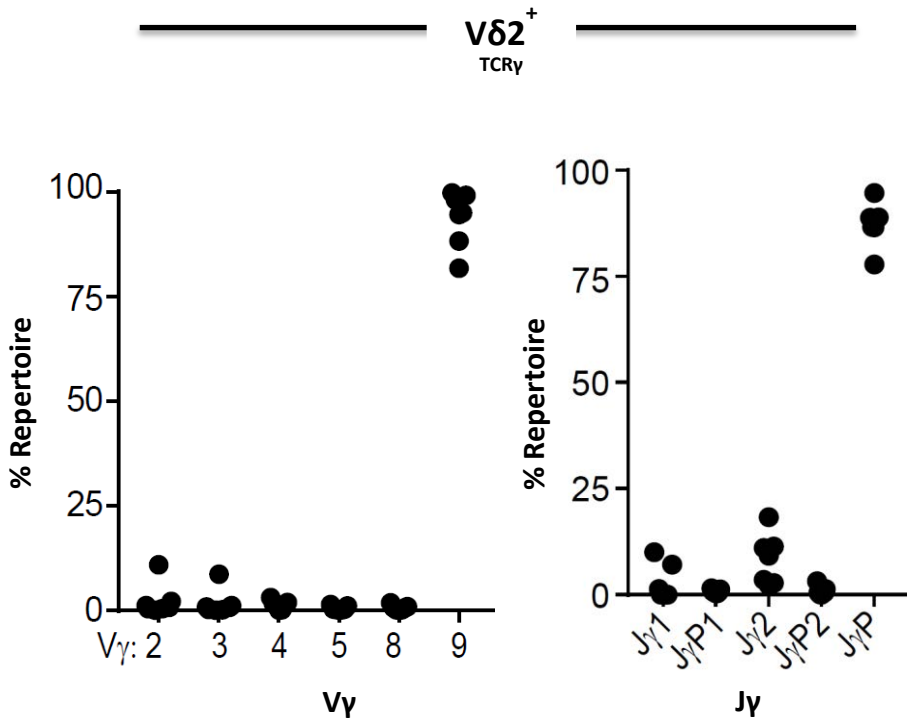

Figure 6.2: Healthy PBMC donor Vδ2$^+$ chain usage is dominated by Vγ9 pairing

V-region and J-region chain usage for Vδ2$^+$ gamma delta T cells from healthy PBMC donor cohort and determined using deep sequencing.

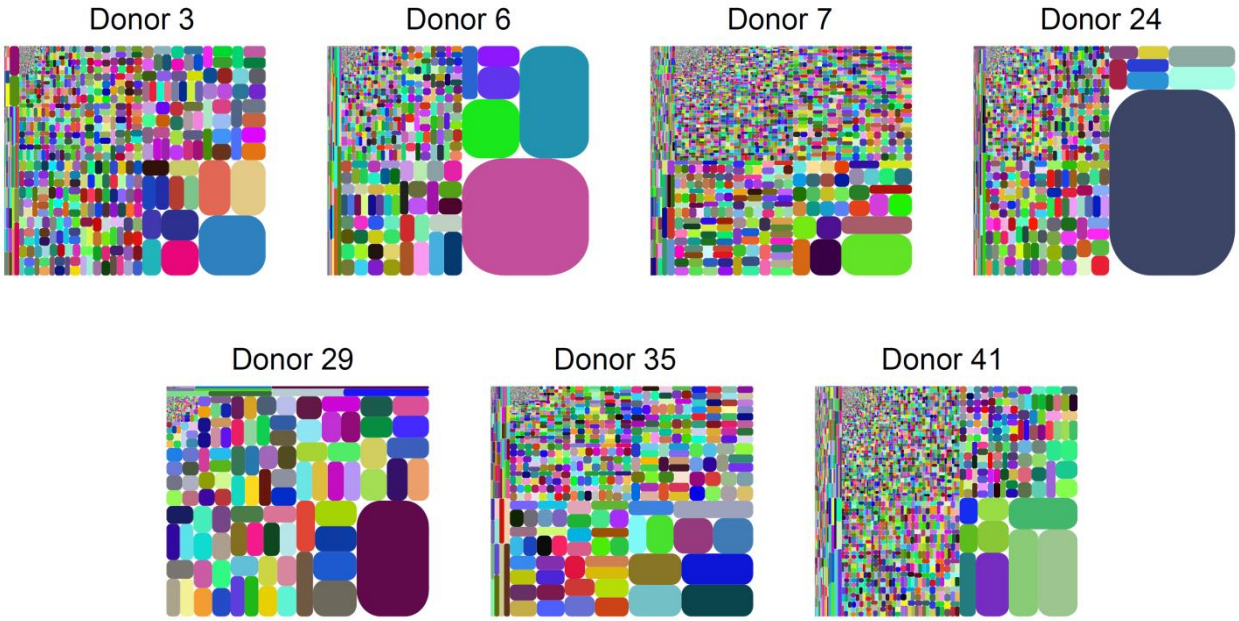

Figure 6.3: PBMC-derived Vδ2^{+} cells display evidence of clonal expansion

Tree maps derived from FACS sorted peripheral blood Vδ2^{+} cells show CDR3 clonotype usage in relation to repertoire size (each CDR3 colour is chosen randomly and does not match between plots). This data is representative of the raw iRepertoire data and has not undergone MiXCR error correction.

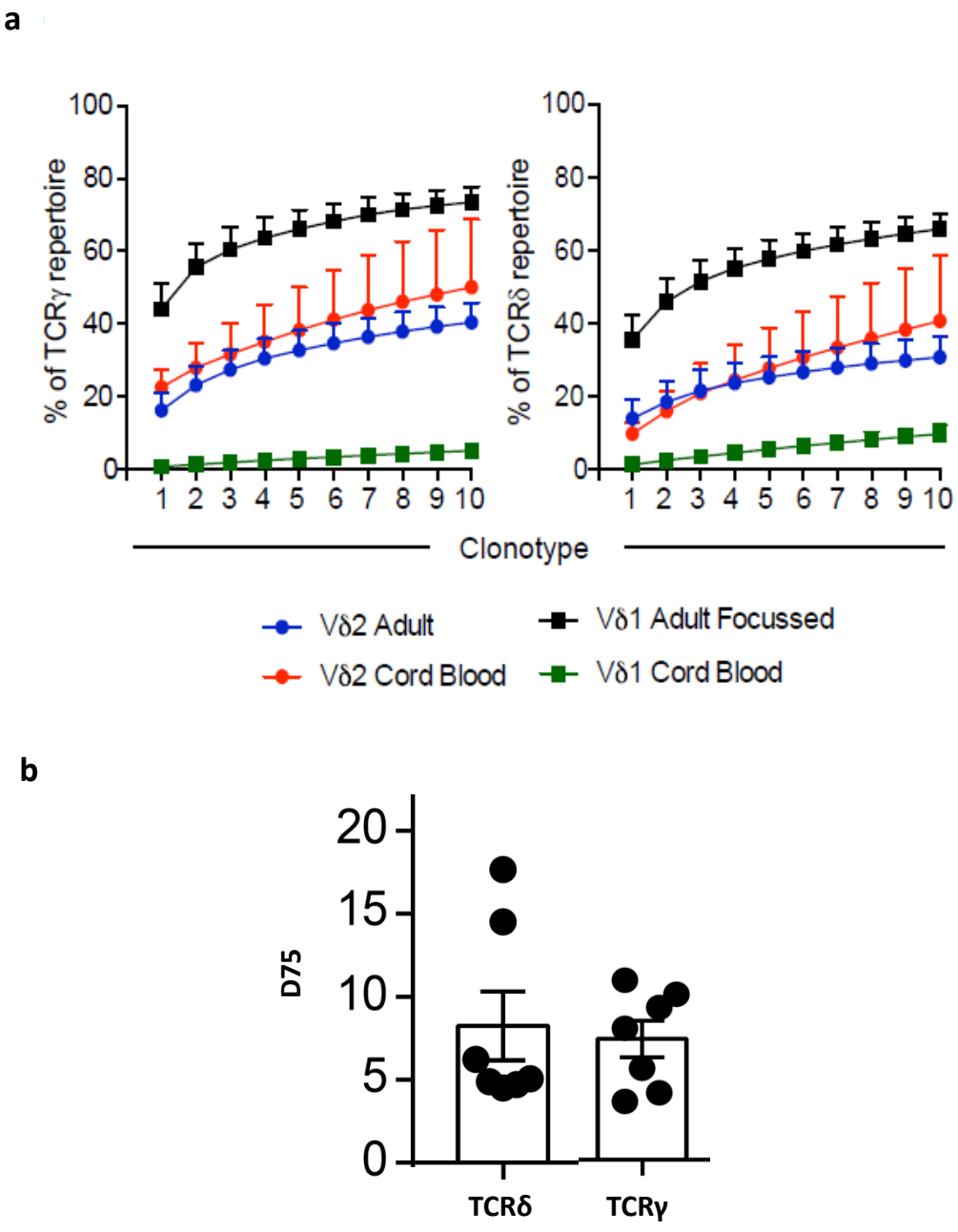

Figure 6.4: PBMC-derived Vδ2$^+$ display intermediate clonal focussing

a) Comparison of frequency of top 10 most prevalent clonotypes across all blood samples for Vδ2$^+$ (blue) as well as Vδ1$^+$ cells identified in "focussed" healthy adult blood donors (black) and cord blood (green) (from Davey *et al*, 2017).

b) D75 diversity estimation for TCRδ and TCRγ sequences from Vδ2$^+$ gamma delta T cell subset for healthy adult blood (n=7)

Vδ2$^+$ cells confirmed previous observations of limited γ-chain diversity (Rock *et al*, 1994), with a strong bias towards 14 amino acids (53.4% ± 4.2%) with a broader range of CDR3 lengths in the δ-chain (Figure 6.5).

Reflective of this difference in observed diversity between TCRγ and TCRδ in Vδ2$^+$ T cells is the degree of sharing found in γ- and δ-chain CDR3 region sequences. Across all donors, an average of 79.1% ± 2.8% of CDR3γ9 sequences were shared by at least 2 donors, demonstrating the high degree of publicity among CDR3γ in Vδ2$^+$ gamma delta T cells. However, as has been reported previously (Cairo *et al*., 2010), the CDR3δ2 were considerably less public, with a mean of 8.7% ± 1.1% of sequences observed in more than one donor (Figure 6.6a). To investigate the nature of the shared clonotypes, the 10 most prevalent shared CDR3γ9 sequences were determined by frequency, filtered from each donor's CDR3γ9 protein lists (n=7). These sequences were then ordered by frequency for sequences that were shared between >2 donors to create a hierarchy of 10 common sequences. The proportion of the repertoire occupied by these sequences is depicted for each donor in Figure 6.6b.

Two CDR3γ sequences were observed in all 7 donors; CALWEVQELGKKIKVF (mean 13.1%) and CALWEVRELGKKIKVF (mean 4.3%). CALWEVQELGKKIKVF has been observed in previous studies in foetal liver and foetal blood (McVay *et al*., 1998, Dimova *et al*., 2015), as well as adults (Sherwood *et al*., 2011). Single cell TCR sequencing analysis of individual Vδ2$^+$ T cells revealed this sequence paired with multiple different CDRδ chains within the same donors, forming a "pseudoclonotype" where the same CDR3γ9 is generated and independently paired with differing CDR3δ2 chains (Table 6.1). Importantly, this sequence can be generated using basic recombination of Vγ9 and JγP gene segments

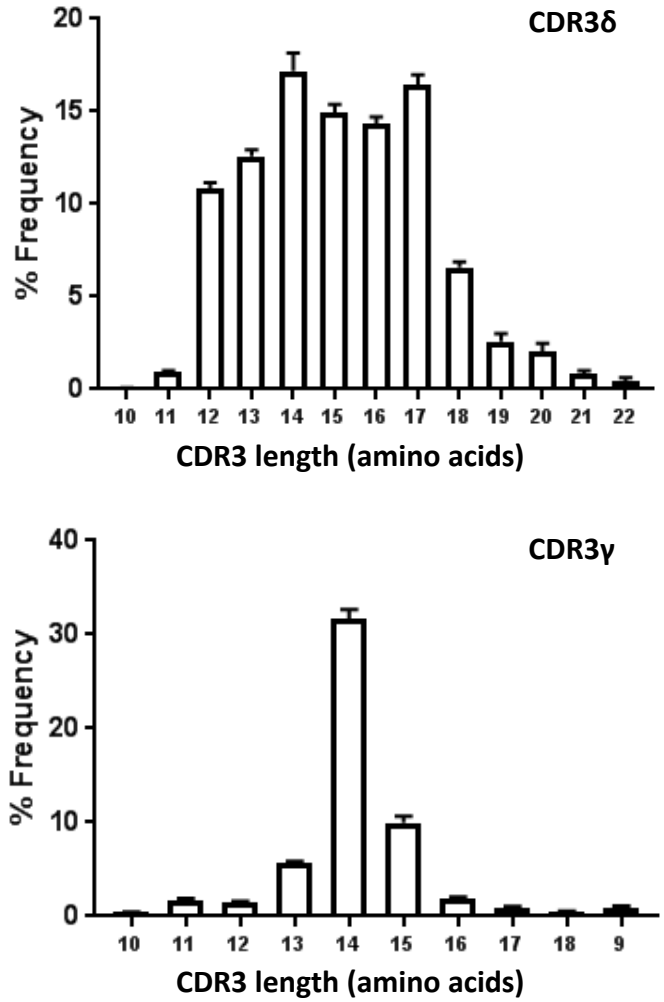

Figure 6.5: PBMC-derived Vδ2$^+$ CDR3 lengths display limited γ-chain diversity

Comparison of mean + s.e.m. CDR3δ (upper) and CDR3γ (lower) pseudo-spectratypes of Vδ2$^+$ T cells from healthy adult blood donors (n=7)

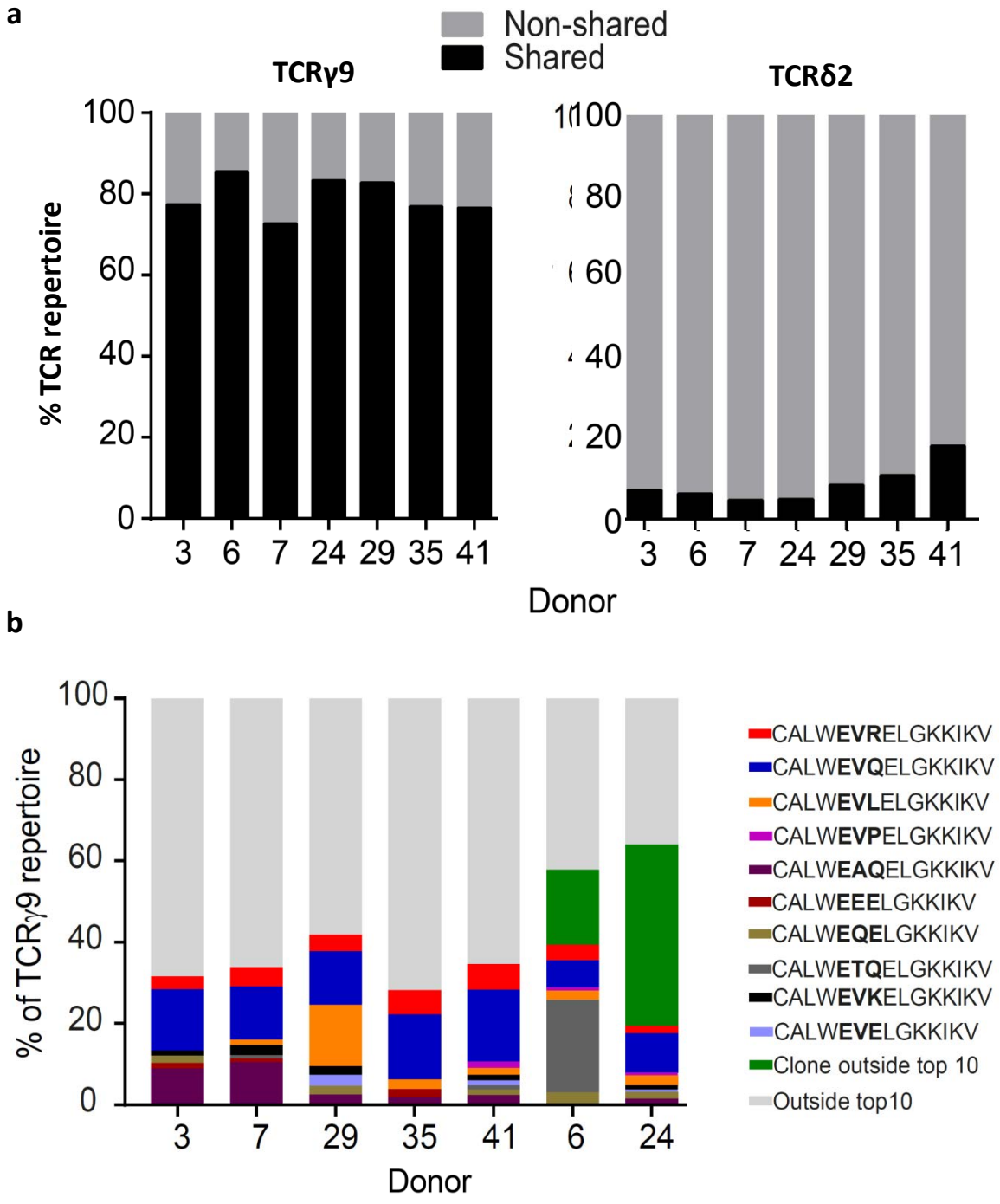

Figure 6.6: Vγ9$^+$ CDR3 sequences in Vδ2$^+$ cells are public

a) Comparison of extent of sequence sharing (i.e. sequences identified in more than one sample) amongst Vδ2Vγ9$^+$ gamma delta T cells from healthy PBMC donors (n=7)

b) Contribution of the 10 most prevalent public Vγ9 sequences to the total Vγ9 repertoire in healthy PBMC donors (n=7)

Donor	CDR3γ9	CDR3γ nucleotide (nt) sequence	N nt addition	CDR3δ2
3	CALWEV**Q**ELGKKIKVF	TGTGCCTTGTGGGAGGTGCAAGAGTTGGGCAAAAAAATCAAGGTATTT	germline	CACDS**L**LGDTPNFDKLIF
	CALWEV**Q**ELGKKIKVF	TGTGCCTTGTGGGAGGTGCAAGAGTTGGGCAAAAAAATCAAGGTATTT	germline	CACDT**G**GAQSWDTRQMFF
28	CALWEV**Q**ELGKKIKVF	TGTGCCTTGTGGGAGGTTCAAGAGTTGGGCAAAAAAATCAAGGTATTT	1	CACDS**L**GTYTDKLIF
	CALWEV**Q**ELGKKIKVF	TGTGCCTTGTGGGAGGTGCAAGAGTTGGGCAAAAAAATCAAGGTATTT	germline	CACDI**I**LGGQYTDKLIF
35	CALWEV**Q**ELGKKIKVF	TGTGCCTTGTGGGAGGTGCAGGAGTTGGGCAAAAAAATCAAGGTATTT	3	CACES**L**GPTGGNPSSDKLIF
	CALWEV**Q**ELGKKIKVF	TGTGCCTTGTGGGAGGTTCAAGAGTTGGGCAAAAAAATCAAGGTATTT	1	CACDT**I**THRTGGPQVTDKLIF
	CALWEV**Q**ELGKKIKVF	TGTGCCTTGTGGGAGGTGCAAGAGTTGGGCAAAAAAATCAAGGTATTT	germline	CACDG**L**GGEYTDKLIF
42	CALWEV**Q**ELGKKIKVF	TGTGCCTTGTGGGAGGTGCAAGAGTTGGGCAAAAAAATCAAGGTATTT	germline	CACDK**V**GYGSPWDTRQMFF
	CALWEV**Q**ELGKKIKVF	TGTGCCTTGTGGGAGGTGCAAGAGTTGGGCAAAAAAATCAAGGTATTT	germline	CACDT**I**PTGGHDPYTDKLIF
3	CALWEV**Q**ELGKKIKVF	TGTGCCTTGTGGGAGGTGCAAGAGTTGGGCAAAAAAATCAAGGTATTT	germline	CACDS**L**LGDTPNFDKLIF
	CALWEV**Q**ELGKKIKVF	TGTGCCTTGTGGGAGGTGCAAGAGTTGGGCAAAAAAATCAAGGTATTT	germline	CACDT**G**GAQSWDTRQMFF

Table 6.1: Prominent shared CDR3γ9 sequences are germline and pair with multiple CDR3δ2 sequences

Single cell PCR analysis of multiple healthy PBMC donors identified common CDR3γ9 sequences shared across one or more donors. Sequence CALWEVQELGKKIKVF was identified in all donors, and paired with multiple different CDR3δ2 sequences. N-nucleotide additions are highlighted in red.

with no N nucleotide addition, thereby indicative of a "germline" sequence. The relative simplicity of this rearrangement combined with likelihood of convergent recombination (Venturi *et al*., 2008), whereby identical CDR3 regions are created through alternate N nucleotide addition and exonuclease activity of initially different sequences, may explain the apparent lack of diversity in the γ-chain repertoire relative to delta as well as the high degree of sharing observed in this analysis. This is very much in contrast with the considerably more diverse repertoire of the intrahepatic and diseased blood $V\delta2^{neg}$ gamma delta T cell repertoire determined in Chapter 4, which exhibited significantly less sharing of γ-chain sequences by comparison (Figure 4.24).

6.2.2 Phenotype of PBMC-derived and intrahepatic $V\delta2^{+}$ T cells

Having established that the healthy $V\delta2^{+}$ T cell repertoire largely consists of shared, expanded clonotypes expressing easily recombined CDR3γ9 sequences, phenotypic analysis of differentiation markers CD27, CD45RA, CCR7 and CD62L was conducted using donor matched PBMC-derived and intrahepatic $V\delta2^{+}$ T cells, in a similar manner to the analysis performed on intrahepatic $V\delta1^{+}$ T cells in Chapter 5. PBMC-derived $V\delta2^{+}$ CD27 expression was 58.1% ± 7.1% (Figure 6.7a), significantly higher than CD27 expression in liver-derived $V\delta2^{+}$ cells (30.1% ± 6.0%, p=0.002, n=10), reflective of a similar loss of $CD27^{+}$ cells observed for the $V\delta2^{neg}$ gamma delta T cells in transition from periphery to liver. In sharp contrast with both PBMC-derived and intrahepatic $V\delta1^{+}$ T cells, only 4.6% ± 0.5% PBMC-derived $V\delta2^{+}$ cells were $CD27^{neg}CD45RA^{+}$, or T_{EMRA}-like.

Analysis of the lymphoid homing markers CCR7 and CD62L showed that expression of these were higher in blood derived $V\delta2^{+}$ cells compared with matched liver derived $V\delta2^{+}$ cells (CCR7: 72.8% ± 6.1% vs. 14.5% ± 3.7%, p=0.25; CD62L: 73.2% ± 7.4% vs. 26.9%

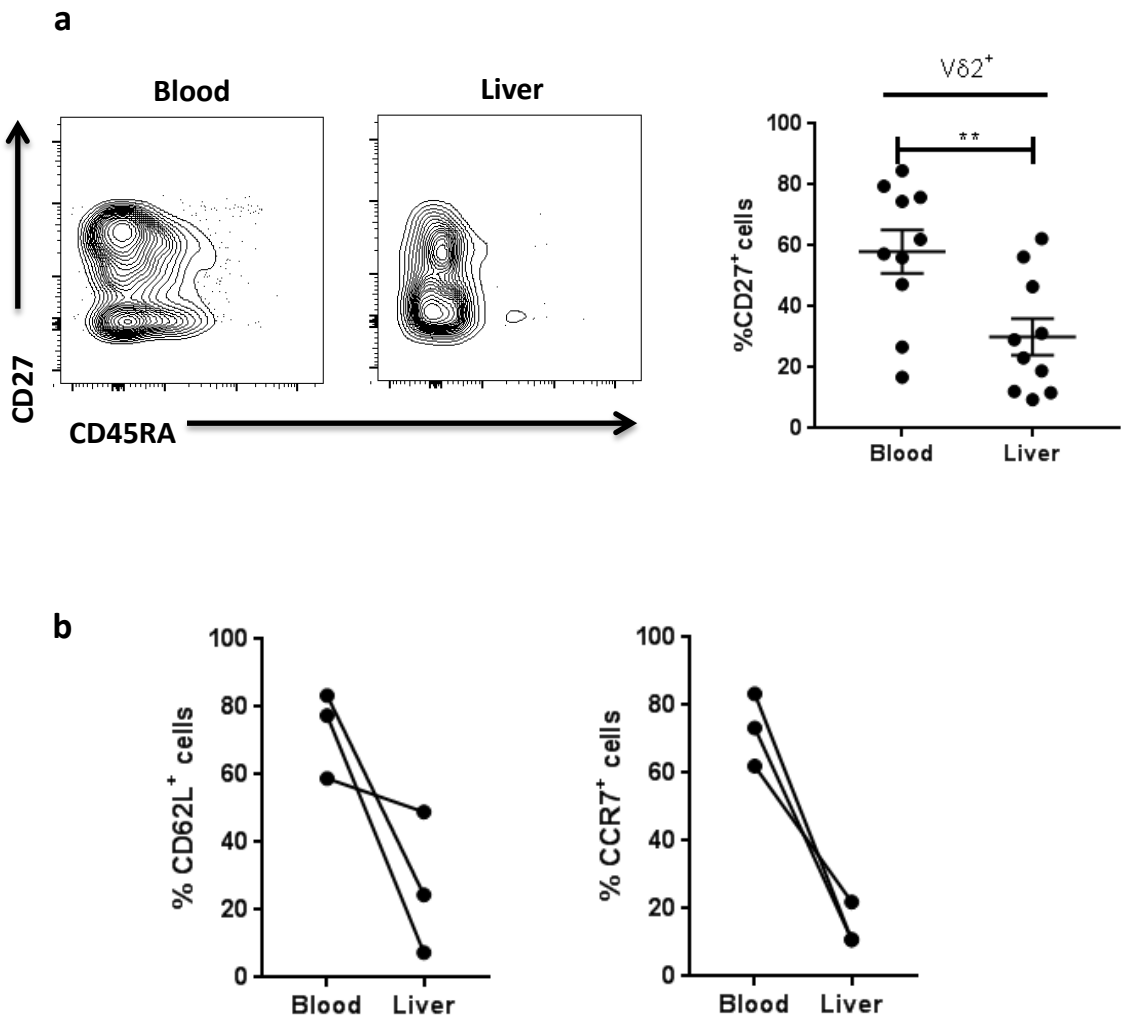

Figure 6.7: Intrahepatic Vδ2$^+$ T cells are less phenotypically naïve than those in the periphery

a) Representative dot plot showing distribution of CD27 and CD45RA expression in Vδ2$^+$ cells from donor matched blood and liver (left) and overall CD27 expression (n=8, **p<0.01)

b) CD62L and CCR7 expression in blood and donor matched liver samples (n=3) for Vδ2$^+$ gamma delta T cells

± 12.5%, p=0.25) (n=3) (Figure 6.7b). Combined with the lower CD27 expression, this is highly suggestive of the loss of a central memory lymphoid homing phenotype in liver associated $V\delta2^+$ populations. This observation is pertinent in light of findings from this group that loss of CD27 and CCR7 and adoption of a T_{EMRA}-like phenotype is observed in certain donor's blood-derived $V\delta2^+$ T cells, concomitant with clonal expansion (Davey *et al*¸ unpublished).

6.2.3 Detection of a novel $V\delta2^+V\gamma9^{neg}$ subset

As indicated by the NGS $V\delta2^+$ samples, flow cytometry based analysis of the repertoire of both healthy blood and matched blood from liver donors also confirmed the presence of a small subset of $V\delta2^+V\gamma9^{neg}$ cells in peripheral blood. Although small, this frequency was similar in magnitude to α-GalCer reactive NKT cells in the same healthy blood donor cohort (Figure 6.8a). This subset represented 4.2% ± 3.1% of the $V\delta2^+$ and 0.19% ± 0.07% of the total $CD3^+$ T cell compartment in healthy donors (n=18) and 17.6% ± 10.2% of $V\delta2^+$ cells in matched blood donors (n=9) (Figure 6.8b). The proportion in blood from liver transplant donors was significantly higher than in the healthy blood donor cohort (p=0.02). It is important to note that this population was only observed when the 123R3 clone was used in the staining panel, and not the B6 clone, which suggests the B6 clone may be specific for a $V\delta2^+V\gamma9^+$ TCR epitope not present in the $V\delta2^+V\gamma9^{neg}$ TCR.

The deep sequencing data of liver gamma delta T cells had suggested that a $V\delta2^+V\gamma9^{neg}$ population may exist in the liver, and accordingly flow cytometry based analysis using the 123R3 Vδ2 TCR antibody and a Vγ9 specific antibody was used to attempt to quantify such a population in a number of explanted human livers (n=16). Firstly, the frequency of $V\delta2^+$ cells was found to be significantly lower in liver than the healthy donor blood cohort

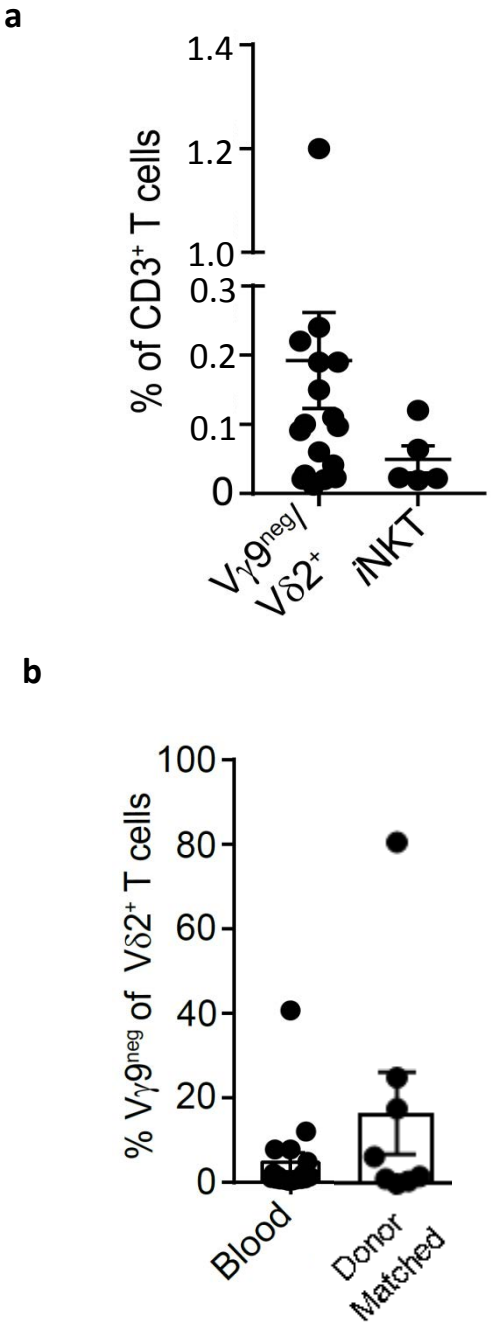

Figure 6.8: Vδ2^{+}Vγ9^{neg} cells are a small but significant subset of human peripheral blood CD3^{+} T cells

a) Frequency of Vδ2^{+}Vγ9^{neg} and iNKT cells in healthy donor blood as a proportion of total CD3^{+} T cells, determined by flow cytometry (n=18 Vδ2^{+}, 5 iNKT)

b) Frequency of Vδ2^{+}Vγ9^{neg} in healthy and liver disease patients as a proportion of all Vδ2^{+} gamma delta T cells (n=18 – 9)

used for the Vδ2 repertoire analysis, comprising 2.3% ± 0.9% of liver infiltrating $CD3^+$ T cells compared with 6.8% ± 2.0% in the periphery (data not shown). However, in the matched blood and liver cohort there was no significant difference between the $V\delta2^+$ proportion of total $CD3^+$ cells observed between liver and blood derived cells (Figure 5.2), suggesting that the difference between healthy blood and liver may be due to differences in the nature of the donors and highlighting the importance of obtaining matched samples whenever investigating differences between tissue and the periphery.

Further to this, a significantly higher proportion of $V\delta2^+V\gamma9^{neg}$ T cells was observed as a proportion of $V\delta2^+$ T cells in the intrahepatic samples compared with the healthy peripheral blood donors (25.9% ± 11.7% liver vs. 4.2% ± 3.1% healthy blood, p=0.0002) and indeed a higher, although not statistically significant, proportion than matched donor blood (17.7% ± 10.2% p=0.25) (Figure 6.9). This enrichment is likely indicative of a tissue-associated nature for this previously uncharacterised population. Consistent with this hypothesis, expression of CD27 and CD45RA in PBMC-derived $V\delta2^+V\gamma9^{neg}$ T cells suggested a generally naïve/ central memory phenotype, with 81.2% ± 3.4% being $CD27^{hi}$. This contrasted with intrahepatic $V\delta2^+V\gamma9^{neg}$ T cells which were predominantly $CD27^{lo}$ (85.7% ± 3.6% vs. 18.8% in blood, p=0.0003) (Figure 6.10a). The overwhelming majority of these cells in the liver were also $CD45RA^+$ (98.5% ± 6.1%), suggestive of a T_{EMRA}-like differentiation status. Interestingly, the expression of CD27 in PBMC derived $V\delta2^+V\gamma9^{neg}$ cells was significantly higher than that of $V\delta2^+V\gamma9^+$ when measured by mean fluorescence intensity, and comparable to that exhibited by $CD27^{hi}$ $V\delta1^+$ T cells (n=3, p=0.008) (Figure 6.10b).

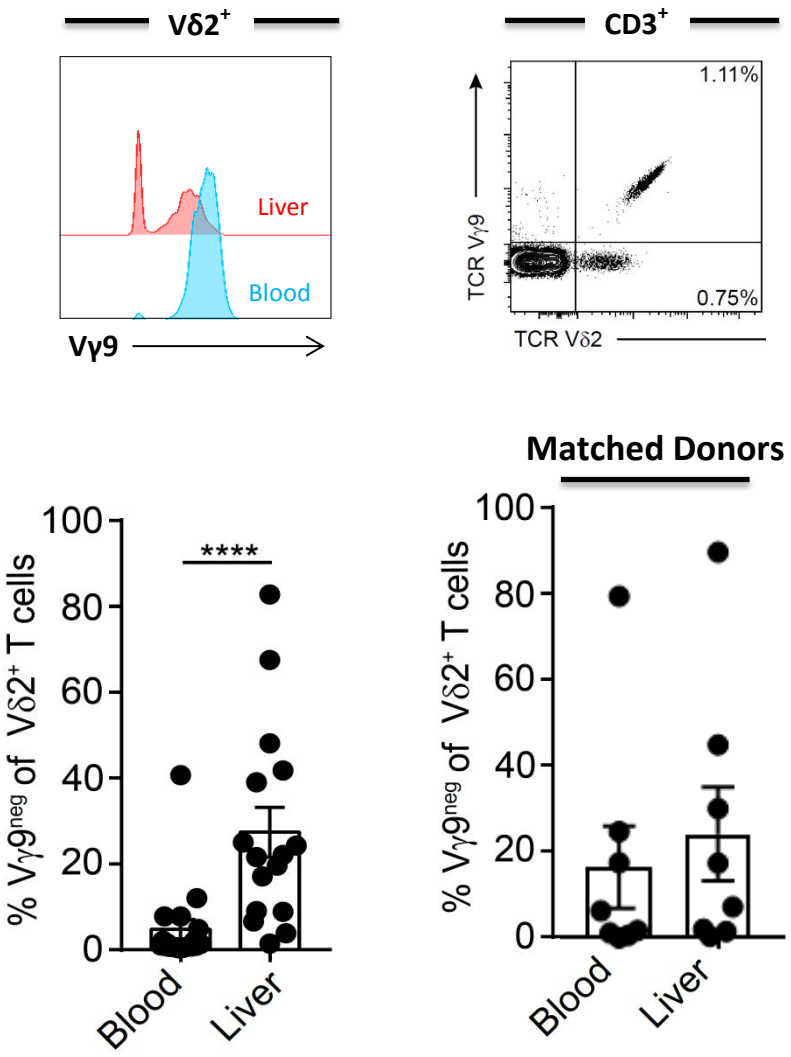

Figure 6.9: Vδ2^{+}Vγ9^{neg} cells are enriched in human liver

a) Representative histogram (left) and dot plots (right) of Vδ2 and Vγ9 expression among CD3^{+} cells isolated from donor matched liver and blood

b) Frequency Vδ2^{+}Vγ9^{neg} cells as a proportion of Vδ2^{+} cells in the same cohorts as a) (left) and a cohort of donor matched blood and liver samples (n=9) (right)

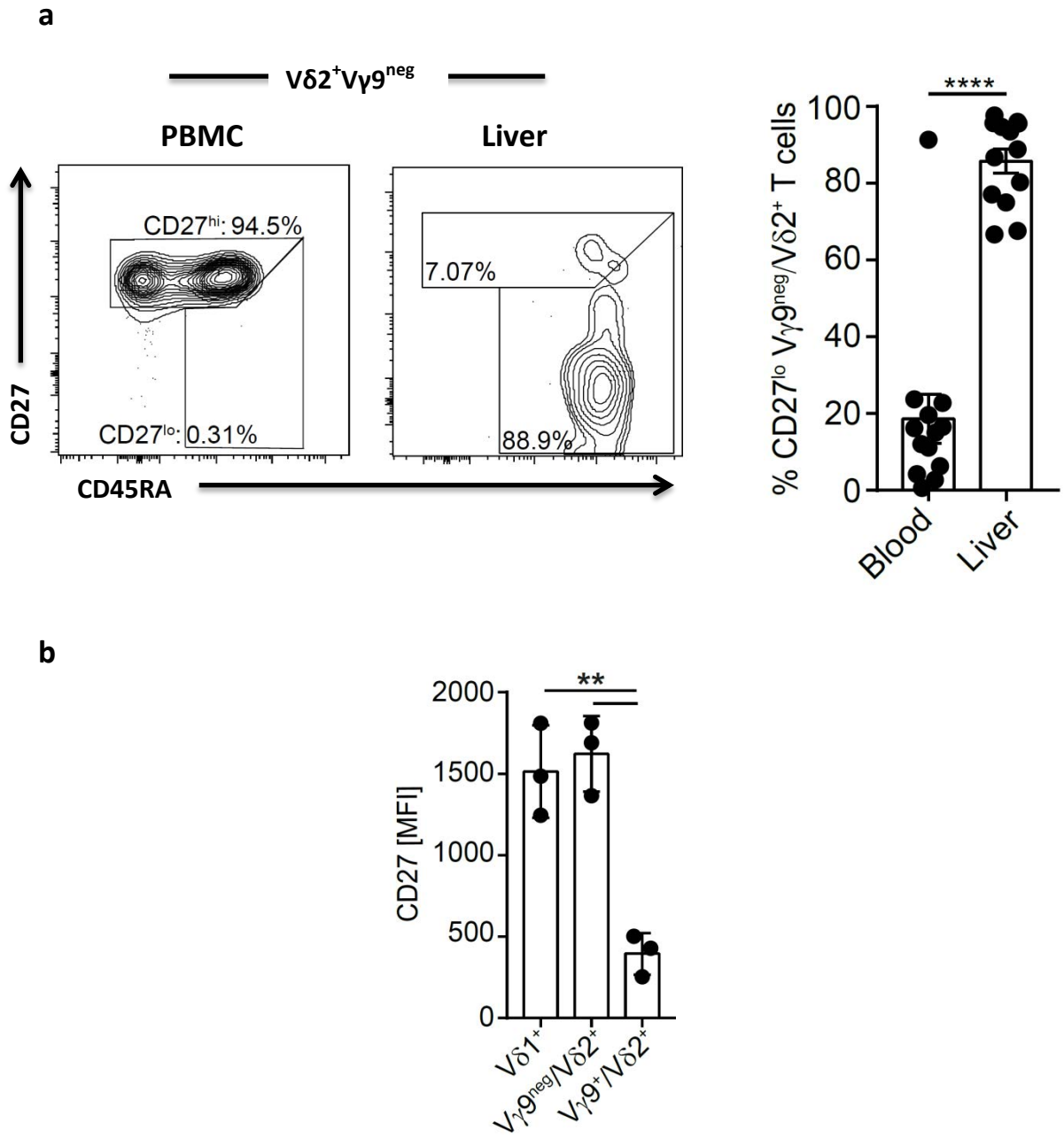

Figure 6.10: Intrahepatic Vδ2^{+}Vγ9^{neg} cells are T_{EMRA}-like

a) Representative dot plots of CD27 and CD45RA expression among Vδ2^{+}Vγ9^{neg} T cells derived from PBMC of healthy donors and liver explants (left). Comparison of CD27$^{lo/neg}$ populations as a proportion of total Vδ2^{+}Vγ9^{neg} T cells between healthy donor (n=18) and explanted liver cohorts (n=16) ****p<0.0001

b) MFI of CD27 expression among various gamma delta T cell subsets (n=3, **p<0.01)

6.2.4 Phenotype and clonotypic overlap of intrahepatic Vδ2^{+}Vγ9^{neg} cells

Next, expression of other surface markers associated with differentiation was also assessed by flow cytometry for PBMC-derived Vδ2^{+}Vγ9^{neg} and intrahepatic Vδ2^{+}Vγ9^{neg} T cells (n=3). Overall, PBMC-derived Vδ2^{+}Vγ9^{neg} T cells expressed higher levels of CCR7 compared with Vδ2^{+}Vγ9^{+} cells (58.8% vs 8.3%, p=0.0006), similar levels of IL-7R (85.2% vs. 82.1%, p=0.99) but significantly lower levels of CX_3CR1 (2.0% vs 43.2%, p=0.0001) (Figure 6.11a). In addition to the marked downregulation of CD27 reported earlier, liver derived Vδ2^{+}Vγ9^{neg} T cells expressed the characteristic clonal-γδ effector marker CX_3CR1 and had downregulated IL-7R (n=1) (Figure 6.11b). These data suggest this subset is phenotypically similar to the Vδ1^{+} T_{EMRA}-like subset identified in both liver and blood in Chapter 5. Finally, expression of CD69, highlighted in the previous chapter as being associated with tissue-specific Vδ1^{+} clonotypes, was significantly upregulated in intrahepatic Vδ2^{+}Vγ9^{neg} T cells compared to matched blood populations (82.5% ± 5.7% vs. 15.4% ± 10.7%, p=0.03, n=6) (Figure 6.11c). These data contrast intrahepatic Vδ2^{+}Vγ9^{neg} T cells with both Vδ2^{+}Vγ9^{+} and Vδ2^{+}Vγ9^{neg} populations derived from peripheral blood, and identifies them as phenotypically analogous to the clonal Vδ1^{+} populations isolated from liver samples in the previous chapter and indeed with Vδ1^{+} cells from the same donor.

To investigate the relationship between these observed phenotypes and TCR clonality, indexed single cell sorting was again used in conjunction with sc-PCR to sequence full TCR CDR3 regions (Chapter 5). To begin, Vδ2^{+}Vγ9^{neg} were sorted from blood of three healthy donors, and in keeping with their CD27^{hi} CCR7^{+} phenotype all the cells sorted across all donors possessed unique CDR3s with no clonotypes shared between any of the analysed

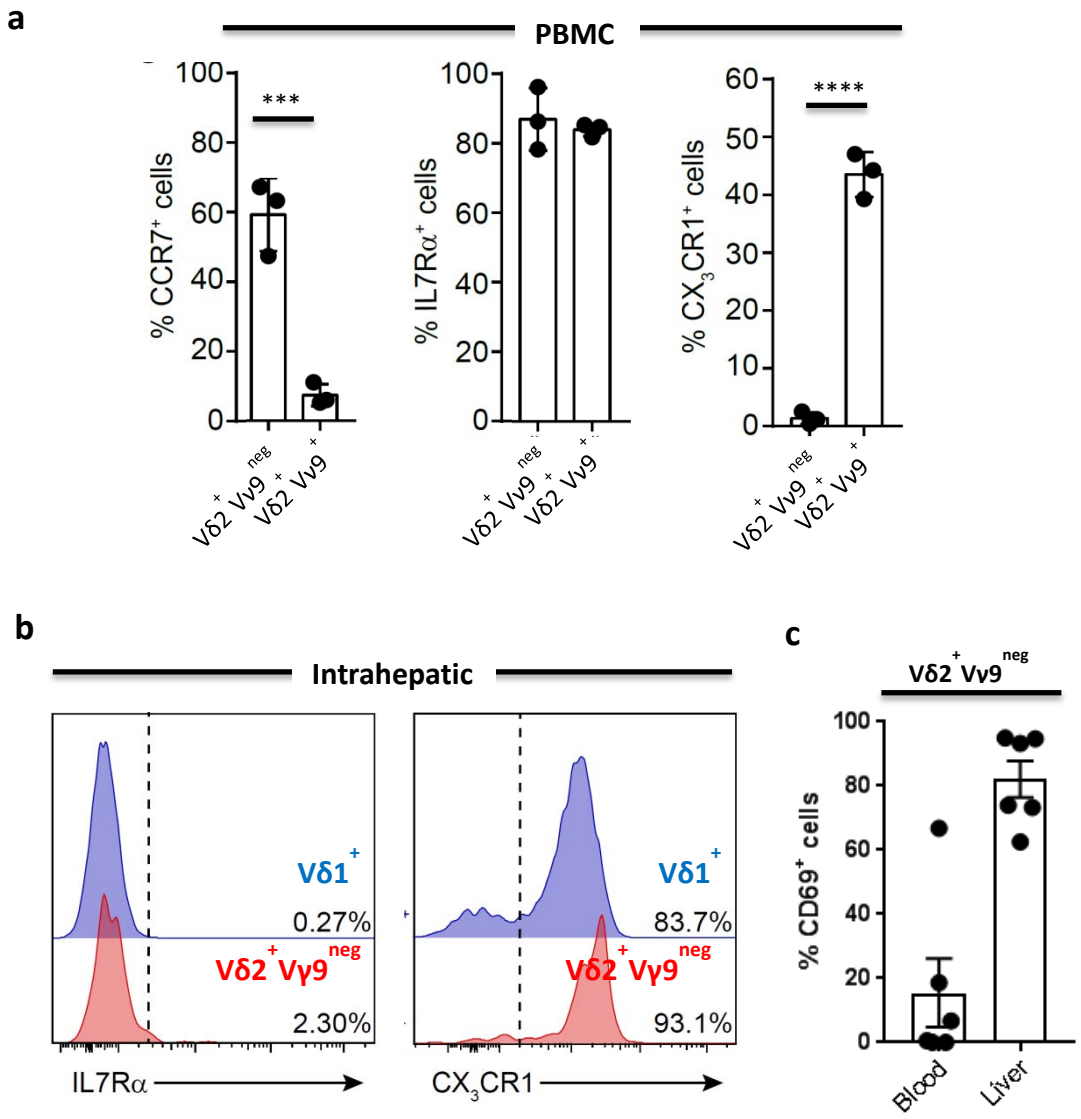

Figure 6.11: Vδ2^{+}Vγ9^{neg} T cells adopt a T_{EMRA}-like phenotype in liver

a) Comparison of expression of surface markers associated with cell differentiation between PBMC-derived Vδ2^{+}Vγ9^{neg} and Vδ2^{+}Vγ9^{+} cells (n=3, ***p<0.001, ****p<0.0001, Mann-Whitney U test)

b) Comparison of expression of surface markers associated with cell differentiation between liver-derived Vδ1^{+} and Vδ2^{+}Vγ9^{neg} T cells (n=1)

c) Comparison of CD69 expression between blood and liver derived Vδ2^{+}Vγ9^{neg} T cells from matched donors (n=6, **p<0.01, Mann-Whitney U test)

cells (Figure 6.12a). This is suggestive of a predominantly naïve population of cells. In contrast, $V\delta2^{+}V\gamma9^{neg}$ isolated from livers appeared to be strongly clonal in nature, with two large clones comprising 21/24 cells sequenced (Figure 6.12b). Again, this is consistent with the strong clonal focussing observed in intrahepatic T_{EMRA}-like $V\delta1^{+}$ T cells observed in the previous chapter, and is strongly suggestive of a similar adaptive biology in the formation of these apparently tissue-associated cells.

Since clonotypically identical $CD27^{lo}CD45RA^{+}$ $V\delta1^{+}$ subsets of gamma delta T cells had been demonstrated to be present in both the liver and blood of matched donors in this study, PBMC and liver-derived $V\delta2^{+}V\gamma9^{neg}$ cells were sorted from an additional donor and sequenced by sc-PCR. In the liver the analysed population of 12 cells consisted entirely of one $V\delta2^{+}V\gamma5^{+}$ clonotype, which was mirrored in the blood for the δ-chain sequence, with the caveat that only 8 of the 12 cells analysed also expressed the same Vγ5 sequence, while the remaining sequences appeared to be an out of frame VγJγP2 (Figure 6.12c). Although the reason for this is unclear, it is evident that the large degree of clonal overlap observed between the blood and liver $V\delta1^{+}$ $CD45RA^{+}$ cells is also possible for $V\delta2^{+}V\gamma9^{neg}$ populations.

6.2.5 Function of the intrahepatic $V\delta2^{+}V\gamma9^{neg}$ subset

It is well established that $V\delta2^{+}V\gamma9^{+}J\gamma P^{+}$ cells are P-Ag reactive, and can be activated by incubation with exogenous HMB-PP (Eberl *et al*., 2003). To determine whether this was also the case for the $V\delta2^{+}V\gamma9^{neg}$ populations identified in this study, PBMC- (n=5) and liver-derived (n=3) T cells were incubated *in vitro* with 10nM HMB-PP and, for blood derived cells, proliferation assessed using CFSE or, for liver derived cells, CD25 upregulation was assessed by flow cytometry. In the case of blood derived cells, a

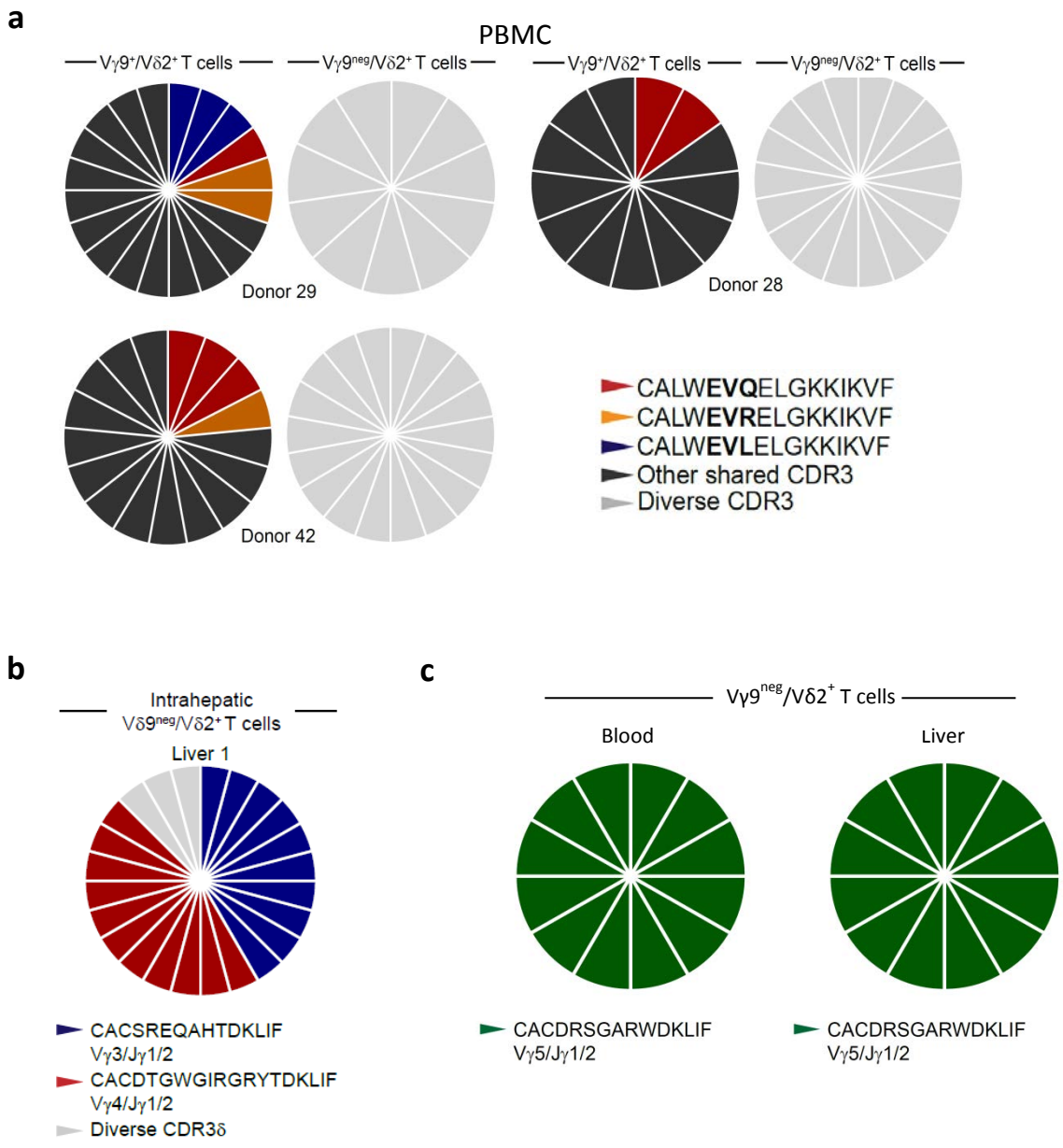

Figure 6.12: Vδ2^{+}Vγ9^{neg} are clonally diverse in blood and focussed in liver

a) Single cell PCR TCR sequencing analysis of Vδ2^{+} subsets derived from healthy PBMC donors. Each slice in the pie chart represents an individual cell and each colour corresponds to a unique CDR3 sequence

b) TCR sequencing of liver derived Vδ2^{+}Vγ9^{neg} cells

c) TCR sequencing of blood and donor matched Vδ2^{+}Vγ9^{neg} cells

strong proliferative response was observed in the Vδ2^{+}Vγ9^{+} cells as expected (82.3% ± 12.7% diluted CFSE), but the Vδ2^{+}Vγ9^{neg} were significantly less responsive (8.2% ± 0.3% diluted CFSE, p=0.0002), in line with CD8^{+} αβ T cells and Vδ1^{+} cells isolated from the same donors (Figure 6.13a). For liver-derived cells, although the response of Vδ2^{+}Vγ9^{+} cells was lower than that observed in blood, there was nevertheless again a significant decrease in response as measured by surface CD25 upregulation between Vδ2^{+}Vγ9^{+} (45.7% ± 4.2%) and Vδ2^{+}Vγ9^{neg} (10.4% ± 1.1%, p=0.025), as well as CD8^{+} αβ T cells and Vδ1^{+} cells (Figure 6.13b). These data suggest that Vδ2^{+}Vγ9^{neg} are minimally responsive to classically Vδ2^{+} activating antigen.

In the previous chapter it was established that both intrahepatic Vδ2^{+} and Vδ1^{+}CD45RA^{neg} gamma delta T cells were activated *in vitro* by exogenous IL-12 and IL-18. This led to the suggestion that these cells may act as part of the protective liver "firewall" that eliminates harmful gut-associated pathogen, responding to TLR-activated myeloid cell production of these cytokines. To investigate this further, heat inactivated *E.coli* bacteria were co-cultured with liver derived mononuclear cells for 48 hours, with and without neutralising antibodies specific for the IL-12 and IL-18 receptors (Figure 6.14). Activation of liver associated lymphocyte populations was then assessed, using flow cytometry to assess the presence of intracellular interferon-γ, a potent inducer of a T_H1 inflammatory response. Following co-culture, little IFN-γ production was observed for intrahepatic CD8^{+} αβ or Vδ1^{+} T cells, and there was no significant difference between the CD45RA^{+} and CD45RA^{neg} Vδ1^{+} T cells. Consistent with previous findings (Hintz *et al*., 2001) and the strong response to IL-12/IL-18 stimulation observed in this study, Vδ2^{+}Vγ9^{+} cells were induced to produce IFN-γ following co-culture with *E. coli*. Inclusion of αIL-12R

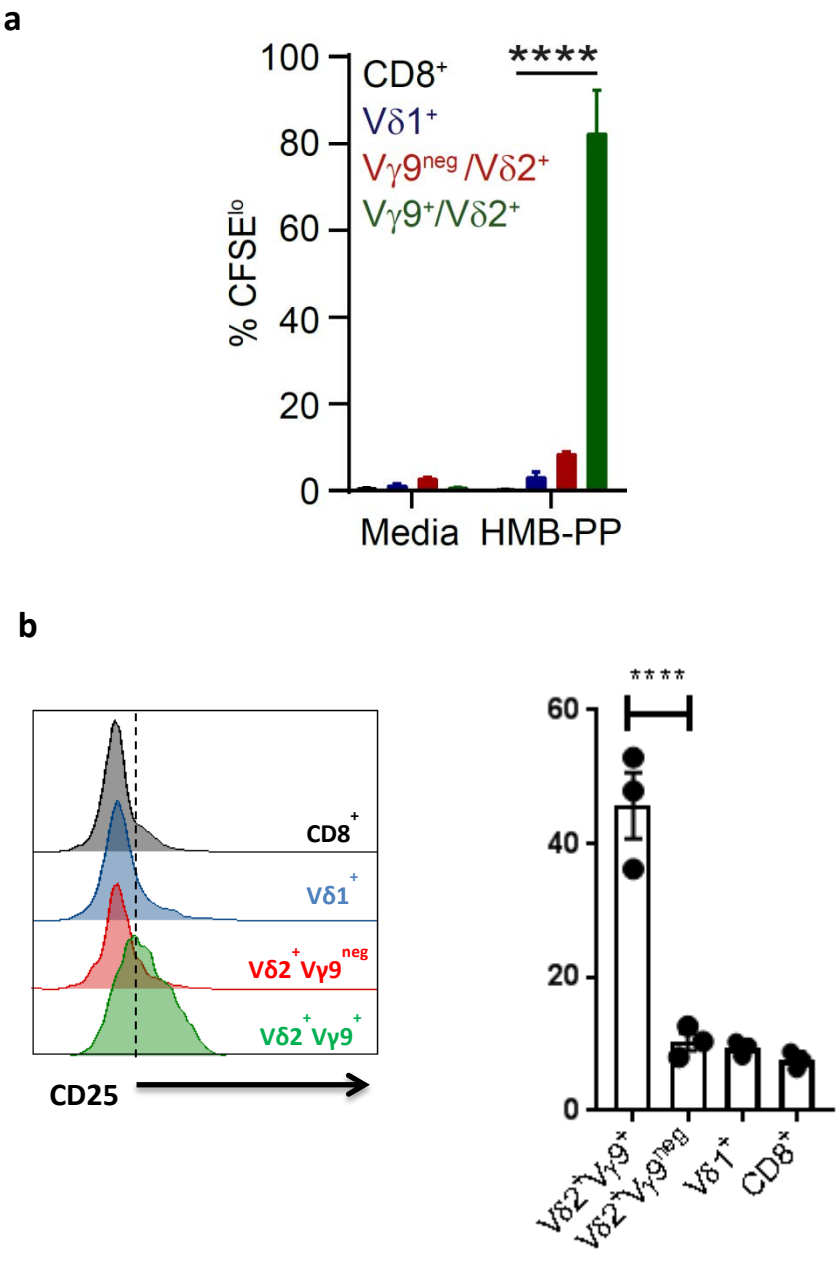

Figure 6.13: Vδ2^{+}Vγ9^{neg} T cells are not HMB-PP reactive

a) Comparison of loss of CFSE staining in PBMC-derived T cell subsets after 48 hours incubation with HMB-PP (n=4, ****p<0.0001, 2-way ANOVA, Tukey's comparison)

b) Representative histogram (left) and comparison of activation by HMB-PP (right) of various liver-derived T cell populations (n=3, ****p<0.0001, 1-way ANOVA, Dunn's comparison)

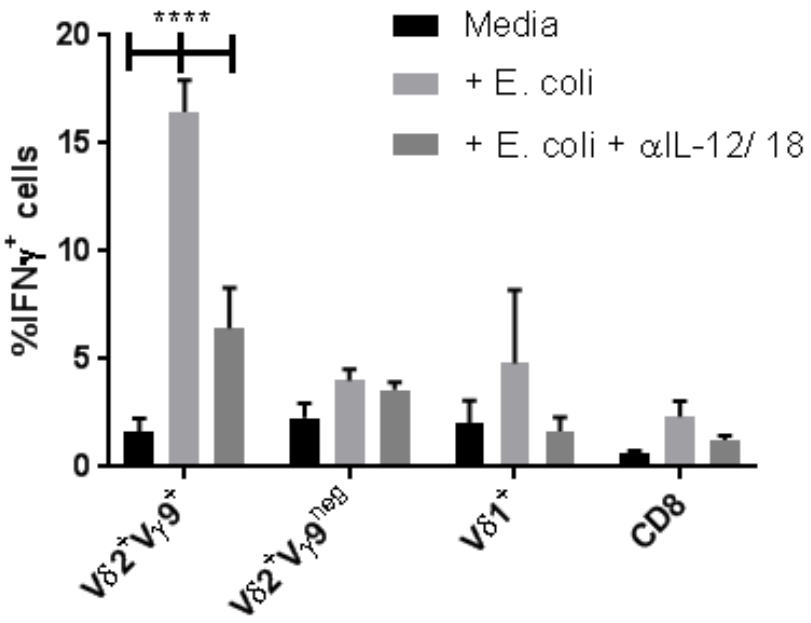

Figure 6.14: Intrahepatic Vδ2^{+}Vγ9^{neg} do not respond to co-culture with *E. coli*

Comparison of interferon-γ production by various liver-derived T cell subsets following 72 hour co-culture with heat killed *E. coli*, either with or without αIL-12 and αIL-18 blocking antibodies.

and αIL-18R blocking antibodies did significantly reduce the frequency of IFN-γ producing $V\delta2^{+}V\gamma9^{+}$ cells, suggesting of a role for these cytokines in the *E. coli* specific response of these cells. Without further experiments, it is unclear whether the liver-derived myeloid cells present in the culture were the source of the cytokines. Interestingly, the intrahepatic $V\delta2^{+}V\gamma9^{neg}$ population did not produce IFN-γ, again suggestive of similar biology to the $V\delta1^{+}$ and $CD8^{+}$ αβ T cells.

In conclusion, the data presented in this section highlights the presence of a previously unreported subset of $V\delta2^{+}V\gamma9^{neg}$ gamma delta T cells in human blood and liver. Additionally these data suggest that unlike the $V\delta2^{+}V\gamma9^{+}$ TCR gamma delta T cell population, which is composed of highly public pseudoclonotypes in the periphery, liver enriched $V\delta2^{+}V\gamma9^{neg}$ cells share a similar biology with blood and liver $V\delta1^{+}$ $CD45RA^{+}$ cells, with highly expanded clonotypes and potential for endothelial homing and cytotoxicity.

6.3 Discussion

In this chapter, the unexpected detection of $V\delta2^{+}$ gamma delta T cells in FACS sorted populations that were expected to be Vδ2 negative led to the discovery of a novel subset of gamma delta T cells that are enriched in the liver and that display the hallmarks of undergoing an adaptive-like immune response, in common with intrahepatic $V\delta1^{+}$ gamma delta T cells described previously in this thesis. These cells were $V\delta2^{+}V\gamma9^{neg}$, although it cannot be ruled out that there may be $V\delta2^{+}V\gamma9^{+}$non-JγP gamma delta T cells that may also share this biology.

Extensive previous research into Vδ2^{+} T cells has described a population that is P-Ag reactive and displays limited TCR diversity, leading to these cells being described as semi-invariant unconventional T cells. The discovery of the essential role of immunoglobulin-like BTN3A1 in P-Ag-mediated activation of Vδ2^{+} T cells seems to confirm a similar biology as that exhibited by MAIT and NKT cells, even if the precise mechanism of this activation mechanism remains unclear. In this study, TCR sequencing analysis of PBMC-derived Vδ2^{+} T cells demonstrated that, although some evidence of clonal focussing was observed, comparison of specific CDR3 region sequences revealed a remarkably high degree of clonal overlap between donors, with several public germline or convergently recombined sequences identified. This was particular prevalent in CDR3γ sequences, where sc-PCR determined the presence of pseudoclonotypes, with multiple common CDR3γ chains pairing with different δ-chains. This is in marked contrast to the intrahepatic Vδ2^{neg} population sequenced in a similar manner in Chapter 4, where γ-chain publicity was orders of magnitude lower, and further strengthens the hypothesis that Vδ2^{neg} gamma delta T cells do not conform to the same innate-like biology exhibited by Vδ2^{+} cells. To this day, many studies investigating gamma delta T cells do not make the distinction between Vδ2 and Vδ2^{neg} cells, classifying all gamma delta T cells under the same umbrella (e.g. Ravens *et al*, 2017), which, under the evidence presented here, may be considered a flawed approach.

Interestingly, there is little distinction between adult- and cord blood-derived Vδ2^{+}Vγ9^{+} repertoires in terms of clonal focussing, CDR3 lengths and phenotypic differentiation status, which is consistent with a post-natal polyclonal expansion specifically tailored to be P-Ag reactive from birth (Davey *et al*, in press). The authors propose that this is at

least in part due to butyrophilin 3 family member A1 (BTN3A1)-mediated shaping of the Vδ2^{+} repertoire *in utero* through sensing of endogenous IPP. This innate-like biology contrasts not only with the Vδ2^{neg} subsets but also with MAIT cells, which emerge from the conventional αβ T cell repertoire only in response to microbial exposure, and suggests the immunological paradigm that applies to Vδ2^{+}Vγ9^{+} T cells is most likely unique.

Phenotypic comparison of Vδ2^{+} cells from liver and blood indicated a modest decrease in expression of CD27 and lymphoid homing associated molecules CD62L and CCR7 in the liver compared with the periphery. While statistically significant in the case of CD27, the loss of the CD27^{+} subset of Vδ2^{+} cells within the liver was not as stark as that observed for the intrahepatic Vδ2^{neg} gamma delta T cell population, presented in the previous chapter. This suggests that although these cells do undergo some phenotypic differentiation and will accumulate in the liver, likely due to similar mechanisms proposed here for Vδ2^{neg} cells, this process is not as defined in the Vδ2^{+} subset, with many intrahepatic Vδ2^{+} cells retaining a blood-like expression pattern of CD27^{+}, CD69^{neg}.

Deep sequencing and flow cytometry analysis of Vδ2^{+} T cells derived from the peripheral blood of healthy donors revealed a small proportion of circulating cells that were not Vγ9^{+} (Vδ2^{+}Vγ9^{neg}), expressing alternative γ-chains paired with Vδ2 and not using the JγP joining region common to P-Ag reactive Vδ2^{+}Vγ9^{+} cells. In the periphery, these cells were highly polyclonal and phenotypically naïve, expression CD27, CCR7 and CD62L. Critically, these cells were enriched as a proportion of all Vδ2^{+} gamma delta T cells in liver tissue compared with healthy blood donors. Further analysis of additional matched blood and liver donors is important to verify whether this is truly the case, as the proportion was

not significantly enriched when donor matched blood and liver was analysed, although the same trend was also observed in these samples. Nevertheless, occupying a mean of over 25% of the intrahepatic $V\delta2^+$ populations, $V\delta2^+V\gamma9^{neg}$ T cells do form a significant and previously unappreciated proportion of liver infiltrating gamma delta T cells in many donors.

Phenotyping of this novel population of cells further discriminated them from the $V\delta2^+V\gamma9^+$ subset and led to intriguingly suggestive possibilities regarding their origin when compared with $V\delta1^+$ cells. In contrast with the polyclonal expansions observed in peripheral $V\delta2^+V\gamma9^+$ T cells, intrahepatic $V\delta2^+V\gamma9^{neg}$ populations were strongly dominated by expanded $CD27^{lo}CD45RA^+$ T_{EMRA}-like clonotypes, and the similarity between these and intrahepatic $CD27^{lo}CD45RA^+$ $V\delta1^+$ T cells is striking. Both exhibit high cytotoxic potential, expression of the fractalkine receptor CX_3CR1, and both populations are composed of few clones that also appear to be shared between the liver and blood. The phenotypic similarity between intrahepatic $V\delta2^{neg}$ gamma delta T cells and virus-specific $CD8^+$ αβ T cells having been established in the previous chapter, it is now possible to extend that comparison to include intrahepatic $V\delta2^+V\gamma9^{neg}$ T cells. The adaptive-like induction of a $CD27^{lo}CD45RA^+$ phenotype under clonal expansion from a $CD27^{hi}$ polyclonal population in the periphery is also suggested here with $V\delta2^+V\gamma9^{neg}$ T cells. This is again indicative of potential transcriptional changes following antigenic stimulation that induce a “vasculature association” phenotype and confers these highly cytotoxic cells the capacity to patrol liver and other tissue vasculature and to mount rapid responses with essentially innate-like kinetics (Vieira Braga *et al*., 2015, McNamara *et al*., 2017). As with $CD45RA^+$ $V\delta2^{neg}$ cells, since identical clonotypes appear to be present in liver and blood, it

is unclear whether these cells are genuinely liver-associated or merely accumulate there due to the upregulation of homing receptors and integrins that accompanies maturation of T cells following TCR engagement, and the nature of the activating ligand remains unknown. What is clear, however, is the enhanced expression of the tissue-association marker CD69 in the intrahepatic $V\delta2^{+}V\gamma9^{neg}$ subset compared with both $V\delta2^{+}V\gamma9^{neg}$ cells from the periphery and $V\delta2^{+}V\gamma9^{+}$ cells from the same liver. Although not as strikingly upregulated as in the liver-derived $V\delta2^{neg}$ $CD45RA^{lo}$ population, this is highly suggestive of a local tissue-associated retention of these cells. . Recent work from Cockburn's group has highlighted potential mechanisms by which $CD8^{+}$ T cells patrol murine hepatic sinusoids (McNamara *et al*., 2017) – further work in this line could reveal a role for phenotypically similar gamma delta T cells.

In addition to being non-responsive to the classical Vδ2-activating ligands, intrahepatic $V\delta2^{+}V\gamma9^{neg}$ T cells did not produce IFN-γ following co-culture with *E. coli*, in contrast to $V\delta2^{+}V\gamma9^{+}$ cells, which did. While this experiment did further ally the $V\delta2^{+}V\gamma9^{neg}$ liver population with $V\delta2^{neg}$ and $CD8^{+}$ αβ T cells, it also demonstrated the potential importance of "conventional" $V\delta2^{+}V\gamma9^{+}$ T cells in the immune response to commensal or pathogenic microbial load in the liver. Further experiments are required to determine the precise cellular mechanism involved, but the activation of these cells was at least in part dependent on IL-12 and IL-18, both readily secreted by TLR-activated myeloid cells. Although direct activation of the $V\delta2^{+}V\gamma9^{+}$ cells, either by TCR or TLR, cannot be ruled out, the fact that the *E. coli* were heat killed prior to co-culture suggests that the TCR is unlikely to be involved as it is sensitive to bacterial metabolites, although the presence of these metabolites cannot be ruled out. Although the $V\delta2^{neg}$ gamma delta subsets are

enriched in liver compared with the periphery, the Vδ2^{+} population is clearly present, has a higher transmigrational capacity than other T cell subsets and likely has a greater potential antimicrobial response than other T cell subsets, suggestive of a greater role in liver immunosurveillance than previously considered, even if extensive phenotypic alterations do not seem to be associated with these cells in liver. It is not inconceivable that local activation may indeed induce phenotypic changes in the liver-associated Vδ2^{+} subset, but that these cells undergo apoptosis after responding and are not retained locally, consistent with the high frequency of central memory Vδ2^{+} cells observed in the periphery.

The data presented in this chapter have established both a tissue-tropism for CD27^{lo} Vδ2^{+} gamma delta T cells and the presence in the liver and periphery of a Vδ2^{+}Vγ9^{neg} T cell population. While the Vδ2^{+}Vg9+ cells are likely to be polyclonally expanded in response to P-Ag exposure, the Vδ2^{+}Vγ9^{neg} cells exhibit the hallmarks of adaptive oligoclonal expansion in response to unknown antigen, and appear to seed the liver with strongly clonally dominated populations that are shared between liver and blood, consistent with a role in vasculature-associated effector function. This is significant as being the first detailed description of such a population in man, and establishes a phenotypic and functional link between these cells and both Vδ2^{neg} and CD8^{+} αβ T cells in the liver.

7

General Discussion

7.1 Introduction

This study was conducted with the ultimate aim of furthering our understanding of an enigmatic subset of unconventional T cells, namely Vδ2^{neg} gamma delta T cells, in the context to which they have often been attributed but rarely investigated – human solid tissue. To this end, in collaboration with clinicians at the Queen Elizabeth II Hospital, Birmingham, explanted human liver tissue was analysed by various means, including immunohistochemistry, flow cytometry and TCR sequencing, with the aim of not only learning more about the general nature of Vδ2^{neg} T cells in solid tissue, but also whether these cells may have an impact on liver disease progression.

7.2 Vδ2^{neg} gamma delta T cells do not appear linked with chronic liver inflammation

Having access to a large depository of historical liver tissue sections and, uniquely, freshly explanted human liver tissue from liver diseases of many aetiologies, a primary aim of this study was to establish whether gamma delta T cells, and specifically Vδ2^{neg} T cells, may have a role in the development or progression of chronic inflammatory liver diseases. Previous studies of human liver tissue had suggested that gamma delta T cells were enriched in diseased liver compared with the periphery, and perturbations in gamma delta T cell frequencies had also been observed in the periphery of patients with various chronic liver diseases, including PBC and HCV. Typically categorised as pro-inflammatory, highly cytotoxic innate-like T cells, a reasonable hypothesis, and indeed one made in several previous studies, would be that activated tissue associated gamma

delta T cells could contribute to liver disease progression, either through activation of a pro-inflammatory immune response or through direct tissue damage.

Accordingly, throughout this study effort has been made to compare normal liver, obtained from discarded donor tissue, with diseased liver. In Chapter 3, immunohistochemical analysis of tissue sections from a variety of chronically diseased explanted livers identified that, at least in terms of proportion of infiltrating T cells, normal livers had a significantly greater level of gamma delta T cells than diseased livers. These findings were subsequently confirmed using flow cytometry analysis of fresh tissue populations, and seem to suggest that while the baseline of healthy, homeostatically regulated tissue contains a relatively high frequency of $V\delta2^{neg}$ gamma delta T cells, under inflammatory conditions the frequency of these cells is reduced, in turn suggesting that it is the conventional αβ T cell population that is most affected by chronic inflammation. Additionally, there was no clear difference in gamma delta T cell numbers in any specific liver disease, suggestive of systemic infiltration and/or expansion of αβ T cells in the liver under inflamed conditions, rather than any disease related gamma delta T cell-specific effect. Although it is conceivable that activation induced cell death may result in a loss of intrahepatic gamma delta T cells under inflammatory conditions, the immunohistochemistry analysis suggested that overall infiltration of the liver by gamma delta T cells remained relatively unchanged in inflammation, and that αβ T cells did indeed hugely increase in number. Although these data don't exclude the possibility that γδ T cells impact on the initiation of inflammation, arguably the simplest explanation for these data is that gamma delta T cells and chronic liver disease actually have little impact on one another. Indeed, perhaps previous studies reporting a relative increase in gamma

delta T cell numbers in liver disease did so simply because compared with the periphery, gamma delta T cell numbers are indeed increased in the liver even during disease.

This possibility was supported by TCR sequencing data presented in Chapter 4 and phenotyping data in Chapter 5. No differences were determined between normal and diseased liver in terms of Vδ2^{neg} TCR repertoire on a chain usage, clonal prevalence, CDR3 length or indeed CDR3 sequence basis in the NGS approach used in Chapter 4. It is not inconceivable that increasing the number of samples analysed may potentially identify disease associated clonotypes but there was no evidence of any clonal overlap in this dataset between any sample. This does not rule out the possibility of disease related antigen-driven private Vδ2^{neg} expansions, but suggests that if such expansions exist they are likely to have multiple private CDR3 sequences. Furthermore, immunophenotyping of Vδ2^{neg} T cells from normal and diseased livers revealed, even in healthy liver samples, a heavy skew towards T_{EMRA}-like clonally expanded populations of Vδ2^{neg} cells, which would likely mask any potential shift in repertoire induced by liver disease, were one to occur. If disease related Vδ2^{neg} clonal expansions do occur, it may be hard to distinguish the disease-influenced repertoire from the likely pre-existing skewed repertoire.

The data presented in this study extend previous findings from other studies that highlight a shift in frequency of circulating Vδ2^{neg} T cells in patients with certain chronic liver diseases to also include autoimmune hepatitis. Here, Vδ2^{neg} cells dominate the peripheral gamma delta T cell population and are at least in part more activated and more differentiated than equivalent populations in healthy donors. As noted in Chapter 4, it is possible that all these observations may be attributable not solely to antigenic TCR stimulation but perhaps also the nature of the therapy or non-TCR specific activatory

signals such as pro-inflammatory cytokines. Whether these enriched Vδ2^{neg} T cells are directly involved in the progression of pathology in these individuals or whether they are "bystanders" in a systemically inflated immune response is unclear, although other work has identified other innate-like lymphocytes that are enriched and activated in autoimmune liver disorders (Schoknecht *et al*., 2017, Chang *et al*., 2015), suggesting the latter hypothesis may be more likely.

Overall then, the data presented in this thesis suggest that, in end stage disease at least, gamma delta T cells do not appear to be significantly changed in comparison with cell isolated from healthy liver. While the possibility of a role in the development of disease cannot be ruled out, it appears that it is likely αβ T cells that are mainly associated with intrahepatic infiltration in chronic liver disease rather than gamma delta T cells. This finding is accordant with findings for other innate-like T cells in human liver, including intrahepatic MAITs, which appear to be enriched in liver compared with the periphery but do not increase in frequency in chronic liver disease (Jeffery *et al*., 2016), and iNKTs, which do not appear to increase in frequency in virally infected livers compared with healthy livers (Yanagisawa *et al*., 2013).

7.3 Gamma delta T cells and tissue

7.3.1 The liver harbours a population of T_{RM}-like gamma delta T cells

The identification of large populations of predominantly MHC Class I restricted CD8$^+$ T cells in the gut (intra-epithelial lymphocytes, or IEL), with high expression of the CD8αα homodimer not readily observed in the periphery (Jarry *et al*., 1990) led to the postulation that these were tissue associated cells, distinct from systemic T cells (Hayday

et al., 2001). This finding was particularly resonant for gamma delta T cell biologists, since a large proportion of the IEL were determined to be γδ TCR^+ (Goodman and Lefrancois, 1988), which in conjunction with the identification of an epidermally restricted population of $Vγ5^+$ gamma delta T cells in murine skin (DETC), suggested gamma delta T cells may have an important role in tissue-specific immunity. Importantly, in humans, the predominant δ-chain used in IEL populations was Vδ1 (Deusch *et al*., 1991). More recent studies have expanded on these observations for gamma delta T cells, and additionally investigated conventional T cells in tissues. Here, a newly characterised subset of cells that do not return to the circulation has been identified, that are retained in the tissue at the site of antigenic stimulation and continue to provide lasting protection against local re-exposure – the tissue resident memory T cells (T_{RM}) (Gebhardt *et al*., 2013).

However, studies of T_{RM} in humans, which began with $CD8^+$ αβ T cells (Thome and Farber, 2015), and latterly included $CD4^+$ αβ T cells (Turner and Farber, 2014) and NK cells (Lugli *et al*., 2016), have not to date addressed whether one of the archetypal tissue associated lymphocyte subsets, gamma delta T cells, conform to the paradigms defined for other lymphocytes in this body of work. Phenotyping by flow cytometry, and indeed functional experiments conducted to determine responsivity to stimulation and cytokine production (Chapter 5), established a strong parallel between $Vδ2^{neg}$ gamma delta T cells and $CD8^+$ αβ T cells in human liver, with one major difference – the majority of liver infiltrating $Vδ2^{neg}$ cells are T_{EMRA}-like, expressing low CD27, IL-7R, CD28, CD62L and CCR7 and high CD45RA. In contrast, intrahepatic $CD8^+$ T cells are predominantly T_{EM}-like, with low CD27, IL-7R, CD28, CD62L and CCR7 expression but also low CD45RA expression. In a separate

study, from the group of Maini at UCL, $CD8^+$ $CD45RA^{neg}$ T_{EM}-like $CD69^+$ cells were identified as being liver-resident in humans (Pallett *et al*., 2017), and the author's ascribed a certain phenotype which mirrored that identified in the smaller T_{EM}-like population in $V\delta2^{neg}$ gamma delta T cells in this study. This included high expression of CD69, CXCR6, CXCR3, as well as low expression of transcription factors Tbet, Hobit and Eomes and lower cytotoxic potential than the $CD45RA^+$ subset. As in the Maini-led study, here, $V\delta2^{neg}$ $CD45RA^{lo/neg}$ T_{EM}-like cells were present within the liver but not detected in the periphery.

However, in this study, further evidence for genuine tissue-association, and indeed putative classification as a T_{RM}-subset, was presented in the form of TCR sequencing. As $V\delta2^{neg}$ T cells are in general highly clonally focussed, whether liver or blood derived, single cell PCR provided a low-depth examination of TCR sequence overlap between blood and liver $V\delta2^{neg}$ from matched donors. Strikingly, a large percentage of T_{EM}-like $V\delta2^{neg}$ TCR sequences were found only in the liver samples, while T_{EMRA}-like $V\delta2^{neg}$ TCR sequences were often identified in both liver and blood. Although the number of cells examined in this study was relatively low, this represents, to the author's knowledge, the first CDR3-based approach to identification of tissue associated gamma delta T cells, and highlights the potential of such an approach in future studies. If sufficient numbers of cells could be sorted from human explanted tissue, deep sequencing of T_{EM}-like and T_{EMRA}-like cells from liver and blood may add weight to this hypothesis. Additionally, if homologous cells could be identified in mice, it may be possible to prove whether or not T_{EM}-like gamma delta T cells are indeed tissue-resident using standard labelling and

parabiosis experiments as have been conducted with αβ T cell studies (Schenkel *et al*., 2014, Steinert *et al*., 2015).

T_{RM} are distinguished from other tissue resident cells as they are genuine memory cells rather than innate or innate-like cells responding to TCR-independent signals such as cytokine stimulation (Masopust *et al*., 2010). Nevertheless, the TCR sequencing data presented in Chapter 4 and 5 suggests that intrahepatic $V\delta2^{neg}$ cells, including the T_{EM}-like subset, have likely undergone private, most likely antigenically-driven clonal expansion and therefore are more similar to $CD8^+$ or $CD4^+$ αβ T_{RM} than innate tissue associated lymphocytes such as NK cells. The apparent increase in sensitivity to cytokines such as IL-12 and IL-18, as well as reduced cytotoxicity compared with T_{EMRA}-like cells may be due to microenvironmental factors in the liver, possibly including IL-15 (Pallett *et al*., 2017), a cytokine that $V\delta2^{neg}$ cells are highly sensitive towards. As discussed in Chapter 3, the potential for using a combination of ISH-based techniques such as BASEscope alongside IHC to identify localisation of specific TCR sequences of T_{RM}-like gamma delta T cells in not just liver but all tissues could also be a powerful tool in future studies exploring tissue associated gamma delta T cells.

7.3.2 The majority of intrahepatic gamma delta T cell appear to be vasculature associated

While the discovery of this T_{RM}-like subset of $V\delta2^{neg}$ T cells in liver is of great interest, the majority of intrahepatic $V\delta2^{neg}$ cells are phenotypically and clonally very similar to those found in the periphery. While there will be some element of overlap between the blood and liver compartments due to the contiguous vascular nature of liver tissue, it should be

emphasised that there are enough differences between the two compartments to suggest that the intrahepatic Vδ2^{neg} cells are not simply "contaminating" blood. Higher expression of CD69, loss of the CD27^{hi}/ CD62L^{+}/ IL-7R^{+} population, not to mention the increase in frequency of these cells in the liver compared with the periphery, both as a proportion of total T cell infiltrate as well as a change from Vδ2^{+} to Vδ2^{neg} dominance within the gamma delta population, all strongly suggest that there is a distinct population of liver-associated Vδ2^{neg} cells in both normal and diseased livers compared to blood.

However, the high degree of clonal and phenotypic overlap between blood and liver in many matched donors is striking. In addition to the clonal overlap, these cells were predominantly T_{EMRA}-like CD27^{lo}CD45RA^{hi}, expressed lower levels of CD69, CXCR3 and CXCR6 but higher CX_3CR1, CD16, Tbet and Hobit as well as being generally non-responsive to cytokine stimulation, in comparison with the T_{EM}/T_{RM}-like population. As with the T_{EM}-like/ T_{RM}-like population, the T_{EMRA}-like Vδ2^{neg} cells were phenotypically and functionally similar to autologous CD8^{+} αβ T cells. CD8^{+} αβ T cells specific for chronic viral infections such as cytomegalovirus (CMV) have been demonstrated to be T_{EMRA}-like, with low expression of CD27, CD28, and re-acquisition of the CD45RA isoform (van Aalderen *et al*., 2014). These cells appear to be long-lived and antigenically induced with reduced potential TCR repertoire compared with other CD8^{+} αβ T cells (Wallace *et al*., 2011, Hamann *et al*., 1999). CX_3CR1 expression has been demonstrated to cluster with loss of CD62L and gain of CD45RA expression in virus-specific T cells in proteomic studies of human CD8^{+} T cell differentiation (Bottcher *et al*., 2015, van Aalderen *et al*., 2017), and was demonstrated to be associated with the subset of both CD8^{+} and Vδ2^{neg} cells in this study. While T_{EMRA}-like CD8+ T cells form a relatively minor proportion of intrahepatic

$CD8^+$ T cells, they are enriched compared with the periphery. Overall enrichment of the T_{EMRA}-like subset of $V\delta2^{neg}$ T cells was not demonstrated in the liver compared with blood, it could be speculated that this is due to the fact that the periphery is already heavily enriched for this phenotype of $V\delta2^{neg}$ cells, even in healthy donors (Davey *et al*., 2017). Indeed, in addition to $V\delta2^{neg}$ T cells, data presented in Chapter 6 revealed a previously unreported population of gamma delta T cells, $V\delta2^+V\gamma9^{neg}$, which are apparently enriched in liver but share a similar phenotype with the T_{EMRA}-like $V\delta2^{neg}$ intrahepatic and blood-derived cells. These cells also had specific clonotypes identified in both liver and blood-derived populations, suggesting a clear analogy to the $V\delta2^{neg}$ population and raising the possibility that they are potentially similarly vasculature-associated in nature. Although $V\delta2^{neg}$ T cell numbers have been demonstrated to increase in CMV-infected donors (Pitard *et al*., 2008) and are capable of targeting CMV-infected endothelium (Halary *et al*., 2005), the antigenic trigger for such expansions is still unclear. Despite this, the parallel between these apparently antigenically induced T_{EMRA}-like populations of $V\delta2^{neg}$ or $V\delta2^+V\gamma9^{neg}$ T cells in both liver and blood and CMV-specific $CD8^+$ αβ T cells is striking. Recent work from the Prinz group has identified clonal response to acute CMV infection following haematopoietic stem cell transplantation in gamma delta T cells (Ravens *et al*., 2017) and unpublished data from this group also supports induction of a clonal response in $V\delta2^+V\gamma9^{neg}$ cells in CMV infection following kidney transplantation. Furthermore, intrahepatic T_{EMRA}-like $V\delta2^{neg}$ cells express high levels of CD16, previously demonstrated to be upregulated in hCMV-induced gamma delta T cells (Couzi *et al*., 2012). One hypothesis that could be worthy of future study is that these T_{EMRA}-like $V\delta2^{neg}$ or $V\delta2^+V\gamma9^{neg}$ cells are vasculature associated, essentially composed of antigenically induced memory populations of cells that remain in circulation

rather than re-entering tissue, perhaps due to a systemic proliferation in response to viral or virally associated antigen, but that remain in close association with vascular endothelium, likely through upregulation of integrins such as LFA-1 (McNamara *et al*., 2017). Since the liver is heavily enriched with vascular endothelium, it is possible that $V\delta2^{neg}$ T cells that have clonally expanded in blood due to virally-associated antigen are then retained within the liver, perhaps through ICAM - LFA-1 interactions, thereby generating a large population of liver associated cells that overlap clonotypically with the periphery. Whether these liver associated $V\delta2^{neg}$ or $V\delta2^{+}V\gamma9^{neg}$ T_{EMRA}-like cells have any specific function in the liver beyond immunosurveillance of the vasculature, although it must be emphasised that these populations do exist in CMV-negative donors, so involvement in anti-viral responses may not be restricted to those directed towards CMV. It would be interesting to investigate how this high apparent level of clonal seeding from the periphery into the liver for $V\delta2^{neg}$ or $V\delta2^{+}V\gamma9^{neg}$ T_{EMRA}-like cells applies to other lymphocyte subsets, particularly if there is any observable correlation with liver disease. This model and the contrasting T_{RM}-like population of liver-specific clonotypes is summarized in Figure 7.1.

How this model may apply to other tissues is unclear, but in the author's opinion this is certainly worth further investigation. In tissues where distinct transmigration across basal membrane, whether epithelial or endothelial, is required for lymphocytic access it could be hypothesised that a greater difference between peripheral and tissue-associated $V\delta2^{neg}$ T cells may be observed than is the case in liver. It would be interesting to compare the extent of the T_{RM}-like population of $V\delta2^{neg}$ in tissues such as

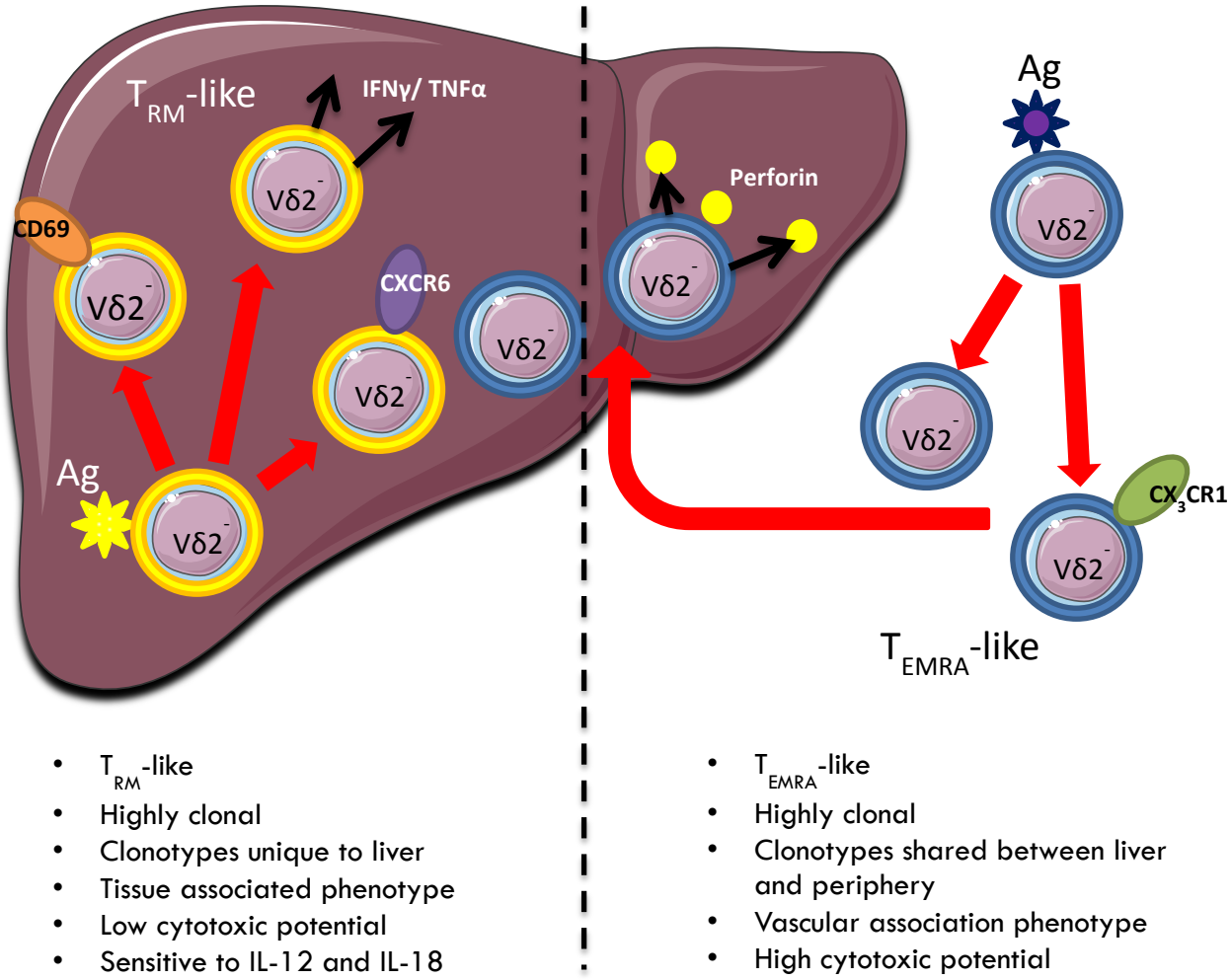

Figure 7.1: Intrahepatic Vδ1+ T cells segregate into cytokine producing and cytotoxic subsets

the gut or lung, where enrichment of Vδ2^{neg} cells has been identified, and also determine the extent of the clonal overlap with the peripheral populations, if indeed there is any.

7.4 Vδ2^{neg} gamma delta T cells conform to an adaptive paradigm

Data presented in Chapters 4, 5 and 6 identify strong, private, complex clonal expansions in parallel with phenotypic variation from naïve-like CD27^{hi}, CD62L^{+}, IL-7R^{+}, CCR7^{+} Vδ2^{neg} T cells present in the periphery to effector-like CD27^{lo} CD62L^{neg}, IL-7R^{neg}, CCR7^{neg} Vδ2^{neg} T cells T cells in the liver. This is strongly suggestive of TCR-associated antigenically driven expansion, in contrast to the essentially semi-invariant like polyclonal expansions of Vδ2^{+}Vγ9^{+} cells presented in Chapter 6. These data highlight the previously overlooked possibility that Vδ2^{neg} T cells are likely predominantly associated with the adaptive immune response, rather than the classical innate-like response that appears to apply to the Vδ2^{+}Vγ9^{+} T cell compartment, which features a semi-invariant TCR repertoire (Chapter 6). Further analysis of Vδ2^{neg} cells in lymphoid tissue may help prove whether Vδ2^{neg} T cells undergo a similar program of lymph node homing, priming and subsequent expansion exhibited by conventional T cells.

Of course, gamma delta T cells are not MHC-restricted, which raises questions as to how they are regulated during development, especially since the majority of *bona fide* TCR ligands so far identified are self-ligands. It can be hypothesised that a combination of TCR binding to self-stress ligands alongside co-stimulation with such surface adhesion molecules as ICAM-1 or CD2 may act in concert in order to activate Vδ2^{neg} T cells via TCR

(Willcox *et al*., 2012) – the "multi-molecular stress signal". What is clear from this dataset is that the repertoire is highly private, with long varied CDR3s, suggestive of a potentially huge variety of TCR ligands, perhaps indicative of why so few ligands have been identified thus far and of the potential for recognition of exogenous ligands, as suggested by studies on γδ TCR-mediated binding to algal protein phycoerythrin (Zeng *et al*., 2012).

7.5 The future of tissue-associated gamma delta T cell research

7.5.1 Vδ2^{neg} gamma delta T cells and cancer immunotherapy

Although a considerable amount of translationally-oriented research has been carried out on the Vδ2^{+} subset of gamma delta T cells in humans, primarily because phosphoantigen-based expansion protocols are readily available, the Vδ2^{neg} subset are also potential vectors of adoptive transfer and chimeric antigen receptor (CAR)-based cellular therapies. Demonstrated to be capable of killing haematologically and epithelially derived malignancies both *in vitro* (Wu *et al*., 2015) and using murine models (Devaud *et al*., 2013), human Vδ2^{neg} T cells share with Vδ2^{+} T cells the advantage of being non-MHC restricted. This means they can by-pass one problem encountered with αβ T cell therapies, namely tumour mediated downregulation of MHC or antigen processing defects. Additionally, they express many NK receptors that enable non-TCR mediated recognition of stressed tumour cells conferring in some cases superior cytolytic potential than other T cell subsets (Choudhary *et al*., 1995).

Finally, and as demonstrated in this study in the transmigration experiment detailed in Chapter 3, Vδ2^{neg} are capable of migrating into and being retained in solid tissues such as liver at a better rate than αβ T cells, meaning they are potentially more likely of reaching

their intended tumour target, and have been demonstrated to be capable of infiltrating tumours in several solid cancers (Kitayama *et al*., 1993, Ferrarini *et al*., 1996, Cordova *et al*., 2012). Moreover, a meta-analysis of 18,000 human tumours identified a gamma delta T cell signature as most highly linked with favourable outcome (Gentles *et al*., 2015), although the basis of this signature is questionable since the TCR itself was not included in the array data analysed and gamma delta T cells do share a strong T_H1 transcriptional profile with many cytotoxic lymphocytes.

Recent work has identified GMP-compliant expansion methods for $V\delta1^+$ gamma delta T cells for adoptive transfer (Almeida *et al*., 2016) and there is also on-going work looking to use gamma delta T cells as CARs, exploiting the natural cytolytic and homing properties of these cells with a recombinant tumour associated antigen specific TCR receptor (Mirzaei *et al*., 2016). Although questions regarding co-stimulation still need to be addressed, there is great potential in such immunotherapy.

7.5.2 $V\delta2^{neg}$ ligand identification

As described in Chapter 1, one of the greatest challenges in gamma delta T cell biology is the identification of TCR ligands for the $V\delta2^{neg}$ subset of cells. Sequence level TCR repertoire studies such as those carried out in this thesis may prove a useful platform for ligand identification by tissue associated gamma delta T cells. Recent studies have suggested that Vδ1 TCRs are capable of recognising antigen via a predominantly non-CDR3 associated interaction (Uldrich *et al*., 2013), throwing into question the extent of the gamma delta CDR3 in antigen binding. However, most ligand identification studies for $V\delta2^{neg}$, including Uldrich *et al*, are based on *a priori* selection of target, for example

from CD1d-reactive cells, which represent a very low proportion of the actual gamma delta T cell population present in most individuals. By placing more emphasis on the immunophenotype and TCR repertoire data generated in studies such as this one, ligand identification studies will focus on physiologically relevant clonotypes that are expanded *in vivo*. This approach could then be used to define TCR ligands with respect to specific stress stimuli such as infectious challenges, including CMV infection.

Having identified whole CDR3 regions from single cell PCR, it is possible to transfect both primary human T cells or cell lines such as Jurkat cells with full length specific expanded TCRs identified in samples obtained in studies such as this one. One could then adopt a screening strategy using tissue-relevant transformed cell lines to identify reactive TCR-transductants, and then in combination with blocking antibodies (Halary *et al*., 2005) and RNAseq of the targets attempt to identify cell surface moieties critical to activation. Further insight may be gained from ACD's BASEscope technology, allowing localisation of T cells with specific TCR sequences within tissue. Knowing where in the tissue specific clonotypes are localised may allow better definition of likely antigenic targets.

7.5.3 Single cell transcriptomics of tissue associated gamma delta T cells

As an extension of the index sorted single cell PCR conducted in Chapter 5, transcriptomics studies, including single cell transcriptomics would be of great interest. Advances in fluidics and RNA sequencing technology now allow analysis of the transcriptome of individual cells by RNASeq (Haque *et al*., 2017), allowing an unprecedented insight into the heterogeneity of individual cells. Algorithms such as TraCeR now also allow interrogation of such transcriptomic data for TCR sequences,

allowing correlation of clonality with transcriptome and tracking of clonal fate in response to infection (Stubbington *et al*., 2016). This algorithm has since been modified to identify gamma delta T cell TCR sequences (Stubbington & Willcox, unpublished). With access to such powerful analytical tools, one can envisage comprehensive tracking of gamma delta clonotypes within blood and solid tissues and in combination with protein level index sorting and RNASeq build a detailed portrait of the processes governing activation, differentiation and migration of these cells.

8

References

Acuto, O. and F. Michel (2003). "CD28-mediated co-stimulation: a quantitative support for TCR signalling." Nat Rev Immunol **3**(12): 939-951.

Adams, E. J. (2014). "Lipid presentation by human CD1 molecules and the diverse T cell populations that respond to them." Curr Opin Immunol **26**: 1-6.

Affo, S., L. X. Yu, et al. (2017). "The Role of Cancer-Associated Fibroblasts and Fibrosis in Liver Cancer." Annu Rev Pathol **12**: 153-186.

Agrati, C., T. Alonzi, et al. (2006). "Activation of Vgamma9Vdelta2 T cells by non-peptidic antigens induces the inhibition of subgenomic HCV replication." Int Immunol **18**(1): 11-18.

Agrati, C., G. D'Offizi, et al. (2001). "Vdelta1 T lymphocytes expressing a Th1 phenotype are the major gammadelta T cell subset infiltrating the liver of HCV-infected persons." Mol Med **7**(1): 11-19.

Ahmed, K. T., A. A. Almashhrawi, et al. (2017). "Is the 25-year hepatitis C marathon coming to an end to declare victory?" World J Hepatol **9**(21): 921-929.

Ajuebor, M. N., Y. Jin, et al. (2008). "GammadeltaT cells initiate acute inflammation and injury in adenovirus-infected liver via cytokine-chemokine cross talk." J Virol **82**(19): 9564-9576.

Allan, R. S., J. Waithman, et al. (2006). "Migratory dendritic cells transfer antigen to a lymph node-resident dendritic cell population for efficient CTL priming." Immunity **25**(1): 153-162.

Almeida, A. R., D. V. Correia, et al. (2016). "Delta One T Cells for Immunotherapy of Chronic Lymphocytic Leukemia: Clinical-Grade Expansion/Differentiation and Preclinical Proof of Concept." Clin Cancer Res **22**(23): 5795-5804.

Asarnow, D. M., T. Goodman, et al. (1989). "Distinct antigen receptor repertoires of two classes of murine epithelium-associated T cells." Nature **341**(6237): 60-62.

Asarnow, D. M., W. A. Kuziel, et al. (1988). "Limited diversity of gamma delta antigen receptor genes of Thy-1+ dendritic epidermal cells." Cell **55**(5): 837-847.

Bai, L., D. Picard, et al. (2012). "The majority of CD1d-sulfatide-specific T cells in human blood use a semiinvariant Vdelta1 TCR." Eur J Immunol **42**(9): 2505-2510.

Balmer, M. L., E. Slack, et al. (2014). "The liver may act as a firewall mediating mutualism between the host and its gut commensal microbiota." Sci Transl Med **6**(237): 237ra266.

Bandeira, A., T. Mota-Santos, et al. (1990). "Localization of gamma/delta T cells to the intestinal epithelium is independent of normal microbial colonization." J Exp Med **172**(1): 239-244.

Barbarin, A., E. Cayssials, et al. (2017). "Phenotype of NK-Like CD8(+) T Cells with Innate Features in Humans and Their Relevance in Cancer Diseases." Front Immunol **8**: 316.

Benechet, A. P. and M. Iannacone (2017). "Determinants of hepatic effector CD8+ T cell dynamics." J Hepatol **66**(1): 228-233.

Benedict, M. and X. Zhang (2017). "Non-alcoholic fatty liver disease: An expanded review." World J Hepatol **9**(16): 715-732.

Berberich, C., J. R. Ramirez-Pineda, et al. (2003). "Dendritic cell (DC)-based protection against an intracellular pathogen is dependent upon DC-derived IL-12 and can be induced by molecularly defined antigens." J Immunol **170**(6): 3171-3179.

Bianchi, M. E. (2007). "DAMPs, PAMPs and alarmins: all we need to know about danger." J Leukoc Biol **81**(1): 1-5.

Bilzer, M., F. Roggel, et al. (2006). "Role of Kupffer cells in host defense and liver disease." Liver Int **26**(10): 1175-1186.

Bjorkstrom, N. K., V. D. Gonzalez, et al. (2008). "Elevated numbers of Fc gamma RIIIA+ (CD16+) effector CD8 T cells with NK cell-like function in chronic hepatitis C virus infection." J Immunol **181**(6): 4219-4228.

Bolotin, D. A., S. Poslavsky, et al. (2015). "MiXCR: software for comprehensive adaptive immunity profiling." Nat Methods **12**(5): 380-381.

Borchers, A. T., S. Shimoda, et al. (2009). "Lymphocyte recruitment and homing to the liver in primary biliary cirrhosis and primary sclerosing cholangitis." Semin Immunopathol **31**(3): 309-322.

Borst, J., A. Wicherink, et al. (1989). "Non-random expression of T cell receptor gamma and delta variable gene segments in functional T lymphocyte clones from human peripheral blood." Eur J Immunol **19**(9): 1559-1568.

Bottcher, J. P., M. Beyer, et al. (2015). "Functional classification of memory CD8(+) T cells by CX3CR1 expression." Nat Commun **6**: 8306.

Braet, F. and E. Wisse (2002). "Structural and functional aspects of liver sinusoidal endothelial cell fenestrae: a review." Comp Hepatol **1**(1): 1.

Brandes, M., K. Willimann, et al. (2005). "Professional antigen-presentation function by human gammadelta T Cells." Science **309**(5732): 264-268.

Brightbill, H. D., D. H. Libraty, et al. (1999). "Host defense mechanisms triggered by microbial lipoproteins through toll-like receptors." Science **285**(5428): 732-736.

Britanova, O. V., E. V. Putintseva, et al. (2014). "Age-related decrease in TCR repertoire diversity measured with deep and normalized sequence profiling." J Immunol **192**(6): 2689-2698.

Bromley, S. K., S. Y. Thomas, et al. (2005). "Chemokine receptor CCR7 guides T cell exit from peripheral tissues and entry into afferent lymphatics." Nat Immunol **6**(9): 895-901.

Butz, E. A. and M. J. Bevan (1998). "Massive expansion of antigen-specific CD8+ T cells during an acute virus infection." Immunity **8**(2): 167-175.

Cairo, C., C. L. Armstrong, et al. (2010). "Impact of age, gender, and race on circulating gammadelta T cells." Hum Immunol **71**(10): 968-975.

Canchis, P. W., A. K. Bhan, et al. (1993). "Tissue distribution of the non-polymorphic major histocompatibility complex class I-like molecule, CD1d." Immunology **80**(4): 561-565.

Carambia, A., C. Frenzel, et al. (2013). "Inhibition of inflammatory CD4 T cell activity by murine liver sinusoidal endothelial cells." J Hepatol **58**(1): 112-118.

Carding, S. R. and P. J. Egan (2002). "Gammadelta T cells: functional plasticity and heterogeneity." Nat Rev Immunol **2**(5): 336-345.

Carding, S. R., J. G. McNamara, et al. (1990). "Characterization of gamma/delta T cell clones isolated from human fetal liver and thymus." Eur J Immunol **20**(6): 1327-1335.

Casorati, G., G. De Libero, et al. (1989). "Molecular analysis of human gamma/delta+ clones from thymus and peripheral blood." J Exp Med **170**(5): 1521-1535.

Chang, C. H., Y. C. Chen, et al. (2015). "Innate immunity drives the initiation of a murine model of primary biliary cirrhosis." PLoS One **10**(3): e0121320.

Chao, A. (1984). "Non-parametric estimation of the number of classes in a population." Scandinavian Journal ofStatistics, **11**:265-270.

Chen, C. Y., S. Yao, et al. (2013). "Phosphoantigen/IL2 expansion and differentiation of Vgamma2Vdelta2 T cells increase resistance to tuberculosis in nonhuman primates." PLoS Pathog **9**(8): e1003501.

Chen, M., P. Hu, et al. (2012). "Enhanced peripheral gammadeltaT cells cytotoxicity potential in patients with HBV-associated acute-on-chronic liver failure might contribute to the disease progression." J Clin Immunol **32**(4): 877-885.

Chen, M., P. Tabaczewski, et al. (2005). "Hepatocytes express abundant surface class I MHC and efficiently use transporter associated with antigen processing, tapasin, and low molecular weight polypeptide proteasome subunit components of antigen processing and presentation pathway." J Immunol **175**(2): 1047-1055.

Chen, M., D. Zhang, et al. (2008). "Characteristics of circulating T cell receptor gamma-delta T cells from individuals chronically infected with hepatitis B virus (HBV): an association between V(delta)2 subtype and chronic HBV infection." J Infect Dis **198**(11): 1643-1650.

Chodaczek, G., V. Papanna, et al. (2012). "Body-barrier surveillance by epidermal gammadelta TCRs." Nat Immunol **13**(3): 272-282.

Chosay, J. G., M. A. Fisher, et al. (1998). "Role of PECAM-1 (CD31) in neutrophil transmigration in murine models of liver and peritoneal inflammation." Am J Physiol **274**(4 Pt 1): G776-782.

Choudhary, A., F. Davodeau, et al. (1995). "Selective lysis of autologous tumor cells by recurrent gamma delta tumor-infiltrating lymphocytes from renal carcinoma." J Immunol **154**(8): 3932-3940.

Cimini, E., C. Bonnafous, et al. (2012). "Interferon-alpha improves phosphoantigen-induced Vgamma9Vdelta2 T-cells interferon-gamma production during chronic HCV infection." PLoS One **7**(5): e37014.

Clevers, H., B. Alarcon, et al. (1988). "The T cell receptor/CD3 complex: a dynamic protein ensemble." Annu Rev Immunol **6**: 629-662.

Compte, E., P. Pontarotti, et al. (2004). "Frontline: Characterization of BT3 molecules belonging to the B7 family expressed on immune cells." Eur J Immunol **34**(8): 2089-2099.

Cordova, A., F. Toia, et al. (2012). "Characterization of human gammadelta T lymphocytes infiltrating primary malignant melanomas." PLoS One **7**(11): e49878.

Costa, G., S. Loizon, et al. (2011). "Control of Plasmodium falciparum erythrocytic cycle: gammadelta T cells target the red blood cell-invasive merozoites." Blood **118**(26): 6952-6962.

Costa, M., E. Cruz, et al. (2015). "Lymphocyte gene expression signatures from patients and mouse models of hereditary hemochromatosis reveal a function of HFE as a negative regulator of CD8+ T-lymphocyte activation and differentiation in vivo." PLoS One **10**(4): e0124246.

Costa, M. F., V. U. Bornstein, et al. (2012). "CCL25 induces alpha(4)beta(7) integrin-dependent migration of IL-17(+) gammadelta T lymphocytes during an allergic reaction." Eur J Immunol **42**(5): 1250-1260.

Coulthard, A. B., D. F. Eberl, et al. (2003). "Genetic analysis of the second chromosome centromeric heterochromatin of Drosophila melanogaster." Genome **46**(3): 343-352.

Couzi, L., V. Pitard, et al. (2015). "Direct and Indirect Effects of Cytomegalovirus-Induced gammadelta T Cells after Kidney Transplantation." Front Immunol **6**: 3.

Couzi, L., V. Pitard, et al. (2009). "Common features of gammadelta T cells and CD8(+) alphabeta T cells responding to human cytomegalovirus infection in kidney transplant recipients." J Infect Dis **200**(9): 1415-1424.

Couzi, L., V. Pitard, et al. (2012). "Antibody-dependent anti-cytomegalovirus activity of human gammadelta T cells expressing CD16 (FcgammaRIIIa)." Blood **119**(6): 1418-1427.

Croft, M., L. Carter, et al. (1994). "Generation of polarized antigen-specific CD8 effector populations: reciprocal action of interleukin (IL)-4 and IL-12 in promoting type 2 versus type 1 cytokine profiles." J Exp Med **180**(5): 1715-1728.

Crowley, M. P., A. M. Fahrer, et al. (2000). "A population of murine gammadelta T cells that recognize an inducible MHC class Ib molecule." Science **287**(5451): 314-316.

Cuff, A. O., F. P. Robertson, et al. (2016). "Eomeshi NK Cells in Human Liver Are Long-Lived and Do Not Recirculate but Can Be Replenished from the Circulation." J Immunol **197**(11): 4283-4291.

Curbishley, S. M., B. Eksteen, et al. (2005). "CXCR 3 activation promotes lymphocyte transendothelial migration across human hepatic endothelium under fluid flow." Am J Pathol **167**(3): 887-899.

Davey, M. S., C. Y. Lin, et al. (2011). "Human neutrophil clearance of bacterial pathogens triggers anti-microbial gammadelta T cell responses in early infection." PLoS Pathog **7**(5): e1002040.

Davey, M. S., C. R. Willcox, et al. (2017). "Clonal selection in the human Vdelta1 T cell repertoire indicates gammadelta TCR-dependent adaptive immune surveillance." Nat Commun **8**: 14760.

Davis, M. M. and P. J. Bjorkman (1988). "T-cell antigen receptor genes and T-cell recognition." Nature **334**(6181): 395-402.

Davis, M. M., J. J. Boniface, et al. (1998). "Ligand recognition by alpha beta T cell receptors." Annu Rev Immunol **16**: 523-544.

Davodeau, F., M. A. Peyrat, et al. (1993). "Peripheral selection of antigen receptor junctional features in a major human gamma delta subset." Eur J Immunol **23**(4): 804-808.

De Libero, G., G. Casorati, et al. (1991). "Selection by two powerful antigens may account for the presence of the major population of human peripheral gamma/delta T cells." J Exp Med **173**(6): 1311-1322.

DeBarros, A., M. Chaves-Ferreira, et al. (2011). "CD70-CD27 interactions provide survival and proliferative signals that regulate T cell receptor-driven activation of human gammadelta peripheral blood lymphocytes." Eur J Immunol **41**(1): 195-201.

Deusch, K., F. Luling, et al. (1991). "A major fraction of human intraepithelial lymphocytes simultaneously expresses the gamma/delta T cell receptor, the CD8 accessory molecule and preferentially uses the V delta 1 gene segment." Eur J Immunol **21**(4): 1053-1059.

Devaud, C., B. Rousseau, et al. (2013). "Anti-metastatic potential of human Vdelta1(+) gammadelta T cells in an orthotopic mouse xenograft model of colon carcinoma." Cancer Immunol Immunother **62**(7): 1199-1210.

Di Marco Barros, R., N. A. Roberts, et al. (2016). "Epithelia Use Butyrophilin-like Molecules to Shape Organ-Specific gammadelta T Cell Compartments." Cell **167**(1): 203-218 e217.

Dieli, F., F. Poccia, et al. (2003). "Differentiation of effector/memory Vdelta2 T cells and migratory routes in lymph nodes or inflammatory sites." J Exp Med **198**(3): 391-397.

Dieude, M., H. Striegl, et al. (2011). "Cardiolipin binds to CD1d and stimulates CD1d-restricted gammadelta T cells in the normal murine repertoire." J Immunol **186**(8): 4771-4781.

Dimova, T., M. Brouwer, et al. (2015). "Effector Vgamma9Vdelta2 T cells dominate the human fetal gammadelta T-cell repertoire." Proc Natl Acad Sci U S A **112**(6): E556-565.

Do, J. S. and B. Min (2009). "IL-15 produced and trans-presented by DCs underlies homeostatic competition between CD8 and {gamma}{delta} T cells in vivo." Blood **113**(25): 6361-6371.

Doherty, D. G. and C. O'Farrelly (2000). "Innate and adaptive lymphoid cells in the human liver." Immunol Rev **174**: 5-20.

Du, G., L. Qiu, et al. (2006). "Combined megaplex TCR isolation and SMART-based real-time quantitation methods for quantitating antigen-specific T cell clones in mycobacterial infection." J Immunol Methods **308**(1-2): 19-35.

Duarte, S., J. Baber, et al. (2015). "Matrix metalloproteinases in liver injury, repair and fibrosis." Matrix Biol **44-46**: 147-156.

Dunne, M. R., L. Elliott, et al. (2013). "Persistent Changes in Circulating and Intestinal gammadelta T Cell Subsets, Invariant Natural Killer T Cells and Mucosal-Associated Invariant T Cells in Children and Adults with Coeliac Disease." PLoS One **8**(10): e76008.

Durante-Mangoni, E., R. Wang, et al. (2004). "Hepatic CD1d expression in hepatitis C virus infection and recognition by resident proinflammatory CD1d-reactive T cells." J Immunol **173**(3): 2159-2166.

Dziubianau, M., J. Hecht, et al. (2013). "TCR repertoire analysis by next generation sequencing allows complex differential diagnosis of T cell-related pathology." Am J Transplant **13**(11): 2842-2854.

Ebe, Y., G. Hasegawa, et al. (1999). "The role of Kupffer cells and regulation of neutrophil migration into the liver by macrophage inflammatory protein-2 in primary listeriosis in mice." Pathol Int **49**(6): 519-532.

Eberl, M., M. Hintz, et al. (2003). "Microbial isoprenoid biosynthesis and human gammadelta T cell activation." FEBS Lett **544**(1-3): 4-10.

Eberl, M. and H. Jomaa (2003). "A genetic basis for human gammadelta T-cell reactivity towards microbial pathogens." Trends Immunol **24**(8): 407-409.

Eberl, M., G. W. Roberts, et al. (2009). "A rapid crosstalk of human gammadelta T cells and monocytes drives the acute inflammation in bacterial infections." PLoS Pathog **5**(2): e1000308.

Ebert, L. M., P. Schaerli, et al. (2005). "Chemokine-mediated control of T cell traffic in lymphoid and peripheral tissues." Mol Immunol **42**(7): 799-809.

Egan, C. E., J. E. Dalton, et al. (2005). "A requirement for the Vgamma1+ subset of peripheral gammadelta T cells in the control of the systemic growth of Toxoplasma gondii and infection-induced pathology." J Immunol **175**(12): 8191-8199.

Eksteen, B. (2016). "The Gut-Liver Axis in Primary Sclerosing Cholangitis." Clin Liver Dis **20**(1): 1-14.

Eksteen, B., A. J. Grant, et al. (2004). "Hepatic endothelial CCL25 mediates the recruitment of CCR9+ gut-homing lymphocytes to the liver in primary sclerosing cholangitis." J Exp Med **200**(11): 1511-1517.

Elliott, J. F., E. P. Rock, et al. (1988). "The adult T-cell receptor delta-chain is diverse and distinct from that of fetal thymocytes." Nature **331**(6157): 627-631.

Emerson, R. O., A. M. Sherwood, et al. (2013). "High-throughput sequencing of T-cell receptors reveals a homogeneous repertoire of tumour-infiltrating lymphocytes in ovarian cancer." J Pathol **231**(4): 433-440.

Exley, M., J. Garcia, et al. (1997). "Requirements for CD1d recognition by human invariant Valpha24+ CD4-CD8- T cells." J Exp Med **186**(1): 109-120.

Farnault, L., J. Gertner-Dardenne, et al. (2013). "Clinical evidence implicating gamma-delta T cells in EBV control following cord blood transplantation." Bone Marrow Transplant **48**(11): 1478-1479.

Fernandez-Ruiz, D., W. Y. Ng, et al. (2016). "Liver-Resident Memory CD8+ T Cells Form a Front-Line Defense against Malaria Liver-Stage Infection." Immunity **45**(4): 889-902.

Ferrarini, M., S. Heltai, et al. (1996). "Killing of laminin receptor-positive human lung cancers by tumor infiltrating lymphocytes bearing gammadelta(+) t-cell receptors." J Natl Cancer Inst **88**(7): 436-441.

Fournie, J. J., H. Sicard, et al. (2013). "What lessons can be learned from gammadelta T cell-based cancer immunotherapy trials?" Cell Mol Immunol **10**(1): 35-41.

Fritsch, R. D., X. Shen, et al. (2005). "Stepwise differentiation of CD4 memory T cells defined by expression of CCR7 and CD27." J Immunol **175**(10): 6489-6497.

Gao, G. F., J. Tormo, et al. (1997). "Crystal structure of the complex between human CD8alpha(alpha) and HLA-A2." Nature **387**(6633): 630-634.

Garboczi, D. N., P. Ghosh, et al. (1996). "Structure of the complex between human T-cell receptor, viral peptide and HLA-A2." Nature **384**(6605): 134-141.

Gardner, T., Q. Chen, et al. (2009). "Characterization of the role of TCR gammadelta in NK cell accumulation during viral liver inflammation." Exp Mol Pathol **86**(1): 32-35.

Gebhardt, T., S. N. Mueller, et al. (2013). "Peripheral tissue surveillance and residency by memory T cells." Trends Immunol **34**(1): 27-32.

Geginat, J., A. Lanzavecchia, et al. (2003). "Proliferation and differentiation potential of human CD8+ memory T-cell subsets in response to antigen or homeostatic cytokines." Blood **101**(11): 4260-4266.

Geissmann, F., T. O. Cameron, et al. (2005). "Intravascular immune surveillance by CXCR6+ NKT cells patrolling liver sinusoids." PLoS Biol **3**(4): e113.

Gentles, A. J., A. M. Newman, et al. (2015). "The prognostic landscape of genes and infiltrating immune cells across human cancers." Nat Med **21**(8): 938-945.

Gerber, D. J., V. Azuara, et al. (1999). "IL-4-producing gamma delta T cells that express a very restricted TCR repertoire are preferentially localized in liver and spleen." J Immunol **163**(6): 3076-3082.

Germain, R. N. (1994). "MHC-dependent antigen processing and peptide presentation: providing ligands for T lymphocyte activation." Cell **76**(2): 287-299.

Gershwin, M. E., A. A. Ansari, et al. (2000). "Primary biliary cirrhosis: an orchestrated immune response against epithelial cells." Immunol Rev **174**: 210-225.

Gibbons, D. L., S. F. Haque, et al. (2009). "Neonates harbour highly active gammadelta T cells with selective impairments in preterm infants." Eur J Immunol **39**(7): 1794-1806.

Gillibert-Duplantier, J., A. Rullier, et al. (2010). "Liver myofibroblasts activate protein C and respond to activated protein C." World J Gastroenterol **16**(2): 210-216.

Girardi, M., D. E. Oppenheim, et al. (2001). "Regulation of cutaneous malignancy by gammadelta T cells." Science **294**(5542): 605-609.

Glatzel, A., D. Wesch, et al. (2002). "Patterns of chemokine receptor expression on peripheral blood gamma delta T lymphocytes: strong expression of CCR5 is a selective feature of V delta 2/V gamma 9 gamma delta T cells." J Immunol **168**(10): 4920-4929.

Golden-Mason, L., A. M. Kelly, et al. (2004). "Hepatic interleuklin 15 (IL-15) expression: implications for local NK/NKT cell homeostasis and development." Clin Exp Immunol **138**(1): 94-101.

Golden-Mason, L. and H. R. Rosen (2013). "Natural killer cells: multifaceted players with key roles in hepatitis C immunity." Immunol Rev **255**(1): 68-81.

Gong, Q., C. Wang, et al. (2017). "Assessment of T-cell receptor repertoire and clonal expansion in peripheral T-cell lymphoma using RNA-seq data." Sci Rep **7**(1): 11301.

Goodman, T. and L. Lefrancois (1988). "Expression of the gamma-delta T-cell receptor on intestinal CD8+ intraepithelial lymphocytes." Nature **333**(6176): 855-858.

Gorgani, N. N., J. Q. He, et al. (2008). "Complement receptor of the Ig superfamily enhances complement-mediated phagocytosis in a subpopulation of tissue resident macrophages." J Immunol **181**(11): 7902-7908.

Grant, A. J., P. F. Lalor, et al. (2001). "MAdCAM-1 expressed in chronic inflammatory liver disease supports mucosal lymphocyte adhesion to hepatic endothelium (MAdCAM-1 in chronic inflammatory liver disease)." Hepatology **33**(5): 1065-1072.

Green, D. R., N. Droin, et al. (2003). "Activation-induced cell death in T cells." Immunol Rev **193**: 70-81.

Greenwald, R. J., G. J. Freeman, et al. (2005). "The B7 family revisited." Annu Rev Immunol **23**: 515-548.

Gregory, S. H., A. J. Sagnimeni, et al. (1996). "Bacteria in the bloodstream are trapped in the liver and killed by immigrating neutrophils." J Immunol **157**(6): 2514-2520.

Groh, V., S. Porcelli, et al. (1989). "Human lymphocytes bearing T cell receptor gamma/delta are phenotypically diverse and evenly distributed throughout the lymphoid system." J Exp Med **169**(4): 1277-1294.

Guermonprez, P., J. Valladeau, et al. (2002). "Antigen presentation and T cell stimulation by dendritic cells." Annu Rev Immunol **20**: 621-667.

Guerville, F., S. Daburon, et al. (2015). "TCR-dependent sensitization of human gammadelta T cells to non-myeloid IL-18 in cytomegalovirus and tumor stress surveillance." Oncoimmunology **4**(5): e1003011.

Guidotti, L. G., D. Inverso, et al. (2015). "Immunosurveillance of the liver by intravascular effector CD8(+) T cells." Cell **161**(3): 486-500.

Guy-Grand, D., P. Vassalli, et al. (2013). "Origin, trafficking, and intraepithelial fate of gut-tropic T cells." J Exp Med **210**(11): 2493.

Haas, J. D., S. Ravens, et al. (2012). "Development of interleukin-17-producing gammadelta T cells is restricted to a functional embryonic wave." Immunity **37**(1): 48-59.

Halary, F., V. Pitard, et al. (2005). "Shared reactivity of V{delta}2(neg) {gamma}{delta} T cells against cytomegalovirus-infected cells and tumor intestinal epithelial cells." J Exp Med **201**(10): 1567-1578.

Hamada, S., M. Umemura, et al. (2008). "IL-17A produced by gammadelta T cells plays a critical role in innate immunity against listeria monocytogenes infection in the liver." J Immunol **181**(5): 3456-3463.

Hamann, D., S. Kostense, et al. (1999). "Evidence that human CD8+CD45RA+CD27- cells are induced by antigen and evolve through extensive rounds of division." Int Immunol **11**(7): 1027-1033.

Hammerich, L., J. M. Bangen, et al. (2013). "Chemokine receptor CCR6-dependent accumulation of gammadelta T-cells in injured liver restricts hepatic inflammation and fibrosis." Hepatology.

Han, J., D. C. Swan, et al. (2006). "Simultaneous amplification and identification of 25 human papillomavirus types with Templex technology." J Clin Microbiol **44**(11): 4157-4162.

Haque, A., J. Engel, et al. (2017). "A practical guide to single-cell RNA-sequencing for biomedical research and clinical applications." Genome Med **9**(1): 75.

Harly, C., Y. Guillaume, et al. (2012). "Key implication of CD277/butyrophilin-3 (BTN3A) in cellular stress sensing by a major human gammadelta T-cell subset." Blood **120**(11): 2269-2279.

Harmon, C., M. W. Robinson, et al. (2016). "Tissue-resident Eomes(hi) T-bet(lo) CD56(bright) NK cells with reduced proinflammatory potential are enriched in the adult human liver." Eur J Immunol **46**(9): 2111-2120.

Havran, W. L., S. Grell, et al. (1989). "Limited diversity of T-cell receptor gamma-chain expression of murine Thy-1+ dendritic epidermal cells revealed by V gamma 3-specific monoclonal antibody." Proc Natl Acad Sci U S A **86**(11): 4185-4189.

Hayday, A., E. Theodoridis, et al. (2001). "Intraepithelial lymphocytes: exploring the Third Way in immunology." Nat Immunol **2**(11): 997-1003.

Hayday, A. and R. Tigelaar (2003). "Immunoregulation in the tissues by gammadelta T cells." Nat Rev Immunol **3**(3): 233-242.

Hayday, A. C. (2009). "Gammadelta T cells and the lymphoid stress-surveillance response." Immunity **31**(2): 184-196.

He, J., G. Lang, et al. (2013). "Pathological role of interleukin-17 in poly I:C-induced hepatitis." PLoS One **8**(9): e73909.

Herkel, J. (2015). "Regulatory T Cells in Hepatic Immune Tolerance and Autoimmune Liver Diseases." Dig Dis **33 Suppl 2**: 70-74.

Himoto, T. and T. Masaki (2012). "Extrahepatic manifestations and autoantibodies in patients with hepatitis C virus infection." Clin Dev Immunol **2012**: 871401.

Hintz, M., A. Reichenberg, et al. (2001). "Identification of (E)-4-hydroxy-3-methyl-but-2-enyl pyrophosphate as a major activator for human gammadelta T cells in Escherichia coli." FEBS Lett **509**(2): 317-322.

Horner, S. M. and M. Gale, Jr. (2013). "Regulation of hepatic innate immunity by hepatitis C virus." Nat Med **19**(7): 879-888.

Horst, A. K., K. Neumann, et al. (2016). "Modulation of liver tolerance by conventional and nonconventional antigen-presenting cells and regulatory immune cells." Cell Mol Immunol **13**(3): 277-292.

Hou, L., Z. Jie, et al. (2013). "Early IL-17 production by intrahepatic T cells is important for adaptive immune responses in viral hepatitis." J Immunol **190**(2): 621-629.

Hua, F., L. Wang, et al. (2016). "Elevation of Vdelta1 T cells in peripheral blood and livers of patients with primary biliary cholangitis." Clin Exp Immunol **186**(3): 347-355.

Huang, D., C. Y. Chen, et al. (2012). "Clonal immune responses of Mycobacterium-specific gammadelta T cells in tuberculous and non-tuberculous tissues during M. tuberculosis infection." PLoS One **7**(2): e30631.

Hudspeth, K., M. Donadon, et al. (2016). "Human liver-resident CD56(bright)/CD16(neg) NK cells are retained within hepatic sinusoids via the engagement of CCR5 and CXCR6 pathways." J Autoimmun **66**: 40-50.

Hwang, Y. Y. and A. N. McKenzie (2013). "Innate lymphoid cells in immunity and disease." Adv Exp Med Biol **785**: 9-26.

Iredale, J. P., G. Murphy, et al. (1992). "Human hepatic lipocytes synthesize tissue inhibitor of metalloproteinases-1. Implications for regulation of matrix degradation in liver." J Clin Invest **90**(1): 282-287.

Itohara, S., A. G. Farr, et al. (1990). "Homing of a gamma delta thymocyte subset with homogeneous T-cell receptors to mucosal epithelia." Nature **343**(6260): 754-757.

Janeway, C. A., Jr., B. Jones, et al. (1988). "Specificity and function of T cells bearing gamma delta receptors." Immunol Today **9**(3): 73-76.

Jarry, A., N. Cerf-Bensussan, et al. (1990). "Subsets of CD3+ (T cell receptor alpha/beta or gamma/delta) and CD3- lymphocytes isolated from normal human gut epithelium display phenotypical features different from their counterparts in peripheral blood." Eur J Immunol **20**(5): 1097-1103.

Jeffery, H. C., B. van Wilgenburg, et al. (2016). "Biliary epithelium and liver B cells exposed to bacteria activate intrahepatic MAIT cells through MR1." J Hepatol **64**(5): 1118-1127.

Jenne, C. N. and P. Kubes (2013). "Immune surveillance by the liver." Nat Immunol **14**(10): 996-1006.

Jorgensen, J. L., P. A. Reay, et al. (1992). "Molecular components of T-cell recognition." Annu Rev Immunol **10**: 835-873.

Kaech, S. M., S. Hemby, et al. (2002). "Molecular and functional profiling of memory CD8 T cell differentiation." Cell **111**(6): 837-851.

Kallies, A. (2008). "Distinct regulation of effector and memory T-cell differentiation." Immunol Cell Biol **86**(4): 325-332.

Kallies, A., A. Xin, et al. (2009). "Blimp-1 transcription factor is required for the differentiation of effector CD8(+) T cells and memory responses." Immunity **31**(2): 283-295.

Kalyan, S. and D. Kabelitz (2013). "Defining the nature of human gammadelta T cells: a biographical sketch of the highly empathetic." Cell Mol Immunol **10**(1): 21-29.

Kaplan, M. H., J. R. Whitfield, et al. (1998). "Th2 cells are required for the Schistosoma mansoni egg-induced granulomatous response." J Immunol **160**(4): 1850-1856.

Kapsenberg, M. L. (2003). "Dendritic-cell control of pathogen-driven T-cell polarization." Nat Rev Immunol **3**(12): 984-993.

Karlsen, T. H., T. Folseraas, et al. (2017). "Primary sclerosing cholangitis - a comprehensive review." J Hepatol.

Kashani, E., L. Fohse, et al. (2015). "A clonotypic Vgamma4Jgamma1/Vdelta5Ddelta2Jdelta1 innate gammadelta T-cell population restricted to the CCR6(+)CD27(-) subset." Nat Commun **6**: 6477.

Kasper, H. U., D. Ligum, et al. (2009). "Liver distribution of gammadelta-T-cells in patients with chronic hepatitis of different etiology." APMIS **117**(11): 779-785.

Kenna, T., L. Golden-Mason, et al. (2004). "Distinct subpopulations of gamma delta T cells are present in normal and tumor-bearing human liver." Clin Immunol **113**(1): 56-63.

Kitayama, J., Y. Atomi, et al. (1993). "Functional analysis of TCR gamma delta+ T cells in tumour-infiltrating lymphocytes (TIL) of human pancreatic cancer." Clin Exp Immunol **93**(3): 442-447.

Klonowski, K. D., K. J. Williams, et al. (2004). "Dynamics of blood-borne CD8 memory T cell migration in vivo." Immunity **20**(5): 551-562.

Klugewitz, K., D. H. Adams, et al. (2004). "The composition of intrahepatic lymphocytes: shaped by selective recruitment?" Trends Immunol **25**(11): 590-594.

Knight, A., A. J. Madrigal, et al. (2010). "The role of Vdelta2-negative gammadelta T cells during cytomegalovirus reactivation in recipients of allogeneic stem cell transplantation." Blood **116**(12): 2164-2172.

Knolle, P., J. Schlaak, et al. (1995). "Human Kupffer cells secrete IL-10 in response to lipopolysaccharide (LPS) challenge." J Hepatol **22**(2): 226-229.

Knolle, P. A., J. Bottcher, et al. (2015). "The role of hepatic immune regulation in systemic immunity to viral infection." Med Microbiol Immunol **204**(1): 21-27.

Knolle, P. A., T. Germann, et al. (1999). "Endotoxin down-regulates T cell activation by antigen-presenting liver sinusoidal endothelial cells." J Immunol **162**(3): 1401-1407.

Knolle, P. A. and D. Wohlleber (2016). "Immunological functions of liver sinusoidal endothelial cells." Cell Mol Immunol **13**(3): 347-353.

Kondo, Y., O. Kimura, et al. (2015). "Differential Expression of CX3CL1 in Hepatitis B Virus-Replicating Hepatoma Cells Can Affect the Migration Activity of CX3CR1+ Immune Cells." J Virol **89**(14): 7016-7027.

Kronenberg, M. and L. Gapin (2002). "The unconventional lifestyle of NKT cells." Nat Rev Immunol **2**(8): 557-568.

Lalor, P. F., S. Edwards, et al. (2002). "Vascular adhesion protein-1 mediates adhesion and transmigration of lymphocytes on human hepatic endothelial cells." J Immunol **169**(2): 983-992.

Lan, R. Y., C. Cheng, et al. (2006). "Liver-targeted and peripheral blood alterations of regulatory T cells in primary biliary cirrhosis." Hepatology **43**(4): 729-737.

Lanca, T., M. F. Costa, et al. (2013). "Protective role of the inflammatory CCR2/CCL2 chemokine pathway through recruitment of type 1 cytotoxic gammadelta T lymphocytes to tumor beds." J Immunol **190**(12): 6673-6680.

Lang, F., M. A. Peyrat, et al. (1995). "Early activation of human V gamma 9V delta 2 T cell broad cytotoxicity and TNF production by nonpeptidic mycobacterial ligands." J Immunol **154**(11): 5986-5994.

Lanier, L. L., A. M. Le, et al. (1986). "The relationship of CD16 (Leu-11) and Leu-19 (NKH-1) antigen expression on human peripheral blood NK cells and cytotoxic T lymphocytes." J Immunol **136**(12): 4480-4486.

Lantz, O. and A. Bendelac (1994). "An invariant T cell receptor alpha chain is used by a unique subset of major histocompatibility complex class I-specific CD4+ and CD4-8- T cells in mice and humans." J Exp Med **180**(3): 1097-1106.

Lawrence, M. B., G. S. Kansas, et al. (1997). "Threshold levels of fluid shear promote leukocyte adhesion through selectins (CD62L,P,E)." J Cell Biol **136**(3): 717-727.

Laydon, D. J., A. Melamed, et al. (2014). "Quantification of HTLV-1 clonality and TCR diversity." PLoS Comput Biol **10**(6): e1003646.

Lepore, M., A. Kalinichenko, et al. (2014). "Parallel T-cell cloning and deep sequencing of human MAIT cells reveal stable oligoclonal TCRbeta repertoire." Nat Commun **5**: 3866.

Li, J. T., Z. X. Liao, et al. (2008). "Molecular mechanism of hepatic stellate cell activation and antifibrotic therapeutic strategies." J Gastroenterol **43**(6): 419-428.

Liaskou, E., G. M. Hirschfield, et al. (2014). "Mechanisms of tissue injury in autoimmune liver diseases." Semin Immunopathol **36**(5): 553-568.

Liaskou, E., E. K. Klemsdal Henriksen, et al. (2016). "High-throughput T-cell receptor sequencing across chronic liver diseases reveals distinct disease-associated repertoires." Hepatology **63**(5): 1608-1619.

Liaskou, E., H. W. Zimmermann, et al. (2013). "Monocyte subsets in human liver disease show distinct phenotypic and functional characteristics." Hepatology **57**(1): 385-398.

Liberal, R., E. L. Krawitt, et al. (2016). "Cutting edge issues in autoimmune hepatitis." J Autoimmun **75**: 6-19.

Limmer, A., J. Ohl, et al. (2000). "Efficient presentation of exogenous antigen by liver endothelial cells to CD8+ T cells results in antigen-specific T-cell tolerance." Nat Med **6**(12): 1348-1354.

Liu, J., H. Qu, et al. (2013). "The responses of gammadelta T-cells against acute Pseudomonas aeruginosa pulmonary infection in mice via interleukin-17." Pathog Dis **68**(2): 44-51.

Liu, W. and S. A. Huber (2011). "Cross-talk between cd1d-restricted nkt cells and gammadelta cells in t regulatory cell response." Virol J **8**: 32.

Lossius, A., J. N. Johansen, et al. (2014). "High-throughput sequencing of TCR repertoires in multiple sclerosis reveals intrathecal enrichment of EBV-reactive CD8+ T cells." Eur J Immunol **44**(11): 3439-3452.

Lu, Y., X. Wang, et al. (2012). "Liver TCRgammadelta(+) CD3(+) CD4(-) CD8(-) T cells contribute to murine hepatitis virus strain 3-induced hepatic injury through a TNF-alpha-dependent pathway." Mol Immunol **52**(3-4): 229-236.

Lugli, E., K. Hudspeth, et al. (2016). "Tissue-resident and memory properties of human T-cell and NK-cell subsets." Eur J Immunol **46**(8): 1809-1817.

Luoma, A. M., C. D. Castro, et al. (2013). "Crystal structure of Vdelta1 T cell receptor in complex with CD1d-sulfatide shows MHC-like recognition of a self-lipid by human gammadelta T cells." Immunity **39**(6): 1032-1042.

Macedo, M. F., G. Porto, et al. (2010). "Low numbers of CD8+ T lymphocytes in hereditary haemochromatosis are explained by a decrease of the most mature CD8+ effector memory T cells." Clin Exp Immunol **159**(3): 363-371.

Mackay, L. K., A. Braun, et al. (2015). "Cutting edge: CD69 interference with sphingosine-1-phosphate receptor function regulates peripheral T cell retention." J Immunol **194**(5): 2059-2063.

Mackay, L. K., M. Minnich, et al. (2016). "Hobit and Blimp1 instruct a universal transcriptional program of tissue residency in lymphocytes." Science **352**(6284): 459-463.

Mackay, L. K., A. T. Stock, et al. (2012). "Long-lived epithelial immunity by tissue-resident memory T (TRM) cells in the absence of persisting local antigen presentation." Proc Natl Acad Sci U S A **109**(18): 7037-7042.

Madi, A., E. Shifrut, et al. (2014). "T-cell receptor repertoires share a restricted set of public and abundant CDR3 sequences that are associated with self-related immunity." Genome Res **24**(10): 1603-1612.

Mangan, B. A., M. R. Dunne, et al. (2013). "Cutting edge: CD1d restriction and Th1/Th2/Th17 cytokine secretion by human Vdelta3 T cells." J Immunol **191**(1): 30-34.

Mao, C., X. Mou, et al. (2014). "Tumor-Activated TCRgamma delta (+) T Cells from Gastric Cancer Patients Induce the Antitumor Immune Response of TCRalpha beta (+) T Cells via Their Antigen-Presenting Cell-Like Effects." J Immunol Res **2014**: 593562.

Marquardt, N., V. Beziat, et al. (2015). "Cutting edge: identification and characterization of human intrahepatic CD49a+ NK cells." J Immunol **194**(6): 2467-2471.

Marra, F. and F. Tacke (2014). "Roles for chemokines in liver disease." Gastroenterology **147**(3): 577-594 e571.

Martinet, L., S. Fleury-Cappellesso, et al. (2009). "A regulatory cross-talk between Vgamma9Vdelta2 T lymphocytes and mesenchymal stem cells." Eur J Immunol **39**(3): 752-762.

Martinez-Esparza, M., M. Tristan-Manzano, et al. (2015). "Inflammatory status in human hepatic cirrhosis." World J Gastroenterol **21**(41): 11522-11541.

Martins, E. B., A. K. Graham, et al. (1996). "Elevation of gamma delta T lymphocytes in peripheral blood and livers of patients with primary sclerosing cholangitis and other autoimmune liver diseases." Hepatology **23**(5): 988-993.

Masopust, D., D. Choo, et al. (2010). "Dynamic T cell migration program provides resident memory within intestinal epithelium." J Exp Med **207**(3): 553-564.

Masopust, D., V. Vezys, et al. (2001). "Preferential localization of effector memory cells in nonlymphoid tissue." Science **291**(5512): 2413-2417.

Masopust, D., V. Vezys, et al. (2004). "Activated primary and memory CD8 T cells migrate to nonlymphoid tissues regardless of site of activation or tissue of origin." J Immunol **172**(8): 4875-4882.

Matloubian, M., C. G. Lo, et al. (2004). "Lymphocyte egress from thymus and peripheral lymphoid organs is dependent on S1P receptor 1." Nature **427**(6972): 355-360.

Matos, J. M., F. A. Witzmann, et al. (2009). "A pilot study of proteomic profiles of human hepatocellular carcinoma in the United States." J Surg Res **155**(2): 237-243.

Matsuzaki, G. and M. Umemura (2007). "Interleukin-17 as an effector molecule of innate and acquired immunity against infections." Microbiol Immunol **51**(12): 1139-1147.

McCarthy, N. E., C. R. Hedin, et al. (2015). "Azathioprine therapy selectively ablates human Vdelta2(+) T cells in Crohn's disease." J Clin Invest **125**(8): 3215-3225.

McNamara, H. A., Y. Cai, et al. (2017). "Up-regulation of LFA-1 allows liver-resident memory T cells to patrol and remain in the hepatic sinusoids." Sci Immunol **2**(9).

McNamara, H. A. and I. A. Cockburn (2016). "The three Rs: Recruitment, Retention and Residence of leukocytes in the liver." Clin Transl Immunology **5**(12): e123.

McVay, L. D. and S. R. Carding (1996). "Extrathymic origin of human gamma delta T cells during fetal development." J Immunol **157**(7): 2873-2882.

McVay, L. D., S. R. Carding, et al. (1991). "Regulated expression and structure of T cell receptor gamma/delta transcripts in human thymic ontogeny." EMBO J **10**(1): 83-91.

McVay, L. D., S. S. Jaswal, et al. (1998). "The generation of human gammadelta T cell repertoires during fetal development." J Immunol **160**(12): 5851-5860.

Medzhitov, R. and C. A. Janeway, Jr. (2002). "Decoding the patterns of self and nonself by the innate immune system." Science **296**(5566): 298-300.

Melsen, J. E., G. Lugthart, et al. (2016). "Human Circulating and Tissue-Resident CD56(bright) Natural Killer Cell Populations." Front Immunol **7**: 262.

Mirzaei, H. R., H. Mirzaei, et al. (2016). "Prospects for chimeric antigen receptor (CAR) gammadelta T cells: A potential game changer for adoptive T cell cancer immunotherapy." Cancer Lett **380**(2): 413-423.

Miyagawa, F., Y. Tanaka, et al. (2001). "Essential requirement of antigen presentation by monocyte lineage cells for the activation of primary human gamma delta T cells by aminobisphosphonate antigen." J Immunol **166**(9): 5508-5514.

Morita, C. T., E. M. Beckman, et al. (1995). "Direct presentation of nonpeptide prenyl pyrophosphate antigens to human gamma delta T cells." Immunity **3**(4): 495-507.

Morita, C. T., C. Jin, et al. (2007). "Nonpeptide antigens, presentation mechanisms, and immunological memory of human Vgamma2Vdelta2 T cells: discriminating friend from foe through the recognition of prenyl pyrophosphate antigens." Immunol Rev **215**: 59-76.

Morita, C. T., H. K. Lee, et al. (1999). "Recognition of nonpeptide prenyl pyrophosphate antigens by human gammadelta T cells." Microbes Infect **1**(3): 175-186.

Morita, C. T., C. M. Parker, et al. (1994). "TCR usage and functional capabilities of human gamma delta T cells at birth." J Immunol **153**(9): 3979-3988.

Mucida, D. and H. Cheroutre (2010). "The many face-lifts of CD4 T helper cells." Adv Immunol **107**: 139-152.

Munoz-Ruiz, M., J. C. Ribot, et al. (2016). "TCR signal strength controls thymic differentiation of discrete proinflammatory gammadelta T cell subsets." Nat Immunol **17**(6): 721-727.

Nakamura, T., Y. Kamogawa, et al. (1997). "Polarization of IL-4- and IFN-gamma-producing CD4+ T cells following activation of naive CD4+ T cells." J Immunol **158**(3): 1085-1094.

Nannini, P. and E. M. Sokal (2017). "Hepatitis B: changing epidemiology and interventions." Arch Dis Child **102**(7): 0.

Nielsen, M. M., D. A. Witherden, et al. (2017). "gammadelta T cells in homeostasis and host defence of epithelial barrier tissues." Nat Rev Immunol **17**(12): 733-745.

Norris, S., C. Collins, et al. (1998). "Resident human hepatic lymphocytes are phenotypically different from circulating lymphocytes." J Hepatol **28**(1): 84-90.

Nuti, S., D. Rosa, et al. (1998). "Dynamics of intra-hepatic lymphocytes in chronic hepatitis C: enrichment for Valpha24+ T cells and rapid elimination of effector cells by apoptosis." Eur J Immunol **28**(11): 3448-3455.

O'Brien, R. L. and W. K. Born (2010). "gammadelta T cell subsets: a link between TCR and function?" Semin Immunol **22**(4): 193-198.

Obar, J. J. and L. Lefrancois (2010). "Memory CD8+ T cell differentiation." Ann N Y Acad Sci **1183**: 251-266.

Okhrimenko, A., J. R. Grun, et al. (2014). "Human memory T cells from the bone marrow are resting and maintain long-lasting systemic memory." Proc Natl Acad Sci U S A **111**(25): 9229-9234.

Oo, Y. H., C. J. Weston, et al. (2010). "Distinct roles for CCR4 and CXCR3 in the recruitment and positioning of regulatory T cells in the inflamed human liver." J Immunol **184**(6): 2886-2898.

Pachnio, A., M. Ciaurriz, et al. (2016). "Cytomegalovirus Infection Leads to Development of High Frequencies of Cytotoxic Virus-Specific CD4+ T Cells Targeted to Vascular Endothelium." PLoS Pathog **12**(9): e1005832.

Pallett, L. J., J. Davies, et al. (2017). "IL-2high tissue-resident T cells in the human liver: Sentinels for hepatotropic infection." J Exp Med **214**(6): 1567-1580.

Pannetier, C., M. Cochet, et al. (1993). "The sizes of the CDR3 hypervariable regions of the murine T-cell receptor beta chains vary as a function of the recombined germ-line segments." Proc Natl Acad Sci U S A **90**(9): 4319-4323.

Pannetier, C., J. Even, et al. (1995). "T-cell repertoire diversity and clonal expansions in normal and clinical samples." Immunol Today **16**(4): 176-181.

Par, G., D. Rukavina, et al. (2002). "Decrease in CD3-negative-CD8dim(+) and Vdelta2/Vgamma9 TcR+ peripheral blood lymphocyte counts, low perforin expression and the impairment of natural killer cell activity is associated with chronic hepatitis C virus infection." J Hepatol **37**(4): 514-522.

Parsons, C. J., M. Takashima, et al. (2007). "Molecular mechanisms of hepatic fibrogenesis." J Gastroenterol Hepatol **22 Suppl 1**: S79-84.

Patsenker, E. and F. Stickel (2011). "Role of integrins in fibrosing liver diseases." Am J Physiol Gastrointest Liver Physiol **301**(3): G425-434.

Pauza, C. D. and C. Cairo (2015). "Evolution and function of the TCR Vgamma9 chain repertoire: It's good to be public." Cell Immunol **296**(1): 22-30.

Pellicci, D. G., A. P. Uldrich, et al. (2014). "The molecular bases of delta/alphabeta T cell-mediated antigen recognition." J Exp Med **211**(13): 2599-2615.

Pellicoro, A., P. Ramachandran, et al. (2014). "Liver fibrosis and repair: immune regulation of wound healing in a solid organ." Nat Rev Immunol **14**(3): 181-194.

Peng, H., X. Jiang, et al. (2013). "Liver-resident NK cells confer adaptive immunity in skin-contact inflammation." J Clin Invest **123**(4): 1444-1456.

Peng, H. and Z. Tian (2015). "Re-examining the origin and function of liver-resident NK cells." Trends Immunol **36**(5): 293-299.

Perdiguero, E. G., K. Klapproth, et al. (2015). "The Origin of Tissue-Resident Macrophages: When an Erythro-myeloid Progenitor Is an Erythro-myeloid Progenitor." Immunity **43**(6): 1023-1024.

Pitard, V., D. Roumanes, et al. (2008). "Long-term expansion of effector/memory Vdelta2-gammadelta T cells is a specific blood signature of CMV infection." Blood **112**(4): 1317-1324.

Pociask, D. A., K. Chen, et al. (2011). "gammadelta T cells attenuate bleomycin-induced fibrosis through the production of CXCL10." Am J Pathol **178**(3): 1167-1176.

Poggi, A., M. R. Zocchi, et al. (2002). "Transendothelial migratory pathways of V delta 1+TCR gamma delta+ and V delta 2+TCR gamma delta+ T lymphocytes from healthy donors and multiple sclerosis patients: involvement of phosphatidylinositol 3 kinase and calcium calmodulin-dependent kinase II." J Immunol **168**(12): 6071-6077.

Poggi, A., M. R. Zocchi, et al. (1999). "IL-12-mediated NKRP1A up-regulation and consequent enhancement of endothelial transmigration of V delta 2+ TCR gamma delta+ T lymphocytes from healthy donors and multiple sclerosis patients." J Immunol **162**(7): 4349-4354.

Purwar, R., J. Campbell, et al. (2011). "Resident memory T cells (T(RM)) are abundant in human lung: diversity, function, and antigen specificity." PLoS One **6**(1): e16245.

Putintseva, E. V., O. V. Britanova, et al. (2013). "Mother and child T cell receptor repertoires: deep profiling study." Front Immunol **4**: 463.

Qi, Q., Y. Liu, et al. (2014). "Diversity and clonal selection in the human T-cell repertoire." Proc Natl Acad Sci U S A **111**(36): 13139-13144.

Racanelli, V. and B. Rehermann (2006). "The liver as an immunological organ." Hepatology **43**(2 Suppl 1): S54-62.

Radaeva, S., R. Sun, et al. (2006). "Natural killer cells ameliorate liver fibrosis by killing activated stellate cells in NKG2D-dependent and tumor necrosis factor-related apoptosis-inducing ligand-dependent manners." Gastroenterology **130**(2): 435-452.

Rani, M., Q. Zhang, et al. (2014). "Gamma Delta (gammadelta) T-Cells Regulate Wound Myeloid Cell Activity After Burn." Shock.

Ravens, S., C. Schultze-Florey, et al. (2017). "Human gammadelta T cells are quickly reconstituted after stem-cell transplantation and show adaptive clonal expansion in response to viral infection." Nat Immunol **18**(4): 393-401.

Remmerswaal, E. B., S. H. Havenith, et al. (2012). "Human virus-specific effector-type T cells accumulate in blood but not in lymph nodes." Blood **119**(7): 1702-1712.

Rhodes, D. A., W. Reith, et al. (2016). "Regulation of Immunity by Butyrophilins." Annu Rev Immunol **34**: 151-172.

Ribot, J. C., S. T. Ribeiro, et al. (2014). "Human gammadelta thymocytes are functionally immature and differentiate into cytotoxic type 1 effector T cells upon IL-2/IL-15 signaling." J Immunol **192**(5): 2237-2243.

Robins, H. S., P. V. Campregher, et al. (2009). "Comprehensive assessment of T-cell receptor beta-chain diversity in alphabeta T cells." Blood **114**(19): 4099-4107.

Rosen, H. R. (2013). "Emerging concepts in immunity to hepatitis C virus infection." J Clin Invest **123**(10): 4121-4130.

Roux, A., G. Mourin, et al. (2013). "Differential impact of age and cytomegalovirus infection on the gammadelta T cell compartment." J Immunol **191**(3): 1300-1306.

Rudolph, M. G., R. L. Stanfield, et al. (2006). "How TCRs bind MHCs, peptides, and coreceptors." Annu Rev Immunol **24**: 419-466.

Russano, A. M., G. Bassotti, et al. (2007). "CD1-restricted recognition of exogenous and self-lipid antigens by duodenal gammadelta+ T lymphocytes." J Immunol **178**(6): 3620-3626.

Sakaguchi, S. (2005). "Naturally arising Foxp3-expressing CD25+CD4+ regulatory T cells in immunological tolerance to self and non-self." Nat Immunol **6**(4): 345-352.

Salerno, A. and F. Dieli (1998). "Role of gamma delta T lymphocytes in immune response in humans and mice." Crit Rev Immunol **18**(4): 327-357.

Salim, M., T. J. Knowles, et al. (2016). "Characterization of a Putative Receptor Binding Surface on Skint-1, a Critical Determinant of Dendritic Epidermal T Cell Selection." J Biol Chem **291**(17): 9310-9321.

Sallusto, F., D. Lenig, et al. (1999). "Two subsets of memory T lymphocytes with distinct homing potentials and effector functions." Nature **401**(6754): 708-712.

Sandstrom, A., C. M. Peigne, et al. (2014). "The Intracellular B30.2 Domain of Butyrophilin 3A1 Binds Phosphoantigens to Mediate Activation of Human Vgamma9Vdelta2 T Cells." Immunity **40**(4): 490-500.

Sato, T., H. Yamamoto, et al. (1998). "Maturation of rat dendritic cells during intrahepatic translocation evaluated using monoclonal antibodies and electron microscopy." Cell Tissue Res **294**(3): 503-514.

Schenkel, J. M., K. A. Fraser, et al. (2014). "Cutting edge: resident memory CD8 T cells occupy frontline niches in secondary lymphoid organs." J Immunol **192**(7): 2961-2964.

Schoknecht, T., D. Schwinge, et al. (2017). "CD4+ T cells from patients with primary sclerosing cholangitis exhibit reduced apoptosis and down-regulation of proapoptotic Bim in peripheral blood." J Leukoc Biol **101**(2): 589-597.

Schrum, A. G., L. A. Turka, et al. (2003). "Surface T-cell antigen receptor expression and availability for long-term antigenic signaling." Immunol Rev **196**: 7-24.

Schrumpf, E., O. Fausa, et al. (1982). "HLA antigens and immunoregulatory T cells in ulcerative colitis associated with hepatobiliary disease." Scand J Gastroenterol **17**(2): 187-191.

Selin, L. K., P. A. Santolucito, et al. (2001). "Innate immunity to viruses: control of vaccinia virus infection by gamma delta T cells." J Immunol **166**(11): 6784-6794.

Shang, H., Z. Wang, et al. (2016). "Liver progenitor cells-mediated liver regeneration in liver cirrhosis." Hepatol Int **10**(3): 440-447.

Shen, Y., D. Zhou, et al. (2002). "Adaptive immune response of Vgamma2Vdelta2+ T cells during mycobacterial infections." Science **295**(5563): 2255-2258.

Sheridan, B. S., P. A. Romagnoli, et al. (2013). "gammadelta T cells exhibit multifunctional and protective memory in intestinal tissues." Immunity **39**(1): 184-195.

Sherwood, A. M., C. Desmarais, et al. (2011). "Deep sequencing of the human TCRgamma and TCRbeta repertoires suggests that TCRbeta rearranges after alphabeta and gammadelta T cell commitment." Sci Transl Med **3**(90): 90ra61.

Sherwood, A. M., R. O. Emerson, et al. (2013). "Tumor-infiltrating lymphocytes in colorectal tumors display a diversity of T cell receptor sequences that differ from the T cells in adjacent mucosal tissue." Cancer Immunol Immunother **62**(9): 1453-1461.

Shetty, S., C. J. Weston, et al. (2014). "A flow adhesion assay to study leucocyte recruitment to human hepatic sinusoidal endothelium under conditions of shear stress." J Vis Exp(85).

Shimoda, S., K. Harada, et al. (2010). "CX3CL1 (fractalkine): a signpost for biliary inflammation in primary biliary cirrhosis." Hepatology **51**(2): 567-575.

Shinkai, Y., G. Rathbun, et al. (1992). "RAG-2-deficient mice lack mature lymphocytes owing to inability to initiate V(D)J rearrangement." Cell **68**(5): 855-867.

Shrivastava, S., A. Mukherjee, et al. (2013). "Hepatitis C virus induces interleukin-1beta (IL-1beta)/IL-18 in circulatory and resident liver macrophages." J Virol **87**(22): 12284-12290.

Shugay, M., D. V. Bagaev, et al. (2015). "VDJtools: Unifying Post-analysis of T Cell Receptor Repertoires." PLoS Comput Biol **11**(11): e1004503.

Shugay, M., D. A. Bolotin, et al. (2013). "Huge Overlap of Individual TCR Beta Repertoires." Front Immunol **4**: 466.

Shugay, M., O. V. Britanova, et al. (2014). "Towards error-free profiling of immune repertoires." Nat Methods **11**(6): 653-655.

Simonetta, F., S. Hua, et al. (2014). "High eomesodermin expression among CD57+ CD8+ T cells identifies a CD8+ T cell subset associated with viral control during chronic human immunodeficiency virus infection." J Virol **88**(20): 11861-11871.

Simonian, P. L., F. Wehrmann, et al. (2010). "gammadelta T cells protect against lung fibrosis via IL-22." J Exp Med **207**(10): 2239-2253.

Sironi, L., M. Bouzin, et al. (2014). "In vivo flow mapping in complex vessel networks by single image correlation." Sci Rep **4**: 7341.

Slifka, M. K., R. Antia, et al. (1998). "Humoral immunity due to long-lived plasma cells." Immunity **8**(3): 363-372.

Spada, F. M., E. P. Grant, et al. (2000). "Self-recognition of CD1 by gamma/delta T cells: implications for innate immunity." J Exp Med **191**(6): 937-948.

Stamenkovic, I. (1995). "The L-selectin adhesion system." Curr Opin Hematol **2**(1): 68-75.

Stegmann, K. A., F. Robertson, et al. (2016). "CXCR6 marks a novel subset of T-bet(lo)Eomes(hi) natural killer cells residing in human liver." Sci Rep **6**: 26157.

Steimle, V., C. A. Siegrist, et al. (1994). "Regulation of MHC class II expression by interferon-gamma mediated by the transactivator gene CIITA." Science **265**(5168): 106-109.

Steinert, E. M., J. M. Schenkel, et al. (2015). "Quantifying Memory CD8 T Cells Reveals Regionalization of Immunosurveillance." Cell **161**(4): 737-749.

Stelma, F., A. de Niet, et al. (2017). "Human intrahepatic CD69 + CD8+ T cells have a tissue resident memory T cell phenotype with reduced cytolytic capacity." Sci Rep **7**(1): 6172.

Strauch, U. G., R. C. Mueller, et al. (2001). "Integrin alpha E(CD103)beta 7 mediates adhesion to intestinal microvascular endothelial cell lines via an E-cadherin-independent interaction." J Immunol **166**(5): 3506-3514.

Stubbington, M. J. T., T. Lonnberg, et al. (2016). "T cell fate and clonality inference from single-cell transcriptomes." Nat Methods **13**(4): 329-332.

Svanborg, C., G. Godaly, et al. (1999). "Cytokine responses during mucosal infections: role in disease pathogenesis and host defence." Curr Opin Microbiol **2**(1): 99-105.

Szabo, G. (2015). "Gut-liver axis in alcoholic liver disease." Gastroenterology **148**(1): 30-36.

Szabo, S. J., S. T. Kim, et al. (2000). "A novel transcription factor, T-bet, directs Th1 lineage commitment." Cell **100**(6): 655-669.

Takahashi, M., K. Ogasawara, et al. (1996). "LPS induces NK1.1+ alpha beta T cells with potent cytotoxicity in the liver of mice via production of IL-12 from Kupffer cells." J Immunol **156**(7): 2436-2442.

Takeda, K., T. Kaisho, et al. (2003). "Toll-like receptors." Annu Rev Immunol **21**: 335-376.

Tam, S., S. Maksaereekul, et al. (2012). "IL-17 and gammadelta T-lymphocytes play a critical role in innate immunity against Nocardia asteroides GUH-2." Microbes Infect **14**(13): 1133-1143.

Thomas, M. L., R. A. Badwe, et al. (2001). "Role of adhesion molecules in recruitment of Vdelta1 T cells from the peripheral blood to the tumor tissue of esophageal cancer patients." Cancer Immunol Immunother **50**(4): 218-225.

Thomas, S. Y., S. T. Scanlon, et al. (2011). "PLZF induces an intravascular surveillance program mediated by long-lived LFA-1-ICAM-1 interactions." J Exp Med **208**(6): 1179-1188.

Thome, J. J. and D. L. Farber (2015). "Emerging concepts in tissue-resident T cells: lessons from humans." Trends Immunol **36**(7): 428-435.

Toulon, A., L. Breton, et al. (2009). "A role for human skin-resident T cells in wound healing." J Exp Med **206**(4): 743-750.

Toutirais, O., F. Cabillic, et al. (2009). "DNAX accessory molecule-1 (CD226) promotes human hepatocellular carcinoma cell lysis by Vgamma9Vdelta2 T cells." Eur J Immunol **39**(5): 1361-1368.

Tramonti, D., E. M. Andrew, et al. (2006). "Evidence for the opposing roles of different gamma delta T cell subsets in macrophage homeostasis." Eur J Immunol **36**(7): 1729-1738.

Tramonti, D., K. Rhodes, et al. (2008). "gammadeltaT cell-mediated regulation of chemokine producing macrophages during Listeria monocytogenes infection-induced inflammation." J Pathol **216**(2): 262-270.

Treiner, E., L. Duban, et al. (2005). "Mucosal-associated invariant T (MAIT) cells: an evolutionarily conserved T cell subset." Microbes Infect **7**(3): 552-559.

Treiner, E. and O. Lantz (2006). "CD1d- and MR1-restricted invariant T cells: of mice and men." Curr Opin Immunol **18**(5): 519-526.

Tribel, F., M. P. Lefranc, et al. (1988). "Further evidence for a sequentially ordered activation of T cell rearranging gamma genes during T lymphocyte differentiation." Eur J Immunol **18**(5): 789-794.

Trivedi, P. J., J. Tickle, et al. (2017). "Vascular adhesion protein-1 is elevated in primary sclerosing cholangitis, is predictive of clinical outcome and facilitates recruitment of gut-tropic lymphocytes to liver in a substrate-dependent manner." Gut.

Tseng, C. T., E. Miskovsky, et al. (2001). "Characterization of liver T-cell receptor gammadelta T cells obtained from individuals chronically infected with hepatitis C virus (HCV): evidence for these T cells playing a role in the liver pathology associated with HCV infections." Hepatology **33**(5): 1312-1320.

Tsuneyama, K., M. Yasoshima, et al. (1998). "Increased CD1d expression on small bile duct epithelium and epithelioid granuloma in livers in primary biliary cirrhosis." Hepatology **28**(3): 620-623.

Tuncer, C., Y. H. Oo, et al. (2013). "The regulation of T-cell recruitment to the human liver during acute liver failure." Liver Int **33**(6): 852-863.

Turner, D. L. and D. L. Farber (2014). "Mucosal resident memory CD4 T cells in protection and immunopathology." Front Immunol **5**: 331.

Turner, D. L., C. L. Gordon, et al. (2014). "Tissue-resident T cells, in situ immunity and transplantation." Immunol Rev **258**(1): 150-166.

Tyler, C. J., D. G. Doherty, et al. (2015). "Human Vgamma9/Vdelta2 T cells: Innate adaptors of the immune system." Cell Immunol **296**(1): 10-21.

Uldrich, A. P., J. Le Nours, et al. (2013). "CD1d-lipid antigen recognition by the gammadelta TCR." Nat Immunol.

Uppenkamp, M. J., K. Schepers, et al. (1993). "Regulation of the T cell receptor-alpha mRNA expression in the human lymphoblastic T cell line CEM." Exp Hematol **21**(2): 331-337.

van Aalderen, M. C., E. B. Remmerswaal, et al. (2014). "Blood and beyond: properties of circulating and tissue-resident human virus-specific alphabeta CD8(+) T cells." Eur J Immunol **44**(4): 934-944.

van Aalderen, M. C., M. van den Biggelaar, et al. (2017). "Label-free Analysis of CD8+ T Cell Subset Proteomes Supports a Progressive Differentiation Model of Human-Virus-Specific T Cells." Cell Rep **19**(5): 1068-1079.

Van de Water, J., A. Ansari, et al. (1995). "Heterogeneity of autoreactive T cell clones specific for the E2 component of the pyruvate dehydrogenase complex in primary biliary cirrhosis." J Exp Med **181**(2): 723-733.

Vantourout, P. and A. Hayday (2013). "Six-of-the-best: unique contributions of gammadelta T cells to immunology." Nat Rev Immunol **13**(2): 88-100.

Venturi, V., H. Y. Chin, et al. (2008). "TCR beta-chain sharing in human CD8+ T cell responses to cytomegalovirus and EBV." J Immunol **181**(11): 7853-7862.

Vermijlen, D., M. Brouwer, et al. (2010). "Human cytomegalovirus elicits fetal gammadelta T cell responses in utero." J Exp Med **207**(4): 807-821.

Vieira Braga, F. A., K. M. Hertoghs, et al. (2015). "Blimp-1 homolog Hobit identifies effector-type lymphocytes in humans." Eur J Immunol **45**(10): 2945-2958.

Voelkerding, K. V., S. A. Dames, et al. (2009). "Next-generation sequencing: from basic research to diagnostics." Clin Chem **55**(4): 641-658.

Wallace, D. L., J. E. Masters, et al. (2011). "Human cytomegalovirus-specific CD8(+) T-cell expansions contain long-lived cells that retain functional capacity in both young and elderly subjects." Immunology **132**(1): 27-38.

Wang, C., C. M. Sanders, et al. (2010). "High throughput sequencing reveals a complex pattern of dynamic interrelationships among human T cell subsets." Proc Natl Acad Sci U S A **107**(4): 1518-1523.

Wang, H. J., B. Gao, et al. (2012). "Inflammation in alcoholic liver disease." Annu Rev Nutr **32**: 343-368.

Wang, H., Z. Fang, et al. (2010). "Vgamma2Vdelta2 T Cell Receptor recognition of prenyl pyrophosphates is dependent on all CDRs." J Immunol **184**(11): 6209-6222.

Wang, J. H. and E. L. Reinherz (2002). "Structural basis of T cell recognition of peptides bound to MHC molecules." Mol Immunol **38**(14): 1039-1049.

Wang, T., Y. Gao, et al. (2006). "Gamma delta T cells facilitate adaptive immunity against West Nile virus infection in mice." J Immunol **177**(3): 1825-1832.

Watanabe, R., A. Gehad, et al. (2015). "Human skin is protected by four functionally and phenotypically discrete populations of resident and recirculating memory T cells." Sci Transl Med **7**(279): 279ra239.

Waters, W. R., M. J. Wannemuehler, et al. (1999). "Cryptosporidium parvum-induced inflammatory bowel disease of TCR-beta- x TCR-delta-deficient mice." J Parasitol **85**(6): 1100-1105.

Wehr, A., C. Baeck, et al. (2013). "Chemokine receptor CXCR6-dependent hepatic NK T Cell accumulation promotes inflammation and liver fibrosis." J Immunol **190**(10): 5226-5236.

Weiskirchen, R. and F. Tacke (2014). "Cellular and molecular functions of hepatic stellate cells in inflammatory responses and liver immunology." Hepatobiliary Surg Nutr **3**(6): 344-363.

Wencker, M., G. Turchinovich, et al. (2014). "Innate-like T cells straddle innate and adaptive immunity by altering antigen-receptor responsiveness." Nat Immunol **15**(1): 80-87.

Willcox, C. R., V. Pitard, et al. (2012). "Cytomegalovirus and tumor stress surveillance by binding of a human gammadelta T cell antigen receptor to endothelial protein C receptor." Nat Immunol **13**(9): 872-879.

Winau, F., G. Hegasy, et al. (2007). "Ito cells are liver-resident antigen-presenting cells for activating T cell responses." Immunity **26**(1): 117-129.

Wirth, T. C., H. H. Xue, et al. (2010). "Repetitive antigen stimulation induces stepwise transcriptome diversification but preserves a core signature of memory CD8(+) T cell differentiation." Immunity **33**(1): 128-140.

Wisse, E., F. Braet, et al. (1996). "Structure and function of sinusoidal lining cells in the liver." Toxicol Pathol **24**(1): 100-111.

Wu, D., P. Wu, et al. (2015). "Ex vivo expanded human circulating Vdelta1 gammadeltaT cells exhibit favorable therapeutic potential for colon cancer." Oncoimmunology **4**(3): e992749.

Wu, P., D. Wu, et al. (2014). "gammadeltaT17 cells promote the accumulation and expansion of myeloid-derived suppressor cells in human colorectal cancer." Immunity **40**(5): 785-800.

Wu, X., J. Y. Zhang, et al. (2013). "Decreased Vdelta2 gammadelta T Cells Associated With Liver Damage by Regulation of Th17 Response in Patients With Chronic Hepatitis B." J Infect Dis **208**(8): 1294-1304.

Wucherpfennig, K. W., Y. J. Liao, et al. (1993). "Human fetal liver gamma/delta T cells predominantly use unusual rearrangements of the T cell receptor delta and gamma loci expressed on both CD4+CD8- and CD4-CD8- gamma/delta T cells." J Exp Med **177**(2): 425-432.

Wunderlich, F., S. Al-Quraishy, et al. (2014). "Liver-inherent immune system: its role in blood-stage malaria." Front Microbiol **5**: 559.

Xin, A., F. Masson, et al. (2016). "A molecular threshold for effector CD8(+) T cell differentiation controlled by transcription factors Blimp-1 and T-bet." Nat Immunol **17**(4): 422-432.

Xu, F., C. Liu, et al. (2016). "TGF-beta/SMAD Pathway and Its Regulation in Hepatic Fibrosis." J Histochem Cytochem **64**(3): 157-167.

Yanagisawa, K., S. Yue, et al. (2013). "Ex vivo analysis of resident hepatic pro-inflammatory CD1d-reactive T cells and hepatocyte surface CD1d expression in hepatitis C." J Viral Hepat **20**(8): 556-565.

Yang, Y., C. Wang, et al. (2015). "Distinct mechanisms define murine B cell lineage immunoglobulin heavy chain (IgH) repertoires." Elife **4**: e09083.

Yi, Y., H. W. He, et al. (2013). "The functional impairment of HCC-infiltrating gammadelta T cells, partially mediated by regulatory T cells in a TGFbeta- and IL-10-dependent manner." J Hepatol **58**(5): 977-983.

Yokoyama, W. M. and B. F. Plougastel (2003). "Immune functions encoded by the natural killer gene complex." Nat Rev Immunol **3**(4): 304-316.

Zaid, A., L. K. Mackay, et al. (2014). "Persistence of skin-resident memory T cells within an epidermal niche." Proc Natl Acad Sci U S A **111**(14): 5307-5312.

Zarnitsyna, V. I., B. D. Evavold, et al. (2013). "Estimating the diversity, completeness, and cross-reactivity of the T cell repertoire." Front Immunol **4**: 485.

Zeissig, S., K. Murata, et al. (2012). "Hepatitis B virus-induced lipid alterations contribute to natural killer T cell-dependent protective immunity." Nat Med **18**(7): 1060-1068.

Zeng, X., Y. L. Wei, et al. (2012). "gammadelta T cells recognize a microbial encoded B cell antigen to initiate a rapid antigen-specific interleukin-17 response." Immunity **37**(3): 524-534.